Discovery of anti-mycobacterial natural products from South African marine algae

A Thesis Submitted in Fulfilment of the Requirements for the Degree of

Master of Science in Pharmaceutical Sciences

University of the Western Cape

School of Pharmacy

By

Zaahirah Mukaddam

5 August 2019

Abstract

Tuberculosis is a communicable disease which affects millions of people around the world. Although the case reports are declining, the eradication rate of this disease is far too slow. Natural products have played a key role in the treatment of the disease. However, tuberculosis is developing resistance to current first-line therapy. In this study, a prefractionated marine algal library was developed in order to identify and prioritise samples for isolation of their active metabolites which exhibit anti-tuberculosis activity. Based on the results of the library screening and chemical profiling, two seaweeds were selected for further investigation, *Laurencia glomerata* and *Plocamium cornutum*. The extraction and fractionation of *Laurencia glomerata* and *Plocamium cornutum* resulted in the isolation of three chamigrane seqsuiterpenes (prepacifenol epoxide, johnstonol and one newly proposed structure) and two monoterpenes (cartilagineal and 1,5,6-trichloro-2-(dichloromethyl)-6-methylocta-1,3,7-triene) respectively. The structures of these compounds were elucidated by 1 and 2D NMR data and were confirmed by literature comparisons. Although some of the initial library factions screened showed rather good activity against *Mycobacterium tuberculosis*, the selected seaweed fractions showed greater activity against *M. aurum*. The isolated monoterpenes showed moderate cytotoxicity against the cancer cell line MCF-12a and the sesquiterpenes however were more selective for MCF-7. The monoterpenes showed both activity and potential selectivity towards *Mycobacterium tuberculosis*.

Keywords: tuberculosis, marine natural product libraries, marine algae, *Laurencia glomerata*, *Plocamium cornutum*, chamigrane sesquiterpenes, monoterpenes, anti-mycobacterial activity.

Zahied and Zumayna Mukaddam – This thesis is dedicated to you

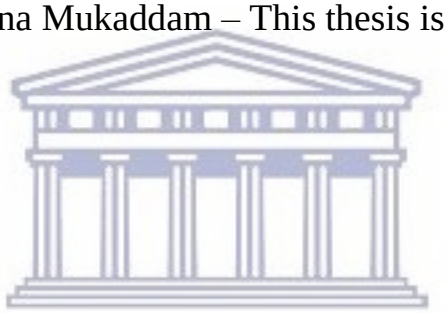

DECLARATION

"I declare that the *Discovery of anti-mycobacterial natural products from South African marine algae* is my own work, that it has not been submitted for any degree or examination in any other university, and that all the sources I have used or quoted have been indicated and acknowledged by complete references".

Full name: Zaahirah Mukaddam Date: 5 August 2019

Signed 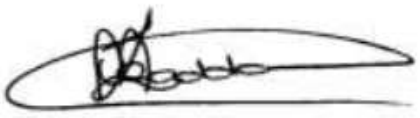

Acknowledgements

"First of all, I would like to say shukran (Thank you) to my creator for blessing me with the strength and courage to pursue my dreams of achieving my masters. It is by your will and decree that I have successfully completed this journey.

I would like to say shukran to my parents for supporting and encouraging me to complete my studies. Thank you for believing in me, when at times I did not believe in myself. To my dad, not many children can say that their father came back from the brink of death for them. I am lucky to have a real superhero in my life. To my mom, all I can say is I was blessed with an amazing, selfless and strong mother who; I aspire to be like one day in'sha Allah (God willing). It is with your sacrifice; I am afforded the opportunity to further my education. I just want to make you proud. I am deeply proud and grateful to have you both as my parents.

Thank you to Prof. Denzil Beukes for all your supervision, effort and guidance in assisting to achieve my masters. Your talent and knowledge in natural product chemistry is incredible.

To my co-supervisor, Dr. Marilize Le Roes-Hill, thank you for being there when I needed help, for providing intellectual input and playing a significant role in supervising me. Thank you for assisting me with the biological aspects of my research.

Many individuals have contributed to the completion of my masters and I would like to express my sincerest gratitude to the following:

- My family for always supporting and encouraging me.
- Prof John Bolton for collecting my marine algal specimens.
- Prof Edith Antunes for all her timeous assistance with NMR experiments and guidance.
- The National Research Foundation for the financial support of this master's project.
- Dr De Sousa for your assistance in preparing my samples for anti-mycobacterial assays.
- Dr Sibuyi for taking the time to conduct and evaluate my cytotoxicity studies.
- Prof. Digby Warner and team for conducting my anti-mycobacterial assays at UCT
- To the Marine BioDiscovery Research group for accepting me, assisting me and for being like a second family to me throughout my studies.
- To my dearest Imaad for always being by my side through all my trials. Your compassion, understanding and continuous motivation is gratefully appreciated. Thank you for having the confidence in my ability and for encouraging me. Lastly for affording me the much-needed break from campus and for gifting me with the greatest memories.
- To my best friends – Saajida and Shameena, your companionship from the very beginning of my B. Pharm career up to today is valued and appreciated. I could not have asked for better friends to see me through the most challenging years of my life.
- To Dr. Mubaiwa, your assistance, guidance, and wisdom has been an enormous help.
- The University of the Western Cape, School of Pharmacy post-graduate students and helpful staff for their unwavering assistance and support"

“I am thankful for my struggle because, without it, I wouldn't have stumbled upon my strength.” - Alexandra Elle

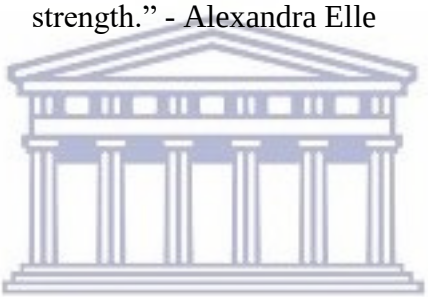

Table of Contents

List of Figures

List of Tables

Scheme List

List of Abbreviations

°C	Degrees Celsius
$CDCl_3$	Deuterated chloroform
^{13}C NMR	Carbon nuclear magnetic resonance
^{1}H NMR	Proton nuclear magnetic resonance
AM	Alveolar macrophage
COSY	Correlation spectroscopy
DEPT-135	Distortionless enhancement by polarization transfer-135
DCM	Dichloromethane
DMSO	Dimethyl sulfoxide
EtOAc	Ethyl acetate
GPP	Geranyl pyrophosphate
HIV	Human immunodeficiency virus
HMBC	Heteronuclear multiple bond correlation
HSQC	Heteronuclear single-quantum correlation
IR	Infrared radiation
J	Spin-spin coupling constant (Hz)
MCF-7	Michigan Cancer Foundation-7
MCF-12a	Michigan Cancer Foundation-12a
MDR	Multi Drug Resistant
MeOH	Methanol
MIC	Minimum inhibitory concentration
MS	Mass spectrometry
Mtb	*Mycobacterium tuberculosis*
MTT	3-(4,5-dimethylthiazol-2-yl)-2,5-diphenyltetrazolium bromide
NMR	Nuclear magnetic resonance
NOESY	Nuclear overhauser enhancement spectroscopy
NP	Natural product
OD	Optical density

PBS	Phosphate buffered solution
SA	South Africa
SDG	Sustainable Development Goals
TB	Tuberculosis
TLC	Thin-layer chromatography
UV	Ultraviolet
WHO	World Health Organisation
WST	Water-soluble tetrazolium salt
XDR	Extensively Drug-resistant
δ	Chemical shift (ppm)

Chapter 1
GENERAL INTRODUCTION

1.1. Background

Tuberculosis (TB) is a disease that has been plaguing early mankind for an estimated three million years. The genus, *Mycobacterium*, is hypothesized to have originated more than 150 million years ago [Daniel, 2006]. It was not until 1839 that J.L. Schönlein coined the term Tuberculosis. Forty-three years later (1882) that *Mycobacterium tuberculosis*, the tubercle bacillus initiating Tuberculosis, was isolated by the German Physician, Robert Koch. He was thus awarded a Nobel Prize in 1905 for his discovery [Sandhu, 2011]. Despite progressing 137 years since the discovery of *Mycobacterium tuberculosis* (Mtb), the disease is presently the leading cause of mortality by a single infective organism. Globally, Tuberculosis was the tenth leading cause of death in 2016 [WHO, Global tuberculosis report, 2018].

1.1.1. The burden of Tuberculosis

Tuberculosis has been an evolving communicable disease; becoming a global pandemic severely burdening especially middle to low-income countries. It is estimated that there are 1.7 billion people infected with latent TB. Approximately 5-10% of latently infected hosts will develop active TB in their lifetime. According to the Global Tuberculosis Report, 2018 released by the World Health organisation (WHO), TB is regarded as an eminent infectious disease due to its significantly high mortality rate. In the year 2017, there were an estimated 10 million incident cases (Figure 1.1) and 1.3 million TB-related deaths worldwide. The report identifies thirty high TB burden countries. Of those, 15 countries are from Africa. South Africa (SA) has the second-highest TB incidence rate of 567 per 100 000 population [WHO, Global tuberculosis report, 2018].

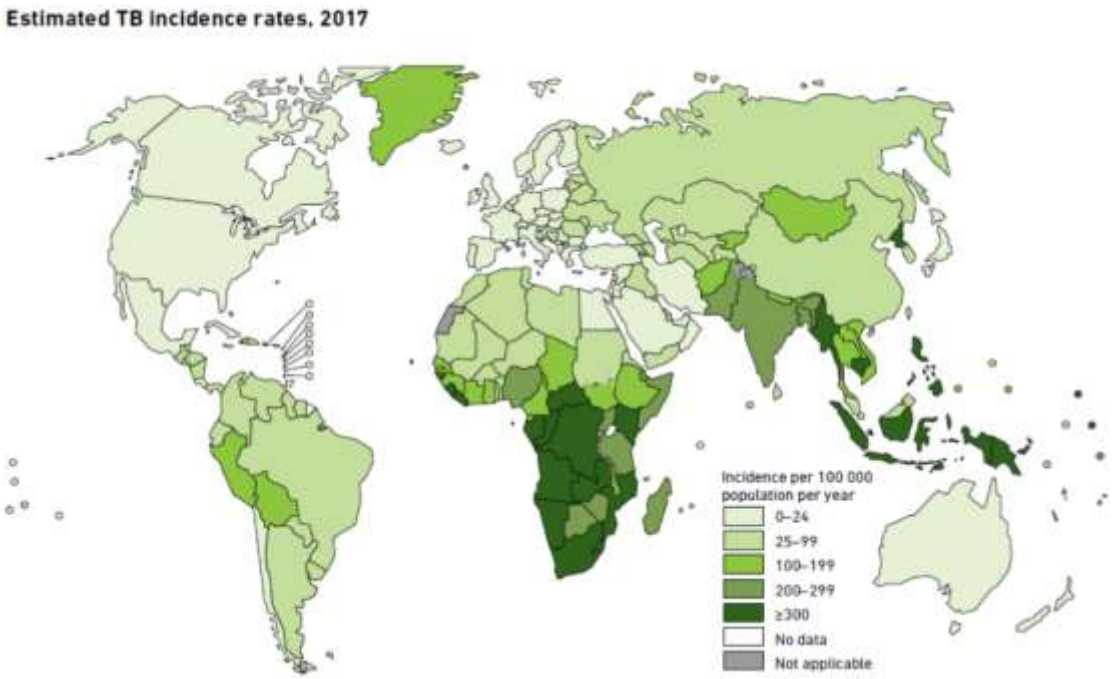

Figure 1.1: WHO World map showing the estimated TB incidence rates in 2017 [WHO, Global Tuberculosis Report, 2018].

Despite having high incident rates, SA has shown a downward trend in TB-related mortality (Figure 1.2). Over a four-year period, TB-related mortality decreased by 2.3% between 2013 and 2016 [Statistics South Africa, 2015-2017].

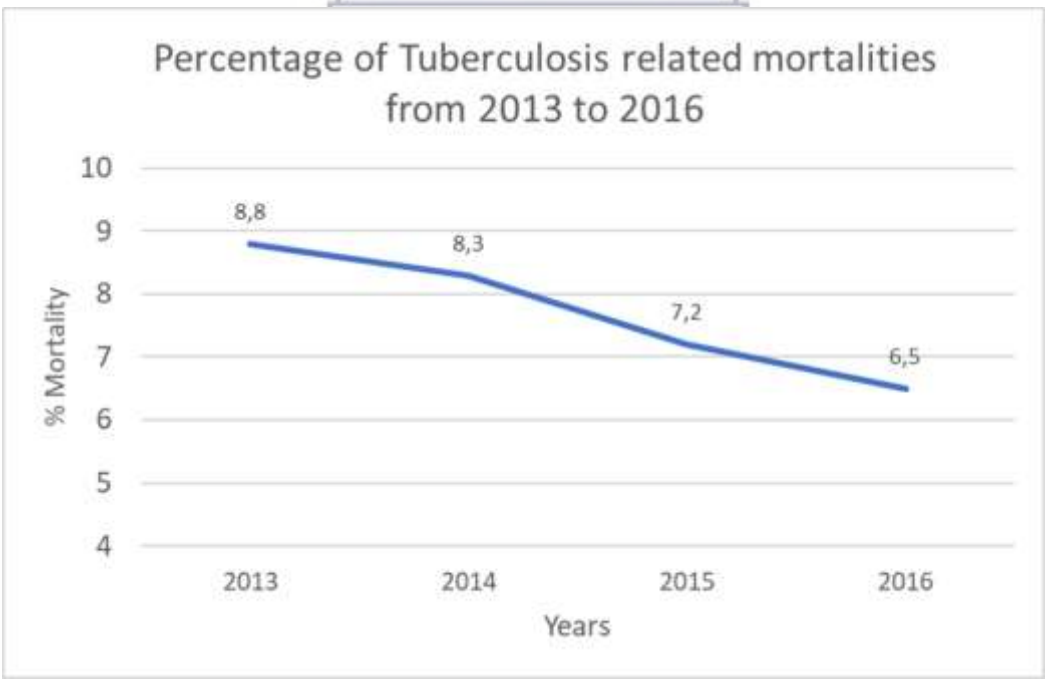

Figure 1.2: Graph showing the percentage decrease in Tuberculosis-related mortality in South Africa from 2013 to 2016.

In 2015, The End TB Strategy® was implemented by the WHO to be aligned with the United Nations Sustainable Development Goals (SDGs). The strategy aims to reduce TB mortality by 95% and targets a 90% reduction in incidence rates by the year 2035. In order to achieve these targets, the strategy focuses on integrated patient-centred care and prevention, bold policies and intensified research and innovation [WHO, End TB Strategy, 2015]. Based on SA's afore-mentioned 2.3% reduction in TB-related mortality, progress is too slow to meet the envisioned 2035 target.

1.1.2. *Mycobacterium tuberculosis*

Mycobacterium tuberculosis (Mtb) is a gram-positive, acid-fast bacillus with a unique cell wall. The mycobacterial-envelope consists of layers which significantly decreases the permeability of the cell walls. The layers are, namely, a plasma membrane surrounded by complex peptidoglycan/ arabinogalactan wall. Additionally, Mtb is protected by a lipid-rich coat (40% of the cell's dry mass). The large lipophilic layer results in tendencies of Mtb to retain acid-fast stains and to grow in clusters [Daffé, 2015]. The thick cell walls and low permeability is critical to the mycobacteria's survival, as it avoids dehydration, chemical harm and prevents permeation by small hydrophilic molecules [Barry, 2001]. Mtb is an aerobic bacillus with the ability to survive in hypoxic conditions. In low oxygen-containing environments, Mtb activates its non-replicating latent form by hindering its growth and decreasing its respiration rate [Starck *et al*., 2004].

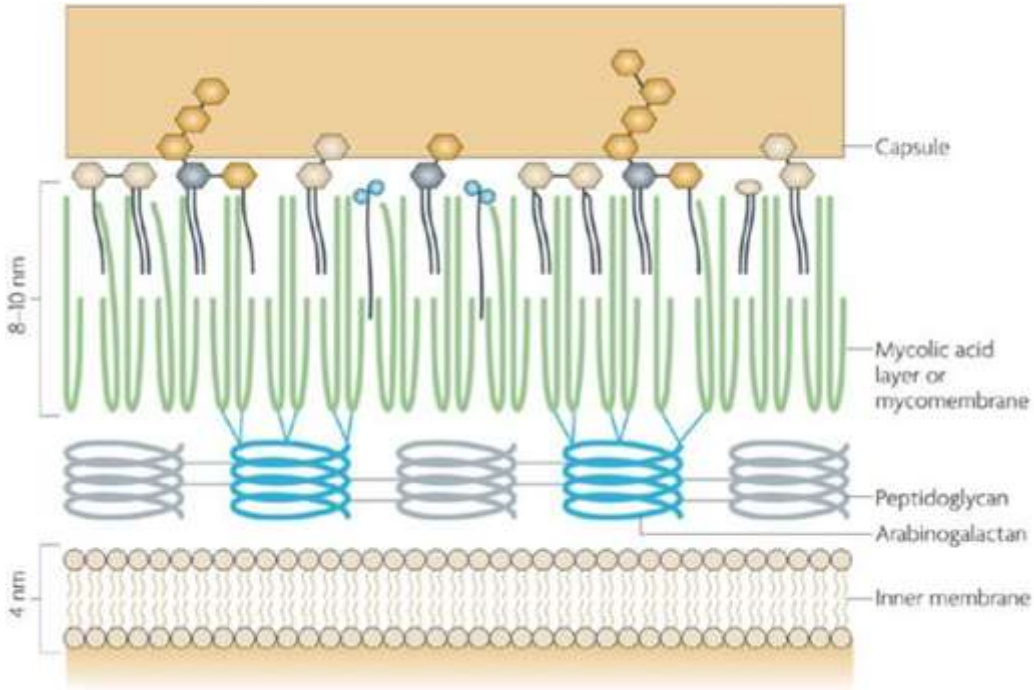

Figure 1.3: Cell wall composition of *Mycobacterium tuberculosis* [Abdallah *et al.* 2007].

1.1.3. The pathogenesis of Tuberculosis

In order for humans (or any host) to be infected by Tuberculosis (Figure 1.4), the Mtb bacilli are required to be released into the air and inhaled as droplets. Upon detection by the immune system, alveolar macrophages (AM) are recruited to the bacillus and subsequently engulf them. Once in the cytoplasm of the AM, Mtb is able to manipulate the macrophage preventing the usual apoptosis of the cell ensuring its survival and it begins the replication process [Cambier *et al.*, 2014]. The AM are necrotised and the process is repeated. Subsequently, this cycle induces an inflammatory response which in turn forms the granuloma. The granuloma encases the infected macrophages and creates a hypoxic and nutrition-deprived environment in which Mtb remains dormant until activation. A stronger immune system of a host maintains granuloma containment. If and when there is a decrease in host immunity due to old age, malnutrition or human immunodeficiency virus (HIV) co-infection, that ability to contain the granuloma is decreased. The granuloma undergoes necrosis which releases infectious tubercle bacilli into the lungs, leading the host to develop active TB [Chatterjee and Pramanik, 2015; Posser *et al.*, 2017].

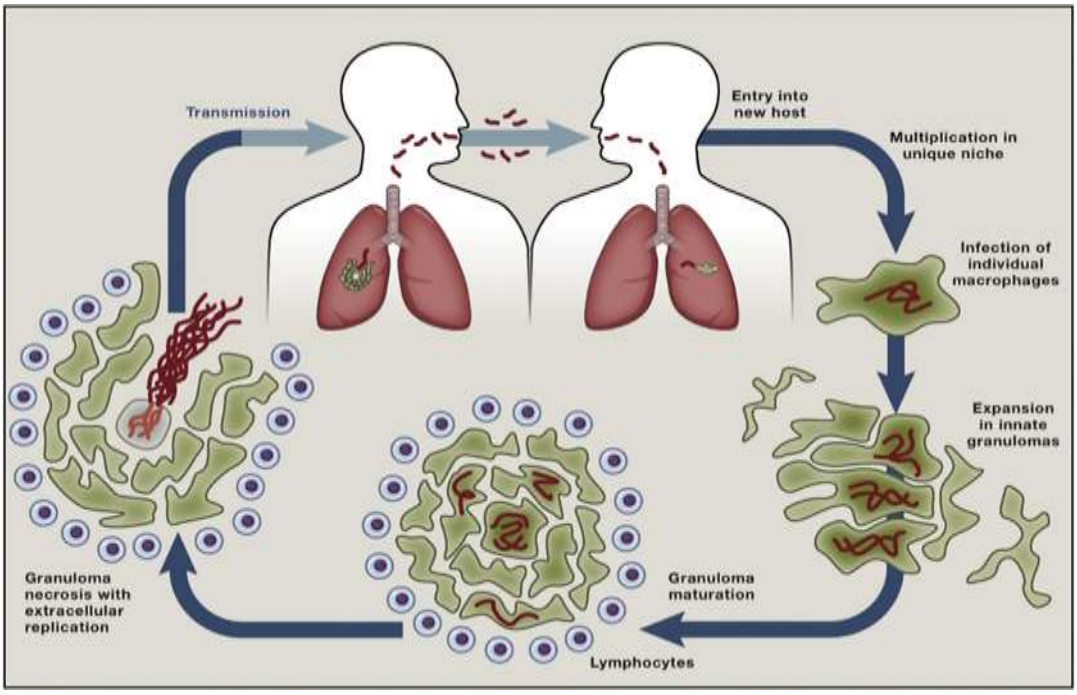

Figure 1.4: *Mycobacterium tuberculosis* infectious and pathogenic lifecycle [Cambier *et al*., 2014].

1.1.4. Presentation of Tuberculosis and treatment.

Tuberculosis is diagnosed based on a screening and sputum test. Patients with active TB usually present with fevers, night sweats, a loss of appetite, coughing, weight loss, fatigue and a productive cough yielding bloody sputum. Once the GeneXpert® results test positive for *M. tuberculosis* and have identified whether the strain is rifampicin-resistant or susceptible, the patient will be started on the appropriate treatment regimen. Should the patient have drug-susceptible tuberculosis, they will begin first-line treatment.

1.1.4.1. First-line TB treatment

The first-line treatment of TB comprises rifampicin, isoniazid, pyrazinamide and ethambutol in a fixed-dose combination tablet. It is an intensive two-month regimen. Following the initial phase (commonly referred to as the intensive phase), the patient will immediately begin the continuation phase. The treatment is for a further four months, comprising of rifampicin and isoniazid [National Tuberculosis Management Guidelines 2014]. Adherence to the six months' treatment regimen under the directly observed therapy patient management programme (DOTS®), results in a >95% cure rate of drug-susceptible TB [Zumla *et al.*, 2013].

1.1.5. Multidrug resistant and Extensively drug resistant Tuberculosis

Subsequent to treatment defaults and non-adherence due to pill burden, the length of treatment time and adverse effects, the TB bacillus developed several mechanisms for drug resistance. The mechanisms include a lipid-rich hydrophobic cell wall, efflux pumps and the ability to change the structure of drug target sites [Padhi *et al*., 2016; Tang *et al*., 2016].

Multidrug resistant (MDR) TB is defined as strains that are resistant to rifampicin and isoniazid, and extensively drug resistant (XDR) TB has additional resistance to one of the fluoroquinolones and aminoglycosides, which are classes of drugs used in the second-line MDR treatment [Maitre *et al.*, 2017]. The WHO estimates that there are 490 000 new MDR-TB incident cases for 2016, which is a cause for concern because the number of patients successfully treated for MDR-TB is 54% and for XDR-TB it is 30%. It is estimated that South Africa has an incident rate of 14 per thousand MDR-TB cases in 2017 [WHO, Global Tuberculosis Report, 2017].

1.1.5.1. Second-line treatment

As mentioned previously, upon detection of resistance to rifampicin or isoniazid or both by a sputum test, patients should be started on second-line TB treatment. The intensive phase is a six-month course consisting of kanamycin, moxifloxacin, ethionamide, terizidone and pyrazinamide. Subsequent to the completion of the intensive phase, patients' progress to the continuation phase for a further 18 months of treatment [DOH South Africa: Policy Framework, 2015].

1.1.6. Tuberculosis and HIV co-morbidities

In many developing countries, TB and HIV-co-morbidity is the leading cause of mortality. The most severely affected are countries in Sub-Saharan Africa, which has an estimated 25.5 million people living with HIV. In 2015, South African records indicated that there was an average of 7 million people infected and living with HIV [Phetlhu *et al.*, 2018]. The most significantly recognised risk factor for TB is the HIV-1 infection [Berkowitz *et al.*, 2018]. The HIV infection increases the risk of latent TB activation and is prevalent when the CD_4 count is below 500 cells/mm^3 [Waruk *et al.*, 2015].

1.2. Natural Products

Natural chemical entities produced by a living organism; such as microorganisms, plants and animals which have the potential to contribute to the drug discovery process are known as natural products [Mathur and Hoskins, 2017]. Natural products are produced through primary or secondary metabolism, primary metabolites being essential for an organism's survival and secondary metabolites, a defence due to environmental pressures [Naman *et al.,* 2017]. Natural products continue to be a source of inspiration for unique and diverse bioactive compounds with 25-50% of marketed drugs originating or derived from them [Anulika *et al.,* 2016].

The Marine environment is able to produce novel lead compounds that can be utilized against pathogenic microbes that are developing resistance. Novel antibiotics are required to counter the spread of resistant pathogens [Habbu *et al*., 2016]. Many marine organisms live a sedentary life and are constantly exposed to a large number of potentially pathogenic microbes that can cause disease and even death. [Kubanek *et al*., 2003]. In a highly competitive habitat, defence strategies are developed by marine organisms in order to survive [Cardozoa *et al*., 2007]. Through evolution, they synthesize toxic protective compounds in order to deter predators, paralyze their prey and fend off any competitors. One defence strategy involves releasing natural products into the water. It is imperative for these compounds to be highly potent to have an effect because once released it is diluted in the surrounding environment. With such a vast amount of uncharted territory, huge marine diversity and interesting biological activity, it is quite possible to discover novel chemical entities. These marine bioactive natural products could have great specificity and efficiency in treating human diseases [Haefner, 2003].

Seaweeds produce an abundantly diverse range of secondary metabolites, categorised by a wide spectrum of biological activities. Once they are isolated, it may be used in the production of pharmaceuticals. The biological activity of the compounds isolated from seaweeds has been documented as anti-mycobacterial, antimicrobial, antiviral, antifungal, antimalarial and antioxidant agents [Daletos *et al*., 2016; Parsaeimehr *et al.*, 2016].

1.3. Research rationale

There is a pressing need to identify and develop new tuberculosis treatment that is inexpensive, effective, and cost-efficient. These drugs need to facilitate a reduced duration of therapy and side effect profiles, subsequently enhancing compliance with the treatment. They should also have a novel mechanism of action to circumvent drug resistance [Tuyiringire *et al.,* 2018].

1.3.1. Hypothesis

Seaweeds are postulated to produce antimicrobial metabolites which may also have anti-mycobacterial activity.

1.3.2. Research Aim

To discover anti-mycobacterial compounds from marine algae.

Research Objectives

- Preparation of a fractionated marine algal compound library.
- Screening for anti-mycobacterial activity and chemical profiling.
- Large scale bio-assay guided isolation of active fractions.
- Structural elucidation and characterization of isolated natural products via spectroscopic methods.
- Confirmation of activity of the pure isolated natural product.

1.4. Thesis outline

This thesis is divided into six chapters. Chapter one provides a general introduction and context of the study. Chapter two briefly reviews natural products as a source of anti-mycobacterial compounds. Chapter three will encompass the development of a marine algal library and bioactivity studies. Chapter four will focus on large scale bioassay guided isolation of compounds from two identified seaweeds, *Laurencia glomerata* and *Plocamium cornutum*. The fifth chapter will cover more biological studies and confirmation of activity of the isolated natural compounds (including cytotoxicity assays). The last chapter will comprise of the conclusion to the thesis, limitations of the study and future work.

References

Abdallah, A. M., Gey van Pittius, N. C., DiGiuseppe Champion, P. A., Cox, J., Vandenbroucke-Grauls, C. M. J. E., Appelmelk, B. J., Bitter, W., Type VII secretions – mycobacteria show the way. *Nature Review Microbiology* **2007**, 5, 883-891.

Anulika, N. P., Ignatius, E. O., Raymond, E. S., Osasere, O. I., Abiola, A. H., The chemistry of natural product: Plant secondary metabolites. *International Journal of Technology Enhancements and Emerging Engineering Research* **2016**, 4(8), 1-8

Barry, E. C. Interpreting cell wall 'virulence factors' of Mycobacterium tuberculosis. *Trends in Microbiology* **2001**, 9(5), 237-241.

Berkowitz. N., Okorie. A., Goliath. R., Levitt. N., Wilkinson. R.J., Oni. T. The prevalence and determinants of active tuberculosis among diabetes patients in Cape Town, South Africa, a high HIV/TB burden setting. *Diabetes Research and Clinical Practice* **2018**, 138, 16-25.

Cambier, C. J., Falkow, S., Ramakrishna, L., Host evasion and exploitation schemes of *Mycobacterium tuberculosis*. *Cell* **2014**, 159(7), 1497-1509.

Cardozo, K. H.M., Guaratini, T., Barros, M. P., Falcão, V. R., Tonon, A. P., Lopes, N. P. S., Campos, M. A., Torres, A. O., Souza, P., Colepicolo, E. P., Metabolites from algae with economical impact, *Comparative Biochemistry and Physiology Part: C Toxicology & Pharmacology* **2007**, 164(1-2), 60-78.

Chatterjee. D., Pramanik. A. K. Tuberculosis in the African continent: A comprehensive review. *Pathophysiology* **2015**, 22(1), 73-83.

Daffé, M. The cell envelope of tubercle bacilli. *Tuberculosis* **2015**, 95 supplement 1, S155-S158.

Daletos, G., Ancheeva, E., Chaidir, C., Kalscheuer, R., Proksch, P., Antimycobacterial metabolites from marine invertebrates, *Arch. Pharm. Chem. Life Sci* **2016**, 349, 763-773.

Daniel, M. T. The history of Tuberculosis. *Respiratory Medicine* **2006**, 100(11), 1862-1870.

Department of Health: Republic of South Africa. National Tuberculosis Management Guidelines 2014. [Accessed August 18, 2018] from: http://www.tbonline.info/media/uploads/documents/ntcp_adult_tb-guidelines-27.5.2014.pdf

Department of Health Republic of South Africa, Introduction of new drugs and drug regimens for the management of drug-resistant tuberculosis in South Africa: Policy Framework Version 1.1, 2015 [Accessed on December 3, 2018] from: http://www.nicd.ac.za/assets/files/Acrobat%20Document.pdf

Habbu, P., Warad, V., Shastri, R., Madagundi, S., Kulkarni, V. H., Antimicrobial metabolites from marine organisms, *Chinese Journal of Natural Medicine* **2016**, 14(2), 101-116.

Haefner, B., Drugs from the deep: marine natural products as drug candidates. *Drug Discovery Today* **2003**, 8(12), 536-544.

Kubanek, J., Jensen, P. R., Keifer, P. A., Sullards, M. C., Collins, D. O., Fenical, W., Seaweed resistance to microbial attack: A targeted chemical defence against marine fungi, *Proceedings of the National Academy of Sciences of the United States of America* **2003**, 100(12), 6916-6921.

Maitre. T., Aubry. A., Jarlier. V., Robert. J., Veziris. N. Bernard, C., Sougakoff, W., Brossier, F., Cambau, E., Mougari, F., Raskine, L. Multidrug and extensively drug-resistant tuberculosis. *Médecine et Maladies Infectieuses* **2017**, 47(1), 3-10.

Mathur, S., Hoskins, C., Drug development: Lessons from nature. *Biomedical Reports* **2017**, 6(6), 612-614.

Naman, C. B., Leber, C. A., Gerwick, W. H., Modern natural products drug discovery and its relevance to biodiversity conservation. *Microbial Resources* **2017**, 103-120.

Padhi, A., Naik, S. K., Sengupta, S., Ganguli, G., Sonawane, A., Expression of Mycobacterium tuberculosis NLP/p60 family protein Rv0024 induced biofilm formation and resistance against cell wall acting anti-tuberculosis drugs in Mycobacterium smegmatis, *Microbes and Infection* **2016**, 18(4), 224-236.

Parsaeimehr, A., Lutzu, G. A., Chapter 18 – Algae as a Novel Source of Antimicrobial Compounds: Current and Future Perspective, *Antibiotic Resistance* **2016**, 377-396.

Phetlhu. D. R., Bimerew. M., Marie-Modeste. R.R., Naidoo. M., Igumbor. J. Nurses knowledge of tuberculosis, HIV and integrated HIV/TB care policies in rural Western Cape, South Africa. *Journal of the Association of Nurses in AIDS Care* **2018**.

Prosser, G., Brandenberg, J., Reiling, N., Barry III, C. E., Wilkinson, R J., Wilkinson, K. A., The bacillary and macrophage response to hypoxia in tuberculosis and the consequences for T cell antigen recognition. *Microbes and Infection* **2017**, 19(3), 177-192.

Sandhu, G. K. Tuberculosis: Current Situation, Challenges and Overview of its Control Programs in India. *Journal of Global Infectious Diseases* **2011**, 3(2), 143-150.

Starck, J., Källenius, G., Marklund, B., Andersson. D. I., Åkerlund. T. Comparative Proteome analysis of Mycobacterium tuberculosis grown under aerobic and anaerobic conditions. *Microbiology* **2004**, 150, 3821-3829.

Statistics South Africa. Statistical Release P0309.3: Mortality and Causes of Death in South Africa, 2015. Findings from Death Notification. Pretoria: Statistics South Africa; 2017. [Accessed 22 June 2018] from: http://www.statssa.gov.za

Statistics South Africa. Statistical Release P0309.3: Mortality and Causes of Death in South Africa, 2016. Findings from Death Notification. Pretoria: Statistics South Africa; 2018. [Accessed 22 June 2018] from http://www.statssa.gov.za

Tang, J., Wing-Cheong, Y., Zhwei, C., Mycobacterium tuberculosis infection and vaccine develop. *Tuberculosis* **2016**, 98, 30-41.

Tuyiringire, N., Tusubira, D., Munyampundu, J. P., Tolo, C. U., Muvunyi, C. M., Ogwang, P. E., Application of metabolomics to drug discovery and understanding the mechanisms of action of medicinal plants with anti-tuberculosis activity. *Clinical and Translational Medicine* **2018**, 7(1), 29.

Waruk, J. L., Machuki, Z., Mesa, C., Juno, J. A., Anzala, O., Sharma, M., Ball. T.B., Oyugi. J., Kiazyk, S. Cytokine and chemokine expression profiles in response to Mycobacterium tuberculosis stimulation are altered in HIV-infected compared to HIV-uninfected subjects with active tuberculosis. *Tuberculosis* **2015**, 95(5), 555-561.

World Health Organisation. Factsheet: Post-2015 Global TB Strategy and Targets. [Accessed June 25, 2018] from: http://www.who.int/tb/post2015_TBstrategy.pdf?ua=1

World Health Organisation. Multidrug-resistant tuberculosis. MDR-TB Factsheet 2017 update. [Accessed August 25, 2018] from: http://www.who.int/tb/challenges/mdr/MDR-RR_TB_factsheet_2017.pdf?ua=1

World Health Organisation. Global Tuberculosis Report 2018. [Accessed November 27, 2018] from: http://apps.who.int/iris/bitstream/handle/10665/274453/9789241565646-eng.pdf?ua=1

Zumla, A., Nahid, P., Cole, S. T., Advances in the development of new tuberculosis drugs and treatment regimens. *Nature Reviews Drug Discovery* **2013**, 12(5), 388-404.

Chapter 2

LITERATURE REVIEW: NATURAL PRODUCTS AS A SOURCE OF ANTI-TUBERCULOSIS DRUGS

2.1. Introduction

Over the past century, natural products have formed the foundation of drug discovery of antibacterial therapies. Antibacterial natural products occupy a unique chemical space, compared to synthetic compounds, which offers multiple opportunities for drug development. In the Dictionary of Natural Products, 40% of all chemical scaffolds occupy a unique chemical space which is not represented by synthetic compounds [Montaser and Luesch, 2011]. New antimicrobials and resistance-modifying agents can be found in natural sources such as terrestrial plants, lichen, fungi, endophytes, aquatic plants, coral, seaweed and other marine organisms [Molone, 2016]. Some of the antibiotics that are currently available have been derived from microbial sources and are often derived through semisynthetic derivatization [Clardy *et al*., 2006]. The number of stated new marine compounds are growing each year, with over 1000 novel compounds with diverse biological activities and potencies reported [Montaser and Luesch, 2011]. Marine natural products could be the key to discovering new treatments for tuberculosis.

Natural products have been a part of the treatment of tuberculosis for several decades since the discovery of streptomycin. Streptomycin (**2.1**) is a natural product isolated from *Streptomyces griseus.* It showed potent bactericidal activity and was recommended as a treatment for tuberculosis in 1944. However, **2.1** was later removed as a first-line treatment due to the *M. tuberculosis* (Mtb) bacillus developing resistance, which informed on how great a challenge TB treatment is for public health institutes in affected countries [Sotgiu *et al.*, 2015].

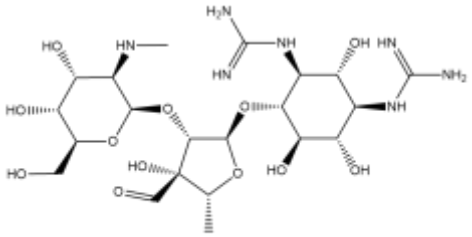

Streptomycin
2,1

In 1963, rifampicin (**2.2**) was discovered when it was isolated from the bacterium *Amycolatopsis mediterranei*, identified from a soil sample. It was later found to produce a macrolide polyketide natural product called rifamycin [Gutierrez-Lugo and Bewley, 2008]. Subsequent to isolation, it was identified that there were five complex forms of rifamycin (rifamycin A, B, C, D and E). Despite being less active than other conformations, rifamycin B (**2.3**) was selected based on the following criteria: it was simple to isolate, proved to be more stable and exhibited good solubility at physiological pH [Lancini and Cavalleri, 1997]. Compound **2.3** provided the lead molecule and the pharmacophore from which **2.2** was derived (Gutierrez-Lugo and Bewley, 2008). Rifapentine (**2.4**) is a semisynthetic derivative of Rifamycin [Mishra *et al.,* 2017]. This derivative **2.4** also exhibits a broad spectrum of antimicrobial activity and has been found to be more active than **2.2** [Jarvis and Lamb, 1998].

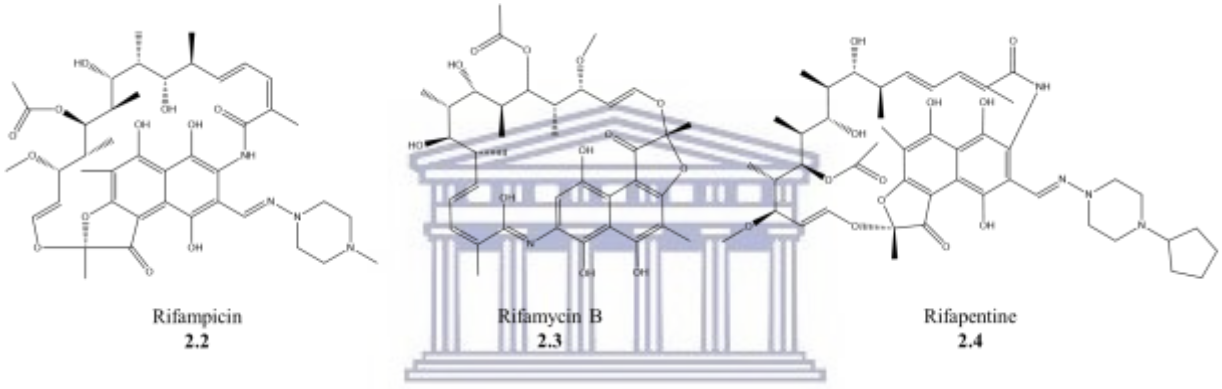

Rifampicin
2.2

Rifamycin B
2.3

Rifapentine
2.4

Vitamin B3, also known as niacin, is found in foods such as bran, seeds, grains, yeast, legumes, poultry, red meat and fish [Peechakara and Gupta, 2018]. Niacin has an important precursor called nicotinamide which through serendipitous observation in animal models revealed it had anti-mycobacterial properties. Analogues of nicotinamide were subsequently synthesized which lead to the discovery and identification of pyrazinamide (**2.5**) [Wabale *et al.,* 2017]. Nicotinamide is a privileged structure for isoniazid (**2.6**) and its activity was discovered in the 1950s together with ethionamide (**2.7**) [Raghunandanan *et al.* 2018] (Figure 2.1). These compounds are therefore synthetically derived analogues with natural origins.

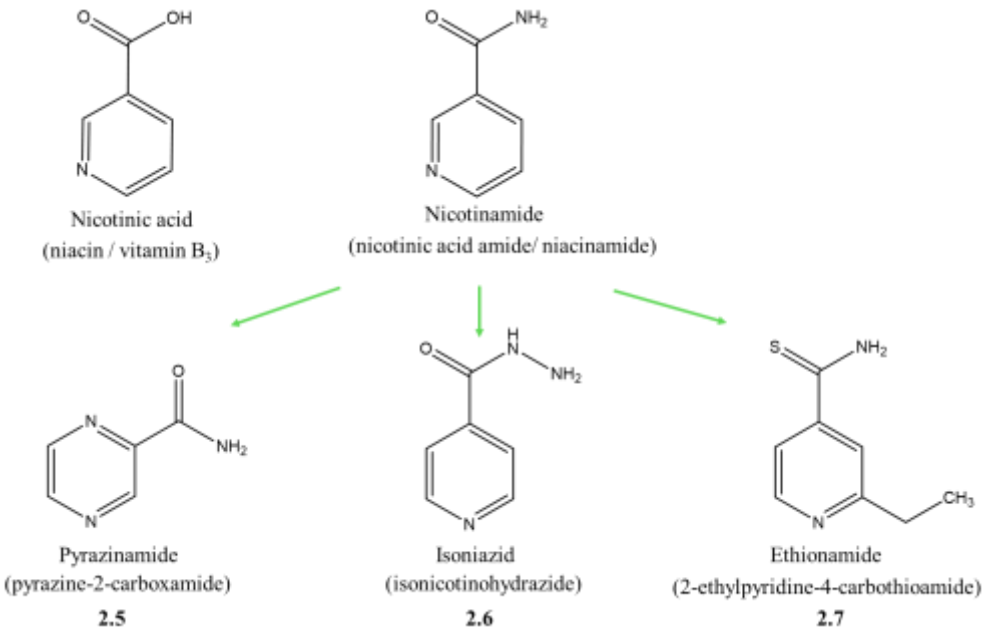

Figure 2.1: Structure of nicotinamide and related anti-tuberculosis compounds

Kanamycin (**2.8**) is an aminoglycoside second-line injectable agent used in the treatment of MDR tuberculosis [Momin *et al.*, 2017]. Discovered in a Japanese soil sample, Kanamycin A was first isolated in 1957 from *Streptomyces kanamyceticus*. An additional second-line tuberculosis drug is amikacin (**2.9**), which is a semisynthetic derivative of Kanamycin A [Pawlowski *et al.*, 2016].

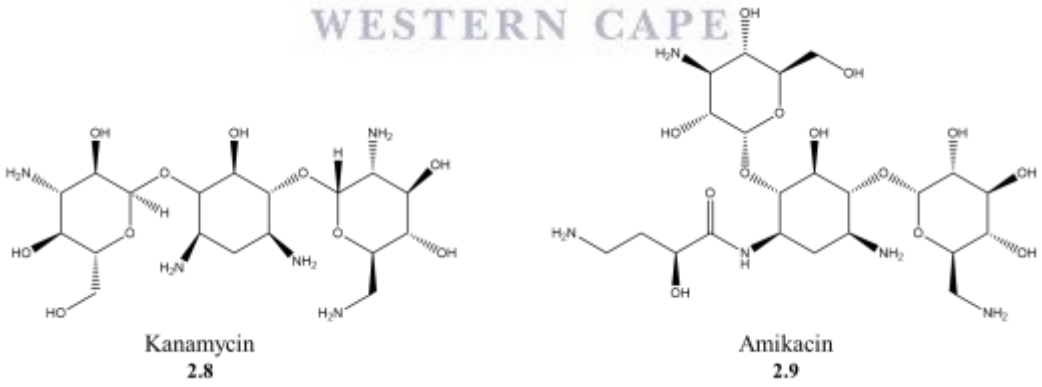

Capreomycin (**2.10**) is a by-product of the Streptomycete species, *Streptomyces capreolus*. It was discovered and isolated in 1960 using a fermentation method [Manning *et al.*, 2014]. Compound **2.10** is an important second-line MDR drug because it has anti-tuberculosis activity against MDR and latent tuberculosis [Fu *et al.*, 2009].

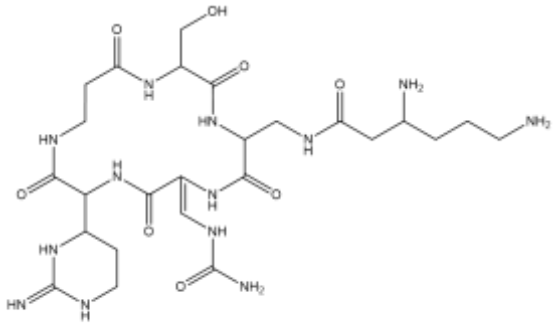

Capreomycin
2.10

D-cycloserine (**2.11**) was discovered in 1954 and it is used in the second-line treatment of MDR tuberculosis. It was isolated from the microorganisms S. *lavendulae* and *S. garyphalus*. It is a structural analogue of D-alanine and it functions by interfering with the formation of the cell wall of the *mycobacterium* [Batson *et al.*, 2017].

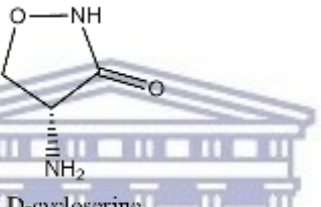

D-cycloserine
2.11

There are a number of other medications that can be used in the treatment of tuberculosis which is denoted as semi-synthetic drugs. The following semi-synthetic drugs are derived from natural sources: Meropenem (**2.12**), clavulanate/clavulanic acid (**2.13**), amoxicillin (**2.14**), imipenem (**2.15**), cilistatin (**2.16**) and clarithromycin (**2.17**) [Mishra *et al.*, 2017].

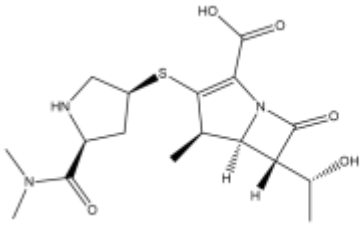

Meropenem
2.12

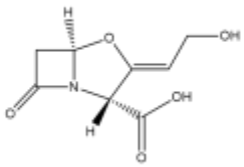

Clavulanic acid
2.13

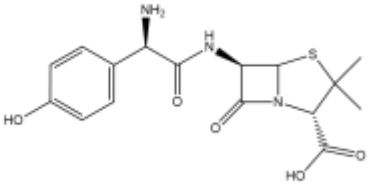

Amoxicillin
2.14

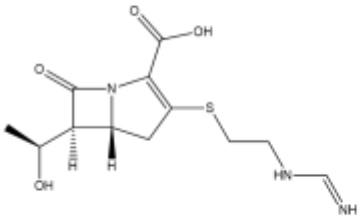

Imipenem
2.15

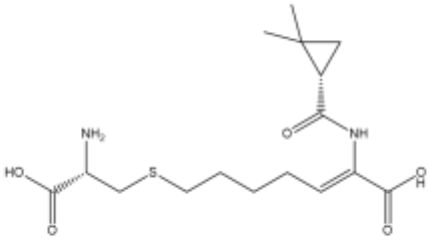

Cilistatin
2.16

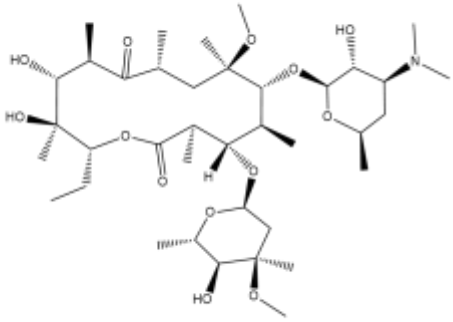

Clarithromycin
2.17

Natural products have been a useful source for identifying compounds that can be used in the treatment of TB, but in order to discover new compounds, exploring uncharted territories is crucial.

2.2. Naturally derived anti-mycobacterial metabolites

2.2.1. Actinobacteria

There are approximately 23 000 antibiotics that have been discovered and isolated from microorganisms. It is estimated that in the region of 10 000 were isolated from actinomycetes [Elsayed *et al.*, 2017]. Actinomycetes play a pivotal role in treating infectious diseases as it has provided a wide range of antibiotic classes. Approximately 45% of known antibiotics on the market were isolated from them and their valuable contribution is attributed to their ability to produce resourceful secondary metabolites.

Chrysomycin A (**2.18**) was isolated from a *Streptomyces* sp. which is an actinomycete. Compound **2.18** produced a MIC of 3.125 µg/ml against *Mycobacterium tuberculosis* H37Rv which is superior to two first-line anti-tuberculosis drugs, pyrazinamide 16 µg/ml and ethambutol 4 µg/ml [Muralikrishnan *et al.*, 2017].

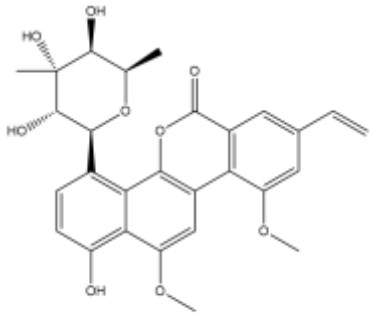

Chrysomycin A
2.18

Thiolactomycin (**2.19**) was initially isolated from a soil-derived *Norcadia* sp. It is a thiolactone antibiotic which has an effective *in vivo* activity against a number of pathogenic bacteria. A MIC evaluation was conducted against Mtb and *M. smegmatis* and was found to produce inhibitory effects at 25 and 75 µg/ml, respectively. The MIC values were then compared to the published values of isoniazid which produced a result of 0.2 and 5 µg/ml and ethionamide which had a 10 µg/ml effect for both mycobacterial species. The MIC results that were published for **2.19** against the selected mycobacteria could be lower as a racemic mixture was used to conduct the tests [Slayden *et al.*, 1996].

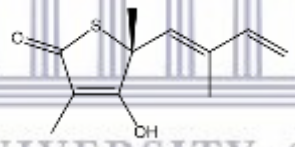

Thiolactomycin
2.19

2.2.2. Plants

More than half the world's population is still reliant on plant medicinal products as a form of primary healthcare. There are many plant species that are yet to be investigated for their medicinal properties and they could provide novel biologically active compounds [Bueno *et al.*, 2011].

Oleanolic acid/ oleanic acid (**2.20**) and Ursolic acid (**2.21**) were isolated from *Lantana hispida* and *Chamaedora tepejilote* respectively, which are plants that are commonly found around Mexico. These plants are used as traditional medicine for the treatment of various respiratory conditions. The hexane extracted fractions which contained Ursolic acid and oleanolic acid were responsible for the anti-mycobacterial activity observed. Ursolic acid and oleanolic acid exhibited MICs of 25 µg/ml and 50 µg/ml respectively against *M. tuberculosis* H37Rv strain.

These compounds were tested against three mono-resistant strains of tuberculosis and the compounds **2.20** and **2.21** both resulted in MIC of 25 µg/ml [Jiménez-Arellanes *et al.*, 2013].

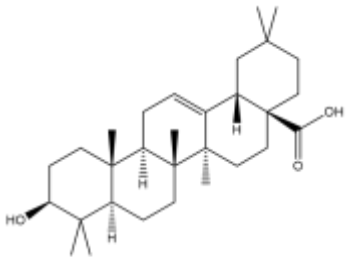

Oleanic acid
2.20

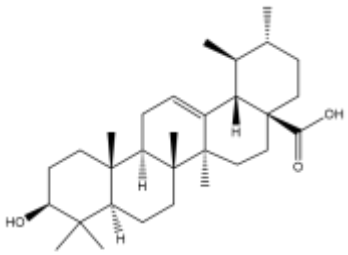

Ursolic acid
2.21

Calanolide A (**2.22)** was isolated from *Calophyllum lanigerum*. At a concentration of 12.5 µg/ml, it exhibited more than 96% inhibition of Mtb H37Rv and demonstrated a MIC of 3.13 µg/ml. Compound **2.22** has a unique structure when compared to the current anti-tuberculosis treatment aids which may aid in a novel mechanism of action and potentially be effective against drug-resistant strains. Compound **2.22** was tested against rifampicin, isoniazid, ethambutol and streptomycin mono-resistant strains and demonstrated a consistent inhibitory activity [Xu *et al.*, 2004].

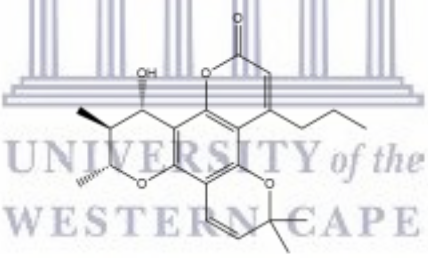

Calanolide A
2.22

During the study of *Strobilanthes cusia*, a Chinese/Taiwanese medicinal plant, it was found to produce an indolo- quinazolinone alkaloid called tryptanthrin (**2.23**). Biological testing of the compound revealed that **2.23** had a similar potency to that of well-known anti-tuberculosis drugs streptomycin, ethambutol and isoniazid. The BACTEC results indicated inhibitory activity of 1 µg/ml against Mtb H37Rv, 4 µg/ml against *M. avium* and 6 µg/ml *M. smegmatis*. Compound **2.23** was also active against MDR-TB and it was proposed to have a different mechanism of action to the existing anti-TB drugs [Mitscher and Baker, 1998].

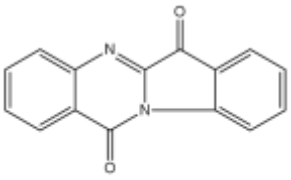

Tryptanthrin
2.23

In the extraction of *Lessonia nigrescens*, a compound saringosterol (**2.24**) was isolated as a racemic mixture of 24R and 24S epimers. The individual epimers were separated via HPLC and were tested in an anti-tubercular assay. The 24S isomer had a MIC of 1 µg/ml against Mtb H37Rv and the 24R isomer was eight times more active with a MIC of 0.125 mg/ml [Kim and Van Ta, 2011].

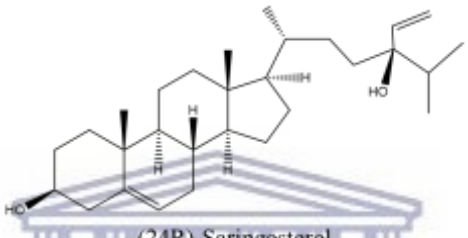

(24R)-Saringosterol
2.24

2.2.3. Marine

The foundation of new/novel natural product drug discovery should be based on the exploration of unique environments [Pye *et al.*, 2017]. Earth has a total oceanic surface area of more than 70% and it has vast ecosystems with great biological diversity. The first census of marine life explored the waters nearer to the coastline and collated data that estimated the number of marine species at 230,000 to 250,000 and microbial organisms at tens to hundreds of millions [Montaser and Luesch, 2011]. The ocean, with its exceptional marine biodiversity and vast chemo diversity, provides an excellent opportunity for the discovery of anti-tuberculosis drug therapies [Wang *et al.*, 2018].

Over the last two decades, the marine environment and marine natural products have gained immense research interest. It is reported that over 25 000 new compounds have been isolated and characterized by marine organisms and most exhibit a wide range of biological activities. Discovering new marine compounds is playing an important role in the discovery of leads, which can be further developed, in order to formulate new drugs for the treatment of human diseases [Pereira *et al*., 2016].

2.2.3.1. Invertebrates (sponge, coral, *etc*.)

Approximately 75% of the afore-mentioned 25 000 compounds, were isolated from marine invertebrates such as sponges, molluscs and echinoderms [Pereira *et al*., 2016]. In a series of review articles, 'Marine Natural Products' published by the Royal Society of Chemistry, a handful of popular invertebrates discussed have been studied for their chemistry. Over the years, sponges, cnidarians, bryozoans, molluscs, ascidians, echinoderms and mangroves have been reviewed [Blunt *et al*., 2018]. Some of the natural products obtained from invertebrates were reported to have anti-mycobacterial activities (Table 2.1) [Donia and Hamann, 2003].

Table 2.1: Summary of interesting marine natural products that have been shown to exhibit activity against Mycobacterium organisms

Natural product	Structures	Source	Phylum	Chemical class	Target strain	Activity MIC
(+)-8-hydroxymanzamine A	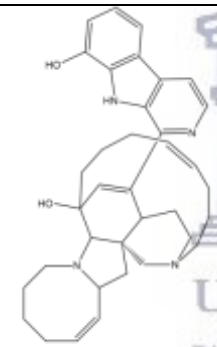 (+)-8-hydroxymanzamine A **2.25**	*Pachypellina* sp	Porifera	Alkaloid	*M. tb* H37Rv35	0.91 µg/mL
Ircinol A	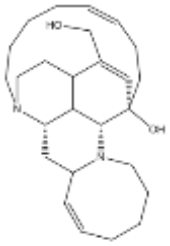 Ircinol A **2.26**	*Indo-Pacific sponge*	Porifera	Alkaloid	*M. tb*	1.93 µg/mL.
Axisonitrile-3 **2.27**	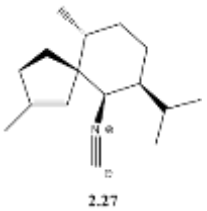 **2.27**	*Acanthella klethra*	Porifera	cyanosesquiterpene	*M. tb.*	2.00 µg/mL

Pseudopteroxazole **2.28**	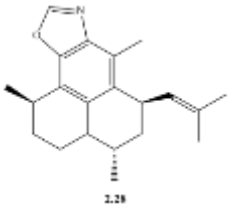	*Pseudopterogorgia elisabethae*	Cnidaria	benzoxazole diterpene alkaloid	*M. tb H37Rv*	12.5 µg/mL
Erogorgiaene **2.29**	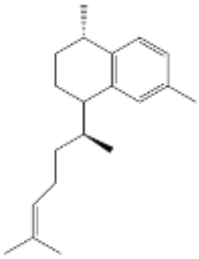	*Pseudopterogorgia elisabethae*	Cnideria	Biflorane	*M. tb H37Rv*	12.5 µg/mL
Litosterol **2.30**	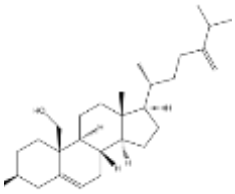	*Litophyton viridis*	Cnideria	hydroxysteroid	*M. tb*	3.13 µg/mL
Puupehenone **2.31**	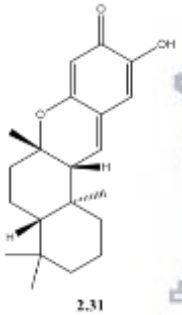	*Verongida* and *Dictyoceratida* and *Hyrtios sp.*	Porifera	Shikimate-sesquiterpene	*M. tb H37Rv*	12.5 µg/mL

2.2.3.2. Seaweeds

For decades, marine algae have been a wealthy source of unusual and new molecules with a wide variety of biological activities. With the drug discovery pipeline for new therapeutic agents being slowed, there is a vast need for new medicinal agents which has intensified the research into the discovery, isolation and structural elucidation of marine algal compounds. Macroalgae, more commonly known as seaweeds, occur all over the world and occupy all kinds of marine habitats. They are the most widely distributed marine plant species. Each algal species has unique distinguishing features and are identified based on their colour, size and shape [Mandrekar *et al*., 2018].

The secondary metabolites in seaweeds are developed by exposure to harsh environmental conditions such as low oxygen concentrations, low water temperatures, inadequate light, high salinity, and high pressure as well as being exposed to a large number of harmful microbes.

In potentially pathogenic environments, with each 1ml of seawater containing about 10^3 fungal cells, 10^6 bacteria and 10^7 viruses including pathogens, seaweeds hardly become infected [Kubanek *et al.*, 2003; Li and Lou, 2018]. The novel compounds that are produced via various metabolic pathways have a significant level of chemical-structural diversity and are required to counter the spread of resistant pathogens [Cardozo *et al.*, 2007; Habbu *et al.*, 2016].

Marine natural products, particularly Macroalgae (seaweeds), has received increased attention as previously mentioned in the search for effective and new compounds. The efforts in studying seaweeds are reflected in the numerous investigations and studies into their bioactivities and the compounds responsible for it. Some examples of the bioactivities exhibited by seaweeds are antiangiogenic activity, inhibition of cell proliferation, anti-tumour, anticancer [Gutiérrez-Rodríguez *et al.*, 2018], antihypertensive, antidiabetic, antioxidant [Admassu *et al*., 2018], anti-obesity, anti-hyperlipidemic [Sun *et al.*, 2018], antimicrobial [Chakraborty *et al.*, 2018], anti-inflammatory, antinociceptive [Abdelhamid *et al*., 2018], antifungal [Mickymaray and Alturaiki, 2018], antiviral [Sun *et al*., 2018] and anti-tuberculosis [Akbari *et al*., 2018] activities and more.

It is estimated that the total number of seaweed species in the oceans and seas is between 8000 - 10500 and the South African coastline has more than 800 species of marine algae. The South African coastline, therefore, encompasses almost one-tenth of the estimated global biodiversity and serves as a rich source of compound discovery [Lategan *et al.*, 2009].

In several studies, crude extracts obtained from seaweeds were tested for anti-mycobacterial activity.

In a study conducted by Swamy in 2011, several marine algal extracts isolated from *Plocamium telfairiae, Sargassum ringgoldianum, Gelidium amansii, Lessonia nigrescens Bory, P. Hamatum* and *Plocamium sp*. exhibited anti-mycobacterial activity [Swamy, 2011]. In 2002, Orhan *et al*., showed that extracts of *Maugeotia sp.* and *Cladophora fracta* exhibited anti-mycobacterial activity at 200 µg/ml and 50 µg/ml respectively [Orhan *et al*., 2002].

In a literature review conducted by Chaudhari and Badole, it stated that the anti-mycobacterial and antimicrobial activity of several Japanese seaweeds were established for *M. avium*, *M. phlei* and *M. tuberculosis*. The inhibition of *M. tuberculosis* growth by a cold-water extract of *Sargassum thunbergii* was established. They also noted a study of 17 brown seaweeds belonging to the genera *Cystoseira, Sargassum* which showed activity against *M. smegmatis*.

Volatile acids such as chonalgin and sarganin from *Sargassum natans* were also shown to exhibit inhibitory activity against the same test strain. Research also reported that a crude extract of a Thai *Dictyota* sp. also displayed anti-mycobacterial activity. Furthermore, an additional study conducted in the British Irish waters reported that *Bifurcaria bifurcate* had a significant anti-mycobacterial MIC of 64 µg/ml [Chaudhari and Badole, 2014].

In another study conducted by Allmendinger *et al*., the brownish red seaweed *Calliblepharis jubata* was found to have a weak anti-mycobacterial activity with a MIC value of 256 µg/ml against *M. tuberculosis* [Allmendinger *et al*., 2010].

Lastly in a study conducted by Süzgeç-Selçuk *et al*., investigations into 11 seaweeds were published and the results showed that three of the seaweeds exhibited weak anti-mycobacterial activity. The three seaweeds were *Ceramium rubrum* with a MIC of 125 µg/ml, *Cystoseira barbata* MIC 256 µg/ml and *Gracilaria verrucosa* MIC 256 µg/ml against *M. tuberculosis* strain H37Rv [Süzgeç-Selçuk *et al*., 2011].

Although there are reports that state some seaweeds have anti-mycobacterial activity, there are very few articles that explore seaweeds and their isolated compounds for anti-tuberculosis leads. The general trend of the research published is merely to establish the anti-mycobacterial activity of the isolated crude extract and its fractions, there is a small number that publishes the compounds responsible for the observed activity.

Saringosterol (**2.24**) has been isolated from *Sargassum ringgoldianum* as well and was reported to have anti-tuberculosis activity. Compound **2.24** had a MIC of 0.25 mg/ml, which when compared with rifampicin in the same assay produced an equivalent MIC of 0.25 mg/ml against the test strain *M. tuberculosis* H37Rv. In addition to having good inhibitory activity, compound **2.24** in low concentrations showed no toxicity towards monkey kidney epithelial (Vero) cells [Kim and Van Ta, 2011].

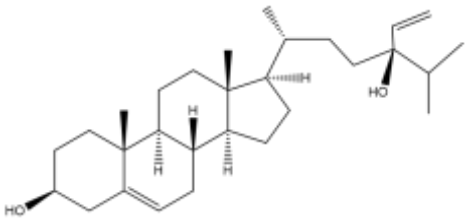

(24R)-Saringosterol

2.24

The bis-indole alkaloid, Caulerpin (**2.32**), isolated from *C. serrulata* and *Caulerpa racemose* is a significant member of the alkaloid family of compounds. Compound **2.32**'s activity varies

from antibacterial, anti-tumour and of particular interest, it has anti-mycobacterial activity against the *M. tuberculosis* strain H37Rv. Compound **2.32**, exhibited an anti-mycobacterial potency of IC_{50} = 0.24 µM, which is more than two times the potency of rifampicin [Cavalcante-Silva *et al.*, 2014]. There were no MIC values determined for this compound.

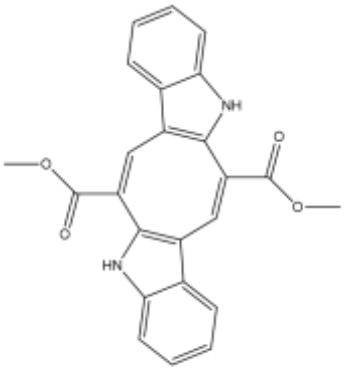

Caulerpin
2.32

There were four fatty acids which were extracted and isolated from the red marine alga *Polysiphonia virgate*, lauric acid (**2.33**), linoleic acid (**2.34**), myristic acid (**2.35**) and oleic acid (**2.36**) which were reported to have anti-tuberculosis activity. The anti-tuberculosis activity was observed for *M. tuberculosis* as well as multidrug resistant tuberculosis. Compounds **2.33**, **2.34**, **2.35**, were tested at 50 µg/ml and **2.36** was tested at 25 µg/ml respectively. Lauric acid and linoleic acid had a 100% inhibition at 50 µg/ml against *M. tuberculosis*, myristic acid exhibited 98% and oleic acid 100% activity at 25 µg/ml against *M. tuberculosis* respectively. The results for the MDR-tb were as follows **2.33** showed 75% inhibition, **2.34** 86%, **2.35** 88%, while **2.36** had no inhibitory effect [Saravanakumar *et al*., 2008].

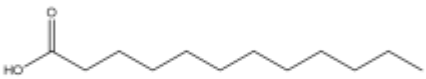

Lauric acid
2.33

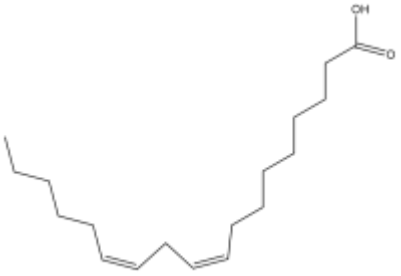

Linoleic acid
2.34

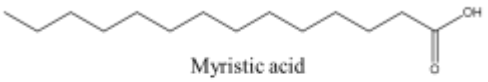

Myristic acid
2.35

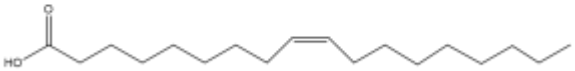

Oleic acid
2.36

Elatol (**2.37**) and deschloroelatol (**2.38**) were isolated from *Laurencia rigidia.* They were tested against *M. tuberculosis* and *M. avium* and **2.37** and **2.38** exhibited a MIC of 32 µg/ml against *M. tuberculosis*. The MIC test results for *M. avium* indicated that **2.37** was non-toxic and **2.38** had inhibitory activity at 8 µg/ml [König *et al.*, 2000].

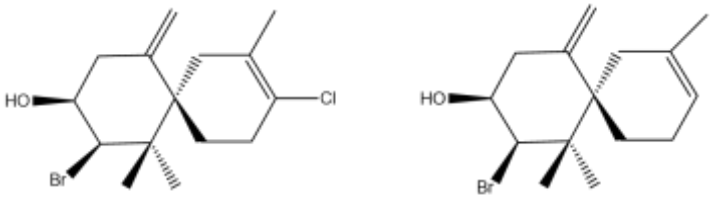

Elatol
2.37

Deschloroelatol
2.38

Debromolaurinterol (**2.39**), a compound isolated from *Laurencia flexilis* showed a MIC inhibitory activity at 64 µg/ml against *M. tuberculosis* and >128 µg/ml for *M. avium*. Aplysistatin (**2.40**) was also isolated from the same species, exhibited poor MIC activity of 128 µg/ml against *M. tuberculosis* and >128 µg/ml for *M. avium* [König *et al.*, 2000].

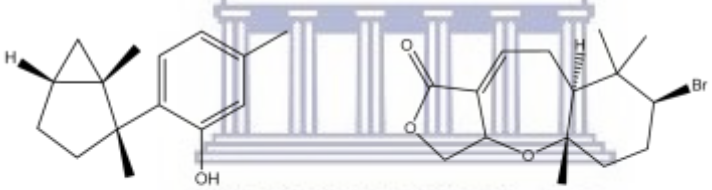

Debromolaurinterol
2.39

Aplysistatin
2.40

Allolaurinterol (**2.41**), was isolated from *Laurencia obtuse.* The compound produced a MIC activity of 16 µg/ml against *M. tuberculosis* and was found to be non-toxic against *M. avium* [König *et al.,* 2000].

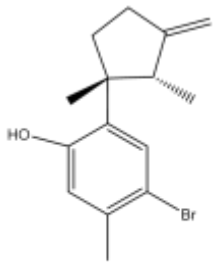

Allolaurinterol
2.41

This review highlights not only the over-all potential of natural products but specifically marine natural products as potential anti-tuberculosis agents. An important area of research is to expand on marine algal natural products and identify compounds which exhibit a desirable potency and display selective anti-tuberculosis activity.

References

Abdelhamid, A., Jouini, M., Amor, H. B. H., Mzoughi, Z., Dridi, M., Said, R. B., Bouraoui, A., Phytochemical Analysis and Evaluation of the Antioxidant, Anti-inflammatory, and Antinociceptive Potential of Phlorotannin-Rich Fractions from Three Mediterranean Brown Seaweeds. *Marine Biotechnology* **2018**, 20(1), 60-74.

Admassu, H., Gasmalla, M. A. A., Yang, R., Zhao, W., Bioactive peptides derived from seaweed protein and their health benefits: Antihypertensive, antioxidant, and antidiabetic properties. *Journal of Food Science* **2018**, 83(1), 6-16.

Akbari, V., Zafari, S., Yegdaneh, A., Anti-tuberculosis and cytotoxic evaluation of the seaweed Sargassum boveanum. *Research in Pharmaceutical Sciences* **2018**, 13(1), 30.

Allmendinger, A., Spavieri, J., Kaiser, M., Casey, R., Hingley-Wilson, S., Lalvani, A., Guiry, M., Blunden, G., Tasdemir, D., Antiprotozoal, antimycobacterial and cytotoxic potential of twenty-three British and Irish red algae. *Phytotherapy Research* **2010**, 24(7), 1099-110.

Batson, S., de Chiara, C., Majce, V., Lloyd, A. J., Gobec, S., Rea, D., Fülöp, V., Thoroughgood, C.W., Simmons, K.J., Dowson, C.G., Fishwick, C.W., Inhibition of D-Ala: D-Ala ligase through a phosphorylated form of the antibiotic D-cycloserine. *Nature Communications* **2017**, 8(1), 1939.

Blunt, J. W., Carroll, A. R., Copp, B. R., Davis, R. A., Keyzers, R. A. Prinsep, M. R., Marine natural products. *Natural Product Reports* **2018,** 35(1), 8-53.

Bueno, J., Coy, E. D., Stashenko, E., Antimycobacterial natural products-an opportunity for the Colombian biodiversity. *Revista Española de Quimioterapia* **2011**, 24(4).

Cardozo, K. H., Guaratini, T., Barros, M. P., Falcão, V. R., Tonon, A. P., Lopes, N. P., Campos, S., Torres, M. A., Souza, A. O., Colepicolo, P., Pinto, E., Metabolites from algae with economical impact. *Comparative Biochemistry and Physiology Part C: Toxicology & Pharmacology* **2007**, 146(1-2), 60-78.

Cavalcante-Silva, L., Falcão, M., Vieira, A., Viana, M., de Araújo-Júnior, J., Sousa, J., Silva, T., Barbosa-Filho, J., Noël, F., de Miranda, G., Santos, B., Alexandre-Moreira, M., Assessment of Mechanisms Involved in Antinociception Produced by the Alkaloid Caulerpine, *Molecules* **2014**, 19, 14699-14709.

Chakraborty, K., Thilakan, B., Kizhakkekalam, V. K., Antibacterial aryl-crowned polyketide from bacillus subtilis associated with seaweed anthophycus longifolius. *Journal of Applied Microbiology* **2018**, 124(1), 108-125.

Chaudhari, S. M., Badole, S. L., Polyphenols and Tuberculosis. In *Polyphenols in Human Health and Disease* **2014**, 723-730. Academic Press

Clardy, J., Fischbach, M. A., Walsh, C. T., New antibiotics from bacterial natural products. *Nature Biotechnology* **2006**, 24, 1541-1550.

Donia, M., Hamann, M. T., Marine natural products and their potential applications as anti-infective agents. *The Lancet Infectious Diseases* **2003**, 3(6), 338-348.

Elsayed, Y., Refaat, J., Abdelmohsen, U. R., Fouad, M. A., The Genus Rhodococcus as a source of novel bioactive substances: A review. *Journal of Pharmacognosy and Phytochemistry* **2017**, 6(3), 83-92.

Fu, L. M., Tai, S. C., The differential gene expression pattern of mycobacterium tuberculosis in response to Capreomycin and PA-824 versus first-line TB drugs reveals stress-and PE/PPE-related drug targets. *International Journal of Microbiology* **2009**. 1-10.

Gutierrez-Lugo, M. T., Bewley C. A., Natural Products, Small Molecules, and Genetics in Tuberculosis Drug Development, *Journal of Medicinal Chemistry* **2008**, 51(9), 2606–2612.

Habbu, P., Warad, V., Shastri, R., Madagundi, S., Kulkarni, V. H., Antimicrobial metabolites from marine microorganisms. *Chinese Journal of Natural Medicines* **2016**, 14(2), 101-116.

Lancini, G., Cavalleri, B., Rifamycins, *Biotechnology of Antibiotics* **1997**, Second Edition, CRC Press, 521–549.

Gutiérrez-Rodríguez, A. G., Juarez-Portilla, C., Olivares-Banuelos, T., Zepeda, R. C., Anticancer activity of seaweeds. *Drug Discovery Today* **2018**, 23(2), 434-447.

Jarvis, B., Lamb, H. M., Rifapentine, *Drugs* **1998**, 56(4), 607-616.

Jiménez-Arellanes, A., Luna-Herrera, J., Cornejo-Garrido, J., López-García, S., Castro-Mussot, M. E., Meckes-Fischer, M., Mata-Espinosa, D., Marquina, B., Torres, J., Hernández-Pando, R., Ursolic and oleanolic acids as antimicrobial and immunomodulatory compounds for tuberculosis treatment. *BMC Complementary and Alternative Medicine* **2013**, 13(1), 258.

John, T., Thomas, T., Abel, B., Wood, B. R., Chalmers, D. K., Martin, L. L., How kanamycin A interacts with bacterial and mammalian mimetic membranes. *Biochimica et Biophysica Acta (BBA)-Biomembranes* **2017**, 1859(11), 2242-2252.

Kim, S. K., Van Ta, Q., Potential beneficial effects of marine algal sterols on human health. *In Advances in Food and Nutrition Research* **2011**, 64, 191-198. Academic Press.

König, G. M., Wright, A. D., Franzblau, S.G., Assessment of antimycobacterial activity of a series of mainly marine derived natural products. *Planta Medica* **2000**, 66(4), 337-342.

Kubanek, J., Jensen, P. R., Keifer, P. A., Sullards, M. C., Collins, D. O., Fenical, W., Seaweed resistance to microbial attack: a targeted chemical defense against marine fungi. *Proceedings of the National Academy of Sciences* **2003**, 100(12), 6916-6921.

Li, G., Lou, H. X., Strategies to diversify natural products for drug discovery. *Medicinal Research Reviews* **2018**, 38(4), 1255-1294.

Mandrekar, V. K., Gawas, U. B., Majik, M. S., Brominated Molecules from Marine Algae and Their Pharmacological Importance. *Studies in Natural Products Chemistry* **2018**, chapter 13, 461–490.

Manning, T., Mikula, R., Lee, H., Calvin, A., Darrah, J., Wylie, G., Phillips, D., Bythell, B. J., The copper (II) ion as a carrier for the antibiotic capreomycin against Mycobacterium tuberculosis. *Bioorganic & Medicinal Chemistry Letters* **2014**, 24(3), 976-982.

Mickymaray, S., Alturaiki, W., Antifungal Efficacy of Marine Macroalgae against Fungal Isolates from Bronchial Asthmatic Cases. *Molecules* **2018**, 23(11), 3032.

Mishra, S. K., Tripathi, G., Kishore, N., Singh, R.K., Singh, A., Tiwari, V. K., Drug development against tuberculosis: Impact of alkaloids. *European Journal of Medicinal Chemistry* **2017**, 137, 504-544.

Mitscher, L. A., Baker, W. R., A search for novel chemotherapy against tuberculosis amongst natural products. *Pure and Applied Chemistry* **1998**, 70(2), 365–371.

Molone, M. G., Natural Products as a Source for Novel Antibiotics, *Trends in Pharmacological Science* **2016**, 37(8), 689-701.

Montaser, R., Luesch H., Marine natural products: a new wave of drugs? *Future Medicinal Chemistry* **2011**, 3(12), 1475–1489.

Momin, M. A., Sinha, S., Tucker, I. G., Doyle, C., Das, S. C., Dry powder formulation of kanamycin with enhanced aerosolization efficiency for drug-resistant tuberculosis. *International Journal of Pharmaceutics* **2017**, 528(1-2), 107-117.

Muralikrishnan, B., Dan, V. M., Vinodh, J. S., Jamsheena, V., Ramachandran, R., Thomas, S., Dastager, S. G., Kumar, K. S., Lankalapalli, R. S., Kumar, R. A., Anti-microbial activity of chrysomycin A produced by Streptomyces sp. against Mycobacterium tuberculosis. *RSC Advances* **2017**, 7(58), 36335-36339.

Orhan, I., Sener, B., Atici, T., Palittapongarnpim, P., In vitro antimycobacterial potential of some fresh-water macroalgae and aqueous plants. *Pharmaceutical Biology* **2002**, 40(8), 568-569.

Pawlowski, A. C., Johnson, J. W., Wright, G. D., Evolving medicinal chemistry strategies in antibiotic discovery. *Current Opinion in Biotechnology* **2016**, 42, 108-117.

Peechakara, B.V., Gupta, M., Vitamin B3. In *StatPearls* **2018** [Internet]. StatPearls Publishing. https://www-ncbi-nlm-nih_gov.ezproxy.uwc.ac.za/books/NBK526107/ [accessed on the 25th November 2018].

Pereira, R., Andrade, P., Valentão, P., Chemical diversity and biological properties of secondary metabolites from sea hares of Aplysia genus. *Marine Drugs* **2016**, 14(2), 39.

Pye, C. R., Bertin, M. J., Lokey, R. S., Gerwick, W. H., Linington, R. G., Retrospective analysis of natural products provides insights for future discovery trends. *Proceedings of the National Academy of Sciences* **2017**, 114(22), 5601-5606.

Raghunandanan, S., Jose, L., Kumar, R.A., Dormant Mycobacterium tuberculosis converts isoniazid to the active drug in a Wayne's model of dormancy. *The Journal of Antibiotics* **2018**, 71(11), 939.

Saravanakumar, D. E. M., Folb, P. I., Campbell, B.W., Smith, P., Antimycobacterial Activity of the Red Alga *Polysiphonia virgata*. *Pharmaceutical Biology* **2008**, 46(4), 254-260.

Slayden, R. A., Lee, R. E., Armour, J. W., Cooper, A. M., Orme, I. M., Brennan, P. J., Besra, G.S., Antimycobacterial action of thiolactomycin: an inhibitor of fatty acid and mycolic acid synthesis. *Antimicrobial Agents and Chemotherapy* **1996**, 40(12), 2813-2819.

Sotgiu, G., Centis, R., D'ambrosio, L., Migliori, G. B., Tuberculosis treatment and drug regimens. *Cold Spring Harbor Perspectives in Medicine* **2015**, p.a 017822.

Sun, Y., Chen, X., Song, L., Liu, S., Yu, H., Wang, X., Qin, Y., Li, P., Antiviral Activity against Avian Leucosis Virus Subgroup J of Degraded Polysaccharides from Ulva pertusa. *BioMed Research International*, **2018**.

Sun, Z., Dai, Z., Zhang, W., Fan, S., Liu, H., Liu, R., Zhao, T., Antiobesity, Antidiabetic, Antioxidative, and Antihyperlipidemic Activities of Bioactive Seaweed Substances. *In Bioactive Seaweeds for Food Applications* **2018**, 239-253. Academic Press.

Süzgeç-Selçuk, S., Meriçli, A. H., Güven, K. C., Kaiser, M., Casey, R., Hingley-Wilson, S., Lalvani, A., Tasdemir, D., Evaluation of Turkish seaweeds for antiprotozoal, antimycobacterial and cytotoxic activities. *Phytotherapy Research* **2011**, 25(5), 778-783

Swamy, M. A., Marine algal sources for treating bacterial diseases. In *Advances in food and Nutrition Research* **2011**, 64, 71-84. Academic Press.

Wabale, V. R., Joshi, A. A., Muthaiah, M., Chowdhary, A. S., Wayne's Assay: A Screening Method for Indirect Detection of Pyrazinamide Resistance in Mycobacterium Tuberculosis Clinical Isolates. *Journal of Bacteriology and Mycology Open Access* **2017**, 5(1), 00123.

Wang, L., Wang, J., Liu, J., Liu, Y., Anti-tubercular Marine Natural Products. *Current Medicinal Chemistry* **2018**, 25(20), 2304-2328.

Xu, Z. Q., Barrow, W. W., Suling, W. J., Westbrook, L., Barrow, E., Lin, Y. M., Flavin, M.T., Anti-HIV natural product (+)-calanolide A is active against both drug-susceptible and drug-resistant strains of Mycobacterium tuberculosis. *Bioorganic & Medicinal Chemistry* **2004**, 12(5), 1199-1207.

Chapter 3
DEVELOPMENT OF A FRACTIONATED LIBRARY OF MARINE ALGAL EXTRACTS

3.1. Introduction

Tuberculosis is a global burden and there is a desperate need for improved tuberculosis treatment. The ideal therapy would have a shortened treatment duration, reduced frequency of drug administration and a regimen that facilitates compliance with a reduced side effect profile [O'Brien and Nunn, 2000]. In order to discover the ideal treatment, scientists are exploring combination therapies to improve the regimen cure rate and changing known drugs chemical structures to create molecules that bind to new drug targets [Gammon, 2014]. But to make an impact in TB treatment, it is crucial to develop and discover novel TB drugs with new mechanisms of action [Ginsberg and Spigelman, 2007].

In the early eras, nature used to be the sole source of pharmaceutical therapeutics and over the past century formed the foundation of the drug discovery process [Montaser and Luesch, 2011]. Living organisms in nature produce secondary metabolites and will continue to be used as a source of potential drugs for many years to come (Figure 3.1) [David *et al.*, 2015].

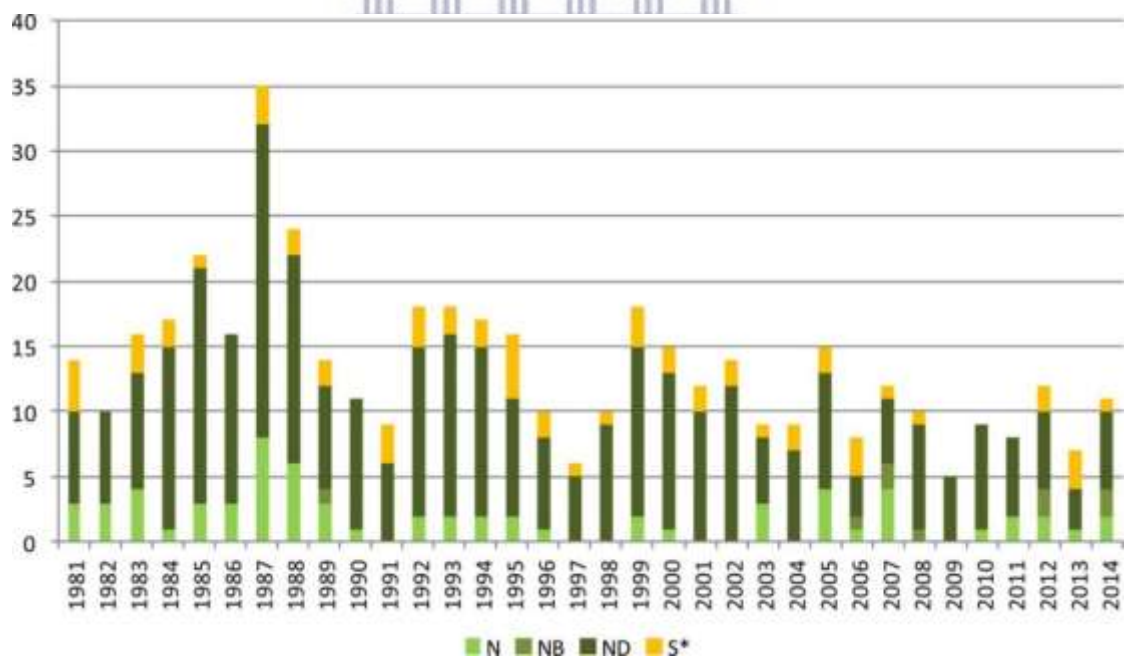

Figure 3.1: The percentage of natural product-based drugs on the market and their derivatives that were isolated and discovered between 1981-2014 [Newman and Cragg, 2016]. Where N = the unaltered natural product, NB = a botanical drug, ND = a natural product derivative, S* = Synthetic drug

3.1.1. Seaweeds as a source of antimicrobial natural products

Seaweeds are classified as marine algae and are categorized according to chemical composition and pigment [MacArtain *et al.,* 2007]. Seaweed compounds exhibit a wide range of biological activities and may be used as leads in the development of pharmaceuticals [Daletos *et al.,* 2016; Khalid *et al*., 2018; Parsaeimehr *et al.,* 2016; Ventura *et al.,* 2015]. Since being isolated, there are a number of marine natural products for sale by commercial providers as research biochemicals. Figure 3.2 highlights the organism collection source of these biochemicals [Gerwick and Moore, 2012].

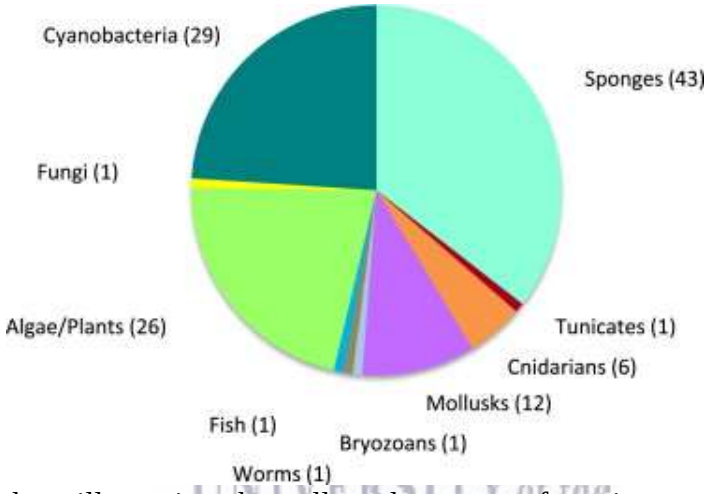

Figure 3.2: Pie chart illustrating the collected sources of marine natural products used as research biochemicals [Gerwick and Moore, 2012].

3.1.2. Lead discovery from natural products

Lead discovery from natural sources is no easy task to achieve because the process is time-consuming, labour intensive, requires specialized equipment and adequate funding. Figure 3.3 indicates the initial steps in identifying lead compounds in natural product drug discovery process. The road to natural product lead discovery is riddled with challenges. Firstly, crude extracts are mixtures of many compounds, has a thick consistency and tend to aggregate and may contain fluorescent quenching or fluorescent compounds, which causes difficulties with isolation, purification and makes them unsuitable for high-throughput screening (HTS) as well as various screening techniques. Secondly, sample quantity harvested at collection sites was limited hence bulk extraction up-scaling was quite small. Thirdly, the purified lead compounds that were isolated, were in very small quantities. Subsequently limiting the number of various

biological activity assays, and chemical analysis become tedious as the recovery of the sample is critical. Fourthly, the activity of minor compounds may be masked by the major compounds and when isolated, the compounds may be highly toxic yielding desirable or undesirable results. Lastly, there is a high probability that the compounds isolated are known compounds [Bernardini *et al.*, 2018; David *et al.*, 2015].

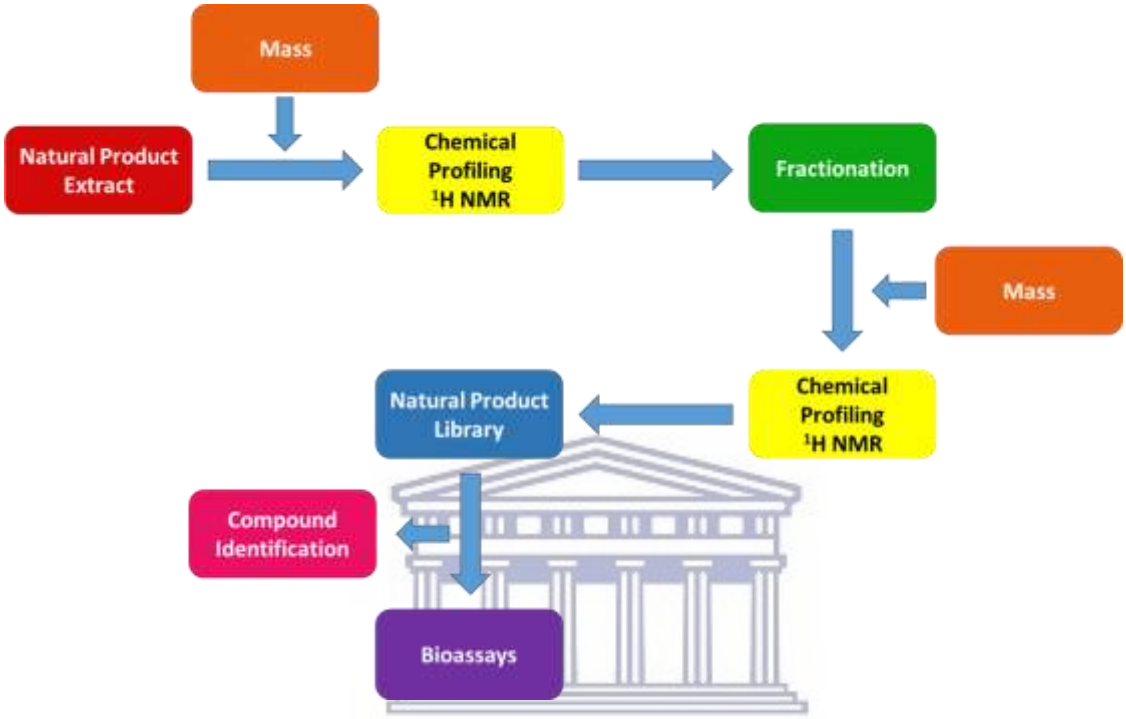

Figure 3.3: Flow diagram of the initial lead identification process followed in the generation of the natural product library utilized in this study.

Based on the challenges with the natural product drug discovery process, which was highlighted above, it was important to develop methods that were suited to improve the screening of marine natural products and to enhance the discovery of potential lead compounds. A suitable way to circumvent these challenges was to develop a natural product library. Natural product libraries are a collection of preselected samples that were isolated, fractionated and chemically analysed. They offer a vast potential in identifying bioactive compounds in bioassay screenings due to their unique physicochemical properties namely the chemical space and property distribution within the molecules, molecular scaffolds and chemical diversity [Gu *et al.*, 2013]. They also offer the opportunity to compare the collection of compounds with other natural product and/or synthetic compound libraries. Natural product libraries can be tailored to the purpose of the screening. The library could be based purely of crude extracts, semi-pure fractions or pure compounds. Pure natural product libraries would then be comparable to

synthetic libraries as the hit compounds are identified immediately and although pure libraries are ideal, they are costly to create and time-consuming. For academic and learning purposes it was more suited to develop a semi-pure natural product library that contains approximately 5-10 compounds per fraction [Butler *et al.,* 2014; Koehn and Carter, 2005].

In order to obtain the crude extract, the biomass of the seaweed needs to be extracted and depending on the amount of sample available, optimized extraction techniques should be used. A few ways to optimize extraction was via ultrasound-assisted extraction, pressure, agitation, heating and maceration, to name a few. The seaweeds should also be immersed initially in methanol as it is polar and is able to extract most of the drug-like molecules, followed by dichloromethane which extracts non-polar compounds [Butler *et al.,* 2014]. The crude extract obtained contains valuable components such as phenolics, phlorotannins, proteins, peptides, essential amino acids, lipids, terpenoids, steroids, polysaccharides, secondary metabolites and vitamins [Kim and Chojnacka, 2015]. Semi-pure or prefractionated libraries are created by processing the crude extract, from the identified marine algae, using a chromatographic technique to obtain various fractions. Prefractionated libraries are less complex than crude extract libraries. It reduces interference caused by mixtures and it shortens the time required to identify the major compound responsible for the activity and isolate it. Although it is not always possible to remove all interfering compounds, this method allows for the detection of minor compounds; assists in exposing antagonist compounds from agonist compounds, active compounds from cytotoxic compounds, and usually only requires one additional purification process [Butler *et al.,* 2014; Koehn and Carter, 2005]. An example of a prefractionated marine algae library can be seen in Figure 3.4 (stored at the University of the Western Cape Marine BioDiscovery laboratory).

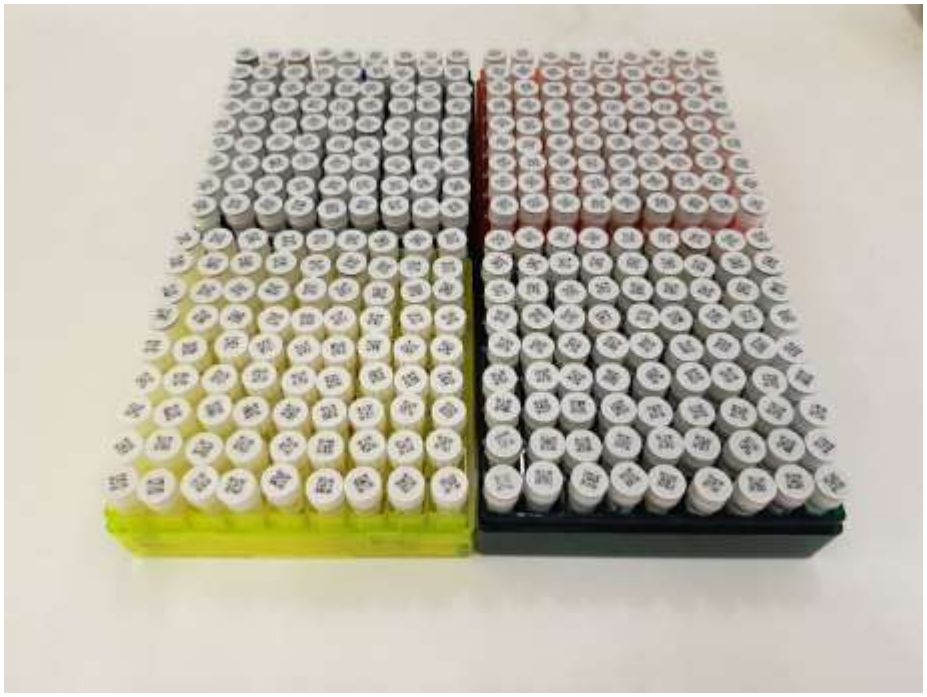

Figure 3.4: A portion of the MBD marine fractionated extract library used in this study.

One important aspect when creating a library is the chemical, spectroscopic and chromatographic profile of each fraction. These profiles ensure chemical identification and allow for results that can be reproduced with confidence and certainty. There are various methods which can be used in order to profile crude extracts and fractions, namely nuclear magnetic resonance (NMR), mass spectrometry (MS), infrared (IR) and ultraviolet (UV). NMR is the preferred tool for chemical analysis and structure elucidation. It provides valuable structural information such as intramolecular relationships, multiplicity, and chemical shifts. In addition, it is non-selective, non-destructive and is able to detect with low sample mass. When working with natural products, the sample mass yields are low hence sample recovery is of the utmost importance [Corcoran and Spraul, 2003]. NMR is able to derive structural features present in a compound and molecules with the same molecular weight but different configuration or constitutions. MS is a useful and sensitive tool for chemical profiling but is unable to differentiate when compounds have the same molecular weights. Lastly, IR and UV provides the least amount of structural information and should only be used when coupled with other spectroscopic techniques for chemical analysis. They only serve as a form of enriching structural information [Zani and Carroll, 2017].

In this chapter the prefractionation of seaweeds used in the development of the library, ^{1}H NMR fingerprinting and *Mycobacterium arum* and *Mycobacterium tuberculosis* assays is discussed as a method of identifying potential anti-tuberculosis compounds from South African marine algae.

3.2. Results and Discussion

3.2.1. Extraction and prefractionation

In this part of the study, the main focus was the development of a library of fractionated algal extracts. A dried voucher sample of each seaweed was catalogued in the Marine Biodiscovery Laboratory herbarium at the University of the Western Cape. Crude extracts produced from the catalogued library are highly complex and require prefractionation in order to obtain simplified fractions. A gradient separation process was used as this method increased the likelihood of identifying minor compounds which may contribute to a sample having biological activity of interest.

To obtain the library of algal fractions, a two-step methodology was followed to produce the collection of marine algal fractions: (i) extraction of algae and (ii) separation of the metabolites by step-gradient chromatography on silica gel. Seventeen marine algae samples were collected at Natures Valley along the South African coastline, this resulted in a collection consisting of nine red, six brown, one green and one unidentified seaweed (Table 3.1).

Table 3.2.1: Samples used in this study to create the South African algal library

#	**Sample**	**Sample code**	**Phylum**
1.	*Laurencia flexuosa*	NV160819-5	Red algae
2.	*Polysiphonia namibiensis*	NV160819-13	Red algae
3.	*Hypnea spicifera*	NV160819-2	Red algae
4.	*Plocamium suhrrii*	NV160820-3	Red algae
5.	*Laurencia stegengae*	NV160819-7	Red algae
6.	*Laurencia glomerata*	NV160819-6	Red algae
7.	*Plocamium rigidum*	NV160820-2	Red algae
8.	*Plocamium cornutum*	NV160819-10	Red algae
9.	*Chondria* sp.	NV160820-9	Red algae
10.	*Plocamium corallorhiza*	NV160819-3	Red algae
11.	*Portieria hornemannii*	NV160820-1	Red algae
12.	*Sargassum elegans*	NV160819-1	Brown algae
13.	*Colpomeria sinuose*	NV160820-10	Brown algae
14.	*Chondracanthus acicularis*	NV160819-11	Brown algae
15.	*Dictyota dichotoma* var. *intricata*	NV160820-7	Brown algae
16.	*Dictyota* sp.	NV160820-8	Brown algae
17.	Unknown	NV160820-101	Unknown

Each sample was thawed and sequentially extracted using sonicated assisted maceration with MeOH and CH_2Cl_2-MeOH. Small amounts of water in the samples was removed by liquid-liquid partitioning between CH_2Cl_2-H_2O. The organic layer was collected, dried under reduced pressure and was fractionated by silica gel gradient column chromatography. The column was eluted with eight solvent mixtures whilst increasing the polarities (Hexane/EtOAc: 10:0, 9:1, 8:2, 6:4, 4:6, 2:8, 0:10 and EtOAc/MeOH: 5:5 and 0:10) to produce a marine algal library comprising of 153 fractions from seventeen seaweeds (Figure 3.5). The Marine BioDiscovery

research group fractionation protocols had previously been established and refined in our laboratory [Afolayan *et al*., 2008]. The protocol was designed to separate compounds based on their polarity, i.e. separating comparatively non-polar to relatively intermediate polarity compounds that are found in the algal biomass.

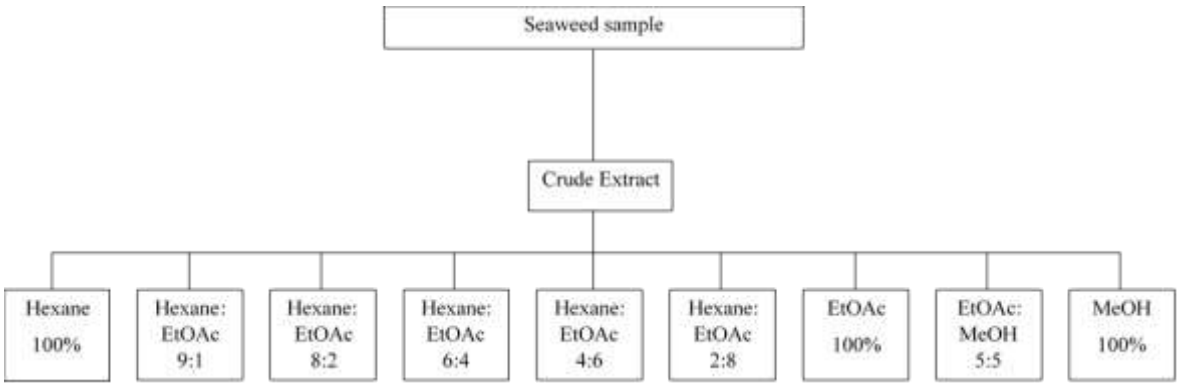

Figure 3.5: Small scale extraction scheme of gradient column chromatography

Figure 3.6 gives a visual representation of the process followed in order to generate the marine algal library.

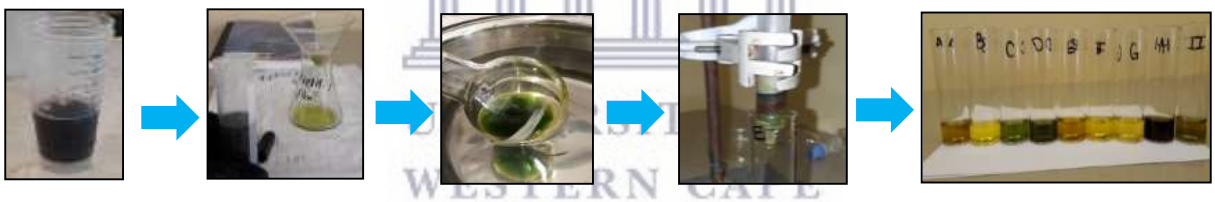

Figure 3.6: Photographic representation of seaweed extraction and fractionation

The 17 seaweeds had varying masses of crude extract and this was depending on their biomass. The crude extract mass varied widely ranging from 31.8 mg to 167 mg with an average recovery of 75 mg. It was interesting to see that even though the amount of seaweed sample used in each extraction was the same, the amount of crude obtained varied. This was largely due to the amount of water in each seaweed sample and the amount of biomass the sample had to offer.

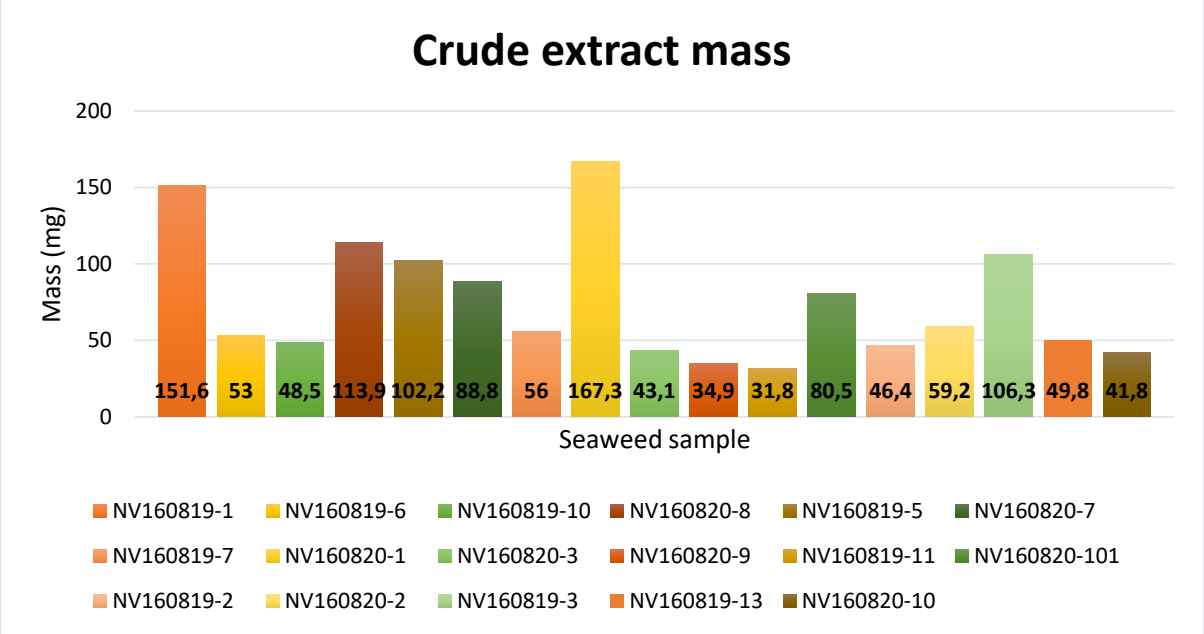

Figure 3.7: A bar graph showing the masses of the crude extracts obtained from the extraction process.

An evaluation of the percentage sample recovery was determined by dividing the total sample recovery from the column with the total extract added (Figure 3.8). Most samples displayed a decent recovery ranging from 49% to 125% with an average recovery of 85%. Samples NV160820-1, NV160820-3, NV160820-9, NV160820-101 and NV160820-2 were all greater than 100% recovery which indicated that there was solvent present in the fraction at the time of weighing which greatly increased the sample masses. More than 60% of the extracts were recovered except for NV160819-5 and NV160820-7, which only had 57% and 49% total extract recovered respectively. The behavioural differences observed with these compounds could be an indication that the samples contain compounds that contain a high affinity for the bonded silica and may require a different stationery phase or the general gradient solvent system used was inadequate for eluting the compounds. These samples may require other solvent combinations. Although silica gel provided a good sample recovery, the recovery was influenced by the type of metabolites being extracted using the predetermined stationery phase. It should also be noted that there was no universal stationery phase that can be applied for all metabolites.

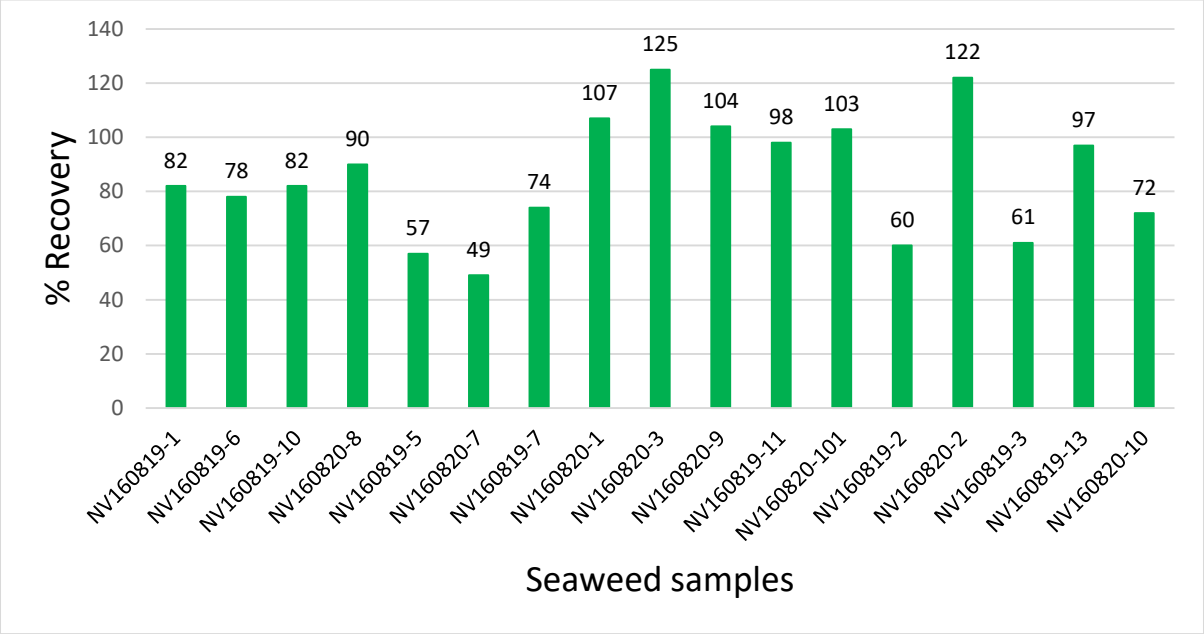

Figure 3.8: Bar graph showing sample recovery after fractionation by silica gel column chromatography (recovery expressed as a percentage of the total extract applied to column).

When the library was developed, it was also important to determine which solvent combinations extracted the most biomass from the sample obtained from the column. The bar graph, Figure 3.9, looked at the average percentage mass recovered per fractions per solvent or solvent combination used. The graph was plotted for all nine fractions. The large standard deviation observed in Figure 3.9 was expected as it gave a general indication of which fraction contained the most sample, it also accounted for the compounds which were not eluted during the gradient fractionation process.

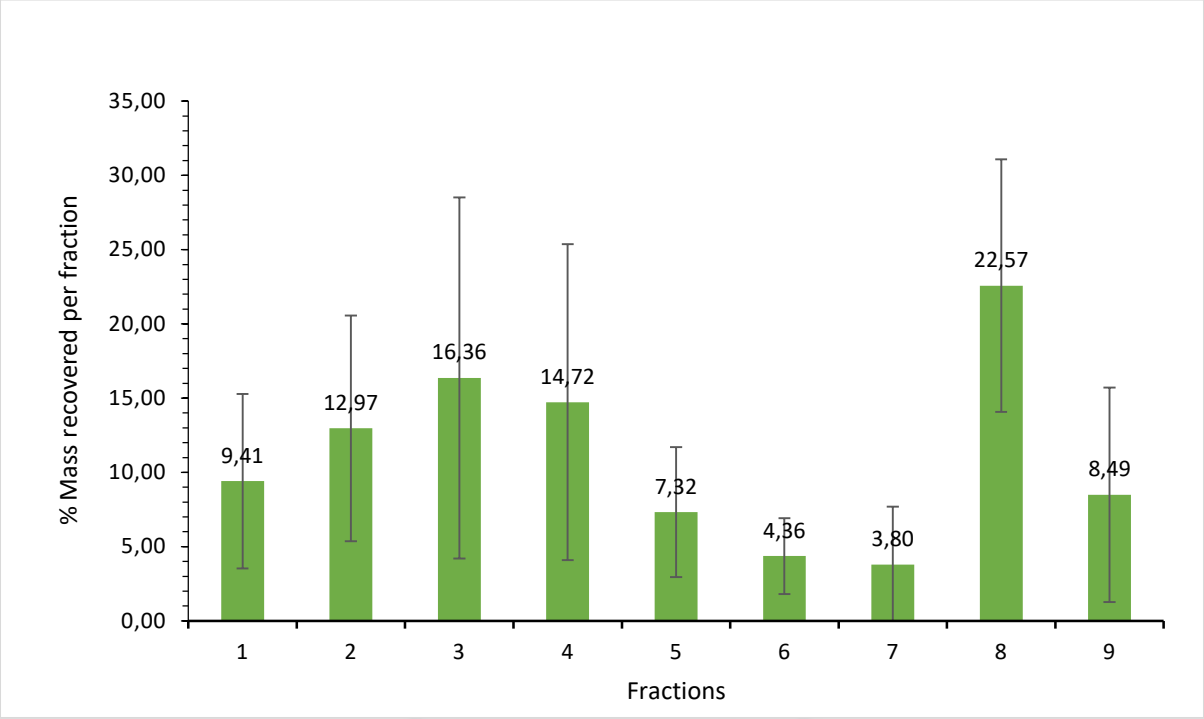

Figure 3.9: Bar graph showing the average percentage of mass recovered per fraction

Approximately, 60% of the recovered organic material was distributed in the first five-column fractions. Fraction seven which was 100% EtOAc extracted the lowest percentage of the metabolites at 3.8%. Fraction eight which was a combination of 50% EtOAc and 50% MeOH had the highest recovery in terms of mass. This was not unexpected since this was a highly polar combination and the solvent would be extracting the cell membrane glycolipids within the sample. It was also important to note how different each sample was in terms of the percentage composition per fraction. It is interesting to note that NV160820-3, NV160820-2, NV160819-10 and NV160819-3, are all *Plocamium* spp. and yet they produced a very different percentage of composition profiles. (Figure 3.10).

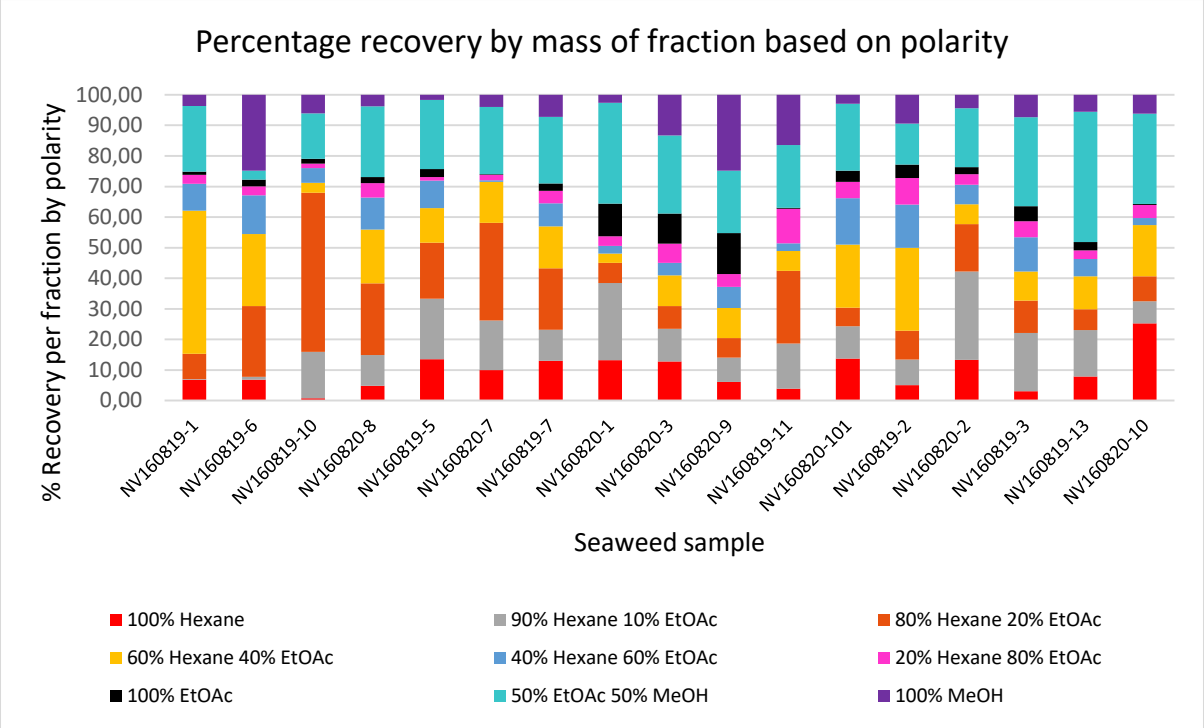

Figure 3.10: A stacked bar graph indicating the percentage composition by mass of fraction based on the polarity.

Once all the fractions were profiled by ^{1}H NMR spectroscopy, they were dissolved and stored in dimethyl sulfoxide (DMSO) at a stock concentration of 10 mg/ml. DMSO was ideal because it dissolves both non-polar and polar compounds and was suitable for short and long term storage. DMSO stock solutions maintain the integrity of the natural product compounds because upon storage at -20 °C the solvent freezes, aiding in compound stability. The library stock samples were placed in screw-cap vials, sealed, labelled and stored in precisely arranged screw-cap vial boxes until they are required for biological tests.

3.2.2. ^{1}H NMR chemical profiling

In this study, chemical profiling was performed on all 153 fractions obtained from the 17 prefractionated seaweeds. Profiling was conducted by ^{1}H NMR spectroscopy. As mentioned before, ^{1}H NMR spectroscopy is a non-destructive technique used to characterize compounds within the crude extract and fractions. Although ^{1}H NMR spectroscopy is insensitive compared to other techniques which are available, it provides information on the classes of metabolites present in each extract. The beauty of this method is that the crude extracts and fractions can be compared and analysed by the ^{1}H NMR software (Figure 3.11).

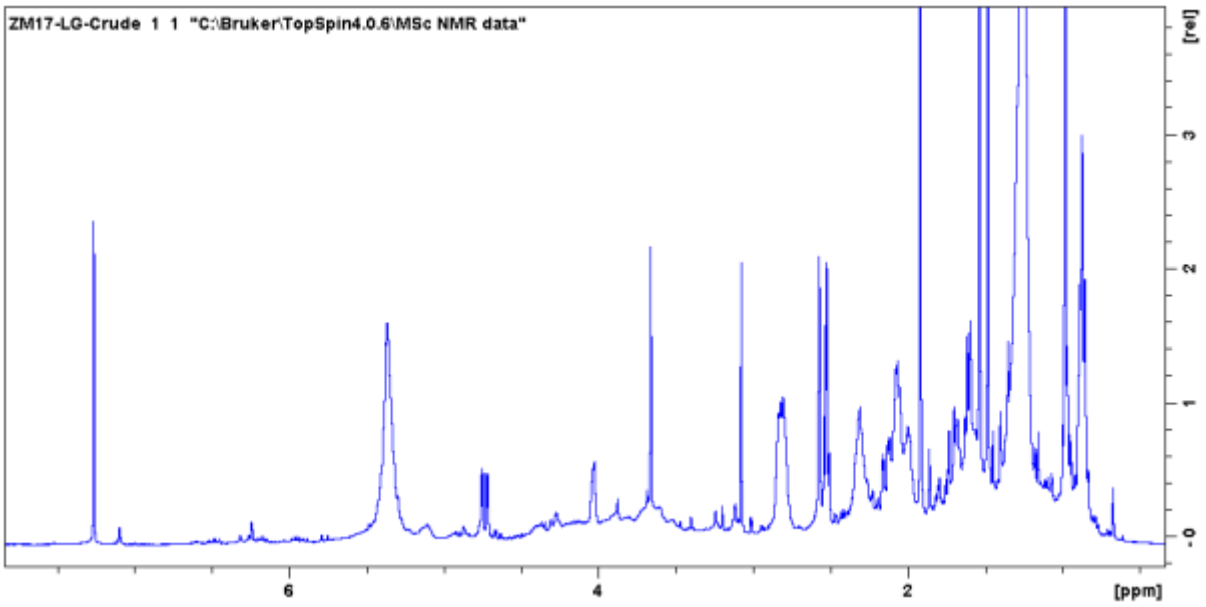

Figure 3.11: ^{1}H NMR spectrum of the crude *Laurencia glomerata* extract

As observed in Figure 3.11, the ^{1}H NMR spectrum of a crude extract contains many compounds and single compounds cannot be identified based on it. A ^{1}H NMR spectrum merely serves as a fingerprint for an individual crude sample. This affords reproducibility in the work as the ^{1}H NMR spectrum of an initial extraction and a subsequent crude extraction occurring at a later date can be compared. The technique was sensitive enough to detect trace amounts of solvent which could be seen at δ 5.23 and δ 7.26 which was CH_2Cl_2 and $CHCl_3$ ($CDCl_3$) respectively. Conducting an initial analysis of the crude extract enabled the identification of compounds which eluted in subsequent silica chromatography column (Figure 3.12a and 3.12b). The advantage of a fractionated library was also apparent from the ^{1}H NMR spectra of the fractions (Figure 3.12a and b). Minor compounds in the crude extract were easily discernible in the spectra of the fractions.

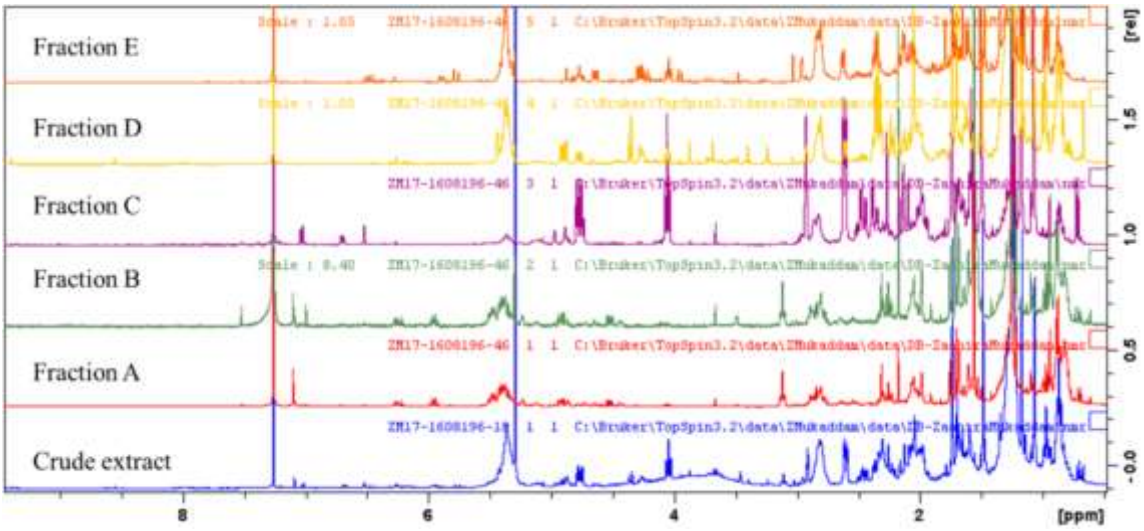

Figure 3.12a: ^{1}H NMR spectra of crude & fractions A-E from *Laurencia glomerata*

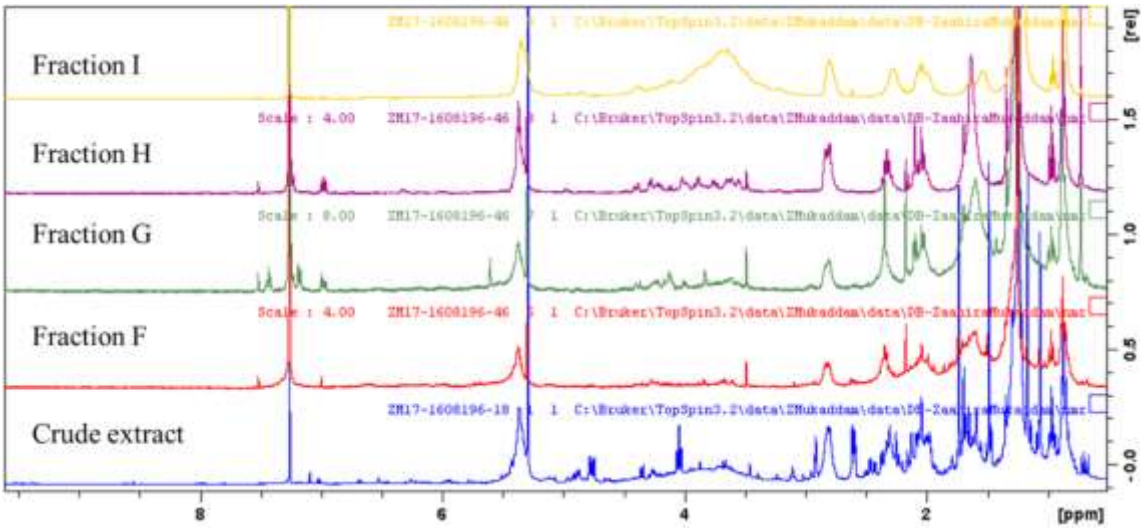

Figure 3.12b: ^{1}H NMR spectra of crude & fractions F-I from *Laurencia glomerata*

The region between δ 0-2.5 in the spectra clearly indicated fatty acids and sterols were present as it was represented by dense cluster peak profiles. Seaweeds are known to produce non-polar fatty acids and it was visible in fractions A-C. The region of interest when identifying interesting chemical shifts are δ 3-10. As can be seen in Figure 3.12a and 3.12b, each fraction had different chemical profiles and when comparing them with the crude extract, it was easy to identify which peaks in the crude eluted in a particular mobile phase. It is possible for two fractions to contain the same compound as depicted in the spectrum. Upon close observation of the intensity of the peaks, it gave a clear indication of which fraction contained the major secondary metabolite and in another fraction, it may have appeared as a minor compound.

It was interesting to note that all 17 seaweeds chemical profiles followed the same trend in the ^{1}H NMR spectra. The first five fractions which were highlighted earlier as containing more than 60% of the sample biomass, were also the most chemically diverse fractions as determined by ^{1}H NMR spectroscopy while fractions 8 and 9 mainly contained glycolipids.

3.2.3. Biological activity

This study has a dedicated aim which was to discover anti-tuberculosis compounds from South African marine algae. It was important that the compound library developed, was screened for anti-tuberculosis activity against *Mycobacterium tuberculosis* H37Rv. It is important to note that there is no universal model used for anti-tuberculosis testing. However, many researchers have reported on the use of *Mycobacterium aurum* A+ for the determination of anti-tubercular activity. The benefits of *M. aurum* A+ are, firstly that it is non-infectious which makes it easier to handle than *M. tuberculosis* (requires trained personnel in a level three infectious disease laboratory). Secondly, *M. aurum* A+ is a slow-growing micro-organism with a replication time of two and a half hours (faster than *M. tuberculosis*), but it is fairly easy to culture and more accessible. Lastly, *M. aurum* A+ has a high genomic similarity as well as a comparable cell wall profile to that of *M. tuberculosis* H37Rv and it was therefore used as a surrogate in bioassay testing [Sood *et al.*, 2016]. Due to the vast number of library fractions that required screening, 50 µg/ml was selected as the test concentration. This was considered a fair starting concentration due to the fact that, the screening was performed to identify potent active compounds. This process would have eliminated a vast number of fractions, which would save time and money. It would also mean that the compounds identified and pursued could be a potential drug upon further research and investigation. Once active compounds were identified a range of concentrations could be tested to establish the potency.

Mycobacterium tuberculosis assay

All *M. tuberculosis* testing was conducted at the University of Cape Town in collaboration with Professor D. Warner (Institute of Infectious Disease and Molecular Medicine). All procedures that required the handling of pathogenic mycobacterial strains are performed in a Biosafety Level III certified and compliant facility.

Table 3.2: Fractions exhibiting an MIC_{90} at a concentration of 50 µg/ml against *Mycobacterium tuberculosis*

Code	Sample name
NV160819-1-D	*S. elegans*
NV160819-1-H	*S. elegans*
NV160819-10-B	*P. cornutum*
NV160819-10-C	*P. cornutum*
NV160820-3-B	*P. suhrrii*
NV160820-2-B	*P. rigidium*
NV160820-2-C	*P. rigidium*

Based on the screening procedure against *M. tuberculosis* of the 153 marine algal fractions submitted for activity testing, only seven fractions showed activity (Table 3.2). Tuberculosis bacillus is a hardy microorganism as mentioned in Chapter 1. It is not surprising that so few fractions exhibited the toxicity required to cause cell death. Out of the seven active fractions identified, five fractions originated from a *Plocamium sp.* The results obtained in combination with the ^{1}H NMR data, identified *Plocamium cornutum* as the candidate for further study.

Mycobacterium aurum assay

In the microbroth assay used to determine the activity of the fractions against *M. aurum* A+, four controls were used to ensure the scientific integrity of the results. The controls were tested in triplicate to maintain the uniformity of the experiment and to ensure technical reproducibility. A sterile control comprising of media and sterile water was used to ensure that no other organisms were interfering with the results obtained and that the techniques employed by the conductor were aseptic and sterile. There were two negative controls utilized in the experiment. The negative controls were used to ensure that the only independent variable influencing the growth of *M. aurum* A+ in the experiment is the respective fraction being tested. The one negative control, comprised of culture and DMSO, which was selected in the experiment to represent 100% growth. The second negative control was culture and media; this

control establishes that the media itself was the correct growth medium as well as that it does not interfere or cause inhibition. In addition, this control also ensured that the DMSO used in the study was not responsible for the inhibitory effect observed, but rather the compounds/ fractions dissolved in the DMSO. The last control was the positive control which comprises of culture and the antibiotic (vancomycin). The positive control indicates the effects of a growth inhibitor and provides a comparison when comparing the effects of the fractions.

Interestingly, *M. aurum* was much more sensitive to the algal fractions. One possibility is that the assay conditions could have affected the sensitivity of the organism to the compounds. *M. aurum* was a weaker mycobacterial strain and the results obtained suggested that. Based on the results of the 153 fractions that were tested against *M. aurum* , 88 fractions showed some inhibitory activity against *M. aurum* at a concentration of 50 μg/ml. This equates to 57.5% of the total fractions submitted. Most of the samples exhibited weak growth inhibition with some seaweed fractions being more active than others. Fractions that resulted in low average growth percentages were NV160820-1 (*Porteria hornamannii* - fraction I), NV160819-13 (*Polysiphonia namibiensis* - fraction E), NV160819-11 (*Chondrocanthus ascicularus* – fraction B), NV160820-3 (*Plocamium suhrrii* – fraction B), NV160819-7 (*Laurencia stegengae* – fraction I) and NV160820-8 (*Dictyota* sp. fractions B and H). The inhibition activity of the mentioned fractions ranged from 32% - 53% growth inhibition.

The anti-mycobacterial activity of the fractions was assigned colours based on how greatly the compound affected the average percentage growth of *M. aurum* A+. Looking at the results in Figure 3.13, it was interesting to note that there was some growth inhibition due to some fractions and other fractions enhanced the growth of *M. aurum* A+. In an article published by Natrah *et al.* (2014), the interaction between microalgae and bacteria is discussed. It suggested that the lysis of cells from both deteriorating and dead microalgae release carbon atoms. The release of carbon has promoted the growth of bacteria. It goes on to note that the bacterial density is high and is proportional to the density of deteriorating microalgae. The article also notes that microalgae contain vitamins which promote bacterial growth [Natrah *et al.*, 2014]. The same logic can possibly be applied to macroalgae that they contain vitamins which promote growth and hence this phenomenon was observed in the results obtained.

The most active fraction based on the tabulated results was fraction G from *Plocamium surrhii*. Unfortunately, this species was not selected for further study due to limited availability, but it was interesting to note that the *Plocamium* spp. in the library contributed a large part of the library activity profile. *Laurencia glomerata* should be highlighted because almost all of the fractions had weak anti-mycobacterial activity against *M. aurum*.

Fractions H and I represented the extraction of fatty acids and glycolipids. There are 34 fractions in the respective categories and 18 of those fractions show increased bacterial growth. The results indicated that 52% of the total number of fractions tested, promoted organism growth. One possibility is that fatty acids and glycolipids could serve as a potential source of carbon, which had promoted the growth of these organisms. It is interesting to note that there were four fractions that have moderate growth inhibition activity.

		A	B	C	D	E	F	G	H	I
NV160819-1	*S. elegans*	144	86	75	**87**	133	95	77	**75**	94
NV160819-6	*L. glomerata*	97	96	84	91	98	86	82	102	96
NV160819-10	*P. cornutum*	100	**79**	**105**	96	91	75	110	96	96
NV160820-8	*Dictote* sp.	76	64	83	79	97	140	81	69	85
NV160819-5	*L. flexuosa*	121	106	102	95	100	93	88	104	108
NV160820-7	*Dictyota dichotoma var. intricata*	100	95	87	98	100	87	170	92	90
NV160819-7	*L. stegengae*	88	166	159	89	99	100	154	133	66
NV160819-4	*Porteria hornamannii*	84	119	99	139	112	148	47	103	108
NV160820-3	*P. suhrrii*	102	**67**	91	101	106	82	98	107	105
NV160820-9	*Chondria* sp.	88	105	106	99	100	92	85	92	175
NV160819-11	*Chondrocanthus asciculatus*	71	64	103	131	93	87	106	116	103
NV160819-2	*Hypnea spicifera*	103	101	115	102	93	91	115	100	97
NV160820-10	Unknown sample	85	104	95	94	104	110	81	75	96
NV160820-2	*P. rigidium*	94	**89**	**92**	97	105	89	75	109	103
NV160819-3	*P. corallohiza*	93	90	102	95	98	86	100	98	94
NV160819-13	*Polysiphonia namibiensis*	77	96	92	78	64	95	106	122	117
NV160820-10	*Colpomeria sinuose*	118	98	104	138	104	98	109	110	102

Figure 3.13: Antimicrobial activity (represented as a heat map) of the South African marine prefractionated library against *M. aurum* A+

Red = excellent activity, orange = moderate activity, yellow = weak activity and white = no antimicrobial activity.

Bolded fractions represent the fractions which showed activity against *M. tuberculosis*

Based on the results of both the *M. tuberculosis* and *M. aurum* studies, there were a few aspects which needed to be highlighted. The assays were performed in different laboratories with their own respective protocols. A second aspect is that the organisms were cultivated in different growth media, which made it difficult to do a direct comparison for the results obtained. As highlighted (Figure 3.13) the seven fractions that exhibited anti-mycobacterial activity also showed varying degrees of growth inhibition for *M. aurum*, except for one fraction. There were a few species utilised in this study which have previously been tested against *M. aurum*. In an article by Lategan *et al*. (2009), *S. elegans, L. flexuosa* and *P. corallorhiza,* all exhibited MICs of 2-4 mg/ml. There was an exception of the hexane fraction of *S. elegans* exhibiting growth at a >4 mg/ml. Although the article had a different method of fractionation and tested fractions at a considerably higher concentration than in this study, there were similarities in the activity which was reported. As seen in Figure 3.13, the hexane fraction of *S. elegans* promoted the growth of *M. aurum* at 50 µg/ml. *P. corallorhiza* exhibited a weak activity profile in this study but at a 2 mg/ml concentration, it inhibited the growth of *M. aurum* [Lategan *et al*., 2009]. There was very little data published on marine algal activity against *M. tuberculosis*. *P. corallorhia* was found to inhibit *M. tuberculosis* in Saravanakumar (2006) thesis, different results were obtained and the possibility was that the fractions were tested at different concentrations. Another possibility was that different polarity test samples were extracted. Due to the differences in the two studies, it cannot be utilized as a comparison but merely as a guide [Saravanakumar, 2006].

Conclusion

In summary, the goal of developing a prefractionated library of marine algae was successfully achieved. The fractionation by silica gel and varying the mobile phase polarity proves to be a time-efficient, reproducible and effective way of obtaining the secondary metabolites, producing a library of 153 fractions. The chemical profiling by ^{1}H NMR spectroscopy and the preliminary screening against *M. tuberculosis* proved helpful in identifying sample candidates for further studies based on distinctive sample chemistry and bioactivity.

From the information obtained in the preliminary screening and chemical profiling, two algae were identified for further studies based on their bioactivity and fascinating chemical profiles: *Plocamium cornutum* and *Laurencia glomerata*. The studies on the selected seaweeds will be explored in the following chapters.

General experimental

All solvents utilized in the extraction process were redistilled. NMR spectra were obtained on a Bruker Avance 400 MHz spectrometer using standard pulse sequences. All samples were prepared in deuterated chloroform as the solvent, chemical shifts were reported in ppm and were referenced to the residual undeuterated solvent signal at δ_H 7.26. Column chromatography was performed using Merck® Silica gel 60 (0.040-0.063 mm), Germany. The library samples stock solutions were prepared using DMSO. The *M. tuberculosis* H37Rv assays were performed by Professor Digby Warner (Institute of Infectious Disease and Molecular Medicine, Faculty of Health Sciences, University of Cape Town). The *M. aurum* A+ assays were performed by the author under the supervision of Doctor Marilize Le Roes-Hill (Biocatalysis and Technical Biology Research Group, Institute of Biomedical and Microbial Biotechnology, Cape Peninsula University of Technology).

Marine algal material

All seaweed samples were collected and identified by Professor Denzil R. Beukes (University of the Western Cape) and Professor John J. Bolton (Biological Sciences, University of Cape Town). Samples used in this study were collected in 2016 from Natures Valley on the Southern Cape coast of South Africa, they were coded and appropriately stored at -20 °C. The selected samples for the library was comprised of 17 algae; nine red, six brown, one green algae and one unidentified species. Dried voucher specimens were stored at the Marine Biodiscovery Laboratory Herbarium, University of the Western Cape.

Extraction and Fractionation of marine algae

Each seaweed was extracted using the following procedure. The bulk sample was removed from the -20 °C freezer and a portion (biomass equivalent to 10 ml of a 50 ml falcon tube) was removed. The sample was extracted via a sonication assisted technique using methanol (MeOH), followed by three successive extractions with MeOH-dichloromethane (CH_2Cl_2) (1:2) for 15 minutes. The extracts were combined and dried under reduced pressure. The crude extracts were partitioned between water and CH_2Cl_2, the organic layer was collected and dried under reduced pressure.

The crude extracts were then fractionated by silica gel 60 (0.040-0.063 mm), column chromatography using a step gradient solvent system. The crude extracts were weighed and masses varied widely (range: 31.8 mg to 167 mg) with an average extract mass of 75 mg. The crude extracts were dissolved in approximately 2 ml of CH_2Cl_2, celite 545 EP (~300 mg) was

added and the solvent removed under reduced pressure. The mass of 1 g silica gel stationary phase was wet packed (in hexane) into a 5 g capacity cartridge and the celite/extract was then added to the column. The column was eluted with 5 ml of hexane 100%, hexane/ethyl acetate (EtOAc): 9:1, 8:2, 6:4, 4:6, 2:8, EtOAc 100%, EtOAc/MeOH 5:5 and MeOH 100%, subsequently nine fractions were obtained. The eluent was collected in pre-weighed polytope vials, dried under reduced pressure and weighed. The respective extract and nine fractions were analysed by ^{1}H NMR spectroscopy. Extracts and prefractions were stored in DMSO at a concentration of 10 mg/ml at -20 °C thus forming the marine algal compound library.

Biological *Mycobacterium* sp. assays

Preparation of extracts

The 17 crude extract samples prepared for the marine algal library were fractionated to yield 153 fractions. The fractions were prepared to a final concentration of 10 mg/ml in DMSO as the library stock solutions.

***Mycobacterium tuberculosis* screening**

The assays were conducted using an approved protocol in a Biosafety Level III certified and compliant laboratory. All samples were initially tested, in 96-well microtiter plates, at a final concentration of 50 µg/ml against *M. tuberculosis* H37Rv using a broth microdilution method (Jorgensen *et al.*, 2007). The lowest concentration of extract that inhibits the growth of more than 90% of the bacterial population is considered to be the MIC_{90}.

A 10 ml sample of the test strain, *M. tuberculosis* H37Rv strain (Ioerger *et al.*, 2010), was grown to the ideal optical density of 0.6-0.7 (OD_{600}). The library stock solutions of 10 mg/ml were diluted to a concentration of 1 mg/ml and 50 µl of each fraction was added to the allocated wells in triplicate. For the single-point assay, 50 µl of the test strain was added to each sample well and to the control wells. The layout of the 96-well plate was a modified version of a method previously described by Ollinger *et al.* (2013). Dose-Response Assays: Duplicate two-fold serial dilutions of the test material are prepared across 10 wells in a 96-well microtitre plate, in a volume of 50 ul, after which, 50 µl of the diluted *M. tuberculosis* culture was added to each well in the plate (including the control wells). The final volume per well was 100 ul.

There were three controls used in this experiment, a minimum growth control (rifampicin at 2 x MIC: 0.150 µM), maximum growth control (DMSO), and a rifampicin dose-response (range 0.15 – 0.0002 µM). The maximum, non-inhibitory, final concentration of DMSO = < 5%. The final concentration of DMSO used in the maximum growth control was equal to the final concentration of DMSO used in the dose-response assay for the test material. The completed plates were sealed in a secondary container and incubated at 37 °C with 5% CO_2 and humidification for six days. On the sixth day, the plates were removed and Alamar Blue reagent was added to each well of the assay plate. The plates were then incubated for a further 24 hours and the results of the MIC_{90} are determined and scored visually. The lowest concentration of material displaying no visible growth was scored as the MIC_{90}.

Plate preparation

Column 1 – each well contains 50 µl of the minimum inhibition control

Column 12 – each well 50 µl contains the maximum inhibition control, 2 X Rifampicin MIC (0.150 µM final concentration).

Row H – contains the 10-point concentration response assay for the reference drug, Rifampicin, concentration response range: 0.150 – 0.0002 µM.

Rows A to G – each row contains a 10-point concentration response range for an individual test.

Two-fold serial dilutions are prepared across 10 wells in the 96-well microtitre plate, for the test compounds and the Rifampicin concentration response, in a volume of 50 µl, after which, 50 µl of the diluted *M. tuberculosis* culture was added to each well (including the control wells). The final well volume per was 100 µl. In the graphical demonstration below, the concentration decreases from right to left.

	1	2	3	4	5	6	7	8	9	10	11	12
A	MIN INHIBITION											MAX INHIBITION
B												
C												
D												
E												
F												
G												
H												

Media used

- sGAST-Fe (glycerol–alanine–salts) medium pH 6.6, supplemented with 0.05% Tween-80 (De Voss et al., 2000). The culture is diluted 1:100.
- Middlebrook 7H9 media (Difco) supplemented with 0.4% Glucose, Middlebrook albumin-dextrose- catalase (ADC) enrichment (Difco) and 0.05% Tween 80 (Franzblau *et al*., 2012). The culture is diluted 1:500.
- Middlebrook 7H9 media (Difco) supplemented with 0.03% Casitone, 0.4% Glucose and 0.05% Tyloxpol (Tang *et al*., 2009). The culture is diluted 1:500.

Media Recipes

Middlebrook 7H9 Broth 1L – 7H9 GLU ADC TW

4.7 g powder

900 ml distilled water

2 g Glucose

100 ml Middlebrook ADC

0.05% Tween 80

Middlebrook 7H9 Broth 1L – 7H9 GLU CAS TX

4.7 g powder

900 ml distilled water

4 g Glucose

0.3 g Casitone

0.81 g NaCl

0.05% Tyloxapol

GAST/Fe 1L:

0.3 g of Bacto Casitone

4.0 g of dibasic potassium phosphate

2.0 g of citric acid

1.0 g of L-alanine

1.2 g of magnesium chloride hexahydrate

0.6 g of potassium sulfate

2.0 g of ammonium chloride

1.80 ml of 10M sodium hydroxide

10.0 ml of glycerol

Mtb. Screening Platform MIC summary protocol – V1 December 2017 RSeldon

0.05% Tween 80

0.05 g of ferric ammonium citrate

Dissolve above components in distilled water. Adjust pH to 6.6 if necessary, then filter sterilize (0.2 μM filter) and store at 37 °C.

Strains used in the respiratory reporter assay:

Mtb H37RvΔ*cyd*KO, and, Mtb H37RvΔ*cyd*KO/QcrBA317T (Arora *et al.,* 2014, Van der Westhuizen *et al.*, 2015)

Data analysis

Relative fluorescence (excitation 540 nm; emission 590 nm) was measured using a SpecraMax i3x Plate reader at day 7. Raw fluorescent data (Relative Fluorescent Units) are acquired using: A SpecraMax i3x Plate reader: (Serial no. 36370 3271), Molecular Devices Corporation 1311 Orleans Drive Sunnyvale, California 94089. RFU data are not acquired for single point assays.

RFU Data were analysed using: Softmax ® Pro 6 software: (Version 6.5.1, Serial no. 1278552768867612530), Molecular Devices Corporation 1311 Orleans Drive Sunnyvale, California 94089.

The onboard Fluorescent Intensity – Endpoint protocol was used in conjunction with the following wavelength filters: Excitation: 540 Emission: 590 nm.

The Softmax ® Pro 6, 4-parameter curve fit protocol, was used to generate a calculated MIC_{90}. Raw RFU data are normalised to the minimum and maximum inhibition controls to generate a dose response curve (% inhibition), using the Levenberg-Marquardt damped least-squares method, from which the MIC_{90} was calculated.

Mycobacterium aurum screening

To prepare the fractions for the antimicrobial activity testing against *M. aurum* A+, 10 µl of each of the 10 mg/ml stock solution was pipetted into a 96-well plate and was diluted with 90 µl of DMSO to obtain a solution concentration of 1 mg/ml.

Preparation of the test strain

The test strain *M. aurum* A+ was inoculated into 5 ml of Luria-Bertani broth. The inoculated broth was then incubated at the ideal growth temperature of 37 °C for 48 hours while shaken at 160 rpm. The lengthy incubation time was due to the slow growth of *M. aurum*. The culture's optical density (OD) was measured at a wavelength of 600 nm and the OD of the culture was adjusted to 0.8 prior to the use in the liquid assay.

Controls

The controls utilized in the antimicrobial tests are as follows:

Negative control:	180 µl culture + 20 µl DMSO
	180 µl culture + 20 µl sterile broth
Positive control:	180 µl culture + 20 µl of 10 mg/ml vancomycin
Sterile control:	180 µl broth + 20 µl sterile distilled water

Antimicrobial *M. aurum* sample setup

To establish a single point concentration test of 50 µg for each fraction, 10 µl of each of the 1 mg/ml sample was pipette into 96-well microtiter plates in triplicate respectively. To each well, an additional 10 µl of DMSO and 180 µl of culture was added to obtain a total volume of 200 µl. This would result in the desired end-concentration of 50 µg to be tested. The microtiter plates were incubated at the optimal growth temperature of 37 °C for 24 hours. After the incubation period, 20 µl of a 0.25% (w/v) of 3-(4,5-dimethylthiazol-2-yl)-2,5-diphenyltetrazolium bromide (MTT)-assay in phosphate-buffered saline (PBS), was added to each well and incubated at 37 °C for an additional 3 hours. Subsequently, 100 µl of DMSO was added to allow for the solubilisation of the formazan dye (incubated at room temperature for three hours). The optical density was measured at a wavelength of 570 nm.

References

Afolayan, A.F., Bolton, J.J., Lategan, C.A., Smith, P.J., Beukes, D.R. Fucoxanthin, tetraprenylated toluquinone and toluhydroquinone metabolites from *Sargassum heterophyllum* inhibit the in vitro growth of the malaria parasite Plasmodium falciparum. Zeitschrift fur Naturforschung C, *Journal of Biosciences* **2008**, 63(11-12), 848-852.

Arora, K., Ochoa-Montaño, B., Tsang, P. S., Blundell, T. L., Dawes, S. S., Mizrahi, V., Bayliss, T., Mackenzie, C. J., Cleghorn, L. A., Ray, P. C., Wyatt, P. G., Respiratory flexibility in response to inhibition of cytochrome C oxidase in Mycobacterium tuberculosis. *Antimicrobial Agents and Chemotherapy* **2014**, 58(11), 6962-6965.

Bernardini, S., Tiezzi, A., Laghezza Masci, V., Ovidi, E., Natural products for human health: an historical overview of the drug discovery approaches. *Natural Product Research* **2018**, 32(16), 1926-1950.

Butler, M. S., Fontaine, F., Cooper, M. A., Natural product libraries: Assembly, maintenance and screening. *Planta Medica* **2014**, 80(14), 1161-1170.

Corcoran, O., Spraul, M., LC-NMR-MS in drug discovery. *Drug Discovery Today* **2003**, 8(14), 624-631.

Daletos, G., Ancheeva, E., Chaidir, C., Kalscheuer, R., Proksch, P., Antimycobacterial metabolites from marine invertebrates. *Archiv der Pharmazie* **2016**, 349(10), 763-773.

David, B., Wolfender, J. L., Dias, D. A., The pharmaceutical industry and natural products: historical status and new trends. *Phytochemistry Reviews* **2015**, 14(2), 299-315.

Gammon, K., Drug discovery: Leaving no stone unturned. *Nature* **2014**, 509, S10-S12.

Gerwick, W. H., Moore, B. S., Lessons from the past and charting the future of marine natural products drug discovery and chemical biology. *Chemistry & Biology* **2012**, 19(1), 85-98.

Ginsberg, A. M., Spigelman, M., Challenges in tuberculosis drug research and development. *Nature Medicine* **2007**, 13(3), 290.

Gu, J., Gui, Y., Chen, L., Yuan, G., Lu, H. Z., Xu, X., Use of natural products as chemical library for drug discovery and network pharmacology. *PLoS One* **2013**, 8(4), e62839

Ioerger, T. R., Feng, Y., Ganesula, K., Chen, X., Dobos, K. M., Fortune, S., Jacobs, W. R., Mizrahi, V., Parish, T., Rubin, E., Sassetti, C., Variation among genome sequences of H37Rv strains of Mycobacterium tuberculosis from multiple laboratories. *Journal of Bacteriology* **2010**, 192(14), 3645-3653.

Jorgensen J. H., Turnidge J. D., Murray P. R., Baron E. J., Jorgensen J. H., Landry M. L., Pfaller M. A., Antibacterial susceptibility tests: dilution and disk diffusion methods, Manual of Clinical Microbiology, **2007**, 9th ed. Washington, DC American Society for Microbiology, 1152-1172.

Khalid, S., Abbas, M., Saeed, F., Bader-Ul-Ain, H., Suleria, H. A. R., Therapeutic Potential of Seaweed Bioactive Compounds. In *Seaweed Biomaterials* **2018**. IntechOpen.

Kim, S. K., Chojnacka, K., editors., *Marine algae extracts: processes, products and applications* **2015.** John Wiley & Sons.

Koehn, F. E., Carter G. T., The evolving role of natural products in drug discovery. *Nature Reviews Drug Discovery* **2005**, 4(3), 206-220.

Krastina, J., Romagnoli, F., Balina, K., SWOT analysis for a further LCCA-based techno-economic feasibility of a biogas system using seaweed feedstock. *Energy Procedia* **2017**, 128, 491-496.

Lategan, C., Kellerman, T., Afolayan, A. F., Mann, M. G., Antunes, E. M., Smith, P. J., Bolton, J. J., Beukes, D. R., Antiplasmodial and antimicrobial activities of South African marine algal extracts. *Pharmaceutical Biology* **2009**, 47(5), 408-413.

MacArtain, P., Gill, C. I., Brooks, M., Campbell, R., Rowland, I. R., Nutritional value of edible seaweeds. *Nutrition Reviews* **2007**, 65(12), 535-543.

Montaser, R., Luesch, H., Marine natural products: a new wave of drugs? *Future Medicinal Chemistry* **2011**, 3(12),1475-1489.

Natrah, F. M., Bossier, P., Sorgeloos, P., Yusoff, F. M., Defoirdt, T., Significance of microalgal–bacterial interactions for aquaculture. *Reviews in Aquaculture* **2014**, 6(1), 48-61.

Newman, D. J., Cragg, G. M., Natural products as a source of new drugs from 1981 to 2014. *Journal of Natural Products* **2016**, 79(3), 629-661.

O'Brien, R., Nunn, P. P., The need for new drugs against tuberculosis obstacles, opportunities and next steps. *American Journal of Respiratory and Critical Care Medicine* **2000**, 163(5). 1055-1058.

Ollinger, J., Bailey, M. A., Moraski, G. C., Casey, A., Florio, S., Alling, T., Miller, M. J., Parish, T., A dual read-out assay to evaluate the potency of compounds active against Mycobacterium tuberculosis. *PloS One* **2013**, 8(4), e60531

Parsaeimehr, A., Lutzu, G. A., Algae as a novel source of antimicrobial compounds: current and future perspectives. *Antibiotic Resistance* **2016**, 377-396.

Saravanakumar, D., Antimycobacterial activity of the red algae *Gelidium pristoides, Plocamium corallorhiza* and *Polysiphonia virgata* **2006**, (Doctoral dissertation, University of Cape Town).

Sood, S., Yadav, A., Shrivastava, R., Mycobacterium aurum is unable to survive mycobacterium tuberculosis latency associated stress conditions: Implications as non-suitable model organism. *Indian Journal of Microbiology* **2016**, 56(2), 198-204.

Tang, Y. J., Shui, W., Myers, S., Feng, X., Bertozzi, C., Keasling, J. D., Central metabolism in Mycobacterium smegmatis during the transition from O 2-rich to O 2-poor conditions as studied by isotopomer-assisted metabolite analysis. *Biotechnology Letters* **2009**, *31*(8), 1233-1240.

Ventura, T. L. B., da Silva Machado, F. L., de Araujo, M. H., de Sousa Gestinari, L. M., Kaiser, C. R., de Assis Esteves, F., Lasunskia, E. B., Soares, A. R., Muzitano, M. F., Nitric oxide production inhibition and anti-mycobacterial activity of extracts and halogenated sesquiterpenes from the Brazilian red alga *Laurencia dendroidea* J. Argardh, *Pharmacognosy Magazine* **2015**, 11(suppl 4), S611.

van der Westhuyzen, R., Winks, S., Wilson, C. R., Boyle, G. A., Gessner, R. K., Soares de Melo, C., Taylor, D., de Kock, C., Njoroge, M., Brunschwig, C., Lawrence, N., Pyrrolo [3, 4-c] pyridine-1, 3 (2 H)-diones: A novel antimycobacterial class targeting mycobacterial respiration. *Journal of Medicinal Chemistry* **2015**, 58(23), 9371-9381.

Zani, C. L., Carroll, A. R., Database for rapid dereplication of known natural products using data from MS and fast NMR experiments. *Journal of Natural Products* **2017**, 80(6), 1758-1766.

Chapter 4

ISOLATION AND STRUCTURE ELUCIDATION OF NATURAL PRODUCTS FROM LAURENCIA GLOMERATA AND PLOCAMIUM CORNUTUM

4.1. Introduction

Screening of the fractionated library for anti-mycobacterial activity and profiling by ^{1}H NMR spectroscopy resulted in the identification of several potential projects for further study. The red algae *Laurencia glomerata* (NV160819-6) and *Plocamium cornutum* (NV160819-10) were selected for further study based on their biological activity, "interesting" chemical profile and availability of the algae.

This chapter will provide a brief overview of the natural products from *Laurencia* and *Plocamium* species of red algae followed by a discussion of the isolation and structure elucidation of the major natural products from the two selected algae.

4.1.1. Natural products from *Laurencia* spp.

Figure 4.1: Underwater photograph of *Laurencia glomerata* [Anderson *et al.*, 2016].

Laurencia glomerata Kützing 1849: 857, belongs to the family Rhodomelaceae and is part of the order Ceramiales. It is a seaweed which is typically found along the Cape Peninsula in South Africa. This species of seaweed was also reported in temperate South America, Indonesia, India and Pakistan. *L. glomerata* can grow up to 40 cm tall and is described as a bush red plant [Andersen *et al*., 2016].

Laurencia spp. serve as a wealthy source of uniquely structured secondary metabolites, mainly of terpenoid origin. Major constituents reported include chamigranes, C15-acetogenins, sesquiterpenes and alkaloids, whilst minor compounds include diterpenes, triterpenes and steroids. Compounds isolated from the *Laurencia* spp. are characteristic due to the compounds containing a high degree of halogenation [Zhang *et al*., 2015]. Along the South African coastline there have been positive identification of fourteen *Laurencia* species namely: *L. glomerata, L. brongniartii, L. natalensis, L. complanata, L. peninsularis, L. corymbosa, L. pumila, L. flexuaosa, L. sodwaniensis, L. dichotoma, L. alfredensis, L. multiclavata, L. digitate* and *L. pumila var. dehoopiensis.* Five of the listed *Laurencia* species are considered to be endemic to South Africa or central and Southern Africa namely: *L. natalensis, L. complanata, L. pumila, L. flexuosa* and *L. peninsularis* [Francis *et al.*, 2017].

Scheme 4.1: Proposed cyclization of a terpene precursor initiated by a theoretical bromonium ion [Butler and Carter-Franklin, 2004].

The biogenesis and biosynthetic pathway of halogenated sesquiterpene molecules are not fully understood and most of them are not fully elucidated (Scheme 4.1) [Wang *et al.*, 2013].

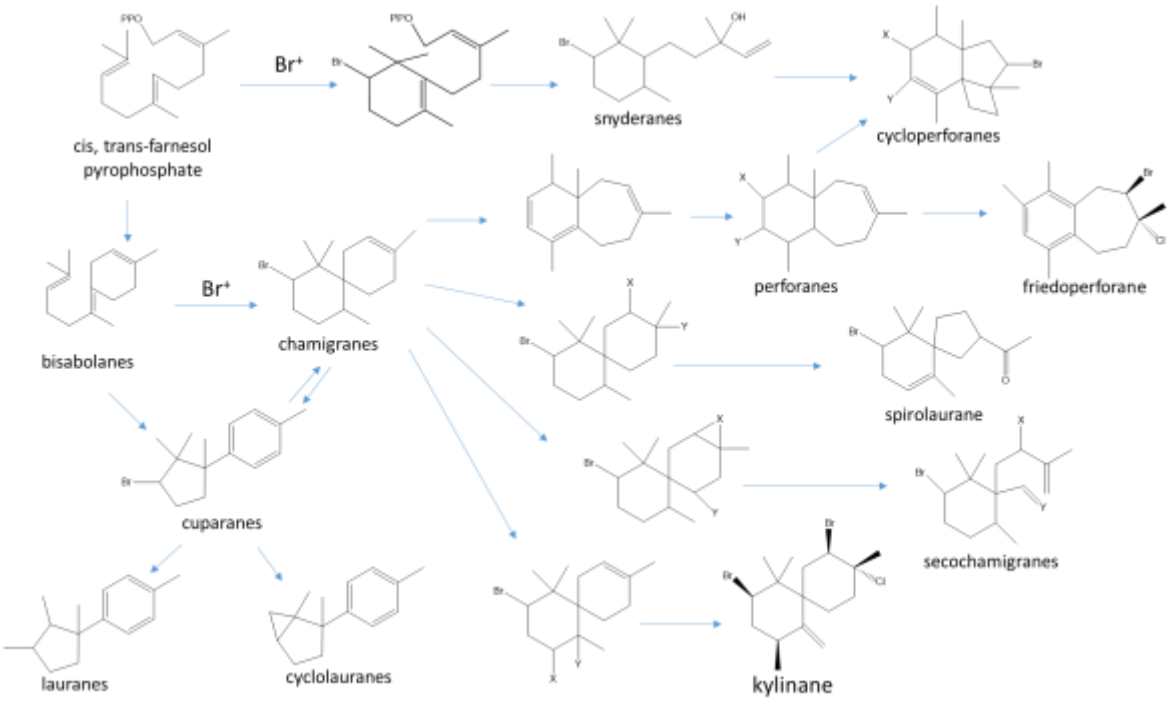

Scheme 4.2: The proposed biosynthesis of sesquiterpenes derived from cis,trans-farnesol pyrophosphate [Wang *et al.*, 2013].

The proposed biogenesis of sesquiterpenes derived from the Rhodomelaceae family is classed into two main categories. There are those arising from the precursors *cis,trans*-farnesol pyrophosphate and *trans,trans*-farnesol pyrophosphate (Scheme 4.2). Chamigranes are derived from the former category and are a crucial intermediate skeleton as it forms the base on which the construction of various more complex sesquiterpenes are built [Wang *et al.*, 2013]. Pacifenol (**4.1**) was the first natural product to be described as containing both chlorine and a bromine atom within the structure and was first discovered in the red algae *Laurencia pacifica* [Pereira *et al.*, 2016]. One well-reported chamigrane from *Laurencia* is elatol (**4.2**), this compound displays the classical terpene core structure, it is positively identifiable by the characteristic four methyl groups, the presence of both chlorine and bromine halogens as well as two cyclohexane rings fused at carbon 6 (C-6) [Chhetri *et al*., 2018]. Elatol (**4.2**) has been reported to be a cytotoxic halosesquiterpene, which is stated to be characteristic of this family. Many of the compounds isolated from *Laurencia* were reisolated from the sea hare *Aplysia dactylomela*. This is due to the fact that it feeds upon this algal species [Wang *et al.*, 2013]. Halogenated sesquiterpene compounds are produced as a defence mechanism to ward off most predators with their antifeedant activity [Mandrekar *et al.*, 2018]. Chamigranes are reported to have weak antibacterial and antiviral biological activities [Kimura *et* al., 1999; Vairappan *et al*., 2008].

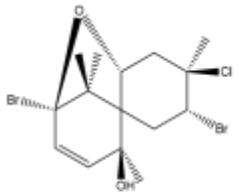

Pacifenol
4.1

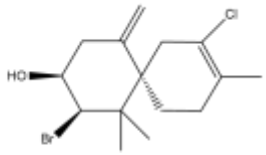

Elatol
4.2

The less commonly discovered sesquiterpene structures are highlighted in Figure 4.2 which indicates the diversity of these compounds.

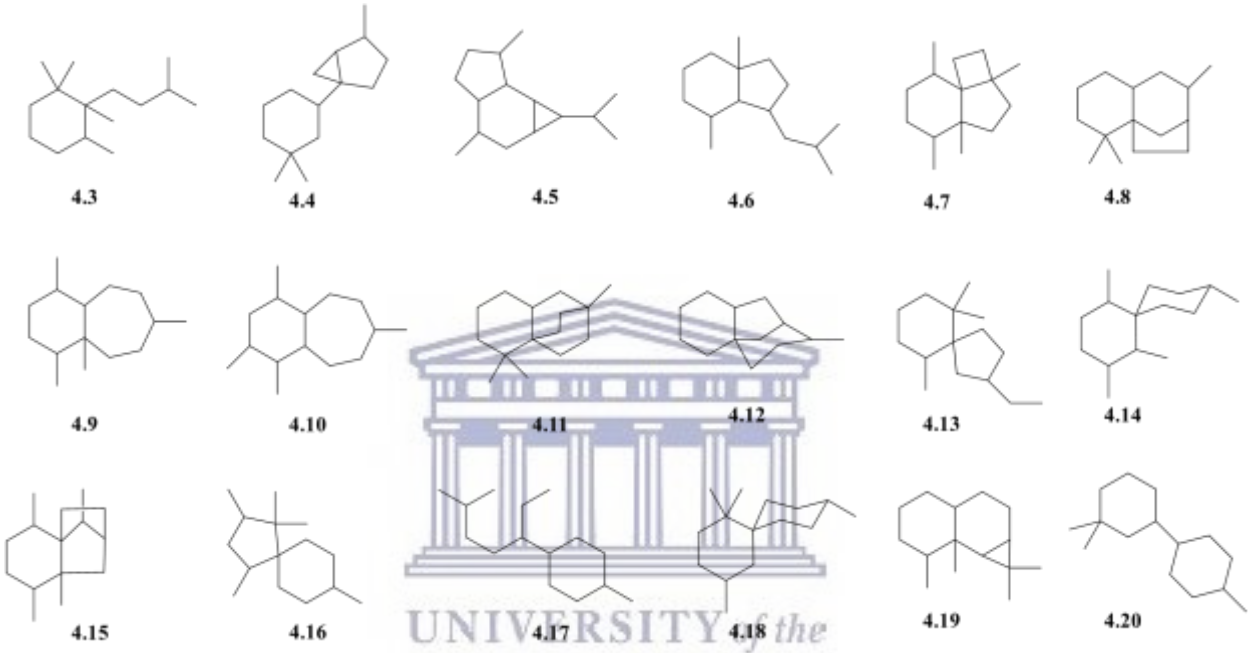

Figure 4.2: Basic scaffolds of less commonly isolated sesquiterpenes [Wang *et al.*, 2013].

4.1.2. Natural products from *Plocamium* spp.

Figure 4.3: Photograph of *Plocamium cornutum* [Anderson *et al.*, 2016].

Plocamium cornutum (Turner) Harvey 1849 (1847-1849), belongs to the family Plocamiaceae and is part of the order Gigartinales. This species of seaweed is endemic to Southern Africa and is usually abundant around the Cape of Good Hope. It was also reported to inhabit the area around Namibia. It inhabits areas where they are exposed to heavy surf and are usually found at low tide levels. *P. cornutum* is reddish-brow in colour and can grow up to 20 cm tall [Andersen *et al*., 2016].

The *Plocamium* genus has a vast distribution in the world's oceans. Along the South African coastline there have been successful identification of the following *Plocamium* species: *P. cornutum, P. glomeratum, P. corallorhiza, P. membranaceum, P. suhrii, P. telfairiae* and *P. beckeri* to name a few [Simon, 1946].

These species are known to produce cyclic and acyclic halogenated monoterpenes and more than 100 of these compounds have been documented [Knott, 2015; Vogel *et al.,* 2014]. The halogenated monoterpenes are reported to have cytotoxic, anticancer, antimicrobial and antifungal biological activities [Afolayan *et al.,* 2009].

Compounds which are structurally composed of five-carbon isoprene subunits are referred to as terpenoids. The vast structural diversity of this natural product class is attributed to the modification of the universal diphosphate precursor geranyl diphosphate (GDP) [Wise, 2003].

There is isoprenoid derived compounds within all living organisms. They are a result of branched isoprene units (C_5) that are repeated, rearranged, cyclized and oxidised to afford the vast structural diversity [Rohmer, 1999]. There are two biosynthetic pathways that utilize isoprene units to form geranyl pyrophosphate, the precursor required to synthesize terpenoid compounds. These pathways are the mevalonate and the non-mevalonate pathway (Scheme 4.3).

4.1.2.1. The mevalonate pathway produces geranyl pyrophosphate

The mevalonate pathway begins with the two acetyl-CoA units which undergo an enzymatically catalysed (acetyl-CoA acetyl transferase) condensation and cleavage reaction to form acetoacetyl-CoA. An additional acetyl-CoA unit is then attached to acetoacetyl-CoA via a catalysed (HMG-CoA synthase) condensation reaction to irreversibly form 3-hydroxyl-3-methylglutaryl-CoA (HMG-CoA). Subsequent to the formation of HMG-CoA, it is then reduced by HMG-CoA reductase in the presence of nicotinamide adenine dinucleotide phosphate (NADPH) to form mevalonic acid (MVA). The MVA is phosphorylated through a reversible reaction by mevalonate kinase in the presence of adenosine triphosphate (ATP) to produce mevalonate 5-phosphate and adenosine diphosphate (ADP). Mevalonate 5- phosphate undergoes a second catalysed (phosphomevalonate kinase) phosphorylation reaction in the presence of ATP to yield mevalonate 5-diphosphate (MVA 5-diphosphate) and ADP. In enzyme catalysed (mevalonate diphosphate decarboxylase) decarboxylation reaction of MVA 5-diphosphate, the establishment of two foundation isoprene units; isopentenyl 5-diphosphate (IPP) and dimethylallyl pyrophosphate (DMAPP) are formed [Miziorko, 2011 and Rohmer, 1999]. The catalysed (prenyltransferases) condensation reaction joins IPP onto DMAPP, in a trans (E) conformation, to form a larger prenyl intermediate geranyl pyrophosphate (GPP). GPP is the preferred universal precursor for the biosynthesis of monoterpenes (Scheme 4.3) [Schilmiller *et al.*, 2009].

4.1.2.2. The mevalonate-independent pathway

The pathway that is mevalonate-independent occurs in algae, eubacteria, plant chloroplasts and some parasites. This pathway is more commonly known as the 2C-methyl-D-erythritol-4-phosphate (MEP) or the 1-deoxy-D-xylulose-5-phosphate (DOXP) pathway. This biosynthetic pathway begins with a catalysed (deoxy-D-xylulose-5-phosphate synthase) condensation reaction between glyceraldehyde 3-phosphate and pyruvate, subsequently, DOXP is formed. In an isomerization reaction (1-deoxy-D-xylulose-5-phosphate reductoisomerase) DOXP is converted to MEP. The precursor molecule dimethyl diphosphate (IPP) is formed when MEP undergoes a sequence of enzymatically catalysed reactions. The enzymes responsible for the catalysed reaction are: 4-diphosphocytidyl-2C-methyl-D-erythritol cytidylyltransferase, 4-diphosphocytidyl-2C-methyl-D-erythritol kinase, 2C-methyl-D-erythritol-2,4-cyclodiphosphate synthase, 1-hydroxy-2-methyl-2-(E)-butenyl-4-diphosphate synthase, 4-hydroxy-3-methyl-2-(E)-butenyl-4-diphosphate reductase and lastly isopentenyl diphosphate isomerase. Comparable to the mevalonate pathway, IPP and DMAPP can undergo an isomerization reaction to form GPP (Scheme 4.3) [Hunter, 2007].

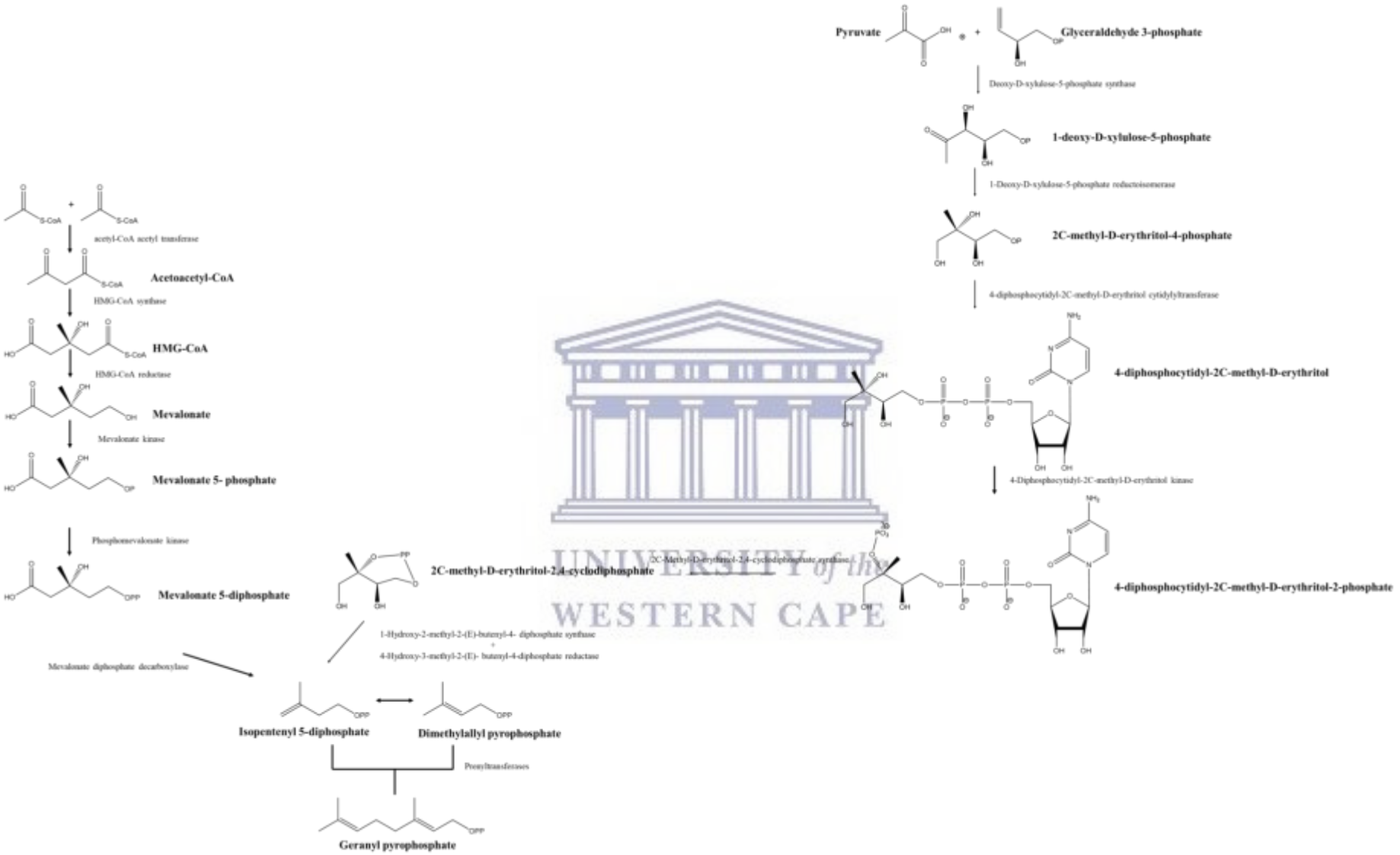

Scheme 4.3: The mevalonate and non-mevalonate pathway for the production of geranyl pyrophosphate

Based on the biosynthesis of geranyl pyrophosphate (GPP), when the precursor GPP loses the diphosphate acid (HOPP) moiety, it generates two important structures for the biosynthesis of various monoterpenes, ocimene and mycrene (Scheme 4.4). Ocimene plays an important role as structural modifications afford preplocamene B and C, which forms the starting point for the cyclization of acyclic monoterpenes to plocamene D and epi-plocamene D (Scheme 4.5). An enzyme catalysed electrophilic addition reaction is responsible for the formation of polyhalogenated monoterpenes [Naylor *et al.,* 1983]. The ocean is a rich source of halide compounds (Cl^-, Br^- and I^-); thus it is not surprising that a large number (15-20%) of newly discovered marine natural products are organohalides. Haloperoxidase is an enzyme found in marine organisms which chlorinate or brominate organic compounds in the presence of these halogens (Scheme 4.4) [Gribble, 2009]. The halogenated monoterpenes found in *Plocamium* is derived from the precursor ocimene [Polzin and Rorrer, 2003].

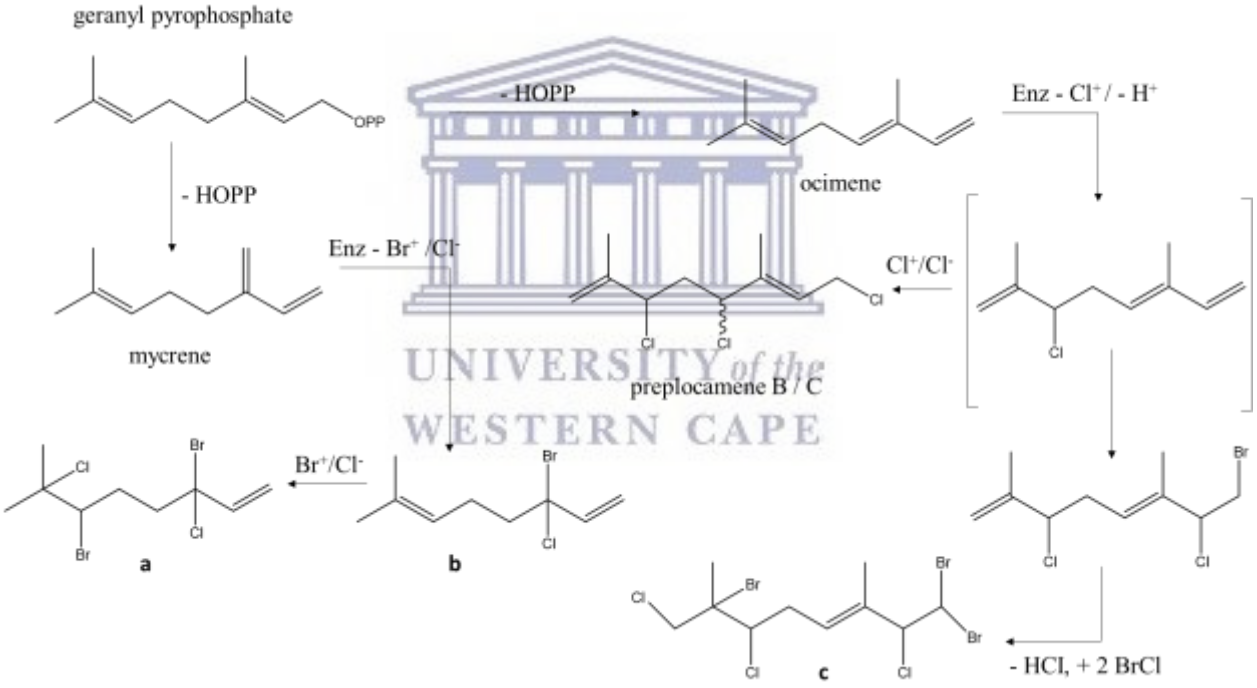

Scheme 4.4: Biosynthetic conversion of ocimene and mycrene to polyhalogenated monoterpenes [Naylor *et al.,* 1983].

Scheme 4.4 depicts the conversion of GPP into the respective precursors, ocimene and mycrene and lastly altering the precursors into various halogenated monoterpenes. A vital part of the biogenesis of halogenated monoterpene compounds is represented by reactions **a**, **b** and **c**, which involves the addition of either Cl^- or Br^-, followed by loss of HX, or addition of Cl^+/Br^- or Br^+/ Cl^- [Naylor *et al.*, 1983].

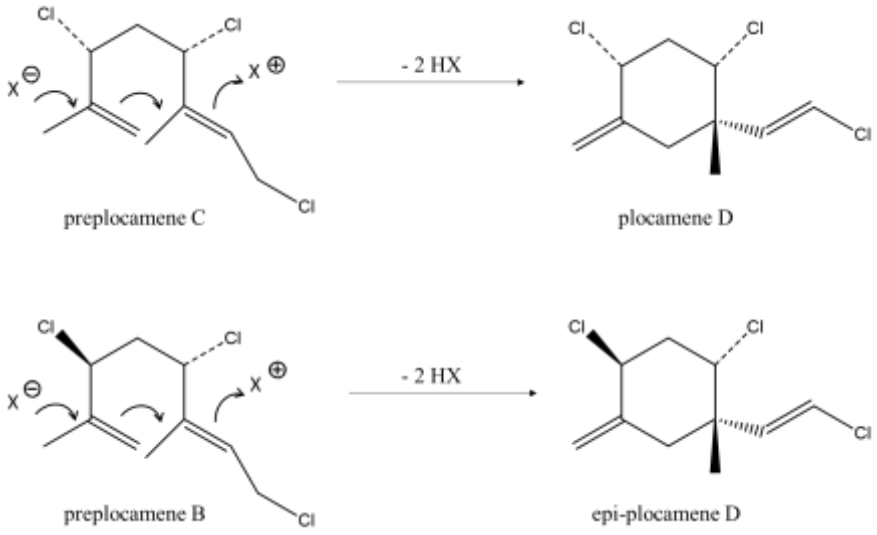

Scheme 4.5: Proposed biosynthesis of cyclic monoterpenes The general monoterpene scaffolds on which most halogenated monoterpenes are based is shown in Figure 4.3 [Naylor *et al.*, 1983].

Figure 4.4: Basic monoterpene scaffolds isolated from various *Plocamium* spp.

4.1.3. Chapter aims and objectives

The aim of this part of the research was to isolate and identify the main anti-mycobacterial natural products from *P. cornutum* and *L. glomerata*.

4.2. Results and Discussions

4.2.1. Extraction and isolation of chamigranes from *L. glomerata* (NV160819-6)

Figure 4.5: A picture of *Laurencia glomerata* collected from Nature's Valley

A portion of the *Laurencia glomerata* (242.0 g) frozen bulk sample was removed and allowed to thaw in de-ionized water for approximately one hour. The alga was removed from the water (Fr W), dried with sheets of absorbent paper, and sequentially extracted with MeOH (Fr M) and MeOH-CH_2Cl_2 (1:2, Fr MD). The de-ionized water (Fr W) was tinted a pink colour, which prompted the filtration of this water fraction and the addition of HP20 to adsorb any organic compound which may have been present. The HP20 was extracted using CH_2Cl_2 and MeOH steeps, each extraction was kept separate. Compound **4.28** was isolated via silica gel column chromatography of the HP20 CH_2Cl_2 extract. The organic extracts (Frs M and MD) was filtered, combined and dried under reduced pressure. The extract contained water and which was extracted with CH_2-Cl_2. The latter was collected and dried to yield a dark green oily crude extract which weighed 1.6 g. Repeated silica gel column chromatography and preparative TLC gave compounds **4.27** and **4.29** respectively (Scheme 4.6) (Figure S4.1).

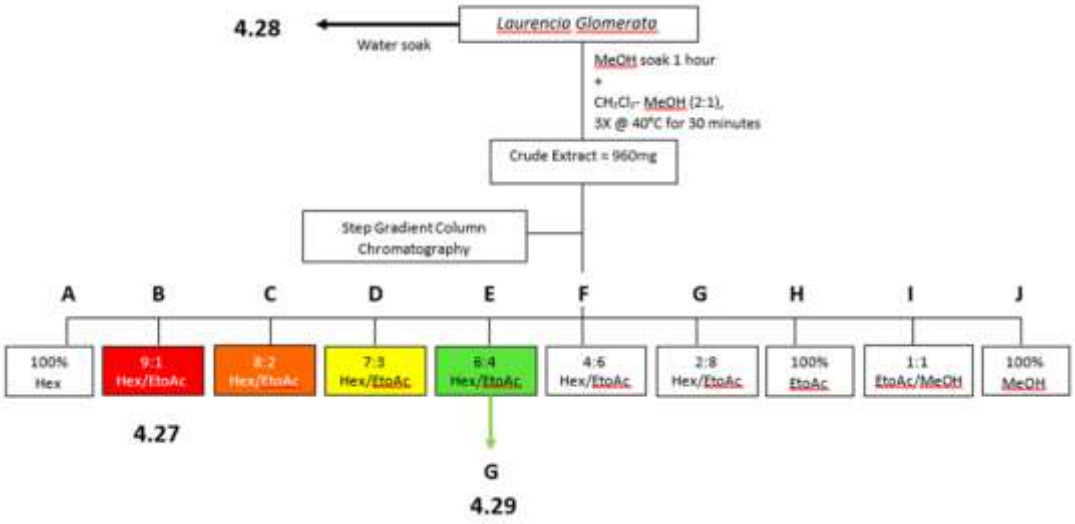

Scheme 4.6: Simplified scheme indicating the isolation of compounds **4.27, 4.28** and **4.29** from *Laurencia glomerata*

4.2.2. Structural elucidation of isolated compounds from *Laurencia glomerata*

4.2.2.1. Compound 4.27 (LG-Fr-B)

Compound **4.27** was isolated as an optically active yellow oil, $[\alpha]_D^{22^\circ}$= +10 ° (CH_2Cl_2), from the initial step gradient fraction B. The molecular formula of $C_{15}H_{21}{}^{79}Br_2{}^{35}ClO_3$ was established on the basis of high resolution ESIMS negative data (m/z 440.9468, the calculated mass was 440.9467). The infrared (IR) spectrum exhibited absorptions of a possible broad hydroxyl stretch slightly outside of the expected range (3576.37 cm^{-1}) (Figure S4.2 and Figure S4.3)

The ^1H NMR spectrum ($CDCl_3$) of compound **4.27** (Figure 4.6), showed four methyl signals at δ 0.99 (H-12), 1.54 (H-13), 1.49 (H-14) and 1.92 (H-15), respectively. There were two methylene signals at δ 2.52 and δ 2.14. Based on the observed signals there were four deshielded methine signals within the molecule at δ 3.08, 3.66, 4.03 (H-1) and 4.73 (H-4).

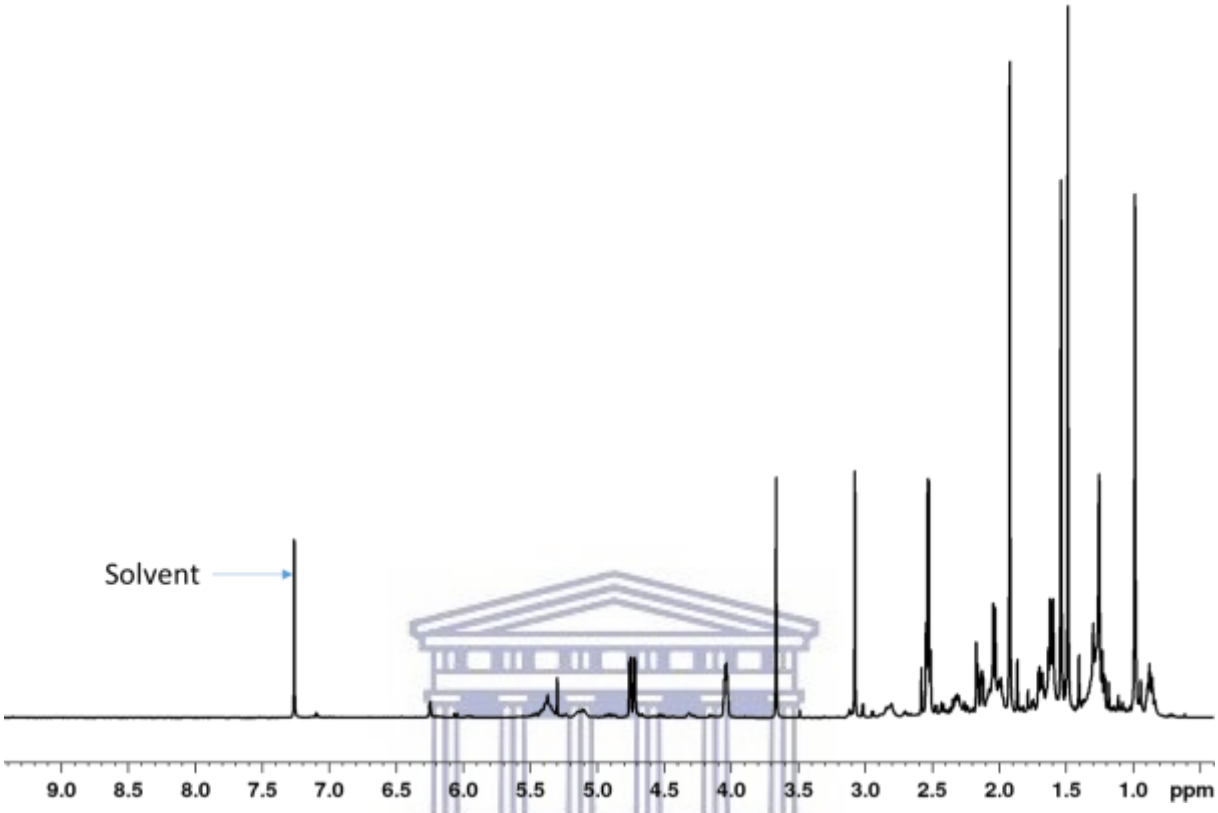

Figure 4.6: ^{1}H NMR spectrum of compound **4.27** (Figure S4.4)

The ^{13}C NMR ($CDCl_3$) spectrum of **4.27** (Figure 4.7) exhibited 15 carbon signals, five quaternary carbon signals at δ 71.6 (C-3), 50.21 (C-6), 61.6 (C-7), 75.57 (C-10) and 46.8 (C-11). The ^{13}C NMR spectrum in combination with the DEPT-135 revealed two methylene signals (CH_2) at δ 47.2 (C-2) and 33.9 (C-5). There were four methyl signals at δ 24.4 (C-12), 27.2 (C-13), 22.2 (C-14) and 28.0 (C-15) (Figure S4.5 and Figure S4.6)

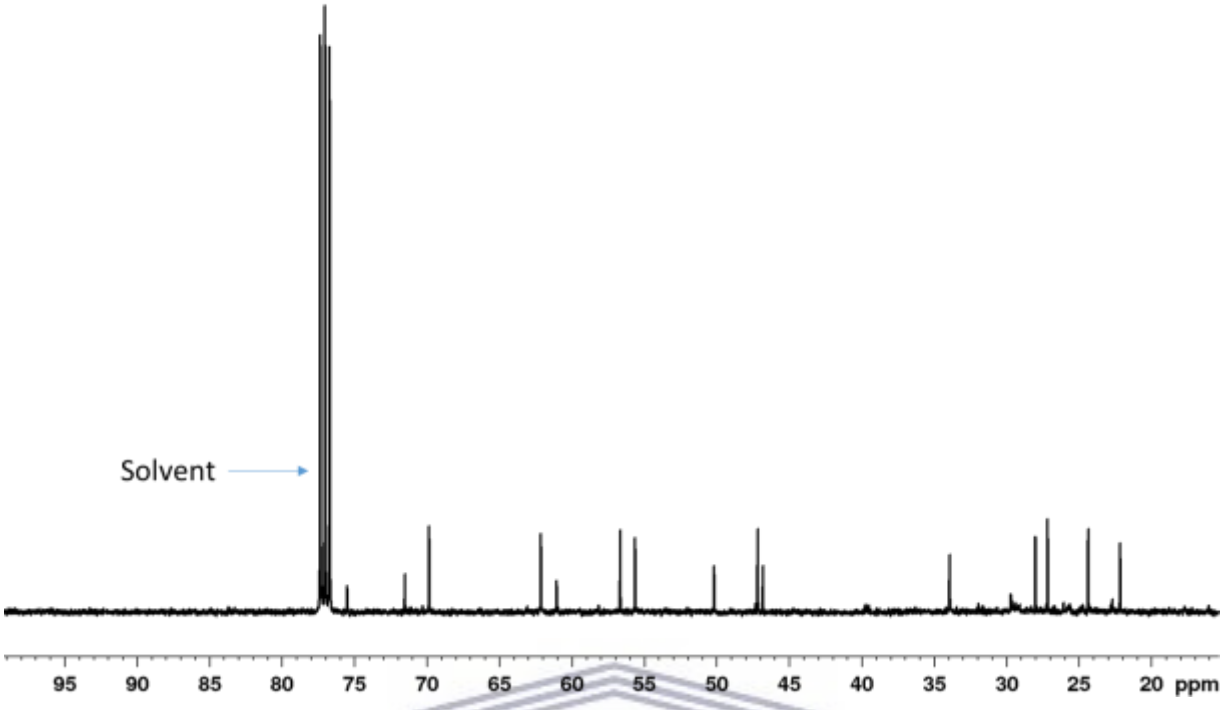

Figure 4.7: ^{13}C NMR spectrum of compound **4.27** (Figure S4.3)

The HMBC and COSY spectra were used to outline the planar structure of the compound. The methylene signal at δ 2.52 (H-2) correlated with a methine signal at 69.9 (C-1), a quaternary carbon signal at 71.6 (C-3) and a methyl signal at 28.0 (C-15). The methine signal at δ 3.08 (H-8) correlated with deshielded carbon signals at δ 61.6 (C-7), 55.7 (C-9), 75.6 (C-10) and a methyl signal at 22.2 (C-14). From the spectrum it was clear C-6, was the linking carbon between the two cyclohexane rings. This was evident from the protons situated on the methyl groups at δ 0.99 (H-12), 1.54 (H-13) and 1.49 (H-14) all showed a positive correlation to C-6. These correlations confirmed the presence of two cyclohexane rings fused at C-6. The geminal dimethyls were situated on C-11, this was confirmed with the correlations from the methyl signal at δ 0.99 (H-12) to a methyl carbon at δ 27.2 (C-13) and the quaternary carbon at δ 46.8 (C-11). The COSY spectrum revealed correlations between H-13 and H-12 and H-4 and H-5 which indicated their close proximity to each other respectively. These correlations assisted in establishing the planar chamigrane structure as seen in Figure 4.8 (Figure S4.7 and Figure S4.9)

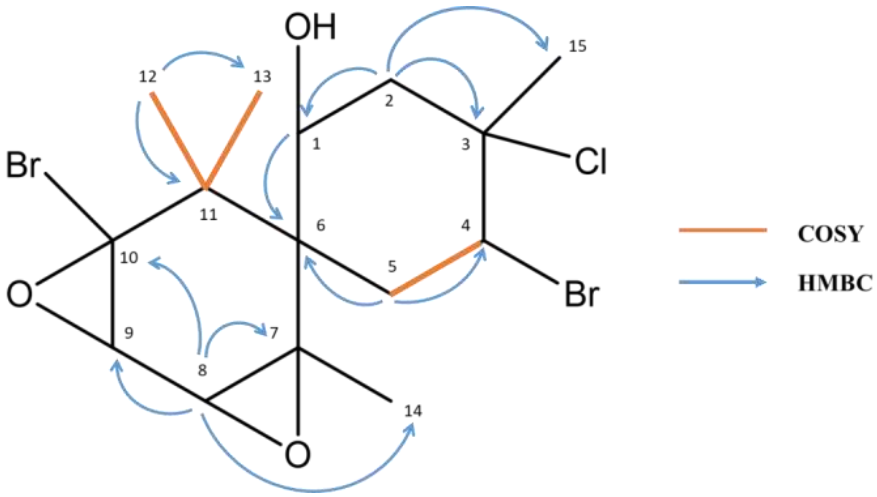

Figure 4.8: HMBC and COSY correlations for compound **4.27**

All spectroscopic data for **4.27** is consistent with the structure of prepacifenol epoxide previously isolated from the sea hare *Aplysia dactylomela* [Faulkner *et al.* 1974; MPhail *et al.*, 1999]. The stereochemistry of compound **4.27** was assigned based on the NOESY spectrum and comparison of the optical rotation data in published literature by Faulkner *et al.* (1974) and MPhail *et al.* (1999).

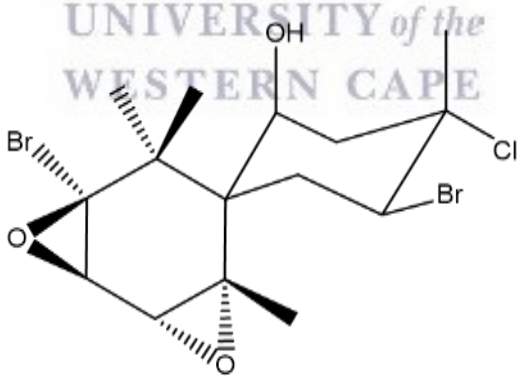

Compound **4.27**

Table 4.1: NMR data for compound **4.27 (LG- Fr-B)** (400 MHz, $CDCl_3$)

Carbon Number	δ_C	δ_C Lit.	Type	δ_H; multi (*J* Hz)	δ_H Lit.	COSY	HMBC
1	69.9	69.8	CH	4.03 *m*	4.03	H-2, H-5	C-3, C- 4, C-5, C-6, C-7
2	47.2	47.2	CH_2	2.52 *m*	2.52	H-5*	C-1, C-3, C-4, C-6, C-11, C-13, C-15
3	71.6	71.5	C	-	-	-	-
4	62.1	62.1	CH	4.73 *dd* (*J* = 4.03, 17.4 Hz)	4.73	H-5*, H-5	C-5, C-3, C-15, C-2, C-6
5	33.9	33.9	CH_2	2.52 *m*	2.54	-	C-6, C-4, C-1, C-15, C-13, C-11, C-3
5*				2.14 *m*	2.14	-	C-6, C-4, C-1, C-3, C-11, C-7
6	50.2	50.2	C	-	-	-	-
7	61.6	61.0	C	-	-	-	-
8	56.7	56.7	CH	3.08 *s*	3.06	H-14	C-9, C-7, C-14, C-10, C-1
9	55.7	55.6	CH	3.66 *s*	3.65	H-14	C-8, C-10, C-7, C-14
10	75.6	75.5	C	-	-	-	-
11	46.8	46.8	C	-	-	-	-
12	24.4	24.3	CH_3	0.99 *s*	0.98	-	C-11, C-13, C-10, C-6, C-14, C-13, C-15, C-2
13	27.2	27.2	CH_3	1.54 *s*	1.53	H-12	C-11, C-6, C-10, C-5, C-2
14	22.2	22.1	CH_3	1.49 *s*	1.48	-	C-7, C-6, C-8, C-12, C-11, C-9, C-4, C-1
15	28.0	28.0	CH_3	1.92 *s*	1.91	-	C-4, C-3, C-7, C-1, C-11

4.2.2.2. Compound 4.28 (LG-DCMHP20)

Compound **4.28** was isolated as an optically active, $[\alpha]_D^{22^\circ}$= -89° (CH_2Cl_2), opaque oil from the aqueous extraction of the *L. glomerata* seaweed. The molecular formula of $C_{15}H_{20}O_3{}^{37}Cl^{79}Br_2$ was established on the basis of high resolution ESIMS negative data (m/z 443.0034, the calculated mass was 443.1108). The infrared (IR) spectrum exhibited an absorption of a broad hydroxyl stretch (3510cm^{-1}) (Figure S4.11 and Figure S4.12)

The ^{1}H NMR spectrum of compound **4.28** (Figure 4.9), showed the presence of four methyl signals at δ 1.16 (H-12), 1.28 (H-13), 1.45 (H-14) and 1.74 (H-15), respectively. There were two methylene signals at δ 2.23 (H-2) and 2.12 (H-5), two epoxy methine signals at δ 4.65 (H-1) and 3.20 (H-8) and lastly, two methine signals at δ 4.30 (H-4) and 4.03 (H-9) (Figure S4.13).

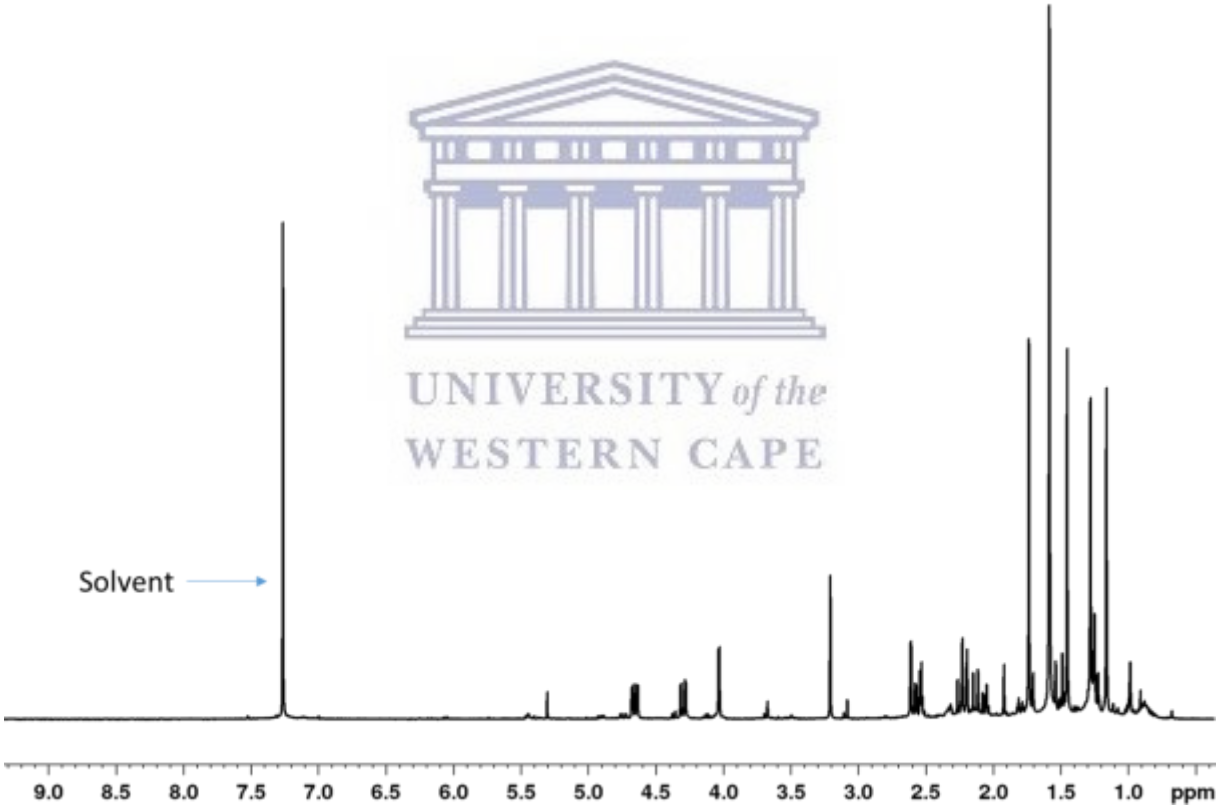

Figure 4.9: ^{1}H NMR spectrum of compound **4.28**

The ^{13}C and DEPT-135 NMR spectra of **4.28** (Figure 4.10) showed 15 signals of which five were quaternary carbon signals at δ 68.1 (C-3), 50.7 (C-6), 61.5 (C-7), 113.6 (C-10) and 49.7 (C-11); four methyl signals at δ 18.5 (C-12), 24.9 (C-13), 21.8 (C-14) and 31.4 (C-15); two methylene signals at δ 45.4 (C-2) and 33.9 (C-5). Lastly, methine signals at δ 74.86 (C-1), 58.1 (C-4), 59.9 (C-8) and 74.80 (C-9). These data sets were suggestive of a chamigrane sesquiterpene (Figure S4.14 and Figure S4.15).

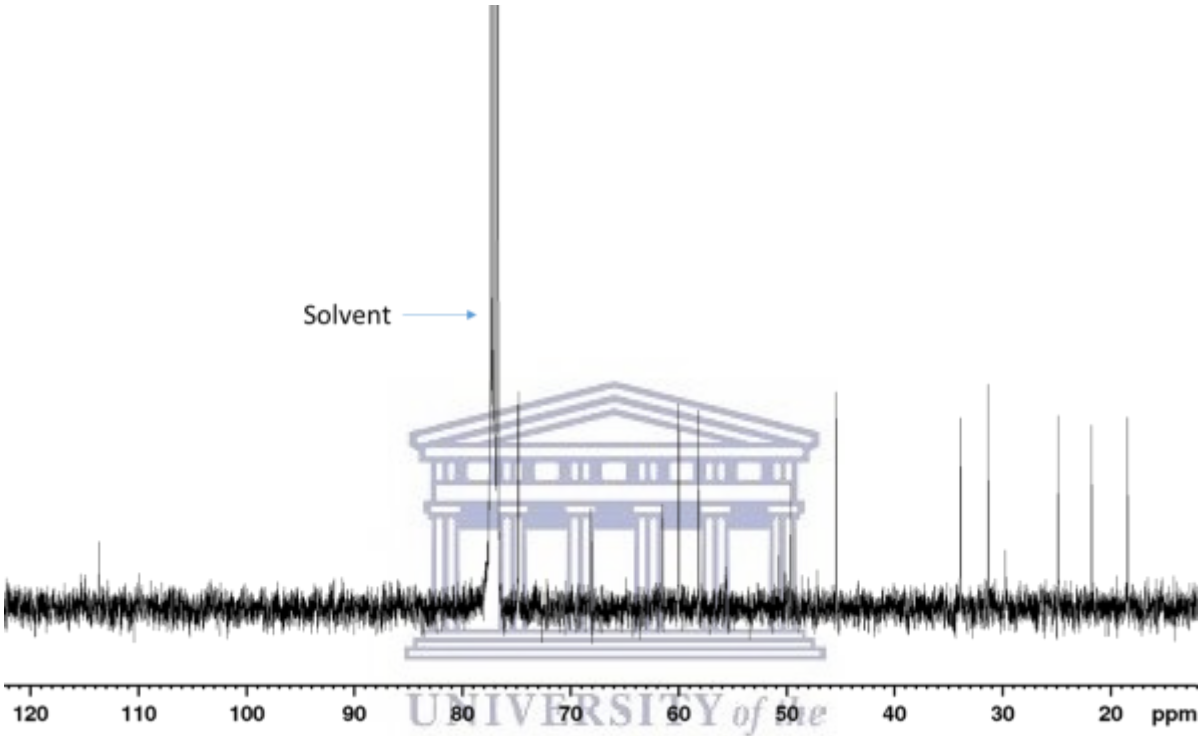

Figure 4.10: ^{13}C NMR spectrum of compound **4.28**

The HMBC and COSY spectra were used to outline the planar structure of the compound, in order to identify the 15 carbon structure. The proton signal at δ 2.23 (H-2) correlated with δ 74.86 (C-1), 68.1 (C-3), 31.4 (C-15) and 58.1 (C-4). The H-9 methine signal correlated to δ 61.5 (C-7), 59.9 (C-8), 113.6 (C-10) and 49.7 (C-11). H-9 correlations confirmed a ring system. Finally, there were correlations from the methyl proton at H-14 to δ 33.9 (C-5), 50.7 (C-6) and 61.5 (C-7), respectively. The long range correlation observed between H-14 to C-6 and C-5 suggested a closed ring system. The COSY spectrum revealed close correlations between H-2 and H-1 and between H-4 and H-5 (Figure 4.11) (Figure S4.16 and Figure S4.18).

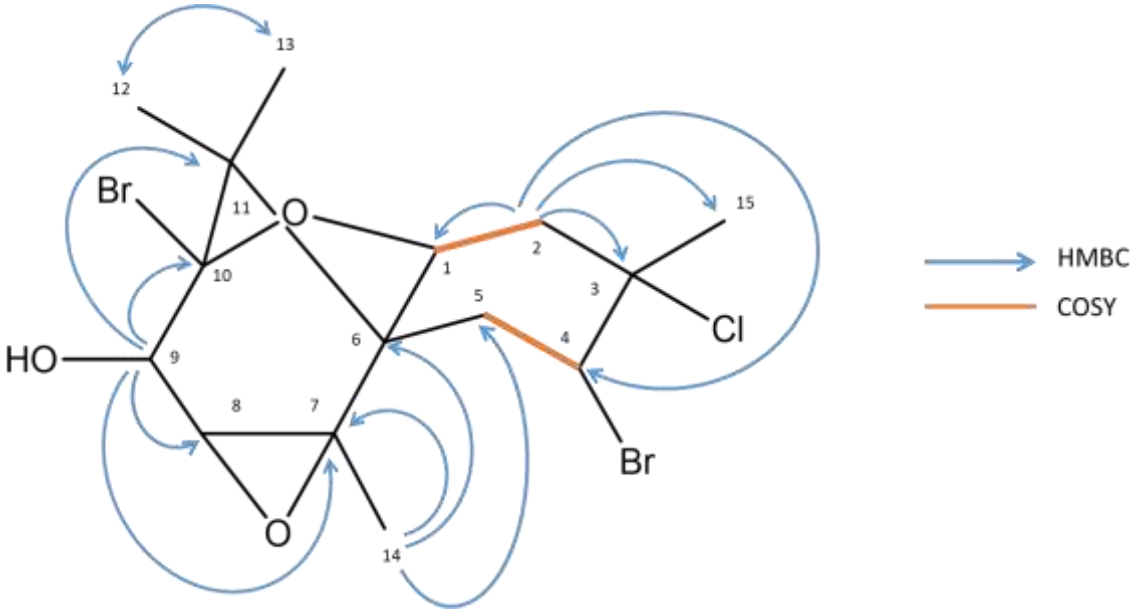

Figure 4.11: HMBC and COSY correlations for compound **4.28**

All spectroscopic data for **4.28** is consistent with the structure of johnstonol previously isolated from the sea hare *Aplysia dactylomela* [Kaiser *et al.*, 2001].

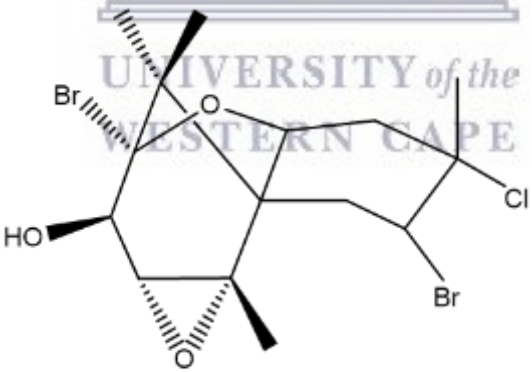

Compound **4.28**

Table 4.2: NMR data for compound **4.28 (LG-DCMHP20)** (400 MHz, $CDCl_3$)

Carbon Number	δ_C	δ_C Lit.	Type	δ_H; multi (*J*, Hz)	δ_H Lit.	COSY	HMBC
1	74.86	74.2	CH	4.65 dd (*J* = 4.8, 13.4 Hz)	4.58 dd	H-5, H-2, H-2*	C-7
2	45.4	45.2	CH_2	2.23 dd (*J* = 3.2, 14.2 Hz)	2.23 dd	H-1	C-1, C-15, C-11, C-3, C-7, C-4
2*				2.54 dd (*J* = 4.5, 14.7 Hz)	2.45 dd	-	C-6, C-4, C-7, C-9
3	68.1	68.0	C	-	-	-	-
4	58.1	58.1	CH	4.30 dd (*J* = 3.0 Hz)	4.22 dd	H-5	C-3
5	33.9	33.6	CH_2	2.12 m	2.13 dd	H-4	
6	50.7	50.4	C	-	-	-	-
7	61.5	61.1	C	-	-	-	-
8	59.9	61.0	CH	3.20 s	3.16s		C-10, C-7, C-14, C-9
9	74.80	73.8	CH	4.03 d (*J* = 3.0 Hz)	4.00 d	H-2*	C-C- 8, C-7, C-11
10	113.6	112.6	C	-	-	-	-
11	49.7	49.3	C	-	-	-	-
12	18.5	18.2	CH_3	1.16 s	1.11s	-	C-13, C-11
13	24.9	24.6	CH_3	1.28 s	1.20s	-	C-12, C-10, C-11
14	21.8	21.5	CH_3	1.45 s	1.35s	-	C-7, C-6, C-8, C-11, C-5
15	31.4	31.0	CH_3	1.74 s	1.64s	-	C-2, C-4, C-3, C-1

There were four chamigrane structures which were reported by Masuda *et al.* in 1996, and under various conditions interconvert from one structural form to another. As seen in Figure 4.12, prepacifenol **4.2** was able to convert to pacifenol and prepacifenol epoxide (**4.27**) while prepacifenol epoxide was able to convert to johnstonol (**4.28**) [Masuda *et al.*, 1996].

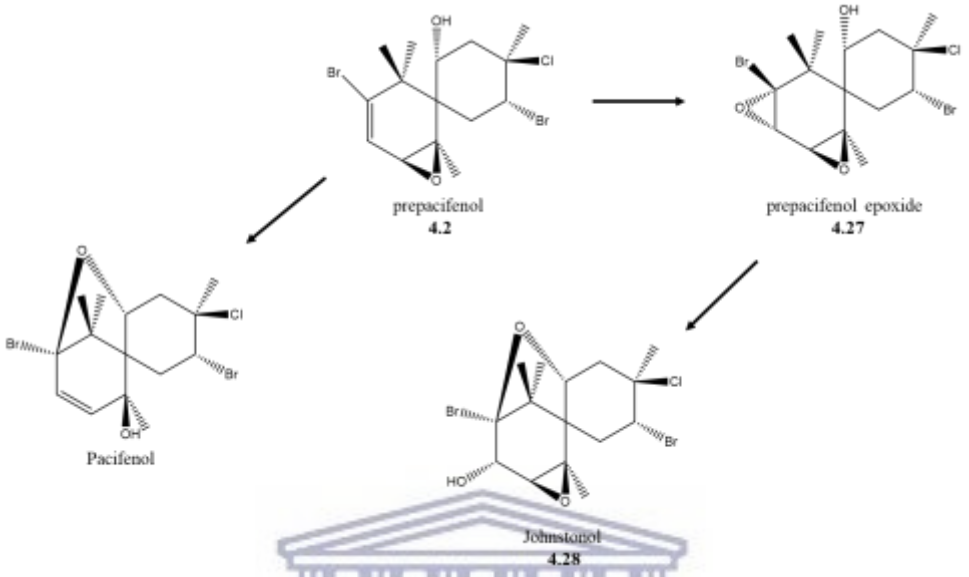

Figure 4.12: Interconversions of various chamigranes [Masuda *et al.*, 1996].

4.2.2.3. Compound 4.29 (LG-Fr-E-G)

Compound **4.29** was isolated as an optically active, $[\alpha]_D^{22^\circ} = -59^\circ$ (CH_2Cl_2), oil from fraction E of the *L. glomerata* seaweed. Although the sample was submitted for HRESIMS no M^+ could be obtained for the compound. Due to insufficient material availability, further investigation was not possible. The infrared (IR) spectrum exhibited absorption of a broad hydroxyl stretch ($3576cm^{-1}$) (Figure S4.20).

The ^1H NMR spectrum ($CDCl_3$) of compound **4.29**, exhibited four methyl signals at δ 1.81 (H-15), 1.27 (H-12), 1.53 (H-13) and 1.56 (H-14), respectively. Two methylene signals at δ 2.17 (H-5) and 1.25 (H-2) and five methine signals at δ 2.90 (H-4), 4.69 (H-1), 4.37 (H-10), 4.18 (H-9) and 6.33 (H-8) were also observed (Figure 4.13) (Figure S4.21).

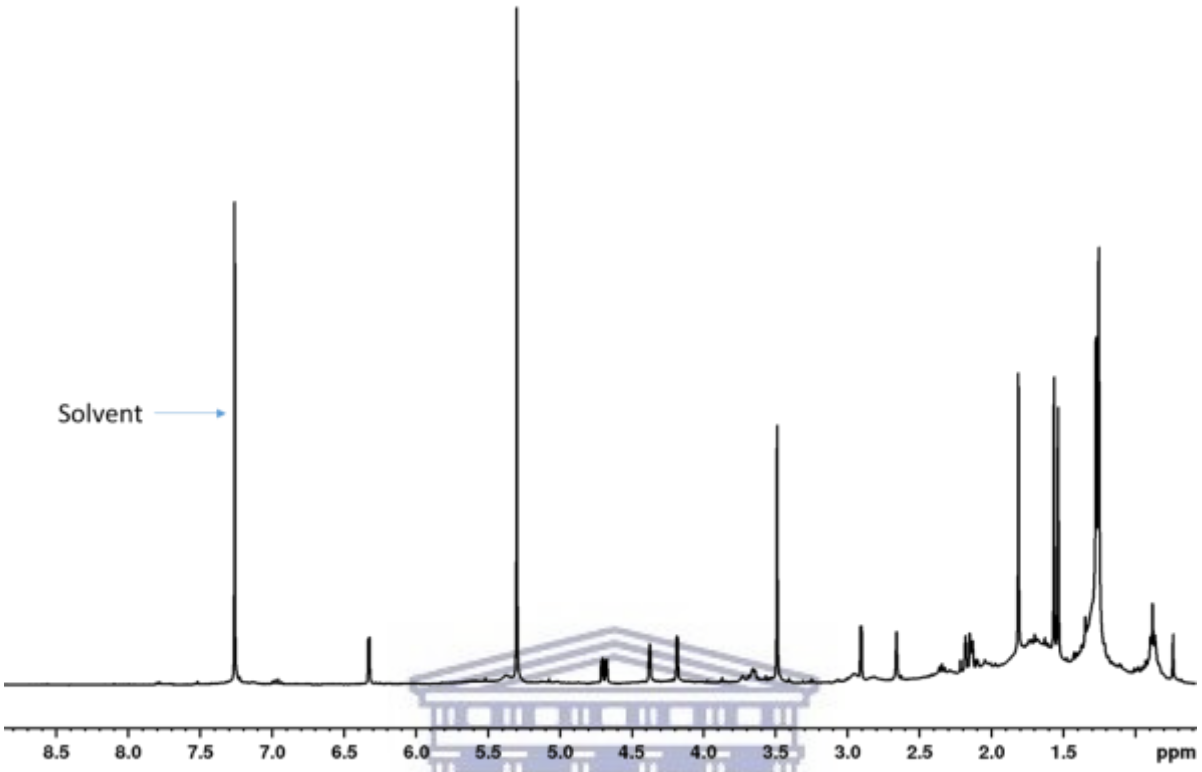

Figure 4.13: ^{1}H NMR (400 MHz, $CDCl_3$) spectrum of compound **4.29**

The ^{13}C NMR spectrum in association with the DEPT-135 showed 16 carbon signals including four methyl groups signals at δ 21.4 (C-15), 23.6 (C-12), 24.6 (C-14) and 26.6 (C-13); two methylene signals at δ 29.7 (C-2) and 34.5 (C-5) and five methine signals at δ 56.9 (C-4), 58.0 (C-1), 73.2 (C-10), 77.3 (C-9) and 123.4 (C-8). Lastly, four quaternary carbon signals were also observed at δ 46.5 (C-11), 50.5 (C-6), 146.7 (C-7) and 78.8 (C-3). The downfield chemical shift of both C-7 and C-8 suggested that they were part of an olefinic bond (Figure 4.14) (Figure S4.22 and Figure S4.23).

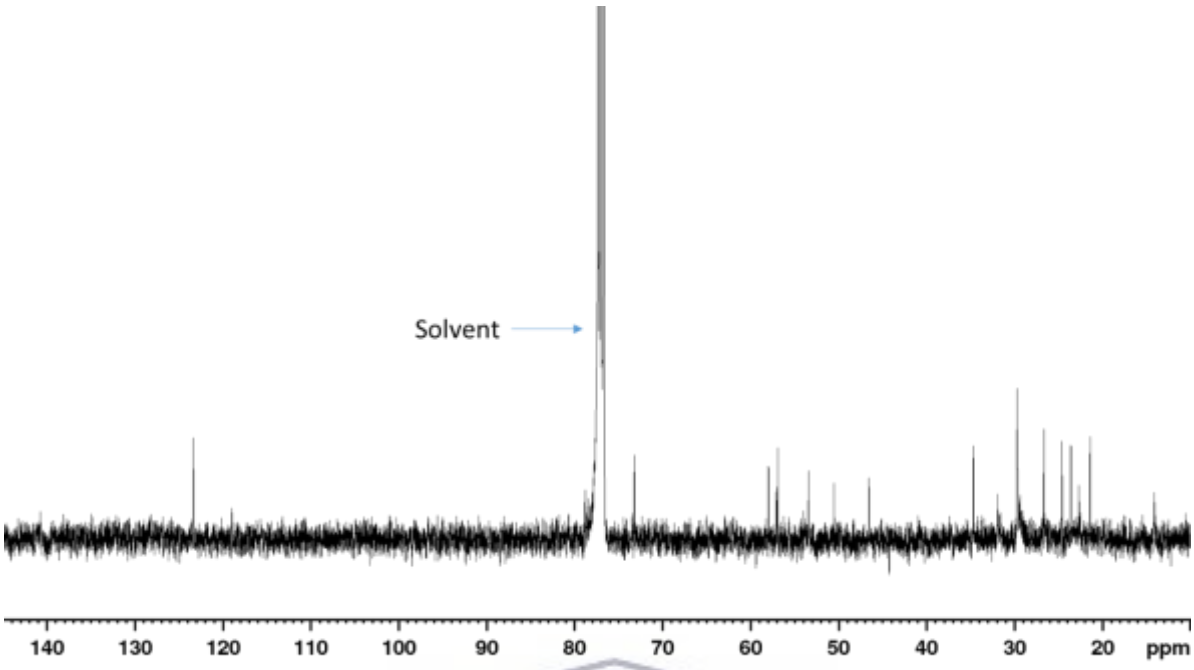

Figure 4.14: ^{13}C NMR spectrum of compound **4.29**

The HMBC and COSY spectra were used to outline the planar structure of the compound, in order to identify the 16 carbon structure. The methine signal at δ 4.69 (H-1) and the methyl protons at δ 1.18 (H-15) correlated with δ 77.8 (C-3). The methine signal at δ 2.90 (H-4) has a number of long range correlations to δ 146.7 (C-7), 123.4 (C-8) and 24.6 (C-14). The protons at δ 2.17 (H-5) and δ 1.53 (H-13), both correlated to δ 50.5 (C-6). These correlations confirmed the placement of C-6 as the link between the two cyclohexane rings. These correlations, together with comparison to compounds **4.27** and **4.28** and literature finalized the planar structure of 4.29 (Figure 4.15) (Figure S4.24 and Figure S4.26).

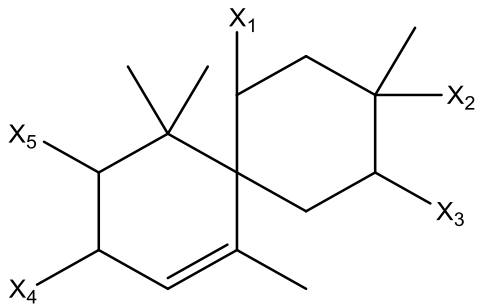

Figure 4.15: Proposed planar structure for compound **4.29**

After an exhaustive literature search, this proposed structure was not found and indicated the possibility of a new chamigrane structure. In Figure 4.16, the basic scaffold of Compositacins H with just the comparator chemical shifts were indicated. As seen in the structure the double bond carbon shifts of δ 143.4 and 123.8 closely matched the shifts observed for compound **4.29** and implied that the double bond was correctly assigned. The methyl carbon observed at δ 25.6 also closely resembled compound **4.29**, thus the assignment of the methyl group at position 14 was correct. The carbon bearing the alcohol moiety has a chemical of δ 73.2 for **4.29** was vastly different from the chemical shift observed for the compound, which was δ56.9. Based on the signal observed it was clear there was a different functional group attached at C-9 and X_4 has been assigned to this moiety. The second difference was observed at position C-4. Compositacins H has a chemical shift of δ 60.7 and compound **4.29** exhibited a chemical shift of δ 58.0. The downfield shift observed could potentially be due to the influence of the functional group attached at C-1. Lastly, the shift at C-1 of δ 30.1 was very different from what was observed for compound **4.29**, which implied there was an additional functional group attached at this point which caused an upfield chemical shift. This observation could support the placement of the methoxy at position C-1 with a chemical shift of δ 77.3. The methoxy signal was initially thought to be an artefact signal in the ^{1}H NMR, upon completion of a second 1 and 2D NMR data set (conducted on different days), the methoxy signal was still present. The two sets of NMR data indicated that the methoxy was possibly attached to the molecule at position C-1 even though there were no HMBC correlations to this moiety [Yu *et al.*, 2017].

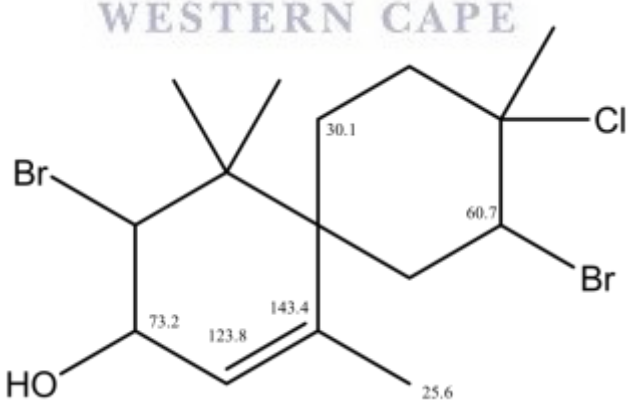

Figure 4.16: Structure of Compositacins H and key carbon chemical shift placements.

The HMBC and COSY spectra were used to outline the planar structure of the compound, in order to identify the 16 carbon structure. The proton signal at δ 4.18 (H-1) which was geminal to the methoxy moiety correlates with δ 77.8 (C-3). The methyl protons at δ 1.18 (H-15) correlated with C-3 and δ 58.0 (C-4). The protons at δ 2.17 (H-5) and δ 1.53 (H-13), both correlated to δ 50.5 (C-6). These correlations confirmed the placement of C-6 as the link between the two cyclohexane rings. Proton H-5 also correlated to C-4. The proton at H-13 also correlated to the germinal methyl carbon at δ 23.6 (C-12). The proton at δ 2.90 (H-9) has correlations to δ 146.7 (C-7), 123.4 (C-8) and 24.6 (C-14). A correlation was observed from δ 1.56 (H-14) to C-7. Lastly, there was a correlation from δ 1.27 (H-12) to δ 46.5 (C-11). There was COSY correlation between δ 4.37 (H-10) and H-12, H-5 and δ 4.69 (H-4) and lastly H-9 to δ 6.33 (H-8) (Figure 4.17).

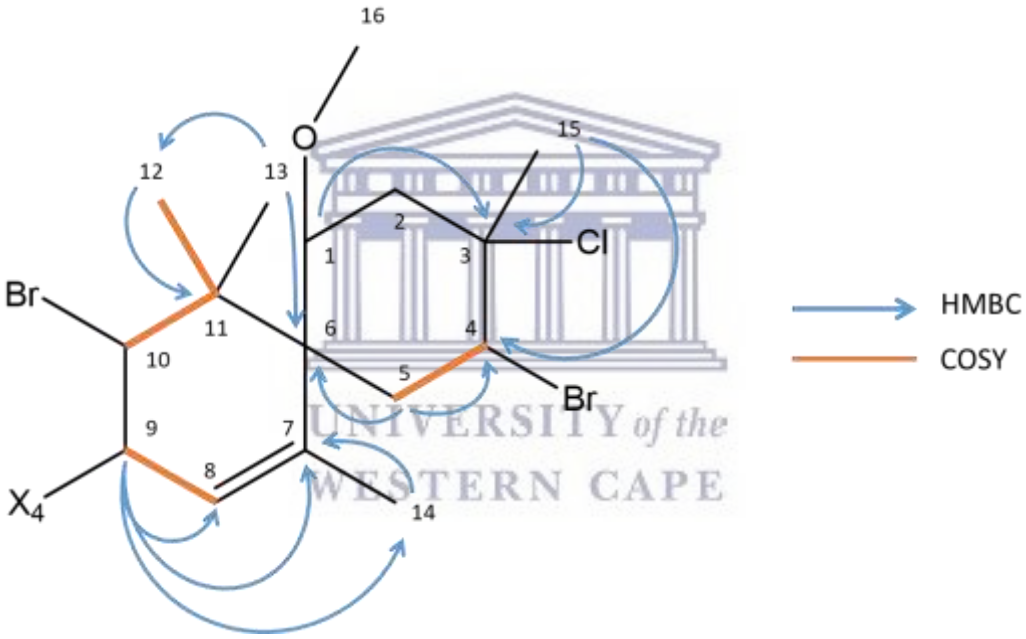

Figure 4.17: Observed HMBC and COSY correlations for proposed planar compound **4.29**

The unknown functional groups X_1, X_2, X_3 and X_5 were assigned based on the standard chamigrane structures observed in the literature. The methoxy was assigned to X_1, the X_2 was assigned a Cl^- functional group and lastly, X_3 and X_5 were assigned Br^- moieties. All unassigned chemical shifts were compared with **4.27** and **4.28**, the observations correspond with the assigned functional groups. The bromine at X_5 was critical for the closure of ring A in the biosynthetic pathway. The X_4 was an unknown due to the lack of material required for further investigation and the M^+ could not be obtained.

Table 4.3: NMR data for compound **4.29 (LG-Fr-E-G)** (400 MHz, $CDCl_3$)

Carbon Number	δ_C	Type	δ_H; multi (*J*, Hz)	COSY	HMBC
1	77.3	CH	4.18 d (*J* = 2.6 Hz)	-	C-3
2	29.7	CH_2	1.25 s	-	-
3	78.8	C	-	-	-
4	58.0	CH	4.69 dd (*J* = 4.3, 12.0 Hz)	H-5	C-3
5	34.7	CH_2	2.17 m	-	C-4, C-3, C-6, C-10
6	50.5	C	-	-	-
7	146.7	C	-	-	-
8	123.4	CH	6.33 d (*J* = 3.3 Hz)	H-14, H-9	C-9
9	56.9	CH	2.90 d (*J* = 3.1 Hz)	-	C-7, C-8, C-14
10	73.2	CH	4.37 s	H-5	C-3
11	46.5	C	-	-	-
12	23.6	CH3	1.27 s	-	C-6, C-7, C-11, C-13
13	26.6	CH3	1.53 s	-	C-6, C-7, C-11, C-12
14	24.6	CH3	1.56 s	H-12	C-9, C-7, C-10
15	21.4	CH3	1.81 s	H-14, H-1	C-4, C-3, C-1
16	50.9	CH3O	3.49 s	H-14	-

Figure 4.18: A picture of *Plocamium cornutum* morphological appearance

4.2.3. Extraction and isolation of monoterpenes from *P. cornutum* (NV160819-10)

A portion of the frozen sample of *Plocamium cornutum* was removed and allowed to thaw. The seaweed material was dried to remove excess moisture and extracted sequentially with MeOH and CH_2Cl_2-MeOH. The organic extracts were combined and dried under reduced pressure to yield 1.45 g of a dark green oily crude sample. A portion of the crude extract was separated on a silica chromatographic column with step-gradient elution using hexane, EtOAc and MeOH. Upon examination of the ^{1}H NMR fraction B [hexane: EtOAc (9:1)] indicated the presence of an aldehyde functional group at δ 9.55 which prompted the investigation into this fraction. Fraction B was chromatographed on an additional silica column to give compound **4.30** and **4.31** (Scheme 4.7).

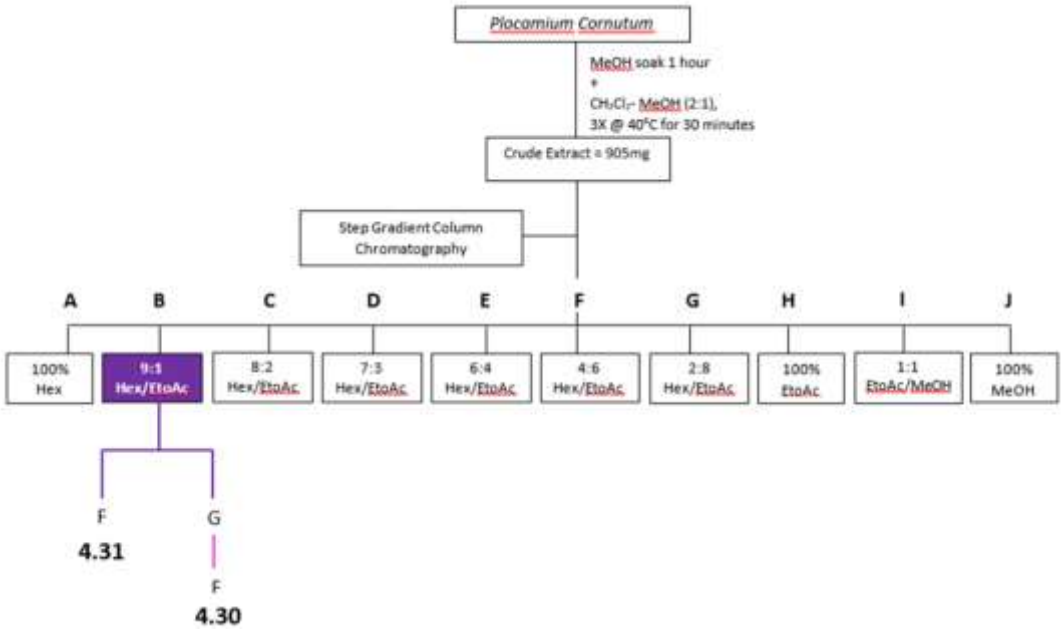

Scheme 4.7: Simplified scheme indicating the isolation of compounds **4.30** and **4.31** from *Plocamium cornutum*

4.2.4. Structural elucidation of isolated compounds from *Plocamium cornutum*

The extraction of the seaweed *Plocamium cornutum* (organic extract) afforded two distinct metabolites compounds **4.30** and **4.31** (Figure S4.28)

4.2.4.1. Compound 4.30 (PC-Fr-B-G-F)

Compound **4.30** was isolated from fraction B as an optically active, $[\alpha]_{\lambda}^{22^{\circ}}$= -68° ($CH_2Cl_2$), yellow oil. Although the sample was submitted for HRESIMS and HRGCMS no M^+ could be obtained for the compound. However, all NMR data are in accordance with published data for the compound and molecular formula of the compound was determined to be $C_{10}H_{11}OCl_3$, calculated mass of 253.55. The IR spectrum revealed the absorptions of an alkene signal (1698.98cm^{-1}) (Figure S4.29).

The ^{1}H NMR ($CDCl_3$) spectrum (Figure 4.19) showed the resonance for an aldehyde signal at δ 9.55 (H-10), olefinic signals at δ 5.30 (H-1), δ 6.07, 6.11 (H-2), δ 7.06, 7.10 (H-5) and δ 6.55 (H-6). A methyl at δ 1.77 (H-9) was also observed. Lastly, two methines situated at δ 4.56 (H-4) and a deshielded proton at δ 7.13 (H-8) (Figure S4.30)

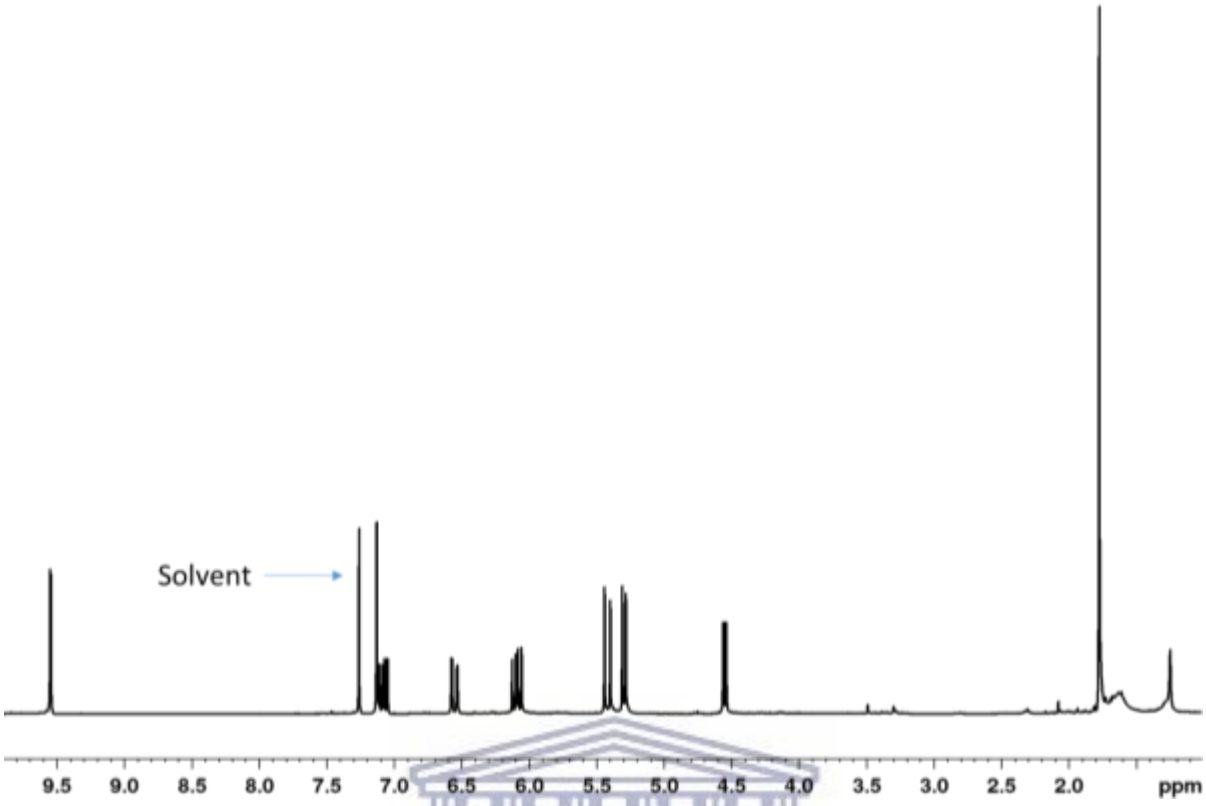

Figure 4.19: ^{1}H NMR spectrum of compound **4.30**

The ^{13}C NMR spectrum revealed signals indicative of 10 carbons (Figure 4.20), five signals in the olefinic region δ 116.5 (C-1), 139.6 (C-2), 134.15 (C-5), 122.6 (C-6) and 144.2 (C-10). This suggested three double bonds within the structure. The signal at δ 189.4 (C-8) was characteristic to a carbon-oxygen double bond which supported the assignment of an aldehyde to the structure, as suggested by the ^{1}H NMR spectrum. The C-1 was shown by the DEPT-135 spectrum to be a methylene signal which was evident that it was terminal in the monoterpene structure. It also indicated that there was one methine within the structure. The data also suggests that there were two quaternary carbons in the structure (Figure S4.31 and Figure S4.32).

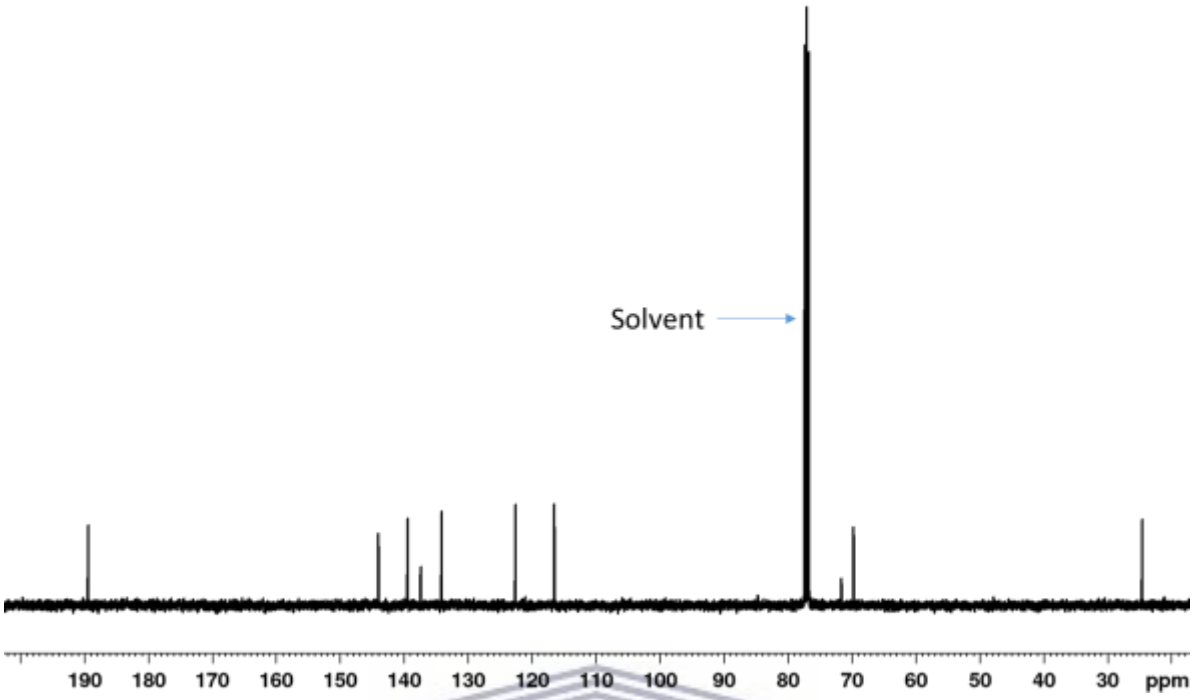

Figure 4.20: ^{13}C NMR spectrum of compound **4.30**

The following HMBC correlations: H-10 to δ 137.6 (C-7),144.2 (C-8) and 122.6 (C-6), H-9 to δ71.6 (C-3), 69.7 (C-4) and 139.6 (C-2). There were single correlations as seen in Figure 4.21, from H-6 to δ 134.15 (C-5) and H-1 to 139.6 (C-2), all of which confirmed the branched straight-chained monoterpene. The ^{1}H-^{1}H COSY spectrum showed correlations between H-1 and H-2, H-4 and H-5 as well as between H-5 and H-6 (Figure S4.33 and Figure S4.35).

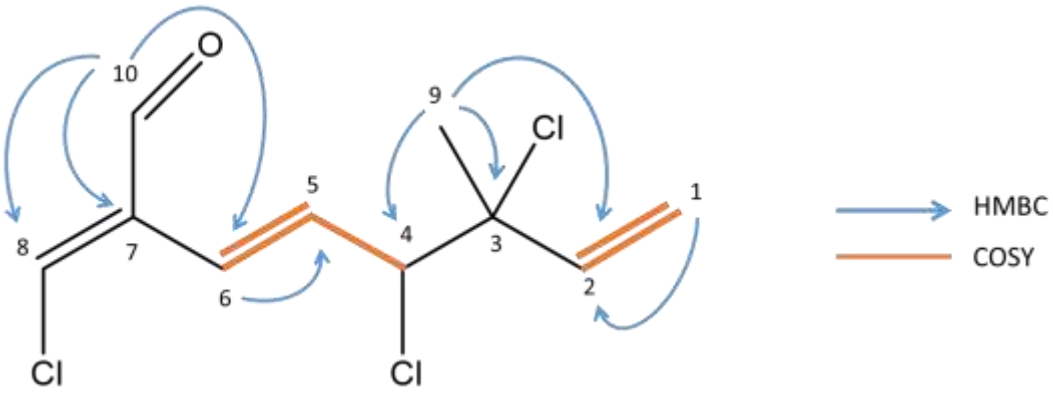

Figure 4.21: HMBC and COSY correlations of compound **4.30**

Based on literature comparisons and the 1 and 2 dimensional NMR data, the compound was identified as cartilagineal. This compound was previously isolated from the marine alga *Plocamium cartilagineum* [Crews and Kho, 1974].

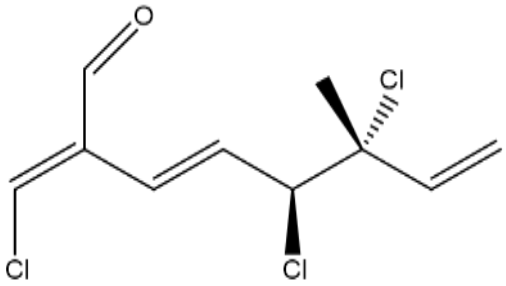

Compound **4.30**

Table 4.4: NMR data for compound **4.30 (PC-Fr-B-G-F)** (400 MHz, $CDCl_3$)

Carbon Number	δ_C	δ_C Lit.	Type	δ_H; multi (*J* Hz)	δ_H Lit.	COSY	HMBC
1	116.5	116.3	CH_2	5.30 (*d*, *J* = 9.9 Hz)	5.26	H-2	C-3, C-4
1*				5.40 (s)	5.40		C-2, C-3, C-4
1**				5.44 (s)	-		C-2, C-3
2	139.6	139.5	CH	6.07, 6.11 (2d, *J* = 9.9)	6.06	H-1	C-9, C-4
3	71.6	71.5	C	-		-	-
4	69.7	69.5	CH	4.56 (*d*, *J* = 9.9 Hz)	4.47	H-5, H-6	C-6, C-5
5*	134.2	134.0	CH	7.06, 7.10 (2d, *J* = 8.9 Hz)	7.05	H-4, H-6	C-6, C-10, C-8
6	122.6	122.5	CH	6.55 (dd, *J* = 2.1, 13.8 Hz)	6.49	H-4, H-5, H-10	C-4, C-5, C-C-10, 8
7	137.6	137.3	C	-		-	-
8	144.2	143.9	CH	7.13 (s)	7.05	-	C-7, C-6, C-8
9	24.7	24.6	CH_3	1.78 (s)	1.71	-	C-2, C-4, C-3
10	189.4	189.3	CHO	9.55 (d, *J* = 2.1 Hz)	9.04	H-6	C-6, C-7, C-8

4.2.4.2. Compound 4.31 (PC-Fr-B-F)

Compound **4.31** isolated as an optically active, $[\alpha]_{\lambda}^{22^{\circ}} = -51°(CH_2Cl_2)$, pale yellow oil. Although the sample was submitted for HRESIMS and HRGCMS no M^+ could be obtained for the compound. However, all NMR data are in accordance with published data for the compound and molecular formula of the compound was determined to be $C_{10}H_{11}C_{l5}$, calculated mass: 308.46. There are many similarities in between compound **4.30** and **4.31**, hence the focus of this section is to identify the differences between the two compounds.

The ^{1}H NMR spectrum shown in Figure 4.22 revealed that the aldehyde signal at δ 9.55 in compound **4.30** was not present in compound **4.31**. The signal at δ 6.76 represents H-10 in the molecule while the signal for H-8 had shifted upfield from δ 7.13 to δ 6.40 (Figure S4.38)

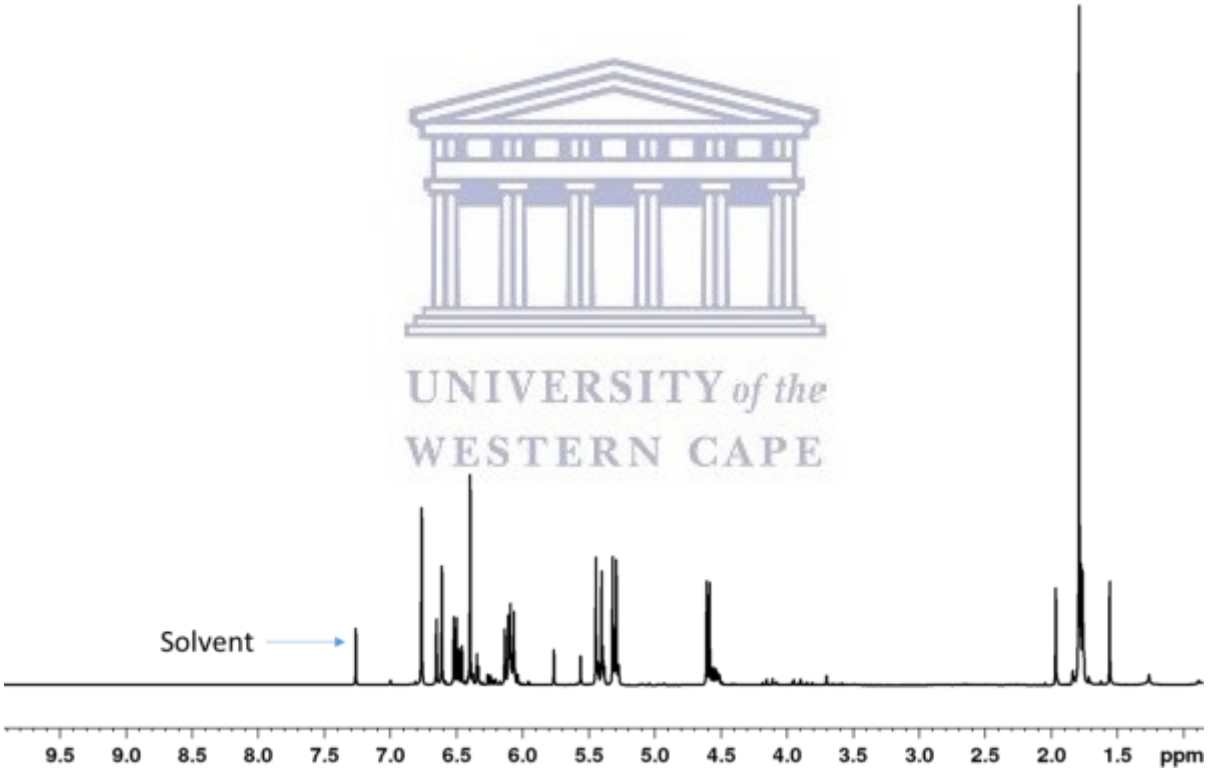

Figure 4.22: ^{1}H NMR spectrum of compound **4.31**

The ^{13}C NMR spectrum revealed 10 signals with a few impurities which were not considered in the elucidation of the structure (Figure 4.23). The stark difference between compound **4.30** and compound **4.31** was the peak at δ 189.4 was no longer present. This indicated that there was no aldehyde moiety within this structure. The signal which corresponds to the previous aldehyde positions chemical shift was δ 124.3 (C-10), this indicated that the present electron

withdrawing moiety caused an upfield shift. The electron withdrawing substituents at δ 71.7 (C-3), 69.45 (C-4), 69.43 (C-8) and 124.3 (C-10) could all be assigned as Cl^- moiety on the basis of their chemical shifts (Figure S4.39).

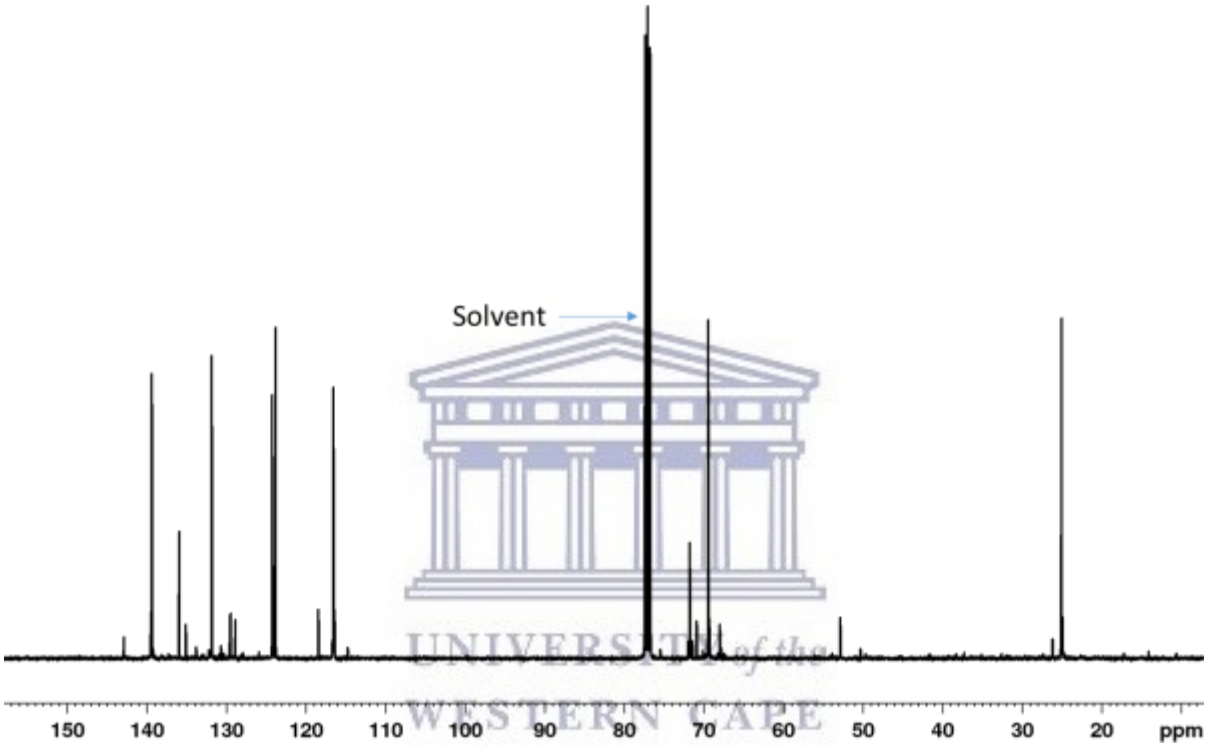

Figure 4.23: ^{13}C NMR spectrum of compound **4.31**

The following HMBC correlations were observed: H-8 to δ 135.2 (C-7), H-4 to δ 131.9 (C-5), H-10 to δ 135.2 (C-7) and 123.9 (C-6), H-9 to δ 71.7 (C-3), 69.45 (C-4), 139.4 (C-2) and 116.6 (C-1). Lastly, H-5 to 123.9 (C-6) as seen in Figure 4.24, confirmed the branched straight-chained monoterpene. There are COSY correlations between H-1 and H-2, H-4 and H-5, H-5 and H-6 and between H-8 and H-10. The correlation allowed for the building of a regular straight chain monoterpene skeleton (Figure S4.41 and Figure S4.43).

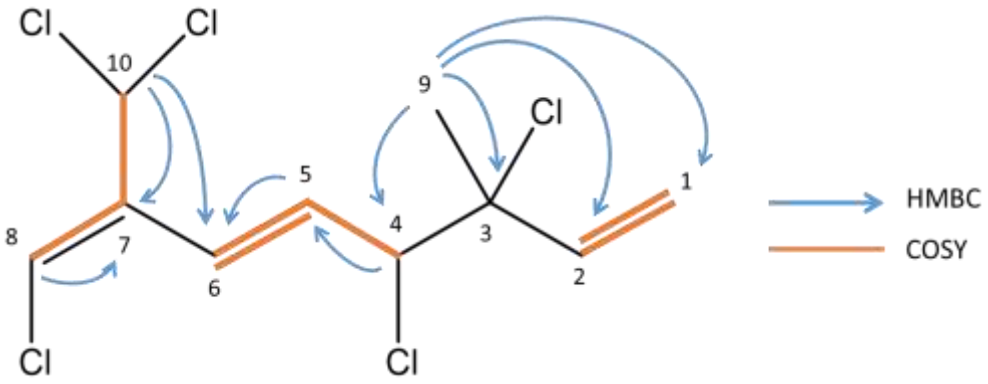

Figure 4.24: HMBC and COSY correlations of compound **4.31**

Based on literature comparisons and the 1 and 2 dimensional NMR data, the compound was identified as 1,5,6-trichloro-2-(dichloromethyl)-6-methylocta-1,3,7-triene and was previously isolated from the marine alga *Plocamium corallorhiza* and *Plocamium cornutum* [Afolayan *et al.*, 2009].

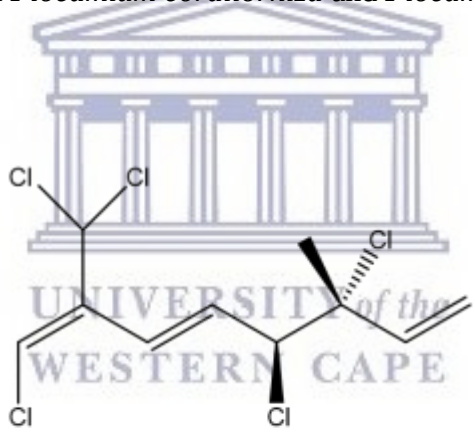

Compound **4.31**

Table 4.5: NMR data for compound **4.31 (PC-Fr-B-F)** (400 MHz, $CDCl_3$)

Carbon Number	δ_C	δ_C Lit.	Type	δ_H; multi (*J* Hz)	δ_H Lit.	COSY	HMBC
1	116.6	116.7	CH_2	5.42 d (*J* = 17.1 Hz)	5.42	H-9, H-2	C-3, C-4, C-2
1*				5.30 d (*J* = 10.8 Hz)	5.31	H-2	C-3
2	139.4	139.5	CH	6.09 dd (*J*=10.7, 17.2 Hz)	6.10	H-1	C-3, C-4
3	71.7	71.9	C	-	-	-	-
4	69.45	69.6	CH	4.59d (*J* = 8.8 Hz)	4.59	H-5	C-3, C-6, C-5, C-7
5	131.9	132.0	CH	6.48 dd (*J*=8.5, 16.20 Hz)	6.49	H-4, H-6	C-4, C-6
6	123.9	124.0	CH	6.62 d (*J* = 15.8 Hz)	6.63	H-5	C-4, C-5, C-10, C-7
7	135.2	136.1	C	-	-	-	-
8	69.43	69.6	CH	6.40 s	6.40	H-10	C-10, C-7
9	25.1	25.2	CH_3	1.79 s	1.79	H-1	C-4, C-3, C-1, C-2
10	124.3	124.4	CH	6.76 s	6.67	H-8	C-4, C-6, C-7

Conclusion

In conclusion, three chamigrane sesquiterpenes (compounds **4.27**, **4.28**, **4.29**) and two monoterpenes (compounds **4.30** and **4.31**) were successfully isolated from *Laurencia glomerata* and *Plocamium cornutum,* respectively. The structural elucidation was achieved by thoroughly evaluating the 1D and 2D NMR data as well as making reference to the available literature. The compounds elucidated are known compounds, except for compound **4.29**, and did not require more in-depth analysis.

In the next chapter, the biological activity was reviewed and the cytotoxicity profiles were established for the isolated compounds.

General Experimental

Silica gel column chromatography was conducted using silica gel 60 (0.040-0.063 mm) from Merck KGaA (Germany) and celite 545 EP from Associate chemical enterprises (PYT) LTD. All the normal phase TLC were visualised under UV light at 254 and 365 nm and were performed on Silica gel 60 F254 aluminium sheets purchased from Merck KGaA (Germany). Preparatory TLC was performed on 20 x 20 cm silica gel 60 F_{254} plates purchased from Merck KGaA (Germany). All solvents utilized in the experiments were redistilled. NMR experiments were obtained on a Avance Bruker 400 MHz spectrometer using standard pulse sequences. The NMR samples were prepared using the deuterated solvent ($CDCl_3$). NMR Chemical shifts were reported in ppm and were referenced to the deuterated solvent peak ($CDCl_3$ δ_H 7.26). The optical rotation of the compounds was determined using a Rudolph Research Analytical Autopol III Automatic Polarimeter. The experiment was conducted at a temperature of 22 °C using the D-line sodium which had a wavelength of 589 nm. The sample was dissolved in 10 ml of DCM and three readings were conducted per sample. IR spectra were obtained with a Perkin Elmer spectrum 400 FT-IR/FT-NIR. High resolution ESIMS data were taken on a Waters Synapt G2, ESI probe.

Plant material (NV160819-6)

Laurencia glomerata was collected by hand at Natures valley which is situated along the Southern Cape coast of South Africa, on August 2016. A dried voucher specimen was stored at the Marine Biodiscovery Laboratory at the University of the Western Cape. Identification of the marine algae was done by Professor John J. Bolton with the department of Biological Sciences, University of Cape Town, South Africa.

Extraction and isolation

The *Laurencia glomerata* material was removed from the -20 °C freezer and a portion was removed from the bulk sample. (wet mass 242 g; dry mass 21.50 g). The sample was allowed to thaw in deionised water. The deionized water (Fr W) was stored at -20 °C until further processing. The algal material was then dried using sheets of absorbent paper. The sample was initially steeped in MeOH (500 ml) for one hour at room temperature, after which the sample was extracted in triplicate with CH_2Cl_2-MeOH (2:1, 500 ml) at a constant temperature of 40 °C for 30 minutes respectively. The organic phases for each respective extraction were collected, combined and dried under reduced pressure. The resulting crude extract was subjected to liquid-liquid partitioning to remove the water. The organic layer was collected and

dried under reduced pressure, which produced a crude extract of 1.6 g (1600 mg) that corresponded to a 6.93% yield [Weight of crude/ (Weight of dry mass + Weight of Crude)]. The crude sample was fractionated using a step gradient elution system of hexane 100%, hexane: EtOAc (9:1, 8:2, 7:3, 6:4, 4:6, 2:8 and 0:10), EtOAc: MeOH (5:5) and MeOH 100% to yield 11 fractions. Fraction B obtained from the step-gradient fractionation was analysed by 2D NMR and fraction E was further purified by preparatory TLC, to give compounds **4.27** (313.6 mg) and **4.29** (3.7 mg) respectively.

The deionised water, which formed the water fraction (Fr W), was removed from -20 °C freezer. Diaion HP20 (25.5 g) was added to the sample, to adsorb any compounds which may be in the water, and it was stored at 4 °C for 48 hours. The HP20ss was filtered and steeped in MeOH for 60 hours and a subsequent second MeOH extraction for a further 48 hours. Finally, the Hp20 was soaked in CH_2Cl_2 for 24 hours. Each extraction was collected separately and dried under reduced pressure. The DCM fraction was further purified via silica gel column chromatography with hexane: EtOAc (7:3) mobile phase. Sub-fraction C gave compound **4.28** (2.3mg).

(GC 180104-1)

Plocamium cornutum was collected by hand at Glen Cairn. It is situated about 4 km north of Simon's Town, on the shore of False Bay Cape Town, South Africa. The sample was collected in January 2018. A dried voucher specimen was stored at the Marine Biodiscovery Laboratory at the University of the Western Cape. Identification of the marine algae was done by Professor John J. Bolton with the department of Biological Sciences, University of Cape Town, South Africa.

The initial biological screening against *M. tuberculosis* conducted in chapter 3 was done using *P. cornutum* collected from Natures Valley. Due to low specimen availability, *P. cornutum* collected from Glen Cairn was used to further the study. A comparative ^{1}H NMR was done to ensure chemical similarity.

Extraction and isolation

A frozen segment of *Plocamium cornutum* was thawed at room temperature prior to solvent extraction (wet mass 134.55 g; dry mass 29.65 g). The sample was dried between sheets of absorbent paper to remove excess water. The sample was steeped in MeOH (500 ml) for one hour at room temperature, after which the sample was extracted in triplicate with CH_2Cl_2-

MeOH (2:1, 500 ml) for 30 minutes at a constant temperature of 40 °C respectively. The organic phases were combined and dried under reduced pressure. The sample underwent

liquid-liquid partitioning between H_2O and DCM, the organic layer was collected and dried under reduced pressure. This process produced a crude extract of 1.45 g (1450 mg) which resulted to a 4.66% yield [Weight of crude/ (Weight of dry mass + Weight of Crude)]. The crude extract was fractionated using a step gradient elution system of hexane 100%, hexane: EtOAc (9:1, 8:2, 7:3, 6:4, 4:6, 2:8 and 0:10), EtOAc: MeOH (5:5) and MeOH 100% to yield 10 fractions. Fraction B showed a spectrum of interest and was further purified by a silica gel column chromatography eluted with hexane 100% to produce 8 more fraction A-H, of which sub-fraction G was subjected to a third silica gel column eluted with hexane: EtOAc (9:1). The purification process gave compound **4.31** (2.7 mg) and compound **4.30** (8.6 mg).

References

Afolayan, A. F., Mann, M. G. A., Lategan, C. A., Smith, P. J., Bolton, J. J., Beukes, D. R., Antiplasmodial halogenated monoterpenes from the marine red alga Plocamium cornutum. *Phytochemistry* **2009**, 70(5), 597–600.

Anderson, R. J., Stegenga, H., Bolton, J. J., Seaweeds of the South African coast, **2016**. World Wide Web electronic publication, University of Cape Town http://southafrseaweeds.uct.ac.za; Accessed on 20 June 2019.

Anderson, R. J., Stegenga, H., Subtidal Algal Communities at Bird Island, Eastern Cape, South Africa. *Botanica Marina* **1989**, 32(4), 299-311.

Butler, A., Carter-Franklin, J. N., The role of vanadium bromoperoxidase in the biosynthesis of halogenated marine natural products. *Natural Product Reports* **2004**, 21(1), 180-188.

Chhetri, B. K., Lavoie, S., Sweeney-Jones, A. M., Kubanek, J., Recent trends in structural revision of natural products, *Natural Product Reports* **2018**, 35(6), 514-531

Crews, P., Kho, E. Cartilagineal. Unusual monoterpene aldehyde from marine alga. *The Journal of Organic Chemistry* **1974**, 39(22), 3303–3304.

Faulkner, J., Stallard, M.O., Ireland, C., Prepacifenol epoxide, a halogenated sesquiterpene diepoxide, *Tetrahedron Letters* **1974**, 15(40), 3571-3574.

Francis, C., Bolton, J. J., Mattio, L., Mandiwana-Neudani, T. G., Anderson, R. J., Molecular systematics reveals increased diversity within the South African Laurencia complex (Rhodomelaceae, Rhodophyta). *Journal of Phycology* **2017**, 53(4), 804-819.

Gribble, G.W., Naturally occurring organohalogen compounds- *A comprehensive update Springer Science & Business Media* **2009** (Vol. 91).

Hunter, W. N., The non-mevalonate pathway of isoprenoid precursor biosynthesis. *Journal of Biological Chemistry* **2007,** 282(30), 21573-21577.

Kaiser, C. R., Pitombo, L. F., Pinto, A. C., Complete 1H and 13C NMR assignments of chamigrenes from *Aplysia dactilomela*. *Magnetic Resonance in Chemistry* **2001**, 39(3), 147-149.

Kimura, J., Kamada, N., Tsujimoto, Y., Fourteen chamigrane derivatives from a red alga *Laurencia nidifica*. *Bulletin of the Chemical Society of Japan* **1999**, 72(2), 289-292.

Mandrekar, V. K., Gawas, U. B., Majik, M. S., Brominated molecules from marine algae and their pharmacological importance. *Studies in Natural Products Chemistry* **2018**, 461–490.

Knott, M. G., A review of secondary metabolites isolated from Plocamium species worldwide, **2015**.

Masuda, M., Abe, T., Suzuki, T., Suzuki, M., Morphological and chemotaxonomic studies on *Laurencia composita* and *L. okamurae (Ceramiales, Rhodophyta). Phycologia* **1996**, 35(6), 550–562.

Miziorko, H. M., Enzymes of the mevalonate pathway of isoprenoid biosynthesis. *Archives of Biochemistry and Biophysics* **2011**, 505(2), 131-143.

MPhail, K. L., Davies-Coleman, M. T., Copley, R. C. B., Eggleston, D. S. New Halogenated Sesquiterpenes from South African Specimens of the Circumtropical Sea Hare *Aplysia dactylomela. Journal of Natural Products* **1999**, 62(12), 1618–1623.

Naylor, S., Hanke, F. J., Manes, L. V., Crews, P., Chemical and Biological Aspects of Marine Monoterpenes. *Fortschritte Der Chemie Organischer Naturstoffe / Progress in the Chemistry of Organic Natural Products* **1983**, 189–241.

Pereira, R., Andrade, P., Valentão, P., Chemical diversity and biological properties of secondary metabolites from sea hares of Aplysia genus. *Marine Drugs* **2016**, 14(2), 39.

Polzin, J. P., Rorrer, G. L., Halogenated monoterpene production by microplantlets of the marine red alga *Ochtodes secundiramea* within an airlift photobioreactor under nutrient medium perfusion. *Biotechnology and Bioengineering* **2003**, 82(4), 415–428.

Rohmer, M., The discovery of a mevalonate-independent pathway for isoprenoid biosynthesis in bacteria, algae and higher plants. *Natural Product Reports* **1999**, 16(5), 565-574.

Schilmiller, A. L., Schauvinhold, I., Larson, M., Xu, R., Charbonneau, A. L., Schmidt, A., Wilkerson, C., Last, R. L., Pichersky, E., Monoterpenes in the glandular trichomes of tomato are synthesized from a neryl diphosphate precursor rather than geranyl diphosphate. *Proceedings of the National Academy of Sciences* **2009**, 106(26), 10865-10870.

Simons, R. H., Species of Plocamium on the South African coast. *Bothalia* **1964**, 8(2), 183-193.

Vairappan, C. S., Suzuki, M., Ishii, T., Okino, T., Abe, T., Masuda, M., Antibacterial activity of halogenated sesquiterpenes from Malaysian *Laurenica* spp., *Phytochemistry* **2008**, 69(13), 2490-2494.

Vogel, C. V., Pietraszkiewicz, H., Sabry, O. M., Gerwick, W. H., Valeriote, F. A., Vanderwal, C. D., Enantioselective divergent syntheses of several polyhalogenated

Plocamium monoterpenes and evaluation of their selectivity for solid tumors. *Angewandte Chemie International Edition* **2014**, *53*(45), 12205-12209.

Wada, N., Kersten, R. D., Iwai, T., Lee, S., Sakurai, F., Kikuchi, T., Fujita, D., Fujita, M., Weng, J. K., Crystalline-sponge-based structural analysis of crude natural product extracts. *Angewandte Chemie International Edition* **2018**, 57(14), 3671-3675.

Wang, B. G., Gloer, J. B., Ji, N. Y., Zhao, J. C., Halogenated organic molecules of rhodomelaceae origin: chemistry and biology. *Chemical Reviews* **2013**, 113(5), 3632–3685.

Wise, M. L., Monoterpene biosynthesis in marine algae. *Phycologia* **2003**, 42(4), 370–377.

Yu, X. Q., Jiang, C. S., Zhang, Y., Sun, P., Kurtán, T., Mándi, A., Li, X. L., Yao, L. G., Liu, A. H., Wang, B., Guo, Y. W., Compositacins A–K: Bioactive chamigrane-type halosesquiterpenoids from the red alga Laurencia composita Yamada. *Phytochemistry* **2017**, 136, 81-93.

Zhang, J., Ding, L. P., Liang, H., Guo, X. Y., Zhang, Q. Y., Sesquiterpenes from red alga, *Laurencia tristicha*, *Biochemical systematics and Ecology* **2015**, 60, 116-119.

Chapter 5

ANTI-MYCOBACTERIAL ACTIVITY AND CYTOTOXICITY OF NATURAL PRODUCTS, FRACTIONS AND CRUDE EXTRACTS OF *LAURENCIA GLOMERATA* AND *PLOCAMIUM CORNUTUM*

5.1. Introduction

The marine environment, containing almost half the overall biodiversity on earth, is potentially a rich source of novel anti-mycobacterial compounds. New antimicrobial compounds are in desperate shortage as pathogenic microorganisms develop resistance to existing antibiotics. Nature has been a productive source of antimicrobial agents while, marine ecosystems are labeled as "particularly promising" in the pursuit of new antimicrobial agents [Habbu *et al*., 2016]. Among the diseases caused by microorganisms, tuberculosis (TB) is a particular global problem and current medicinal therapy is rapidly becoming ineffective due to non-compliance [Tiberi *et al.,* 2017]. The emergence of multidrug resistant TB (MDR-TB), which has a treatment success rate of 55% is driving the drug discovery process for new anti-tuberculosis compounds. Due to the high incidence of TB in South Africa [WHO Global Tuberculosis Report 2018], and based on the preliminary screening results obtained in this study against *Mycobacterium aurum* A+ and *Mycobacterium tuberculosis* H37Rv, we investigated the anti-mycobacterial activity and cytotoxicity of the isolated compounds, selected fractions and extracts.

A general search for seaweeds and anti-mycobacterial activity highlighted only a few studies conducted on red algae. These seaweeds are known to contain a vast range of secondary metabolites, such as halogenated di- and monoterpenes and phenols [Allmendinger *et al.,* 2015]. In Saravanakumar's doctoral thesis, she investigated the anti-mycobacterial activity of the red algae *Plocamium corallorhiza* as one of her seaweed samples. It was found that *P. corallorhiza* extracts were active against *Mycobacterium smegmatis* and *M. tuberculosis* [Saravanakumar, 2006]. In another study conducted by König *et al* (2000)., 39 marine-derived natural product fractions/compounds were screened for anti-mycobacterial activity against *Mycobacterium avium* and *M. tuberculosis*. The seaweeds used in the study were preselected based on functionality. Eight compounds were derived from a *Laurencia* sp. and three were derived from a *Plocamium* sp. [König *et al.,* 2000]. Pure metabolites and organic extracts of various *Laurencia* sp. exhibited significant pharmacological activities such as antiviral, antifungal, antitumor, antimalarial and anti-mycobacterial to name a few [Ventura *et al.,* 2015].

In order to establish whether compounds showing anti-mycobacterial activity are selective, it is crucial to conduct biological evaluations and screening tests of the compounds by means of cytotoxicity tests. Cytotoxicity assays are preferred because they are relatively fast, simple, has high sensitivity and can spare the need for animal testing [Li *et al.*, 2015]. A great degree of emphasis has been placed on seaweed constituents and their anti-cancer activity. Cytotoxic compounds such as laminarians, fucoidans and terpenoids have been isolated from seaweeds possessing antitumor, anticancer and antiproliferative properties [El-Kassas and El-Sheekh, 2014].

By 2030, the world's cancer burden in low- and middle-income countries, such as South Africa, is estimated to be more than 70%. The most frequently diagnosed cancer among South African women is breast cancer [Lince-Deroche *et al.*, 2017]. It is therefore imperative that cytotoxicity screening is conducted against a breast cancer cell line (MCF-7) and a non-tumorigenic breast cancer cell line (MCF-12a). The studies assess cytotoxicity in order to demonstrate selectivity for mycobacteria. These cell lines were selected for the cytotoxicity tests used in this study.

5.1.1. Antimicrobial susceptibility testing

Antimicrobial susceptibility testing is an *in vitro* method which can be utilized in the drug discovery process, by screening extracts, fractions or pure compounds to establish their activity profile. The principle behind conducting these tests is to establish the potency of a compound against a selected, potentially susceptible, bacterium. A micro-organism/bacterium is considered susceptible if the tested compound successfully results in growth inhibition. In these tests, the inhibition is directly proportional to the potency of the compound [Kenny *et al*., 2015]. These *in vitro* methods that assess the activity of compounds and extracts are quantified by numeric values such as minimum inhibitory concentration (MIC), half maximal inhibitory concentration (IC_{50}) and IC_{90} to name a few [Sanchez and Kouznetsov, 2010].

The most common susceptibility tests are diffusion method (quantitative), thin-layer chromatography (TLC) bioautography (qualitative) and dilution methods (quantitative) [Balouiri *et al*., 2016]. The choice of method is dependent on the fact that each individual assay is not based on the same principles. Based on the method selected by the researcher, the results achieved may be influenced by chemical complexity, degree of sample solubility, stereochemistry, choice of the organism and the size of the inoculum [Kenny *et al*., 2015]. Other factors which may influence the results include temperature (affecting the growth and

time taken to grow adequate organism), supplementation (test strains that do not grow satisfactorily due to the lack of supplements), moisture (a moist environment is ideal but a wet incubation environment can adversely affect results) and pH (ideal is between 7.2 and 7.4, extremes affect compound potency) The choice of method is also dependent on time spent (from start to obtaining results) when conducting the experiment, reproducibility of the method as well as cost [Lalitha, 2004].

5.1.2. Macrobroth dilution tests

The broth dilution methods were mostly utilized in the early days of antimicrobial susceptibility testing. This method entailed preparing two-fold dilutions in test tubes with the addition of a liquid bacterial culture and an overnight incubation at 35 °C. Upon completion, the turbidity observed was an indication of bacterial growth. These tests generated the quantitative results of the minimal inhibitory concentration (MIC), which was the lowest concentration that prevented bacterial growth. The disadvantages of this method are that it is a manual task with the possibility of error as well as being tedious and requiring large amounts of reagent. All these factors promoted the miniaturization of this technique to form the microbroth dilution method [Kenny *et al*., 2015; Reller *et al*., 2009].

5.1.3. Agar diffusion

In 1940, the agar disk-diffusion method was developed [Balouiri *et al*., 2016]. This method entailed inoculating the surface of an agar medium (set in a petri dish) with the standardized strain of choice. Small filter paper discs are impregnated with the test compounds at the chosen concentration and are placed on the surface of the agar. The petri dishes are then incubated at the ideal growth temperature, the antimicrobial agents diffuse into the agar and inhibit the organism's growth. The inhibition produces a clear zone around the active disc and the diameter of the circle is measured. The difficulties encountered with this method is that firstly, it is difficult to distinguish between bacteriostatic and bactericidal compounds. Secondly, the MIC cannot be determined as the amount of compound which diffused into the agar cannot be quantified [Balouiri *et al*., 2016].

5.1.4. Bioautography

Bioautography is a screening tool that can indicate bioactive compounds in natural product extracts. The analytical screening can adopt the principle of bioassay-guided fractionation. This method typically utilizes thin-layer chromatography (TLC) as the test medium. The advantages of this method is that natural products can be effortlessly screened; it can serve as an isolation method for bioactive compounds by extracting fractions that show activity after separating the complex crude extract; less material is required to conduct the experiment (ideal for natural products which yields low mass); saves money and time; lastly many extracts and fractions can be spotted on the same TLC plate and parallel bioactivity comparisons between similar/same species can be identified. The bio-guiding method is conducted by spotting the crude, initial parent fractions and subsequent secondary purification fractions on a TLC plate and identifying the path of activity. This method can identify masked compounds that deserve further investigation and structural analysis. The preparative TLC method is conducted by applying the natural product crude as a band along the glass-backed silica plate, the plates are developed in the desired mobile phase, the fractions identified as active are then scraped off the plate and they are analysed [Kenny *et al*., 2015].

There are several other antimicrobial methods which can be utilized such as agar plug diffusion, time-kill test, antimicrobial gradient method (E-test), ATP bioluminescence assay, cross streak method, automated antimicrobial susceptibility testing and flow cytoflourometric method to name a few [Balouiri *et al*., 2016; Kenny *et al*., 2015].

As indicated in Chapter 3, *M. aurum* A+ is often used as a surrogate for bioassay testing and therefore has been selected as the organism of choice for the antimicrobial assays. In this chapter there are two main aims, to determine the antimicrobial activity using bioautography and microbroth dilution assays and to evaluate the cytotoxicity profiles of the fractions generated from the large scale extraction in Chapter 4. In this study, it is important to note that *Plocamium cornutum* (*P. cornutum*) was identified based on its activity in preliminary screening results. *Laurencia glomerata* (*L. glomerata*) was selected for its interesting chemistry and based on previous reports that sesquiterpene compounds have exhibited anti-mycobacterial activity [Ventura *et al.*, 2015].

5.2. Results and discussion

5.2.1. Thin-layer bioautography

Direct bioautography is a procedure which is capable of analysing a given sample to establish the presence or absence of antimicrobial compounds, with results providing a "yes, no, or maybe" response (yes = active; no = no activity; maybe = too low concentration of the active compound present resulting in regrowth). Bioautography has a high sensitivity, it was a quick, inexpensive, simplistic method and did not require complex analytical equipment. The thin-layer chromatography plate, comprised of silica gel was spotted with compounds/fractions. The plate was dipped in the inoculum/dabbed, overlaid or sprayed with the inoculum and the compounds diffused from the chromatographic layer into the inoculated medium at the surface of the plate. Upon incubation in a humid atmosphere, the surface of the plate promoted microbial growth and where antimicrobial compounds were spotted, zones of inhibition would occur. The visualization of the organism growth occurred when the plates are sprayed with the 3-(4,5-dimethylthiazol-2-yl)-2,5-diphenyl tetrazolium bromide (MTT) reagent. The microorganism converted the tertrazolium salt to formazan which was a purple colour and was a direct indication of growth (active respiration). In the case of a zone inhibition by the compound, a white spot appeared against a purple background [Choma and Grzelak, 2011].

There are currently three TLC bioautography methods which could be used to establish antimicrobial activity: direct, contact and immersion contact. The contact method was quite similar to the disc diffusion method. The prepared TLC plate was placed on the surface of an inoculated agar surface and the compounds diffused into the agar, subsequently, the TLC is removed and the agar plate is incubated. Compounds with antimicrobial activity created clear zones of inhibition. The immersion method was a mixture of both the direct and contact bioautography, where the inoculated agar was laid over the developed TLC plate, the antimicrobial compounds diffused into the agar and are incubated. Subsequently, clear zones were observed [Kenny *et al*., 2015].

It was important to conduct the bioautography first to give an indication of how the fractions interacted with *M. aurum*. This process would set the baseline for comparison when the microdilution assays were conducted. It was also a more cost-effective method, which utilized minimal material and served as a great trial and error process. It was a more robust method that has very few troubleshoot errors associated with it.

As mentioned above, the first aim of this chapter was to establish the antimicrobial activity of *L. glomerata* and *P. cornutum* extracts and fractions. The 78 fractions generated (described in Chapter 4) were tested against *M. aurum* A+. On the first TLC plate, block 1 represented *L. glomerata* crude extract and blocks 2-12 represented the step-gradient fractions A-K. The subsequent *L. glomerata* block allocations were for the fractions obtained from a secondary fractionation process. Blocks 13-18 were for the secondary fractionation of LG-Fr-B, blocks 19-23 for LG-Fr-C and 24-30 for LG-Fr-D sub-fractions. Block 31 represents *P. cornutum* crude and blocks 32-41 represent the step-gradient fractions A-J. Plate 2 started with sub-fractions of LG-Fr-E blocks 51-61 and blocks 62-65 represented water fractions of *L. glomerata.* Blocks 66-71 represented PC-Fr-B first set of sub-fractions and 72-77 were from the second set of sub-fractions of PC-Fr-B-G. Figure 5.1 was a graphical representation of the zones of activity observed. A qualitative approach was used in order to assign a value to the size of the zone of activity that was observed as an indication of the samples' activity.

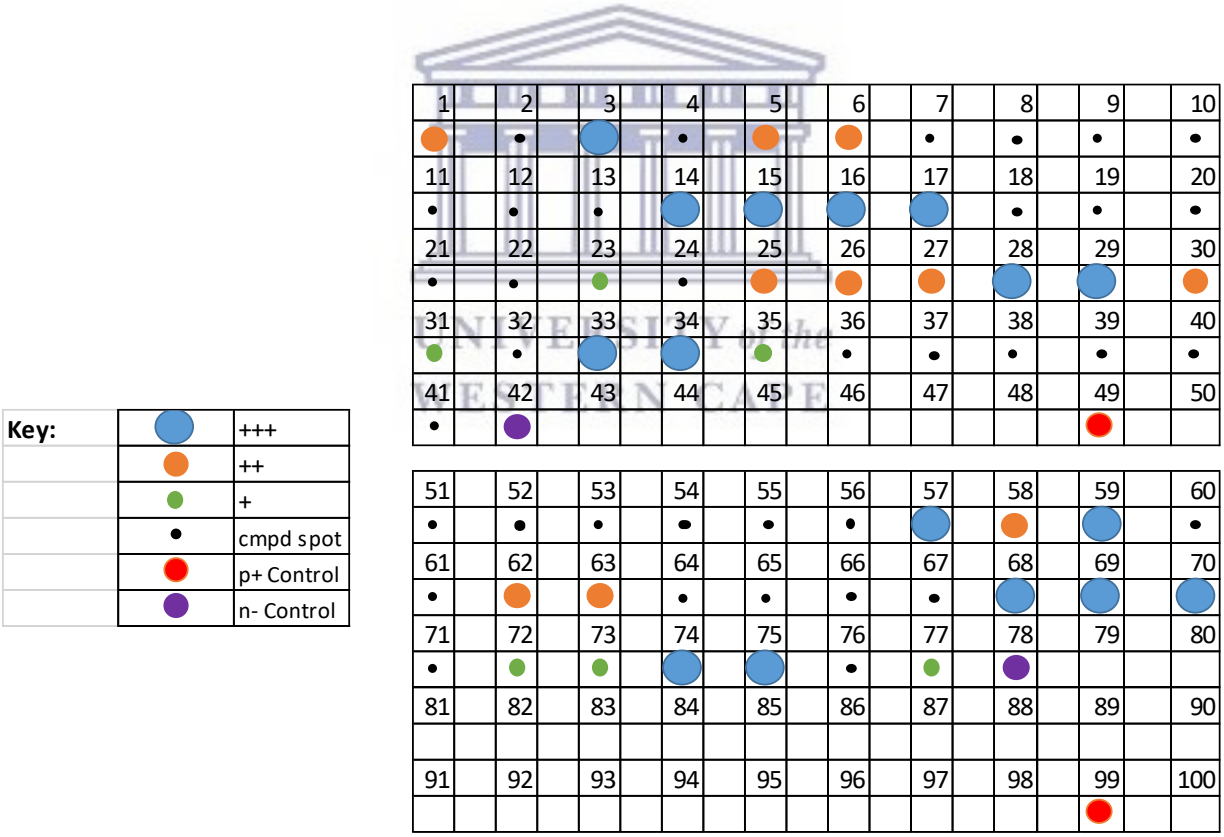

Figure 5.1: Graphical representation of the tested bioautography plates and the activity profiles observed for the various fractions against *M. aurum.* Blocks 1 and 31 are the crude extracts of *L. glomerata* and *P. cornutum* respectively. Blocks 2-12 represent the step-gradient fractions A-K for *L. glomerata*. Blocks 32-41 represent the step-gradient fractions A-J for *P. cornutum*. Pure compounds **4.27**, **4.28**, **4.29**, **4.30** and **4.31** are situated at blocks 3, 57, 63, 75 and 70 respectively.

As can be seen in Figure 5.1, the potency of the fraction was determined by the size of the zone of activity. If more active compounds were present, the full spot will reflect that (large circle) versus the ones with only a few bioactive compounds resulted in a smaller active spot. More active spots may also be an indicator of the ability of an active compound to diffuse outside the confines of the area in which the sample was spotted. The largest circle, i.e. the blue circle, was assigned when the zone of activity size was approximately 0.2 millimeters from the boundary to a size that exceeded its allocated square area. The orange circle was assigned when approximately half of the allocated square was occupied by the zone of activity and the green circle was assigned when only a small zone was present. A black spot was placed where no zone was observed and only the compound spot can be seen. The purple spot was representative of the negative control dichloromethane (CH_2Cl_2) and the red spot represented the positive control (Vancomycin). Regrowth was observed for the majority of the compounds. One possible reason for the regrowth observed was the incubation time (it is usually 24 hours). Regrowth was not necessarily only linked to the length of incubation, but may also be linked to the number of bioactive compounds present. If a sub-lethal amount of the bioactive compound was present, it would kill some of the bacteria present and when this was depleted (i.e., in this case, extended incubation). The surviving *M. aurum* will start growing over the area where growth inhibition occurred, showing the effect of regrowth. Although regrowth was observed, the compounds were still considered to be "active". There were 32 of the 77 fractions that were tested that showed zones of activity. Sixteen fractions had fairly large zones of activity. Numbers 1-30 and 51-65 were all the *L. glomerata* fractions. It could be seen that nine of the largest zones of activity was due to this seaweed. Numbers 31-41 and 66 -77 represent the *P. cornutum* fractions. There were seven fractions that had large zones of activity. Interestingly, fractions 1 and 31 represents the crude extracts of *L. glomerata* and *P. cornutum* respectively, both crude samples showed less activity than the purified compounds (position 3, 75, 70, 57 and 63). This indicated that the process of purification enhanced the antimicrobial activity possibly by removing any interfering/masking compounds. The four isolated Compounds **4.27 (LG-Fr-B), 4.30 (PC-FrB-G-F), 4.31 (PC-Fr-B-F)** and **4.29 (LG-Fr-E-G)** situated at position 3, 75, 70, 57 respectively, had large zones of activity. Compound **4.28 (LG-DCMHP20)** was the weakest of the pure compounds, it only exhibited moderate activity (position 63). It can, therefore, be inferred that the compounds in question were responsible for the anti-mycobacterial activity observed in the *M. aurum* A+ assay.

Due to the limitation of sample quantity, it was not possible to test one of the fractions generated in chapter 4. It was also not possible to conduct the experiment for a second time to shorten the incubation period to avoid regrowth. It was an unfortunate downfall that the yield when working with natural products is low. This does complicate experiments as there was a limit to how many times an experiment could be repeated.

5.2.2. Assessment of antimicrobial activity

The microdilution experiment was conducted in disposable, sterile, plastic 96-well plates which were small in size (wells accommodate 0.4 ml maximum). This method rapidly became popular because of its practicality, cost, less reagent was used and quantitative MICs can be determined. An additional benefit was that the entire process could be automated, reducing the chances of error [Reller *et al*., 2009]. There are two concerning downfalls with the dilution method. Firstly, non-polar compounds could precipitate and reduce contact with the inoculum and secondly, it was not always possible to compare the results obtained by diffusion or bioautographic, to dilution results [Kenny *et al*., 2015].

The next set of tests was to establish if varying the test concentration of the 78 fractions (described in Chapter 4), would affect the average percentage growth of *M. aurum* A+. The test which was selected was a microdilution assay. Each fraction's stock solution required serial dilution to obtain the desired concentrations of 100 µg, 90 µg, 80 µg, 70 µg, 60 µg, 50 µg, 25 µg and 12.5 µg. The microdilution assay was conducted in sterile 96-well plates and each concentration was tested in triplicate.

Based on the results of the bioautography antimicrobial assays, it was important to establish the activity of the 78 fractions in a microdilution assay. The importance of conducting both assays was to give a more realistic activity profile of the crude extracts, fractions and pure compounds. In Figures 5.2a and 5.2b, the values indicated were the average percentage growth observed for the respective fractions. The activity of the fractions in the liquid medium was assigned colours to evaluate their potency. Yellow represented weaker activity and this was assigned from 75-99% average percentage growth. Orange represented moderate potency with the average percentage growth ranging from 50-74%. There were no compounds which exhibited activity resulting in percentage growth of below 50%, hence there were no red indicators. The microdilution assay starting concentration was 100 µg/ml because this was one

of the standard concentrations which was used when conducting this method. Looking at Figure 5.2a it was noted that the majority of the dilutions obtained for *L. glomerata* produced weak antimicrobial activity against *M. aurum*. There were 32 of the 96 fractions tested, that promoted the growth of *M. aurum*. The results indicated that 66% of the dilutions tested exhibited some activity against *M. aurum.* The most active dilution was fraction K at a concentration of 90 µg/ml.

	LG Crude	LG-Fr-A	LG-Fr-B	LG-Fr-C	LG-Fr-D	LG-Fr-E	LG-Fr-F	LG-Fr-G	LG-Fr-H	LG-Fr-I	LG-Fr-J	LG-Fr-K
100µg	96	91	101	86	101	102	89	100	92	91	90	90
90µg	101	99	96	100	96	104	98	99	102	98	91	76
80µg	102	94	98	86	94	95	98	95	89	106	95	86
70µg	108	98	94	94	90	90	100	92	94	105	97	85
60µg	105	87	99	103	97	90	97	96	95	107	88	94
50µg	106	97	98	101	100	100	99	90	87	105	99	83
25µg	106	104	97	98	103	126	104	92	89	110	91	98
12.5µg	116	106	95	108	93	101	107	95	85	95	97	81

Figure 5.2a: Heat map indicating the antimicrobial activity of the *L. glomerata* crude and step-gradient fractions at varying concentrations

	PC Crude	PC-Fr-A	PC-Fr-B	PC-Fr-C	PC-Fr-D	PC-Fr-E	PC-Fr-F	PC-Fr-G	PC-Fr-H	PC-Fr-I	PC-Fr-J
100µg	75	104	101	91	88	91	82	75	76	93	108
90µg	70	104	92	84	96	80	83	81	82	91	106
80µg	72	110	108	100	102	86	87	82	80	81	101
70µg	70	102	104	86	96	83	76	79	85	81	101
60µg	60	91	93	85	95	83	78	64	67	76	104
50µg	58	113	99	93	107	84	81	85	77	79	98
25µg	64	105	111	97	99	85	80	79	76	71	98
12.5µg	60	103	100	104	95	85	76	85	71	75	98

Figure 5.2b: Heat map indicating the antimicrobial activity of the *P. cornutum* crude and step-gradient fractions at varying concentrations

In Figure 5.2b it could be seen that there were a number of fractions from *P. cornutum* which exhibited moderate growth inhibition. The fraction with the most activity observed was the crude extract. This could possibly indicate that during the fractionation process minor compounds that produced the activity observed could have been removed. The second possibility was that compounds with synergistic activity were separated into different fractions. There were a total of 11 dilutions of the 88 tested exhibited moderate activity, the contribution to the activity observed is 12.5%. There were 21 dilutions that promoted the growth of *M. aurum* and the main contribution was due to fraction A and J. It is understandable that fraction J would promote growth as it was a polar fraction and many glycolipids and fatty acids were found in these fractions. The remaining 64% (56) of the *P. cornutum* dilutions exhibited weak antimicrobial activity.

In Figure 5.3 a comparison is made between the *Laurencia glomerata* crude extract and the activity observed for the pure compounds isolated against *M. aurum*.

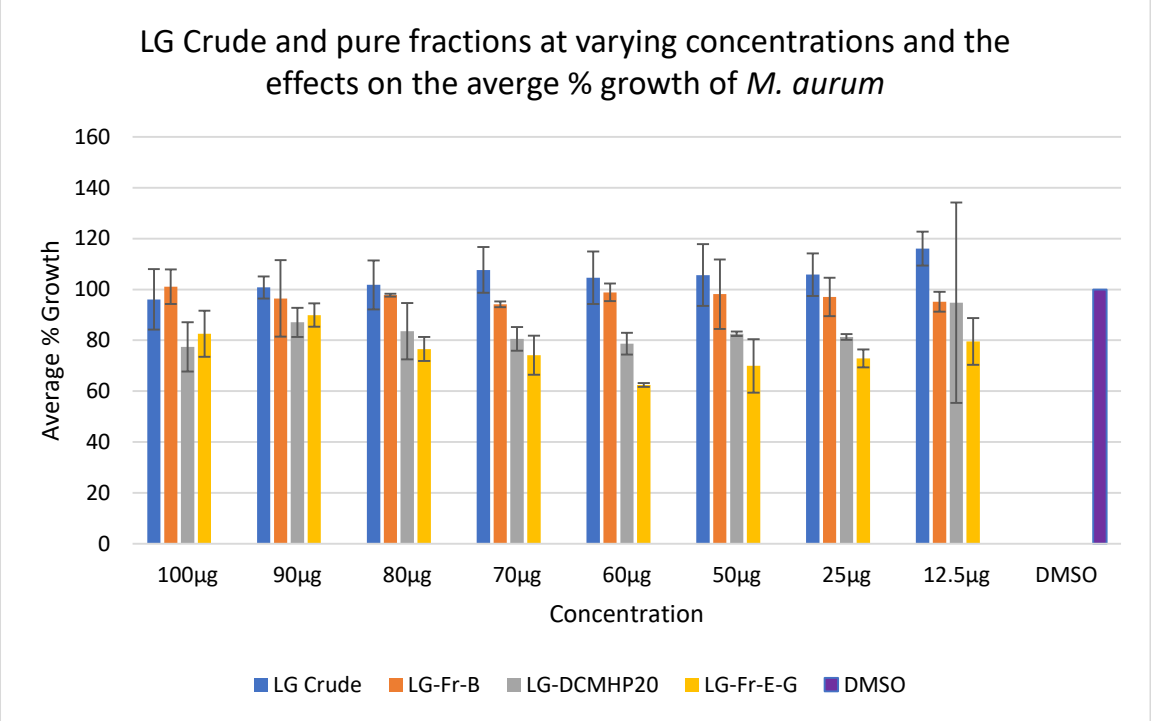

Figure 5.3: *L. glomerata* crude and pure fractions at varying concentrations and the effects on the average % growth of *M. aurum*

In the microdilution assay, the crude and pure compounds were compared to evaluate the impact of fractionation on activity. In Figure 5.3 the crude dilutions appear to be on par with the dimethyl sulfoxide (DMSO) control. Also looking at the error bars the results obtained were closely related, the crude fraction does not appear to have any activity. At lower concentrations, the crude appeared to be promoting the growth of *M. aurum*. The activity observed for the bioautography showed slight activity and therefore corresponds with what was observed in the microdilution assay. It was a possibility that there were masking compounds that could be hiding/suppressing the activity of potential bioactive compounds.

When looking at LG-Fr-B, the trend followed a similar pattern to the crude extract dilutions. It showed a slight downward trend indicating a minor increase in activity. LG-Fr-B was identified from the ^{1}H NMR and was obtained from the step-gradient fractions. There was no further purification and hence masking compounds could potentially still be present. When comparing it to the results of the bioautography, it was interesting that LG-Fr-B had quite a potent activity (indicated by a large zone of activity at block 3). In the bioautography assay, the microorganism was in direct contact with the compound. The discrepancies in activity could be attributed to the possibility of solubility issues. The compounds in the assay are in a 20% (v/v) DMSO

solution in broth, which could lead to compounds (possibly the bioactive compounds) precipitating out of solution. This would effectively reduce the microorganisms' contact area with the active compound (loss of bioavailability), therefore reducing the potency.

When evaluating LG-DCMHP20, the fraction shows an overall inhibitory effect of approximately 20% reduction in bacterial growth. It could be seen that 12.5 µg was a low concentration of the bioactive compound, but not quite sub-lethal, the fraction still inhibits the growth of *M. aurum*. It is important to note the large error bar at 12.5 µg; it would have been best to repeat this fractions testing to obtain a more accurate result. Unfortunately, due to the limited amount of material, a retest could not be performed for this fraction. When comparing the results with the bioautography, LG-DCMHP20 had slight activity against *M. aurum* (block 63, orange circle). This was an interesting comparison as it appeared that the fraction had greater activity in the microdilution assay than in the bioautography assay. One possible explanation was that the compound had a greater affinity to bind to the TLC solid support (silica) and therefore was not bioavailable resulting in decreased activity.

When looking at LG-Fr-E-G dilution results, the trend observed was a bit unusual. The bioactivity of growth inhibition was definitely present, but the activity seems to be masked until further diluted. It could be seen as the sample becomes more dilute, the activity increased until 12.5 µg where the amount of compound was too diluted. An increase in the percentage growth was observed. This trend could be seen by approximately 40% growth inhibition at 60 µg vs 20% growth inhibition at 100 µg. Based on the error bars the values are relatively close to each other and the results obtained are fairly accurate. The average error observed for LG-Fr-E-G is 6.2, this was calculated based on the eight dilutions utilized in the experiment. The error value was low and therefore indicated accuracy in the data. When comparing with the bioautography, a large zone of activity (block 57, blue circle) was observed and this corresponds to the activity observed in the microdilution assay.

In Figure 5.4 the crude extract obtained from *Plocamium cornutum* was compared to the activity profile of the isolated compounds against *M. aurum.*

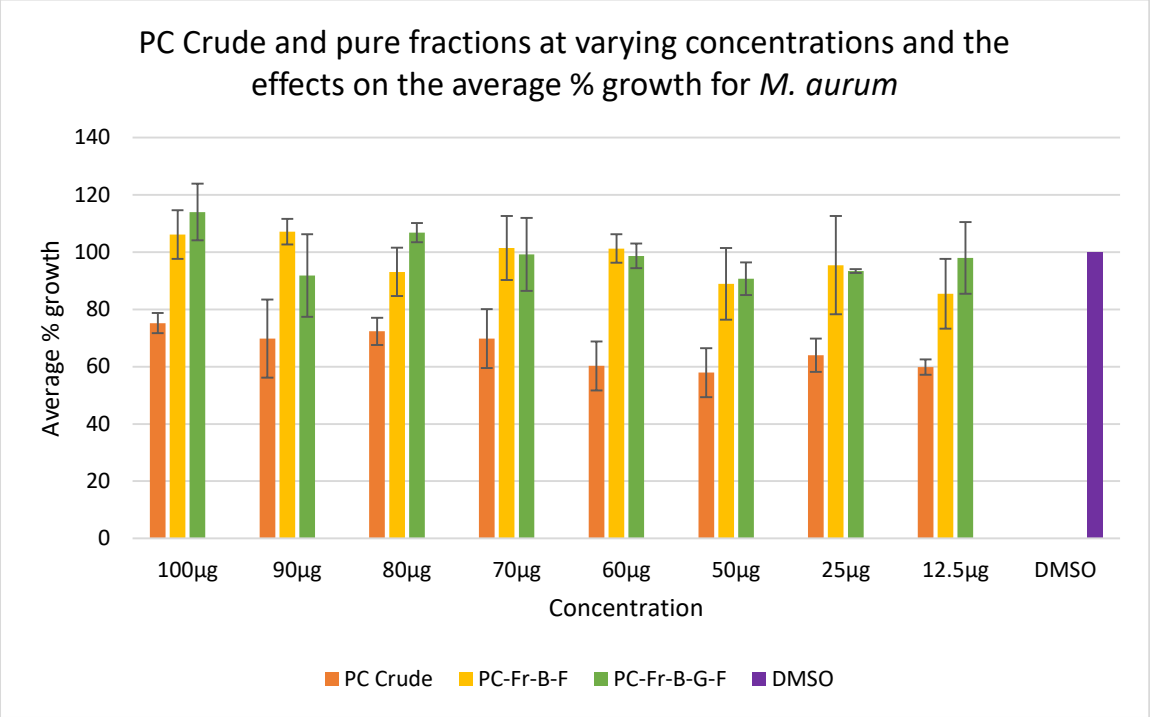

Figure 5.4: *P. cornutum* crude and pure fractions at varying concentrations and the effects on the average % growth for *M. aurum*.

In Figure 5.4 it seemed that the trends observed for *P. cornutum* are the reverse of what was seen for *L. glomerata.* When looking at the crude fraction, the activity of the extract increased as the sample became more dilute. The possible situation was that as the sample was diluted, the masking agents were diluted out. The bioactivity was more pronounced and it was seen on the effect of the *M. aurum* average percentage growth. When comparing to the results obtained in the bioautography, (block 31, small green circle) it was quite surprising that the activity in the microdilution assay was greater than observed for the bioautography. This observation could potentially support the proposal that the dilution enhanced activity by diluting masking compounds thus enhancing the bioactive compounds.

When comparing PC-Fr-B-F and PC-Fr-B-G-F to the crude it can be seen that there was no real bioactivity. Although the pure compounds follow a similar trend as the crude, as it was being diluted the more "active" the fractions become. This trend observed could possibly be due to the compounds being insoluble, forming a precipitate and therefore lost bioactivity. Another possibility could be that there was an interaction between the compounds and the broth components or the test strain has a resistance mechanism to the two compounds being tested (e.g. production of degradation enzymes, binding the compounds in some way resulting in

inactivation, etc.). Comparing PC-Fr-B-F and PC-Fr-B-G-F to the results obtained from the bioautography assay, it was interesting to note that both fractions had a good potency against *M. aurum* (PC-Fr-B-F, block 70 blue circle and PC-Fr-B-G-F, block 75 blue circle). This observation could potentially support the theory that the compounds are either precipitating out of the solution or that the broth itself is interfering with the compounds' activity.

Looking at the pure compounds in Figure 5.3 and Figure 5.4, their bioactivities in either the liquid or solid support could imply potential anti-mycobacterial applications. Compounds **4.27**, **4.28**, and **4.29** isolated from *L. glomerata* showed better antimicrobial activity in the liquid medium (microdilution assay) which therefore could indicate their potential in a liquid treatment preparation. Compounds **4.30** and **4.31** isolated from *P. cornutum* indicated a better antimicrobial activity profile in the bioautography assay (solid support). The possible application could be to prepare antimicrobial surfaces (e.g. to prevent biofilm formation, functionalisation of surfaces in hospitals, etc.). Although marine algae offer great biologically active compounds, realistically there are insufficient yields and material isolated to consider using this approach on a large scale. It would be more financially feasible to discover the natural product compounds, establish their biological impact and then attempt a synthetic approach that could produce greater compound yields. Also the time it takes to isolate natural products is lengthy, when trying to curb the spread of a communicable disease, time is crucial.

5.2.3. Effect of *L. glomerata and P. cornutum* seaweed extracts on human breast cancer cells

The second aim of this chapter was to investigate the cytotoxic activity of *L. glomerata* and *P. cornutum* in order to establish the selectivity of the compound towards tuberculosis. The selection of these seaweed extracts was based on their interesting chemical profile and biological activity, respectively. The crude extracts and their fractions were tested against human breast cancer (MCF-7) and non-tumorigenic breast (MCF-12a) cells. The two cell lines were used to establish the cytotoxic effects of the compounds, to evaluate their selectivity and to determine the possible outcomes if they were to be administered to a patient. The ideal compounds would be the ones that had selective toxicity towards diseased cells and not the normal cells. The two cell lines were exposed to 50 µg/ml of the seaweed compounds over a period of 48 hours, their effect on cell proliferation was assessed by light microscope followed by a water-soluble tetrazolium (WST-1) assay.

The seaweed compounds did not show any visible morphological changes under light microscopy on both MCF-7 and MCF-12a cells after 24 hours of treatment (data not shown). Definite morphological changes on MCF-7 cells treated with 50 µg/ml of selected fractions after 48 hours are shown in Figure 5.5. The MCF-7 cells usually grow as adherent clusters, as reflected in untreated cells and *L. glomerata* (LG) crude treated cells. Major cellular changes were observed in cells treated with LG-Fr (B, G, H and I). The dark spots observed indicated that the cells were dying were as healthy cells were clear. The cells treated with LG-Fr-B displayed apoptotic cell death features, the cells rounded up, detached from the surface and from each other. In contrast, the size of cells treated with LG Fr (G, H and I) shrunk and did not detach from the surface. Thereafter, the WST-1 assay was used to measure the metabolic activity of live cells in order to quantify the proliferation rate of the treated cells.

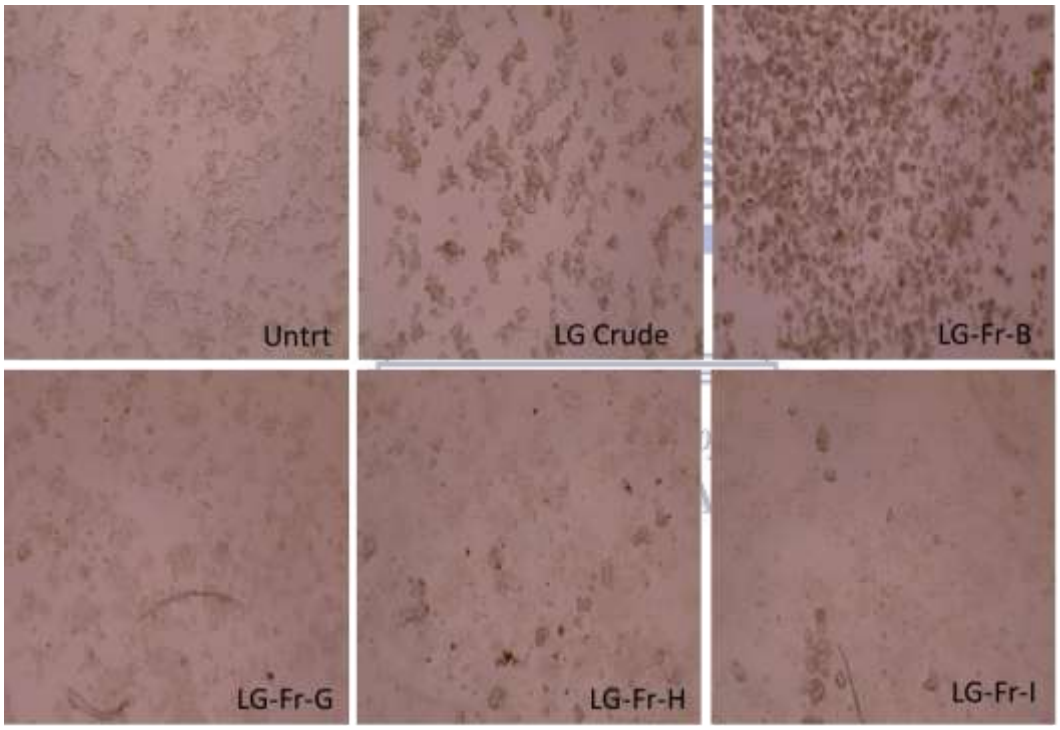

Figure 5.5: Effect of *L. glomerata* on cellular morphology. MCF-7 cells were treated with 50 µg/ml *L. glomerata* compounds for 48 hours. Representative images of cells treated with LG-Fr B, G, H, and I were captured under a light microscope at 10X magnification.

The untreated cells served as the negative control in order to compare the effects each compound has on the cell viability. Since the compounds were dissolved in DMSO, DMSO at the same concentration in the compounds was also included as a negative control. DMSO only had an effect on the cell viability at the concentration >5%. Compared to the untreated cells,

the *L. glomerata* compounds had weak cytotoxic activity against the MCF-7 and MCF-12a cells with >80% cell viability (Figure 5.6). The majority of the *L. glomerata* fractions had higher MCF-12a cell proliferation compared to the untreated cells, especially LG-Fr-A, E, F, H, I and LG-DCMHP20. The general cytotoxic trend was, as the polarity of the fraction increases from the crude, the activity decreased. LG-Fr-B and LG-Fr-E-G were the most active fractions towards MCF-7 cells, however, it was also toxic to non-cancerous cells (MCF 12a). LG-Fr-B had a percentage of cell viability of 58% and 61% against MCF-7 and MCF 12a, respectively. The LG crude and some of the fractions (LG-Fr-A, E, F, H, I) showed selectivity against the cancer cells. LG-Fr-J and LG-Fr-G were highly toxic towards the normal breast cells and has negligible activity against the cancer cells. Interestingly, the selective activity of the parent fraction LG–Fr-E against MCF-7 cells was reduced in the pure compound LG-Fr-E-G.

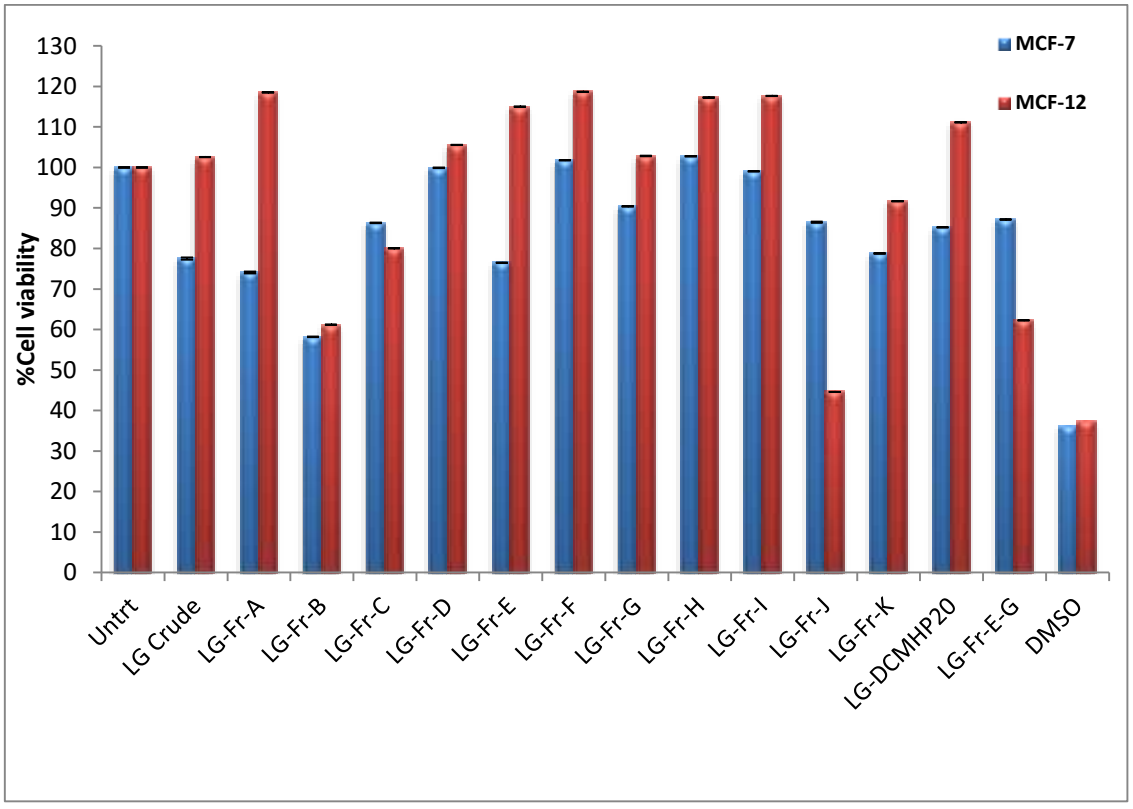

Figure 5.6: Effect of *L. glomerata* compounds on human breast cell lines. Breast cancer (MCF-7) and non-cancer (MCF-12a) cells were treated with 50 µg/ml of the compounds for 48 hours, cellular response to treatment was assessed by WST-1 assay.

The *P. cornutum* (PC) compounds compared to the *L. glomerata* compounds had poor activity against the breast cancer cells. As shown in Figure 5.7, the MCF-12a cells were most susceptible to these compounds. The cytotoxicity of PC compounds increased with the increase in the polarity of the fractions. PC-Fr-E was the only PC fraction with higher inhibitory effects on MCF-7 cells at 78% cell viability. PC-Fr-B-G-F was most toxic to MCF-12a cells with cell viability of 19%, which was less than the parent fraction (PC-Fr-B). Thus, the toxicity of the fractions against MCF-12a cells increased with further fractionation of the parent compound. This trend was observed with the PC-Fr-B, PC-Fr-B-F and PC-Fr-B-G-F which resulted in reduced cell viability from 65% to 37%, and 19%, respectively. The most active fraction (PC-Fr-E) against MCF-7 cells had an inhibitory activity of 66%, which was three times the activity against the MCF-12a cells (22%).

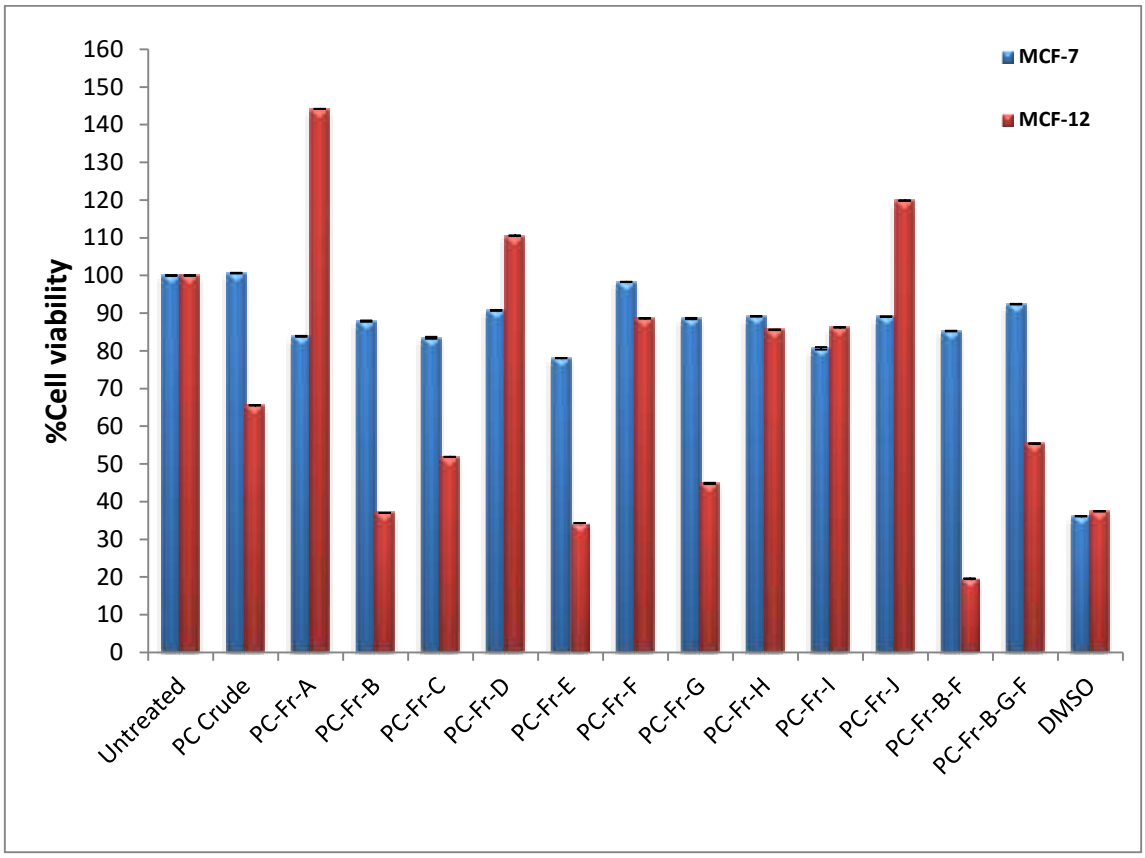

Figure 5.7: Effect of *P. cornutum* compounds on human breast cell lines. Breast cancer (MCF-7) and non-cancer (MCF-12a) cells were treated with 50 µg/ml of the compounds for 48 hours, cellular response to treatment was assessed by WST-1 assay.

5.2.4. Cytotoxicity

Based on the results obtained for *L. glomerata*, it could be seen that there was general weak toxicity towards breast cancer cells. The results imply that the activity towards *M. aurum*+ could potentially be due to non-selective toxicity. Due to the fact that the *L. glomerata* fractions did not display activity towards *M. tuberculosis*, it was difficult to establish the selectivity of the compounds.

It was not surprising that the fractions obtained from *P. cornutum* were more toxic to normal cells as two fractions were responsible for the anti-mycobacterial activity in the library screening. The mycobacterium bacillus is a hardy microorganism and required toxic compounds to cause cell death. This cytotoxicity study indicated the anti-mycobacterial potential of these compounds **4.30** (PC-Fr-B-G-F) and **431** (PC-Fr-B-F). Based on the toxicity towards normal cells, the compounds appeared to be selective for tuberculosis and their activity observed in the library screening was not due to non-selective toxicity. Although these compounds **4.30** and **4.31** were toxic to normal cells many anticancer agents show toxicity to normal cells as well and with possible structural modification, these compounds could be made less toxic to normal breast cells.

Conclusion

In conclusion, this chapter reported on the antimicrobial activity of halogenated sesquiterpenes (compounds **4.27, 4.28, 4.29**) and PC-Fr-B-F and PC-Fr-B-G-F halogenated monoterpenes (compounds **4.30** and **4.31**) against *M. aurum* A+. It was successfully established that the isolated compounds were responsible for the antimicrobial activity observed by the large zones of activity. Compounds **4.30** and **4.31** were also observed to be active in the *M. tuberculosis* MIC_{90} assay reported in Chapter 3. The cytotoxicity results revealed that the fractions obtained from *L. glomerata* were relatively non-toxic towards MCF-7 and MCF-12a except for compound **4.27** which was shown to be toxic towards both cell-lines. The fractions obtained from *P. cornutum* were more toxic to MCF-12a and less toxic to MCF-7. It could be seen that compounds **4.31** and **4.30** were relatively the most toxic of all the fractions indicating that the purification process increased the toxicity observed. The fact that these compounds do not appear to have great toxicity towards MCF-7, indicated that the activity observed with *M. aurum* and *M. tuberculosis* was, in fact, selective for *Mycobacterium* spp. It was also quite possible that the compounds could also be active towards other Gram positive organisms, but this was not assessed during the course of this study.

In the future, it would be a great follow up study to conduct structural modifications to these compounds to increase selectivity and potency towards *Mycobacterium* spp. and decrease the toxicity towards normal human breast cells. It would also be interesting to establish the activity of the isolated compounds **4.27**, **4.28**, **4.29**, **4.30** and **4.31** against tuberculosis and investigate synergistic effects with current tuberculosis treatment.

General Experimental

The test strain, *Mycobacterium aurum* A+ (not an ATCC strain), was prepared by Dr. Marilize Le Roes-Hill at the Institute of Biomedical and Microbial Biotechnology, Cape Peninsula University of Technology.

Test strain *M. aurum* preparation: *M. aurum* A+ was used to determine the antibacterial activity of the extracts and fractions. The *M. aurum* A+ strain was inoculated into 5 ml of Luria-Bertani broth and was incubated for 48 hours at 37 °C and was constantly shaken at 160 rpm. The optical density (OD) was measured at 600 nm and was then adjusted to 0.5 for bioautography experiments and the culture OD is adjusted to 0.8 in liquid assays such as MIC and microbroth dilution assays.

Bioautography: In order to conduct the bioautography using *M. aurum*, the thin-layer chromatography (TLC) plates required the correct preparation. TLC plates, 20 X 20 cm Silica gel 60 $F_{254,}$ were cut in half to afford two 10 X 20 cm plates. A 5mm border was drawn around the edges of the plate to demarcate the working area of the TLC. On the inside of the border, a 1 cm X 1 cm grid was created using pencil lines. Every alternate block was allocated a number such that each sample spotted had a large enough clearance diameter for a sample that may cause a large activity zone. The large clearance was allocated to prevent overlap in the activity zones.

Sample preparation: All the fractions that were generated from the large scale extraction were weighed in order to determine the accurate mass. Based on the masses the samples were then diluted using dichloromethane (DCM) to a concentration of 10 mg/ml and followed a second dilution the final concentration was 1 mg/ml. Using a 200 µl pipette, 20 µl of each fraction was spotted on to the TLC plate under their allocated number. The plate was then left for roughly 10 minutes which allowed the residual DCM solvent to evaporate. The negative control was DCM and the positive control was vancomycin 10 mg/ml. All plates were prepared in duplicate to ensure reliable results. Incubation containers were lined with a sterile water moistened paper towel. The prepared plates were dipped in the *M. aurum* culture until the plates were evenly coated and were removed with tweezers to not disturb the plate. The excess culture was allowed to run off the plate to avoid any oversaturation with culture. The inoculated plates were placed in the incubation container, sealed and were incubated at the test strain's optimal growth temperature of 37 °C for 40 hours. After completing the incubation period, the plates were sprayed with thiazolyl blue (MTT) dissolved in phosphate buffered

saline (4.26 g $Na_2HPO_4.7H_2O$, 2.27 g KH_2PO_4, 8.00 g NaCl per litre, pH to 7.0) at a final concentration of 0.25% (w/v), and incubated for a further three hours in order for the reagent to develop. The size of the activity zones and the efficacy of the extract against *M. aurum* was determined on a qualitative basis.

Antimicrobial assessment experimental

All antimicrobial broth microdilution assays were conducted by Dr. Le Roes-Hill at Cape Peninsula University of Technology (CPUT). The samples to be tested were stored at a concentration of 10 mg/ml in DMSO. The preparation of the test strain, *M. aurum* A+, was as described above. Serial dilutions of the compounds were conducted with the stock solutions to obtain eight varying concentrations of 100, 90, 80, 70, 60, 50, 25, 12.5 µg/ml for each test compound. The dilutions were calculated so that the addition of 20 µl of sample to 180 µl of culture would result in the desired end-concentration to be tested. Sterile 96-well plates were used to conduct the antimicrobial assay. The prepared concentrations for each sample were dispensed into the wells in triplicates. There were four controls used in the assay to ensure the integrity of the results obtained. The antibiotic control (positive control) comprised of culture and antibiotic (vancomycin). The solvent control (negative control) was made up of culture and DMSO. The sterile control (negative control) comprised of media and sterile water. Lastly, culture control, which was made up of media and culture. The controls were prepared in triplicate to ensure a cohesive result. Once the plates were completed, a Diversified Biotech breathe-easier membrane was firmly placed on the 96-well plate. The test plates were incubated at 37 °C, which is optimum growth temperature, for 48 hours. After the incubation period was completed, 20 µl off a 0.25% (w/v) MTT dye was added to each well and the plates were incubated for an additional three hours to allow the dye to develop. Upon detection of precipitation of the formazan dye, 100 µl of DMSO was added to dissolve the precipitate and was incubated for another four hours at room temperature. Once the plates completed the incubation period, the OD of each plate was read at 570 nm on a Rayleigh UV-9200. The absorbance values were used to determine the percentage growth.

$$\% \text{ growth} = \frac{Absorbance\ of\ sample}{absorbance\ of\ negative\ control\ (culture+DMSO)} \times 100\%$$

The average of the three percentage growth values obtained from the triplicate assay was determined by:

$$\text{Average \% growth} = \frac{(Growth\ \%\ A)+(Growth\ \%\ B)+(Growth\ \%\ C)}{3} \times 100\%$$

Finally, the mean of the % growth values was established in order to determine the standard deviation for each set of triplicates. This is an indication of the amount of error that was introduced in the experiment.

$$\text{Standard deviation} = \sqrt{\frac{(Growth\ \%\ A - mean)^2 + (Growth\ \%\ B - mean)^2 + (Growth\ \%\ C - mean)^2}{n-1}}$$

Cytotoxicity

All cytotoxicity assays were conducted by Dr. Nicole Sibuyi under the supervision of Professor Mervin Meyer at the Department of Biotechnology, University of the Western Cape.

The cell lines MCF-7 and MCF-12a were obtained from the American Type Culture collection.

Cell seeding: The MCF-7 and MCF-12a cell lines were removed from the -150 °C storage, thawed and harvested by centrifugation. The MCF-7 and MCF-12a cell lines were grown in the appropriate growth media and were incubated at 37 °C in a humidified 5% CO_2 incubator, which was the standard culture conditions. Cells were grown until >70% confluence was achieved.

Cell counting: Cell counting was conducted by Countess ™ cell counting chamber slide, which is an automated cell counter. The viability measurement and cell count were conducted using trypan blue stain. Living cells appear as clear round bodies whereas dead cells appear blue.

Cell trypsinizing: Once the cells reach 70-90% confluence, they are trypsinized which was the process of detaching cells from the culture flask and to allow the cells to be recovered via centrifugation. The cells were then re-suspended in growth medium to begin experimentation.

WST-1 assay: To visualize the effect the sample has on the cells the cytotoxicity assay was performed using tetrazolium salt WST-1 which in the presence of living cells is converted to formazan which was a purple dye. A plate density of 100 µl of $1x10^5$ cells of MCF-7 and MCF-12a cell lines were seeded into each well of a 96-well plate and was incubated at 37 °C for 24 hours in a 5% CO_2 humidified incubator. Upon completion of the incubation period, fresh medium containing 50 µg/ml of each test fraction replaced the initial growth medium for the treated cells and the negative control cells received fresh growth medium as well. All assays were conducted in triplicate and were incubated for another 48 hours under the standard culture conditions. Subsequent to the completion of the second incubation period, 50 µl of the WST-1

dye was added to each well and was incubated under standard culture conditions for an additional three hours after which the absorbance was read. The microplate reader measures the plates at a wavelength of 440 nm. The formula for calculating cell percentage viability is as follows:

$$\% \text{ Cell proliferation inhibition} = 100 - \frac{Absorbance\ of\ treated\ cells}{Absorbance\ of\ negative\ control} \times 100\%$$

References

Allmendinger, A., Spavieri, J., Kaiser, M., Casey, R., Hingley-Wilson, S., Lalyani, A., Guiry, M., Bluden, G., Tasdemir, D., Antiprotozoal, antimycobacterial and cytotoxic potential of twenty-three British and Irish red algae. *Phytotherapy Research* **2010**, 24(7), 1099-1103.

Balouiri, M., Sadiki, M., Ibnsouda, S. K., Methods for in vitro evaluating antimicrobial activity: A review. *Journal of Pharmaceutical Analysis* **2016**, 6(2), 71-79.

Choma, I. M., Grzelak, E. M., Bioautography detection in thin-layer chromatography. *Journal of Chromatography A* **2011**, 1218(19), 2684-2691.

El-Kassas, H. Y., El-Sheekh, M. M., Cytotoxic activity of biosynthesized gold nanoparticles with an extract of the red seaweed *Corallina officinalis* on the MCF-7 human breast cancer cell line. *Asian Pacific Journal of Cancer Prevention* **2014**, 15(15), 4311-4317.

Habbu, P., Warad, V., Shastri, R., Madagundi, S., Kulkarni, V. H. Antimicrobial metabolites from marine microorganisms. *Chinese Journal of Natural Medicines* **2016**, 14(2), 101–116.

Kenny, C. R., Furey, A., Lucey, B., A post-antibiotic era looms: can plant natural product research fill the void?, *British Journal of Biomedical Science* **2015**, 72(4), pp.191-200.

König, G. M., Wright, A. D., Franzblau, S. G., Assessment of antimycobacterial activity of a series of mainly marine derived natural products. *Planta Medica* **2000**, 66(04), 337-342.

Lalitha, M. K., Manual on antimicrobial susceptibility testing. *Performance standards for antimicrobial testing: Twelfth Informational Supplement* **2004,** 56238, 454-456.

Li, W., Zhou, L., Xu, Y., Study of the in vitro cytotoxicity testing of medical devices. *Biomedical Reports* **2015,** 3(5), 617-620.

Lince-Deroche, N., Rayne, S., van Rensberg, C., Benn, C., Masuku, S., Holele, P., Breast cancer in South Africa: developing an affordable and achievable plan to improve detection and survival. *South African Health Reviews* **2017**, 2017(1), 181-188.

Reller, L. B., Weinstein, M., Jorgensen, J. H., Ferraro, M. J., Antimicrobial susceptibility testing: a review of general principles and contemporary practices. *Clinical Infectious Diseases* **2009**, 49(11), 1749-1755.

Sánchez, J. G. B., Kouznetsov, V. V., Antimycobacterial susceptibility testing methods for natural products research. *Brazilian Journal of Microbiology* **2010**, 41(2), 270-277.

Saravanakumar, D., Antimycobacterial activity of the red algae *gelidium pristoides, plocamium corallorhiza* and *polysiphonia virgate* **2006** (Doctoral dissertation, University of Cape Town).

Sood, S., Yadav, A., Shrivastava, R., Mycobacterium aurum is unable to survive mycobacterium tuberculosis latency associated stress conditions: Implications as non-suitable model organism. *Indian Journal of Microbiology* **2016**, 56(2), 198-204.

Tiberi, S., Buchanan, R., Caminero, J. A., Centis, R., Arbex, M. A., Salazar, M., Potter, J., Migliori, G. B., The challenge of the new tuberculosis drugs. *La Presse Médicale* **2017**, 46(2), 41-51.

Ventura, T. L. B., da Silva Machado, F. L., de Araujo, M. H., de Sousa Gestinari, L. M., Kaiser, C. R., de Assis Esteves, F., Lasunskia, E. B., Soares, A. R., Muzitano, M. F., Nitric oxide production inhibition and anti-mycobacterial activity of extracts and halogenated sesquiterpenes from the Brazilian red alga *Laurencia dendroidea* J. Argardh, *Pharmacognosy Magazine* **2015**, 11(suppl 4), S611.

World Health Organisation. Global Tuberculosis Report **2018**. page 6, 27, 34. [Accessed November 15, 2018] from: http://www.who.int/tb/publications/global_report/Main_text_21Sept2018_v1.1.pdf

Chapter 6

Conclusion

6.1. General summary

The marine environment and its vast biodiversity remain an area that requires more exploration. It is evident that interest in the marine environment for the discovery of novel compounds, with medicinal potential, is indeed growing [Cikoš *et al*., 2018]. The South African coastline is rich with marine life and has a large diversity of seaweed species, some of which are potentially endemic [Anderson *et al.*, 2016]. The investigation of seaweed as a source of drug leads compounds is still in the early stages and has a wealth of potential for the drug discovery process as well as many other applications [Rampelotto and Trincone, 2018]. The investigation into seaweed may lead to the discovery of new metabolites and possibly uncover new mechanisms of action [Terekhov *et al*., 2018]. The current research study demonstrates that South African marine algae could potentially be a new and exciting source of anti-tuberculosis lead compounds.

A prefractionated South African marine algal library was successfully developed and chemically characterized and profiled by ^{1}H NMR. The fractionation method used to develop the library proved successful as there was a high column recovery as well as distinct chemical profiles per fraction. The library was screened against *Mycobacterium tuberculosis* (Mtb) and *M. aurum* in order to identify fractions with anti-tuberculosis activity. Based on the activity and chemical profiles observed, one species (*Plocamium cornutum*) was selected for its anti-mycobacterial activity and another species (*Laurencia glomerata*) was chosen based on the uniqueness of the spectra. Two halogenated monoterpenes were isolated from *P. cornutum* (compound **4.30** and **4.31**) and three halogenated sesquiterpenes were isolated from *L. glomerata* (compound **4.27**, **4.28**, **4.29**). Although some of the initial library factions screened showed fair activity against Mtb, the selected seaweed fractions showed good activity against *M. aurum*. Further studies of the pure compounds against Mtb are required. *M. aurum* may be a useful test organism, but it is not always an effective surrogate for Mtb. The isolated monoterpenes showed moderate cytotoxicity against cancer cell line MCF-12a, whilst showing little activity towards MCF-7 indicating the activity observed against Mtb and *M. aurum* appears to be selective for the mycobacterium organism. The sesquiterpenes, however, were more selective for MCF-7 and exhibited little activity against MCF-12a. This result corresponds with the fact that the *L. glomerata* fractions did not exhibit much *M. tuberculosis*

and *M. aurum* activity. The continued exploration of marine algae could potentially uncover lead compounds with the desired biological activity. Modifications to the isolated structures and establishing these compounds' pharmacophores will be an invaluable contribution to the discovery of anti-mycobacterial compounds.

6.2. Limitations encountered

The biggest difficulty when working with natural products is the amount of sample obtained per fraction and the pure compound is limited. This heavily impacted the quality of the results obtained. Having a limited sample also meant that it was not ideal to repeat experiments several times as in the case of direct bioautography. The incubation period was too long and allowed for regrowth of the *M. aurum*, hence the light purple zones of inhibition were considered as active. The solubility of natural products is another great concern as the compounds are usually highly lipophilic. Although these compounds are stored in DMSO which is commonly used for bioassays and storage, the compounds could form a precipitate and not display an accurate activity. Due to time constraints, the pure compounds isolated in this study were not retested to establish their activity against *M. tuberculosis*. Lastly, another limitation to this study was only two seaweeds were selected of the 17 which were screened for anti-mycobacterial activity. The seaweeds selected may not have been the only seaweeds that could prove useful to the study. In an ideal situation, the four seaweeds which exhibited anti-mycobacterial activity should have been explored further.

6.3. Recommendations for future work

It was not possible to test all the fractions that showed anti-mycobacterial activity against both *M. tuberculosis* and *M. aurum*, it would be a good follow up study to identify the compounds which are responsible for the activity. Exploring the potential of enhancing the isolated compounds' activity through structure-activity relationships and identifying the isolated compounds pharmacophores could prove beneficial in designing new anti-mycobacterial drugs. It would have been useful to assess the "druggability" of the compounds, such as amenability to synthesis, their logP, solubility, Lipinski, metabolism, etc. Only the crude sample and fractions obtained from *L. glomerata* and *P. cornutum* were screened for MCF-7 and MCF-12a activity; it would be interesting to establish the cytotoxicity profiles of the entire marine algal library. The last recommendation for follow up study is the effects of these isolated compounds and known anti-tuberculosis therapies, to establish whether it is synergistic or antagonistic.

References

Anderson, R. J., Stegenga, H., Bolton, J. J., Seaweeds of the South African Coast. World Wide Web electronic publication, University of Cape Town, http://southafrseaweeds.uct.ac.za; Accessed on 24 July 2019.

Cikoš, A. M., Jokić, S., Šubarić, D., Jerković, I., Overview on the application of modern methods for the extraction of bioactive compounds from marine macroalgae. *Marine Drugs* **2018**, 16(10), 348.

Rampelotto, P. H. and Trincone, A. eds., *Grand Challenges in Marine Biotechnology*. *Springer* **2018**.

Terekhov, S. S., Osterman, I. A., Smirnov, I. V., High-Throughput Screening of Biodiversity for Antibiotic Discovery. *Acta Naturae* **2018**, 10(3), 23.

Supplementary Data

Chapter 3: Supplementary data

S/N	Seaweed Code	PERCENTAGE BY MASS OF FRACTIONS									Total % Recovered
		100% Hex	90% Hex/ 10% EtAOc	80% Hex/ 20% EtAOc	60% Hex/ 40% EtAOc	40% Hex/ 60% EtAOc	20% Hex/ 80% EtAOc	100% EtOAc	50% CH_3OH / 50% EtOAc	100% CH_3OH	
1	NV160819-1	6,83	0,16	8,36	46,70	8,84	2,89	1,05	21,46	3,70	100,0
2	NV160819-6	6,81	0,97	23,11	23,60	12,65	2,92	2,19	2,92	24,82	100,0
3	NV160819-10	0,76	15,15	52,02	3,28	4,80	1,52	1,52	14,90	6,06	100,0
4	NV160820-8	4,81	10,11	23,45	17,57	10,40	4,81	1,96	23,06	3,83	100,0
5	NV160819-5	13,52	19,76	18,37	11,27	9,01	1,21	2,60	22,53	1,73	100,0
6	NV160820-7	9,95	16,20	31,94	13,43	0,46	1,85	0,23	21,99	3,94	100,0
7	NV160819-7	13,04	10,14	20,05	13,77	7,49	4,11	2,42	21,74	7,25	100,0
8	NV160819-4	13,20	25,22	6,63	3,01	2,51	3,17	10,69	32,96	2,62	100,0
9	NV160820-3	12,78	10,74	7,41	10,00	4,07	6,30	9,81	25,56	13,33	100,0
10	NV160820-9	6,06	7,99	6,34	9,92	6,89	4,13	13,50	20,39	24,79	100,0
11	NV160819-11	3,86	14,79	23,79	6,43	2,57	11,25	0,32	20,58	16,40	100,0
12	NV160820-101	13,73	10,60	6,02	20,60	15,18	5,42	3,61	21,93	2,89	100,0
13	NV160819-2	5,07	8,33	9,42	27,17	14,13	8,70	4,35	13,41	9,42	100,0
14	NV160820-2	13,28	28,91	15,49	6,50	6,36	3,46	2,35	19,23	4,43	100,0
15	NV160819-3	3,07	19,05	10,60	9,52	11,21	5,22	4,92	29,03	7,37	100,0
16	NV160819-13	7,88	15,15	6,85	10,79	5,60	2,90	2,70	42,53	5,60	100,0
17	NV160820-10	25,25	7,21	8,20	16,72	2,30	4,26	0,33	29,51	6,23	100,0

Figure S3.1: Data for percentage recovery by mass of fraction based on polarity data

Ave % by Mass of Fraction	9,41	12,97	16,36	14,72	7,32	4,36	3,80	22,57	8,49
STD	5,88	7,60	12,17	10,64	4,37	2,56	3,89	8,50	7,22

Figure S3.2: Data for the bar graph showing the average percentage of mass recovered per fraction

S/N	Seaweed Code	Mass of Extract (g)
1	S. Elegans NV16	0,1516
2	L. Glomerata NV	0,053
3	P. Cornutum NV	0,0485
4	Dictyote SP NV	0,1139
5	L. Flexuosa NV1	0,1022
6	Dictyote Dichot	0,0888
7	L. Stegengae NV	0,056
8	Porteria Hornar	0,1673
9	P. Suhrrii NV16	0,0431
10	Chondria SP NV	0,0349
11	Chondrocanthu	0,0318
12	No Name NV16	0,0805
13	Hypnea Specife	0,0464
14	P. Rigidium NV	0,0592
15	P. Corallorhiza	0,1063
16	Polysiphonia of	0,0498
17	Colpomeria Sin	0,0418

Figure S3.3: Data for bar graph showing the masses of the crude extracts obtained from the extraction process

S/N	Seaweed Code	Percentage Recovery
1	*S. elegans* NV160819-1	82,1
2	*L. glomerata* NV160819-6	77,5
3	*P. cornutum* NV160819-10	81,6
4	*Dictyote sp.* NV160820-8	89,5
5	*L. flexuosa* NV160819-5	56,5
6	*Dictyote dichotoma var. intricata* NV160820-7	48,6
7	*L. stegengae* NV160819-7	73,9
8	*Porteria hornamannii* NV160819-4	107,4
9	*P. suhrrii* NV160820-3	125,3
10	*Chondria sp*. NV160820-9	104,0
11	*Chondrocanthus ascicularus* NV160819-11	97,8
12	No Name NV160820-101	103,1
13	*Hypnea specifera* NV160819-2	59,5
14	*P. rigidium* NV160820-2	122,1
15	*P. corallorhiza* NV160819-3	61,2
16	*Polysiphonia namibiensis* NV160819-13	96,8
17	*Colpomeria sinuose* NV160820-10	73,0

Figure S3.4: Data for bar graph showing sample recovery after fractionation by silica gel column chromatography

Chapter 4: Supplementary data

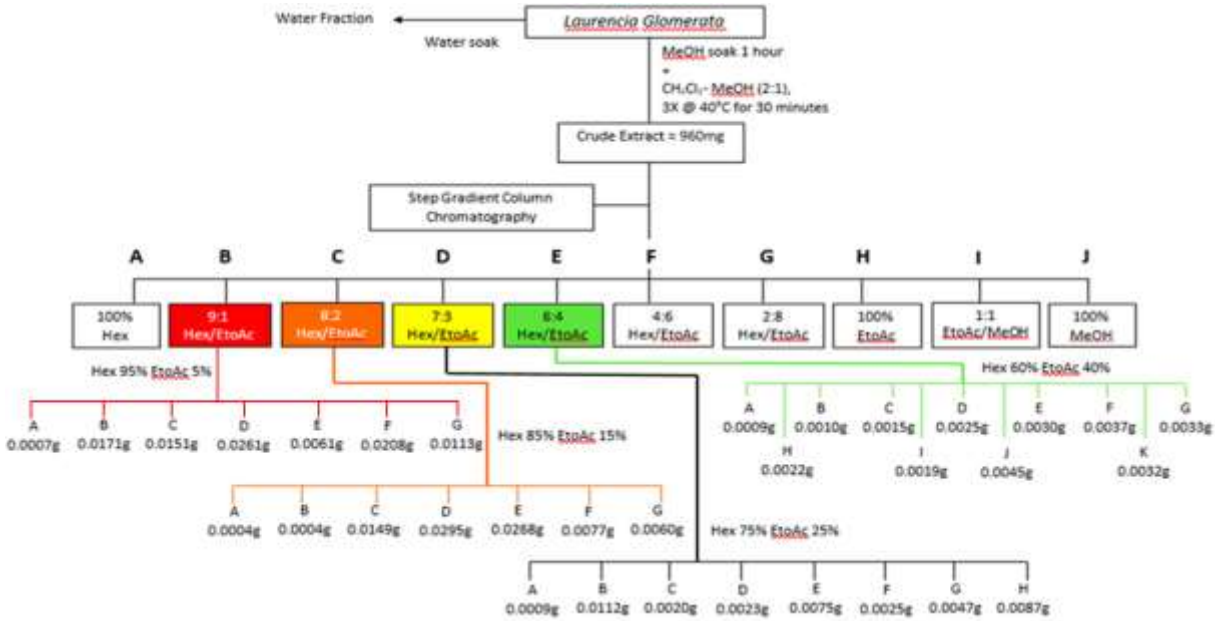

Figure S4.1: The total extraction and fractionation of *Laurencia glomerata*

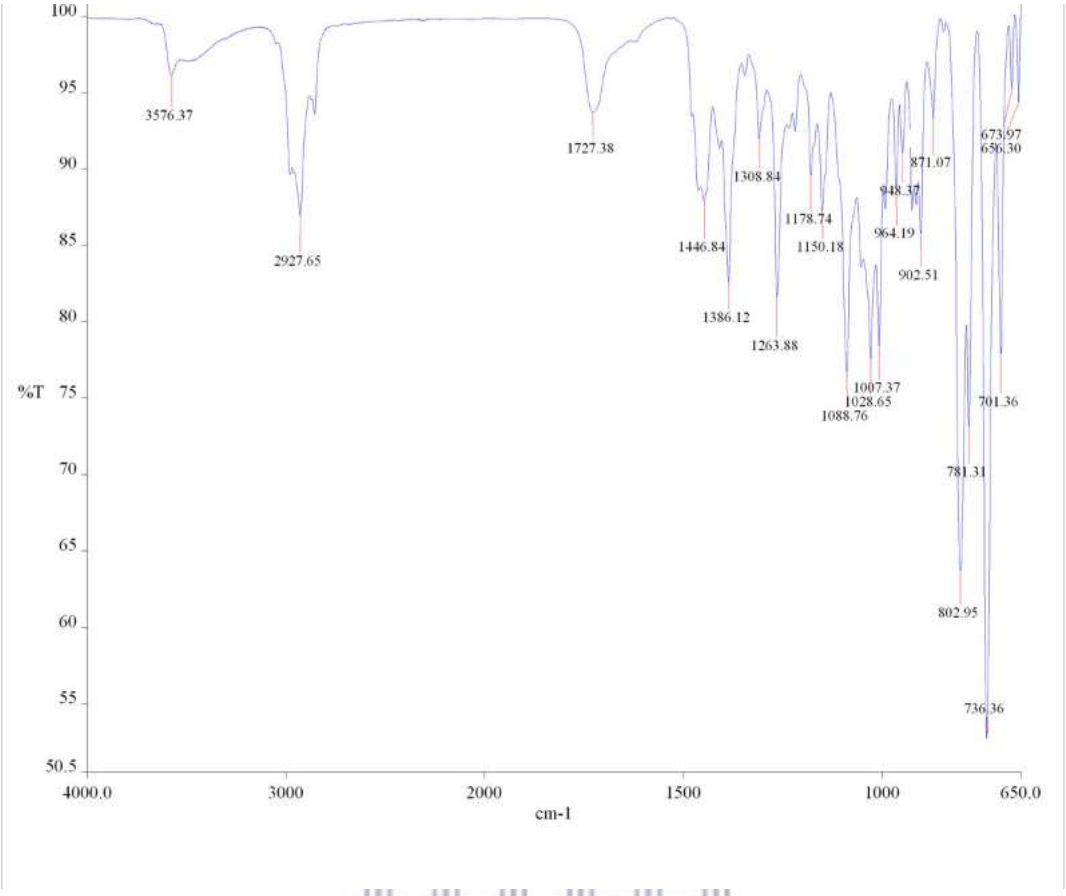

Figure S4.2: FTIR data for compound **4.27**

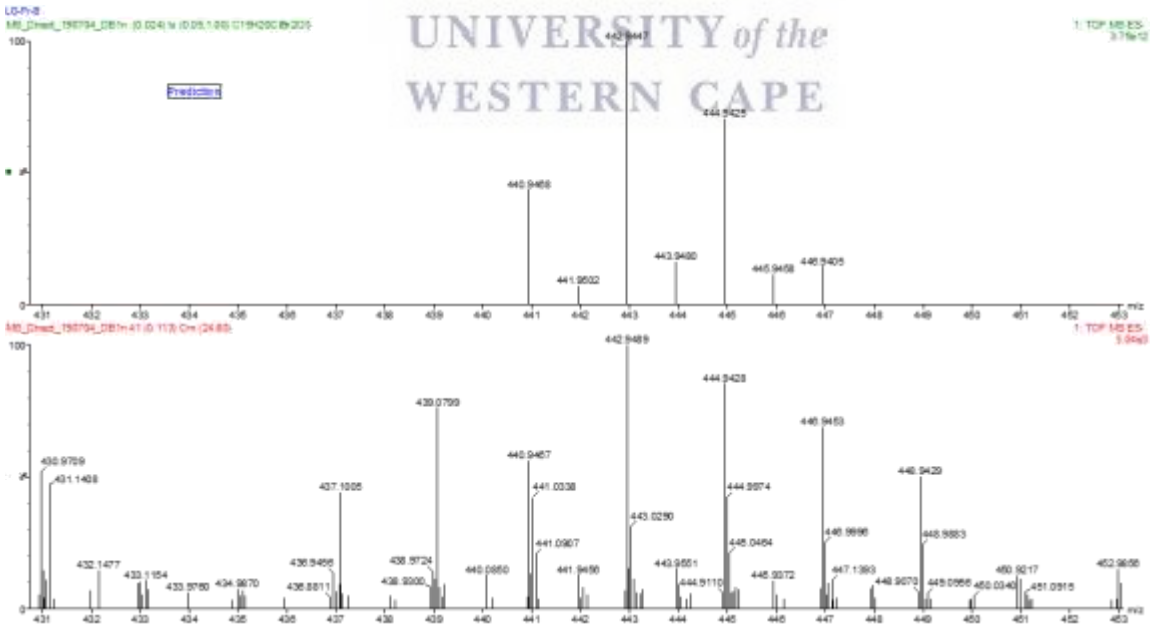

Figure S4.3: HR-ESIMS data for compound **4.27**

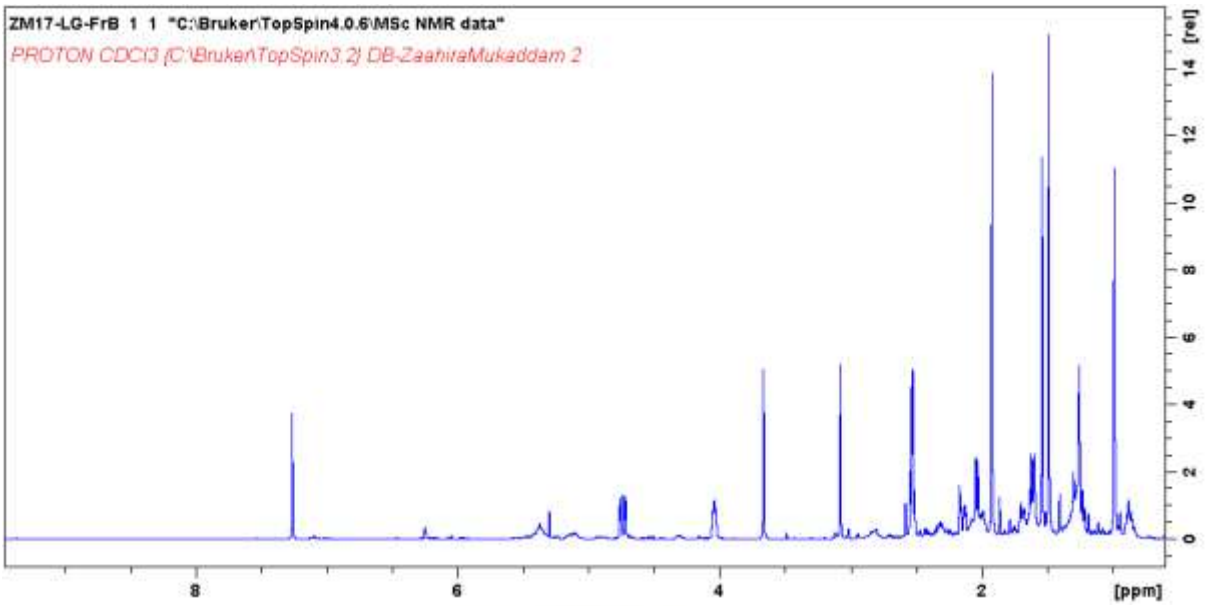

Figure S4.4: ^{1}H NMR spectra of compound **4.27** ($CDCl_3$, 400 MHz)

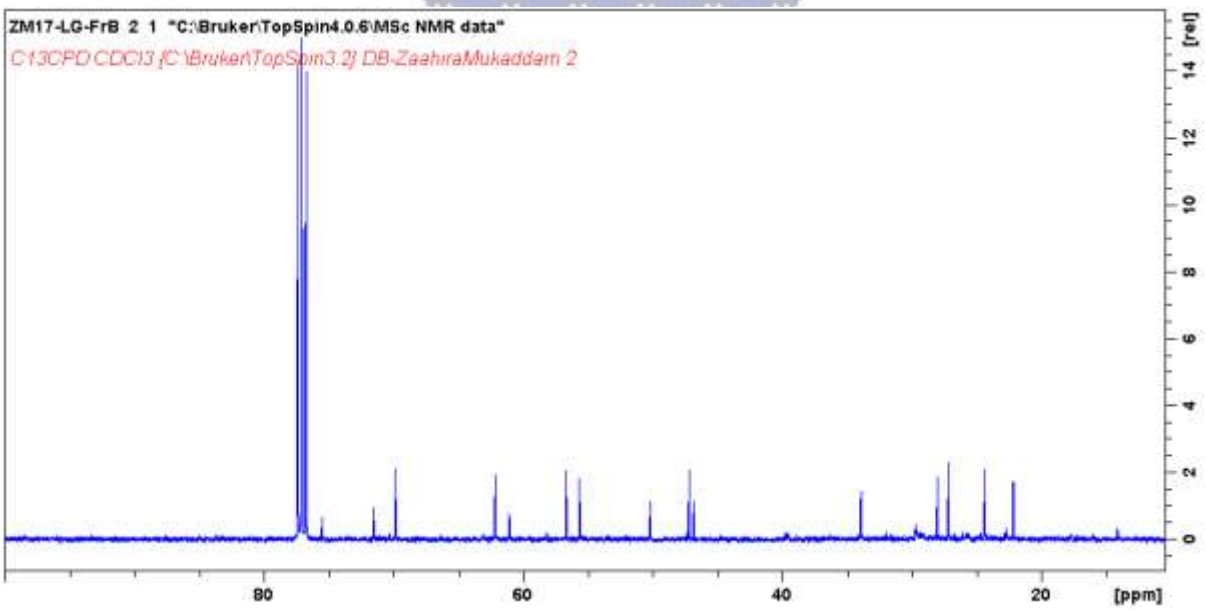

Figure S4.5: ^{13}C NMR spectra of compound **4.27** ($CDCl_3$, 400 MHz)

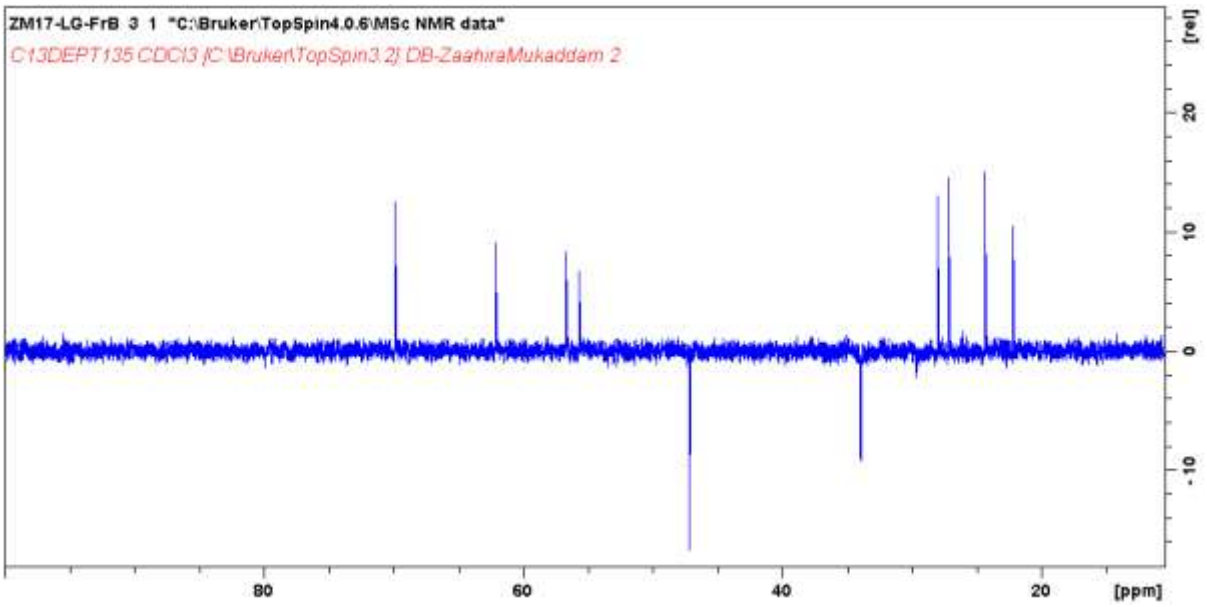

Figure S4.6: DEPT-135 spectra of compound **4.27** ($CDCl_3$, 400 MHz)

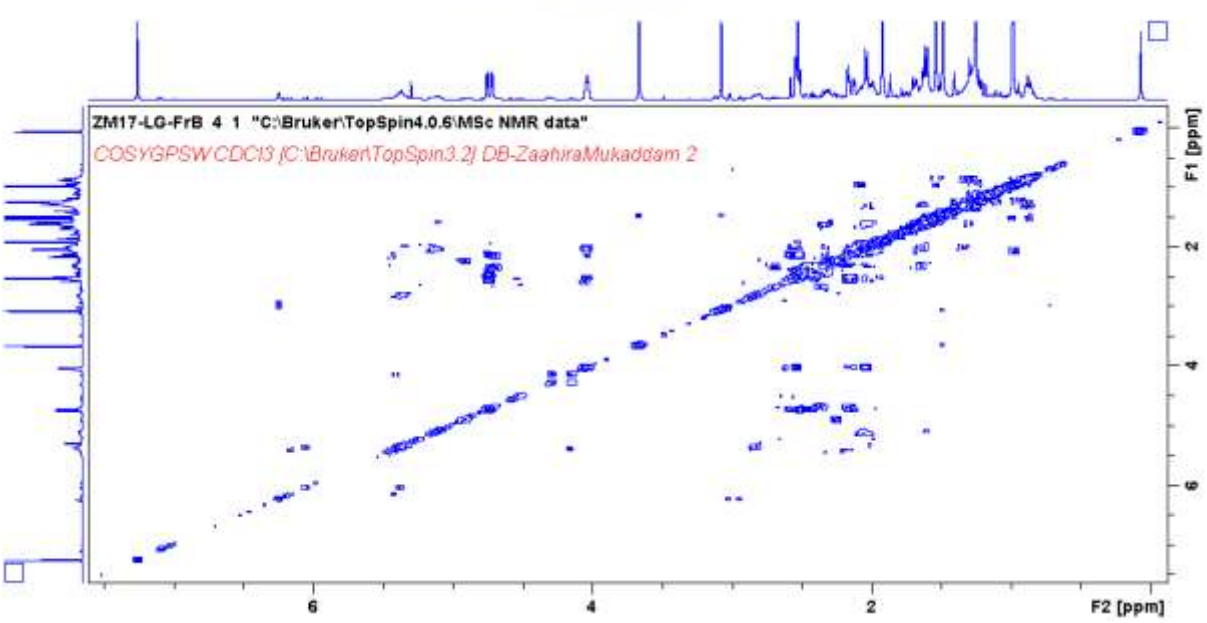

Figure S4.7: COSY spectra of compound **4.27** ($CDCl_3$, 400 MHz)

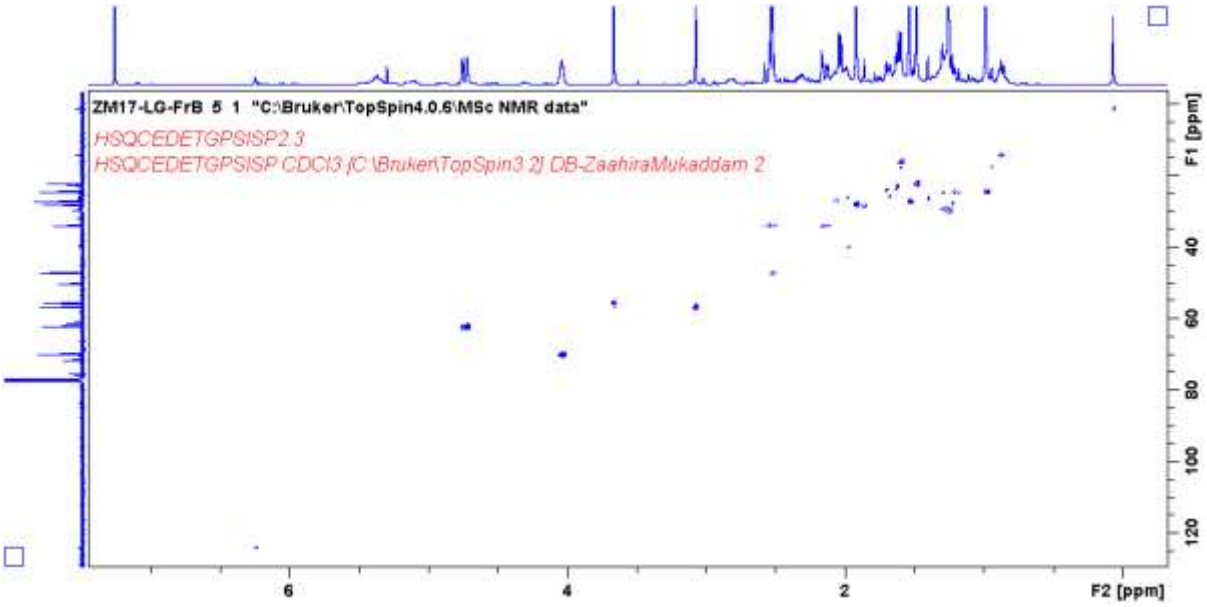

Figure S4.8: HSQC spectra of compound **4.27** ($CDCl_3$, 400 MHz)

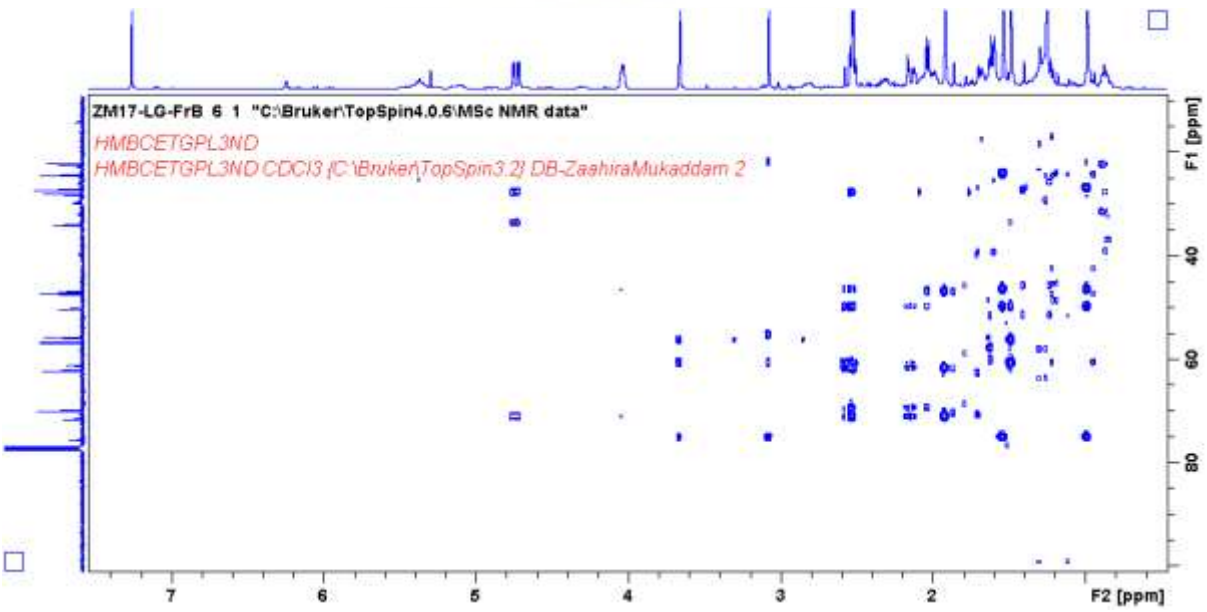

Figure S4.9: HMBC spectra of compound **4.27** ($CDCl_3$, 400 MHz)

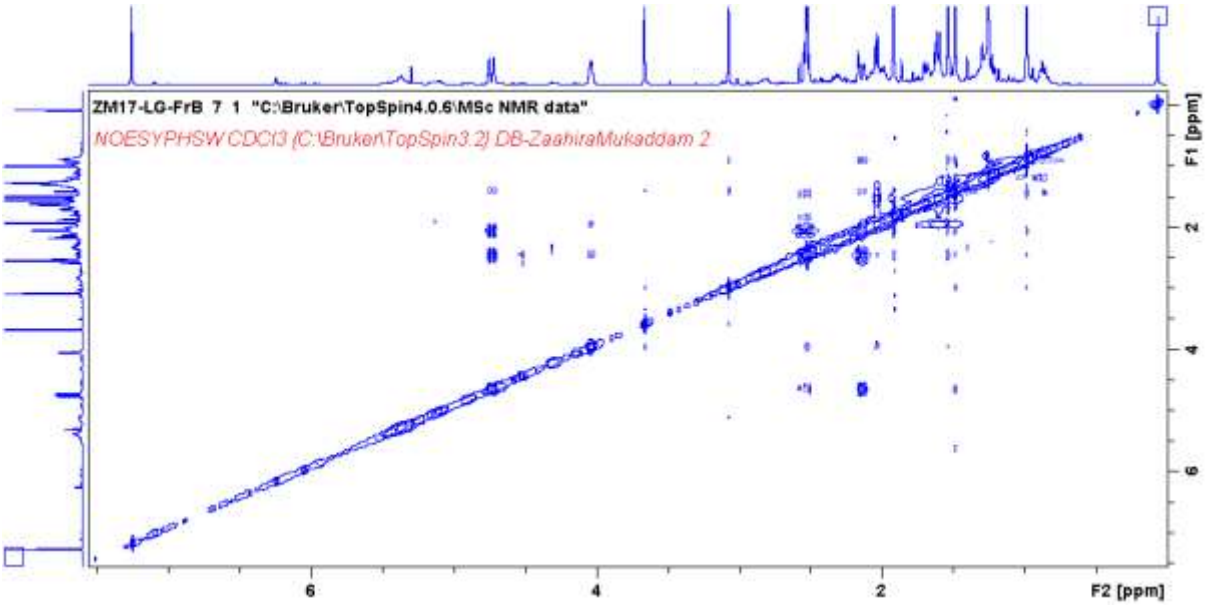

Figure S4.10: NOESY spectra of compound **4.27** ($CDCl_3$, 400 MHz)

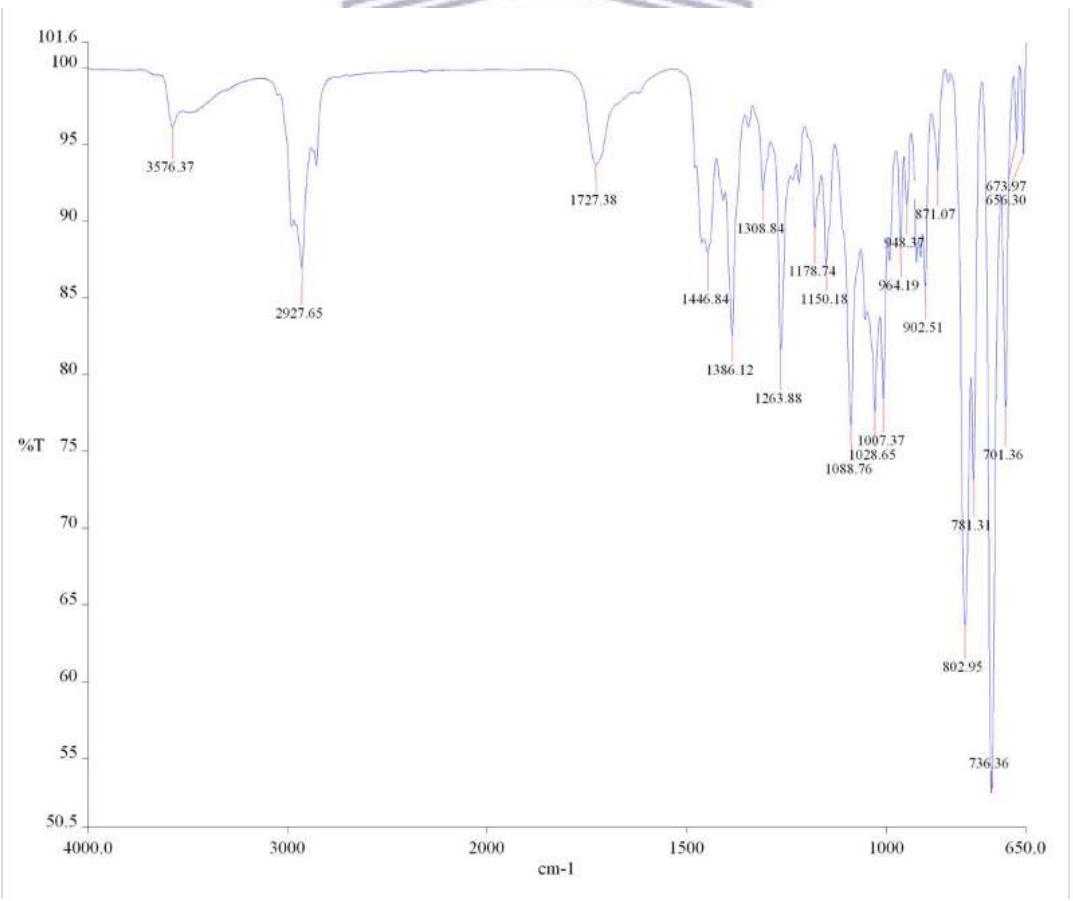

Figure S4.11: FTIR data for compound **4.28**

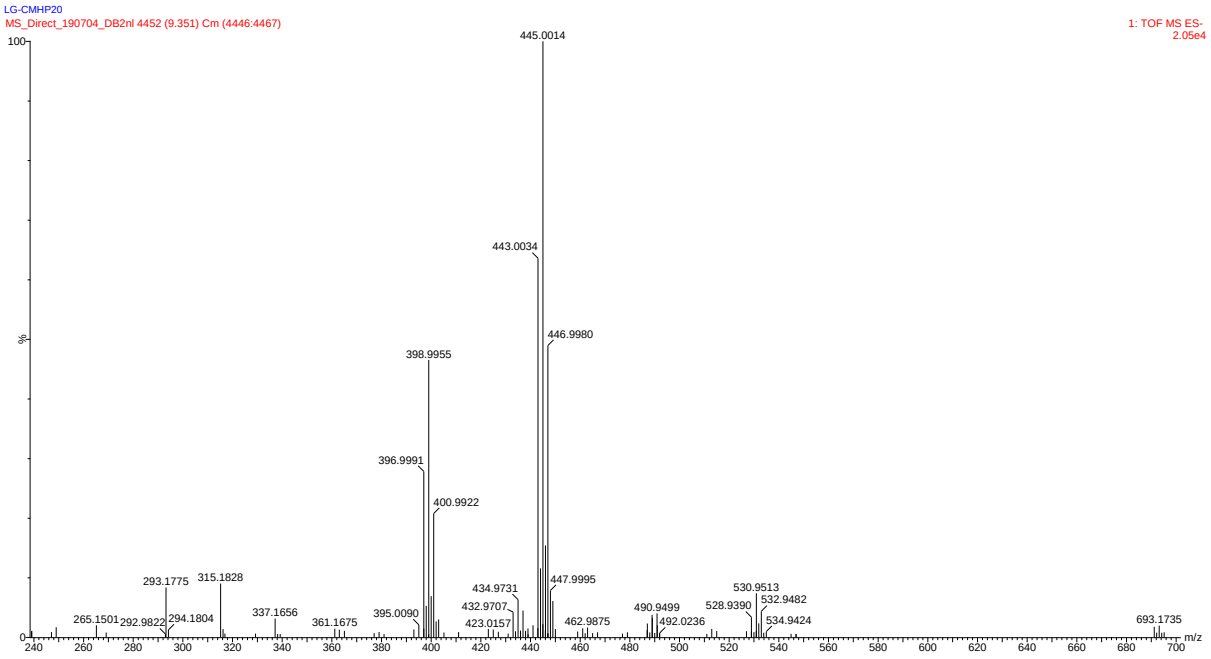

Figure S4.12: HR-ESIMS data for compound **4.28**

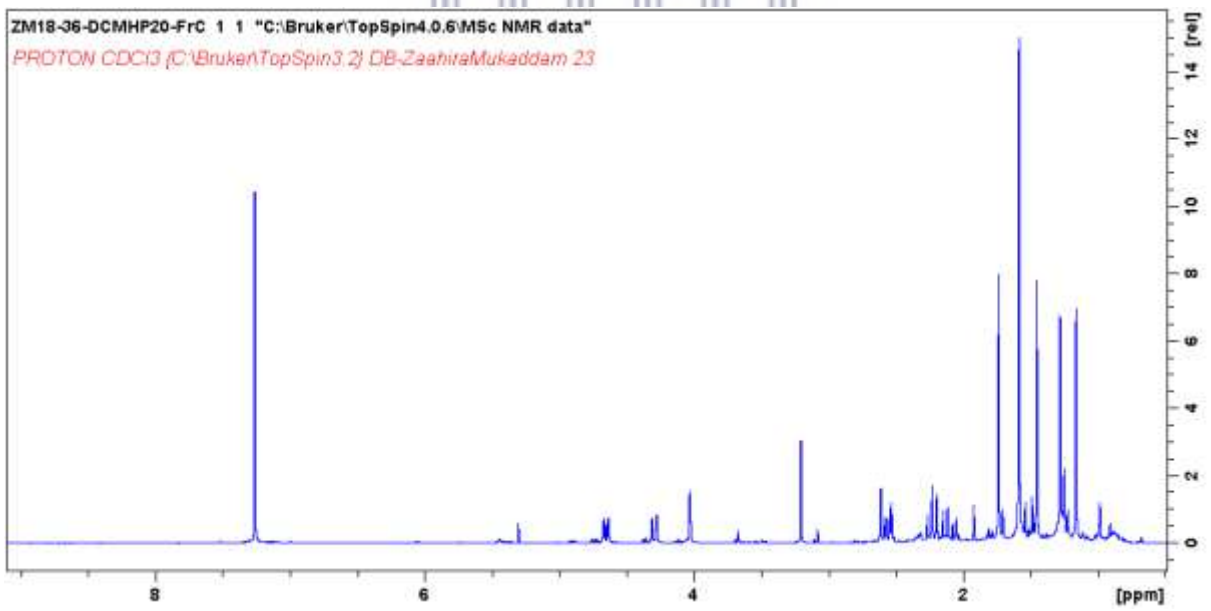

Figure S4.13: ^{1}H NMR spectra of compound **4.28** ($CDCl_3$, 400 MHz)

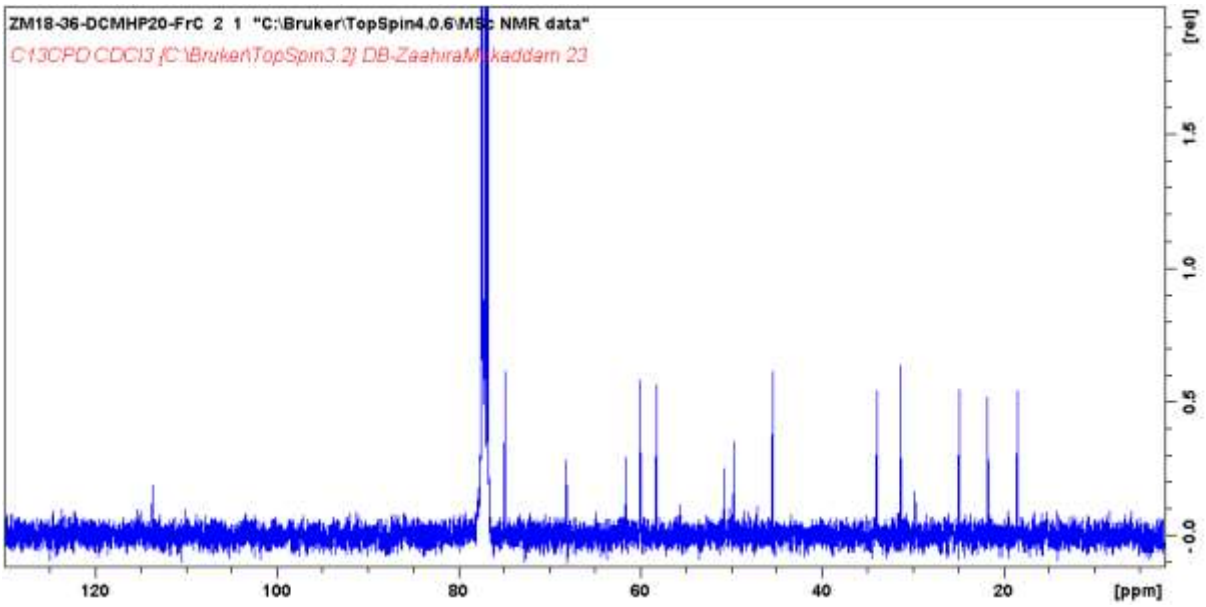

Figure S4.14: ^{13}C NMR spectra of compound **4.28** ($CDCl_3$, 400 MHz)

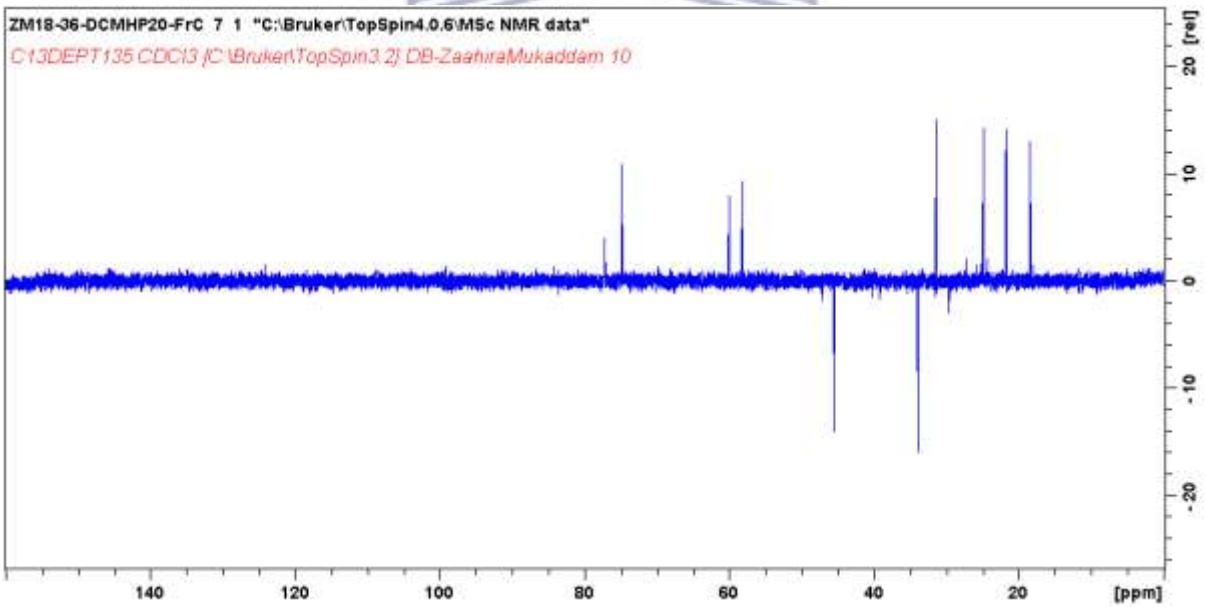

Figure S4.15: DEPT-135 spectra of compound **4.28** ($CDCl_3$, 400 MHz)

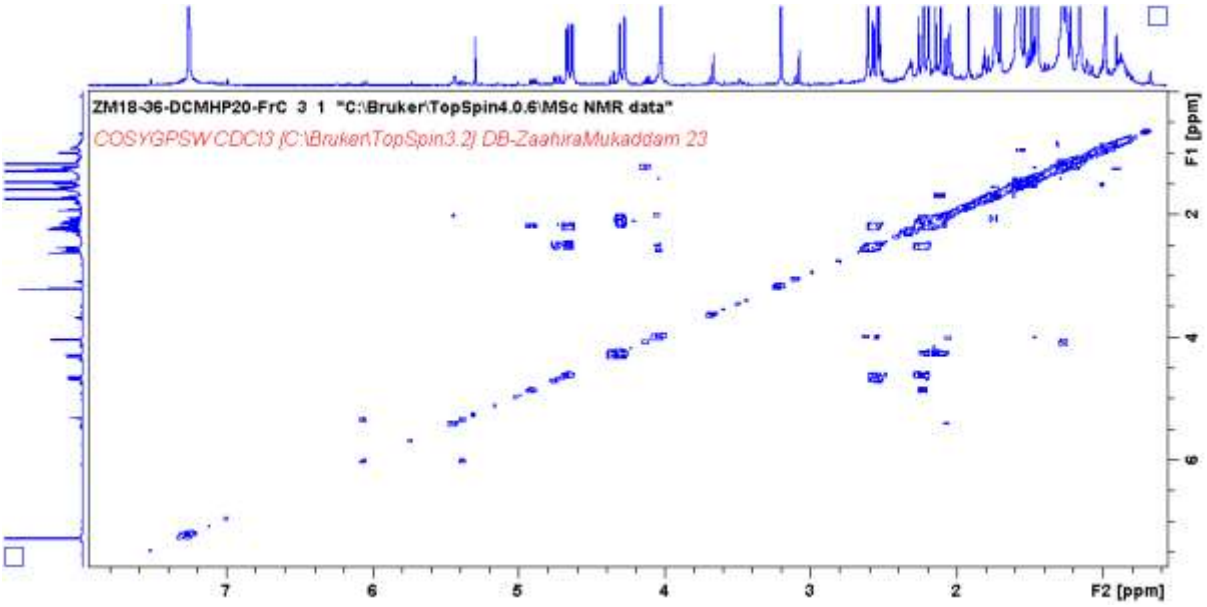

Figure S4.16: COSY spectra of compound **4.28** ($CDCl_3$, 400 MHz)

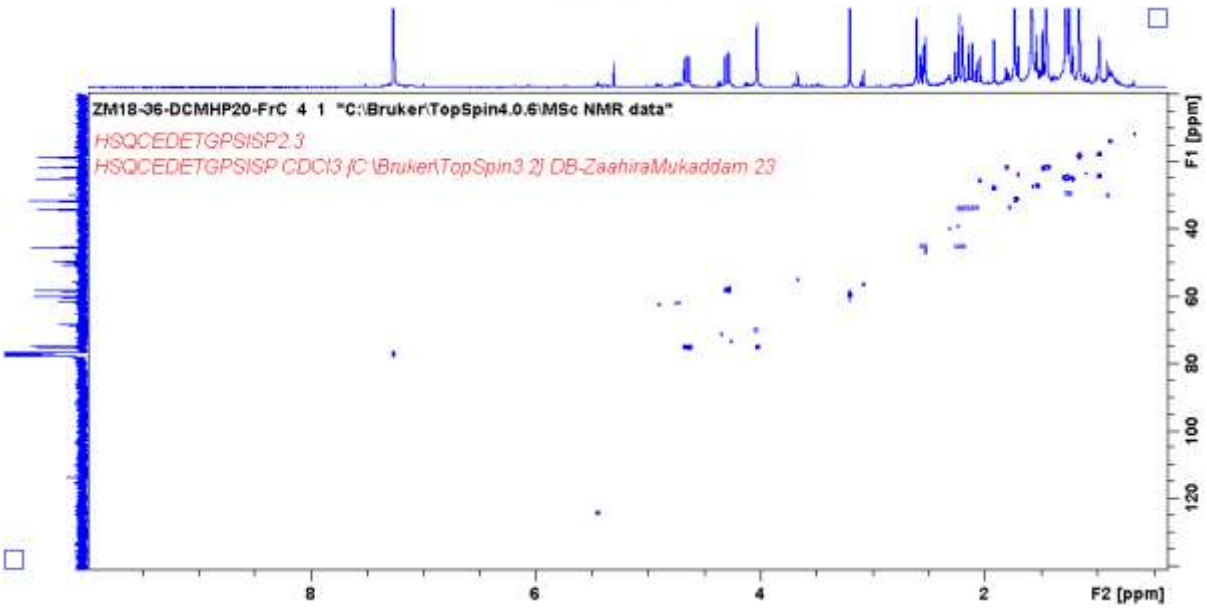

Figure S4.17: HSQC spectra of compound **4.28** ($CDCl_3$, 400 MHz)

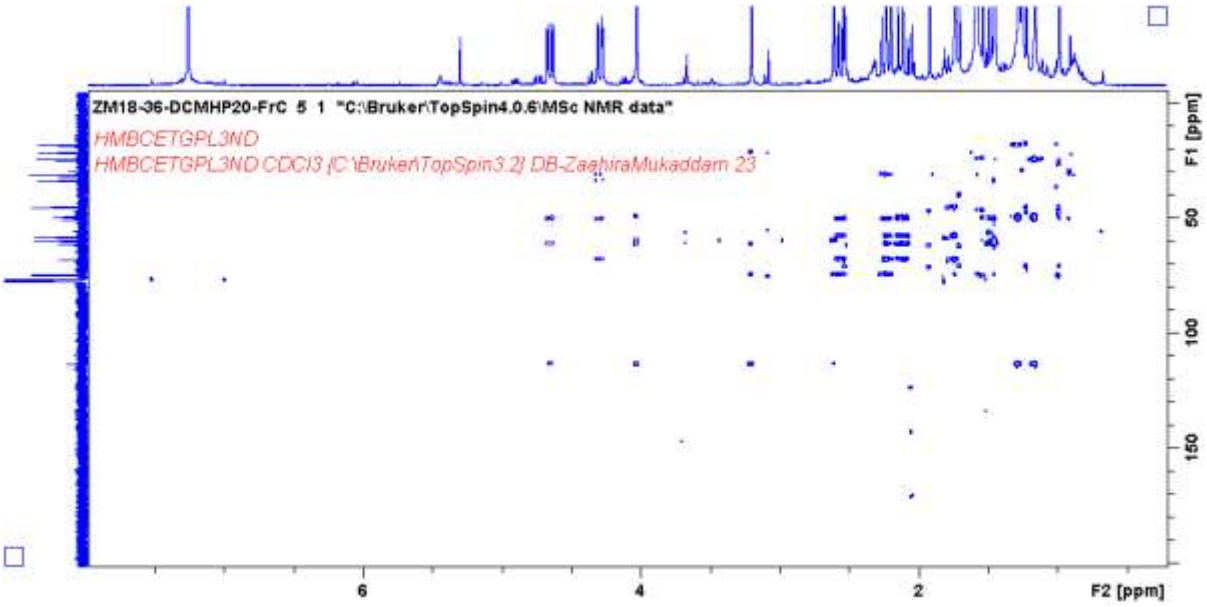

Figure S4.18: HMBC spectra of compound **4.28** ($CDCl_3$, 400 MHz)

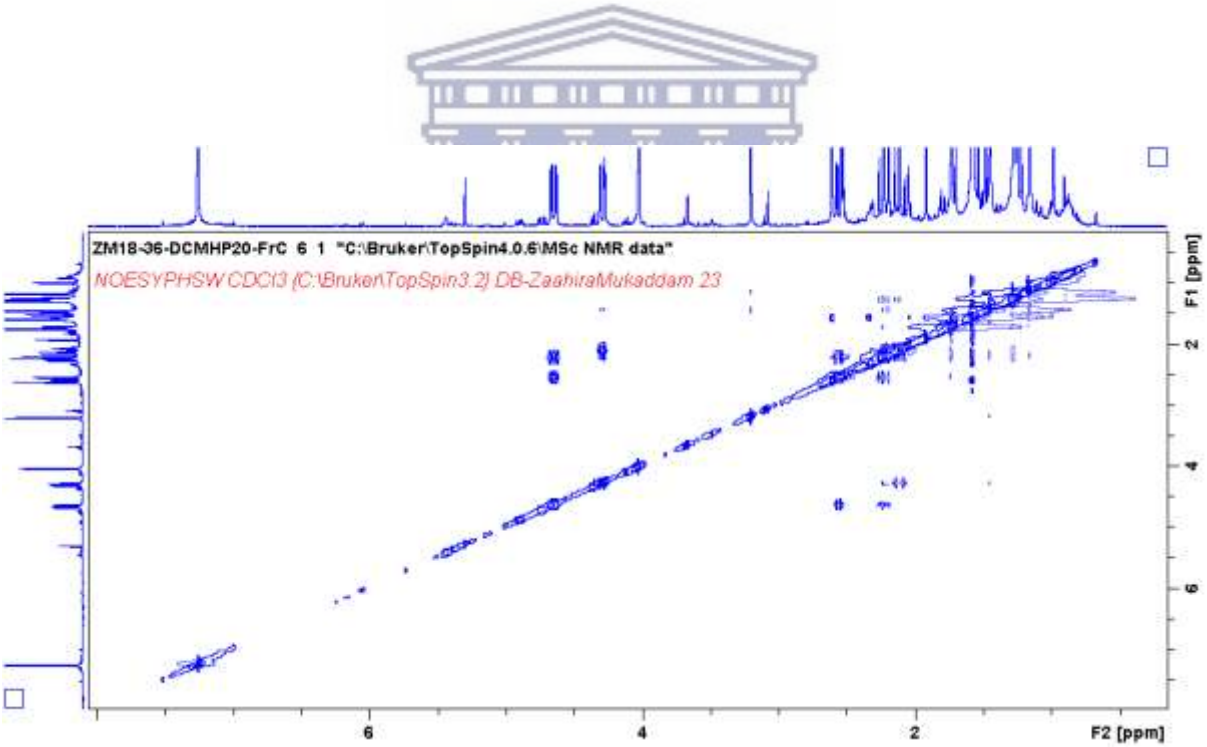

Figure S4.19: NOESY spectra of compound **4.28** ($CDCl_3$, 400 MHz)

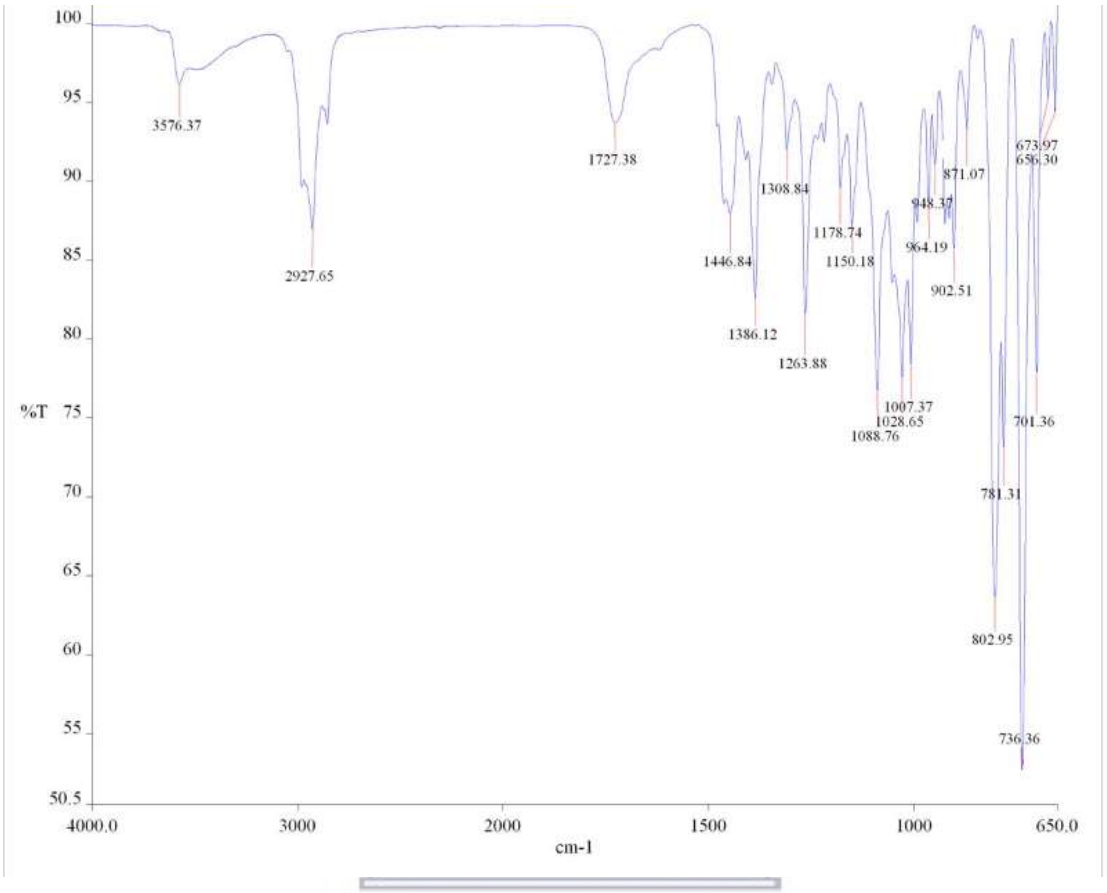

Figure S4.20: FTIR data for compound **4.29**

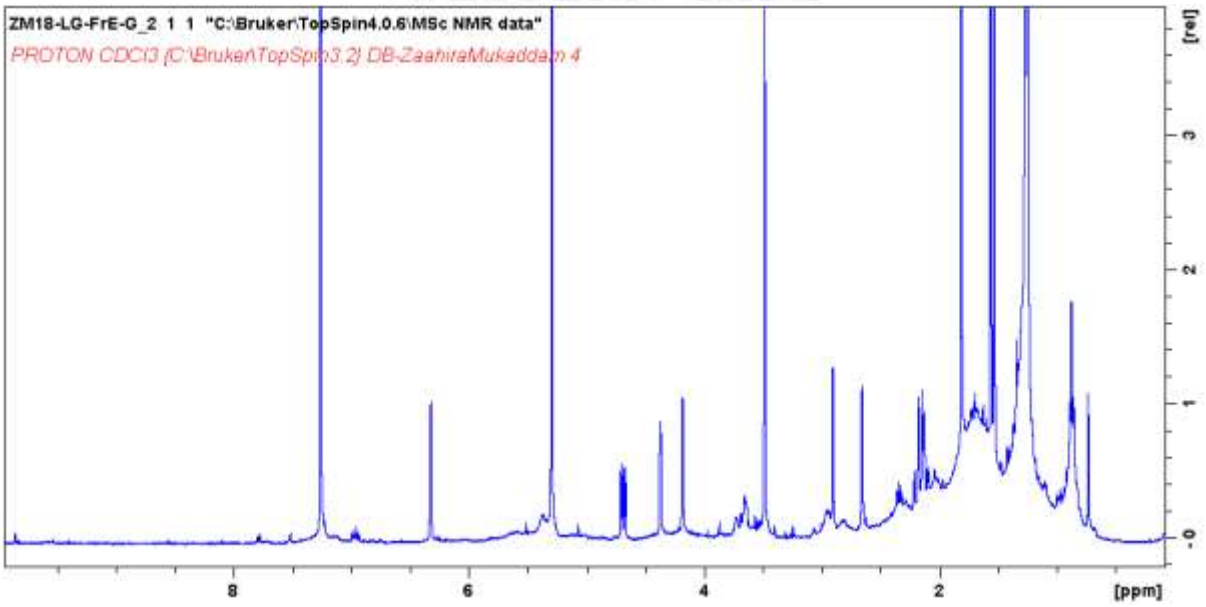

Figure S4.21: ^{1}H NMR spectra of compound **4.29** ($CDCl_3$, 400 MHz)

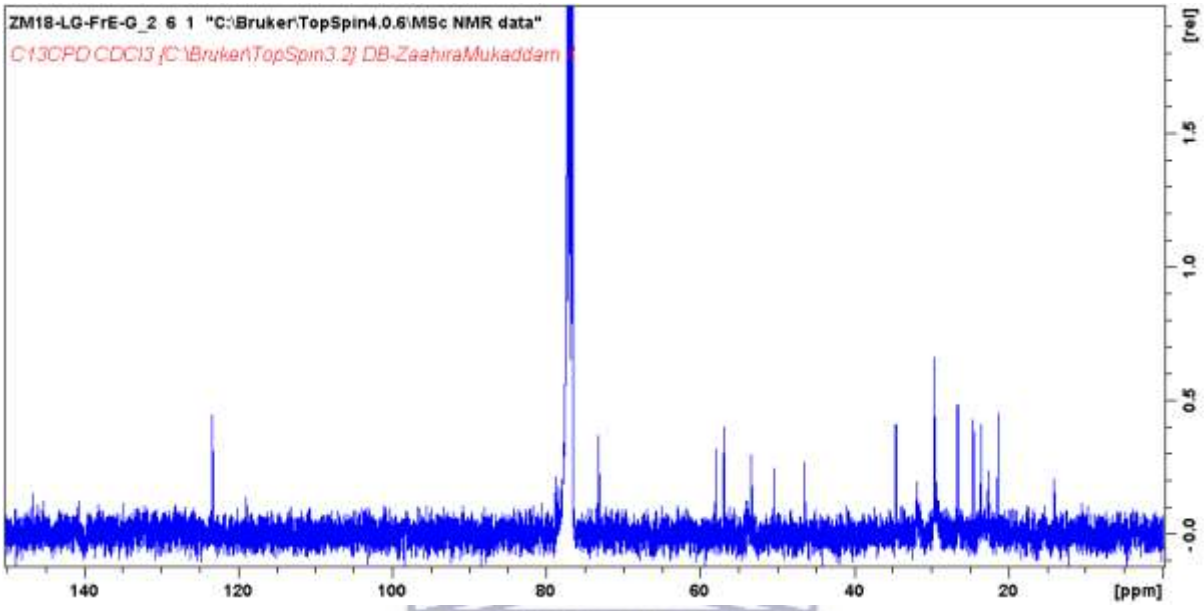

Figure S4.22: ^{13}C NMR spectra of compound **4.29** ($CDCl_3$, 400 MHz)

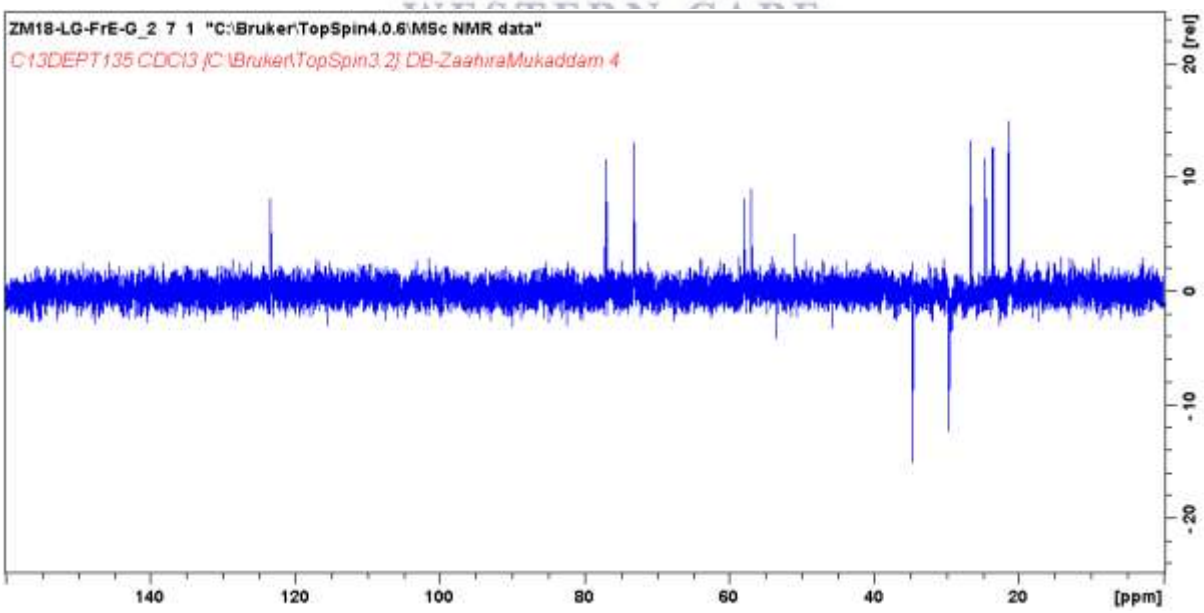

Figure S4.23: DEPT-135 spectra of compound **4.29** ($CDCl_3$, 400 MHz)

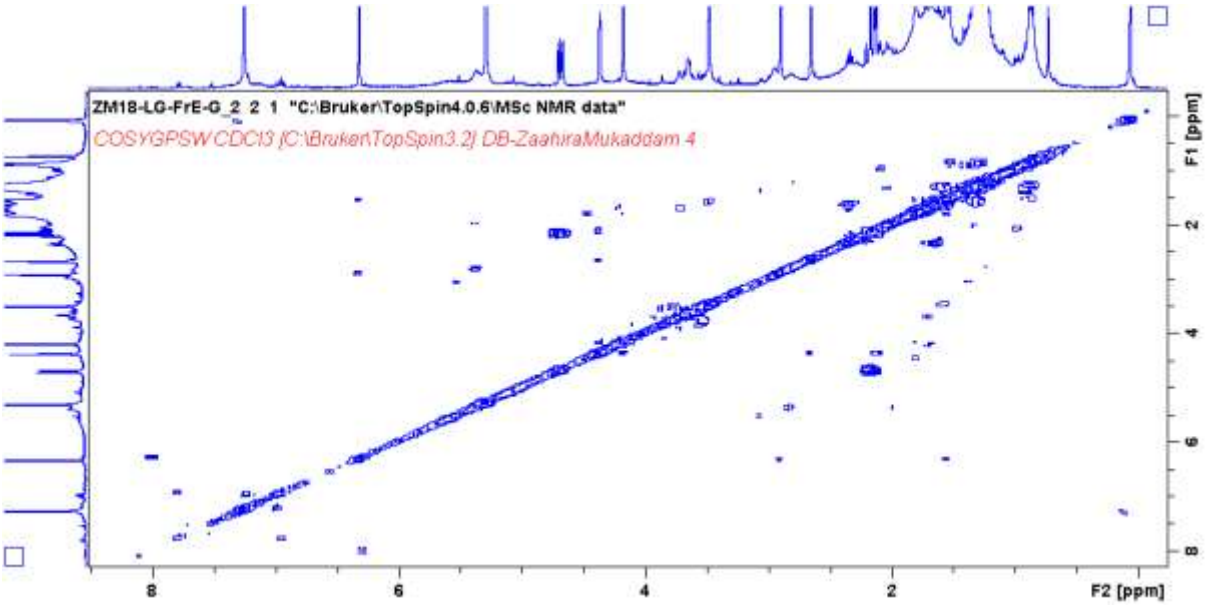

Figure S4.24: COSY spectra of compound **4.29** ($CDCl_3$, 400 MHz)

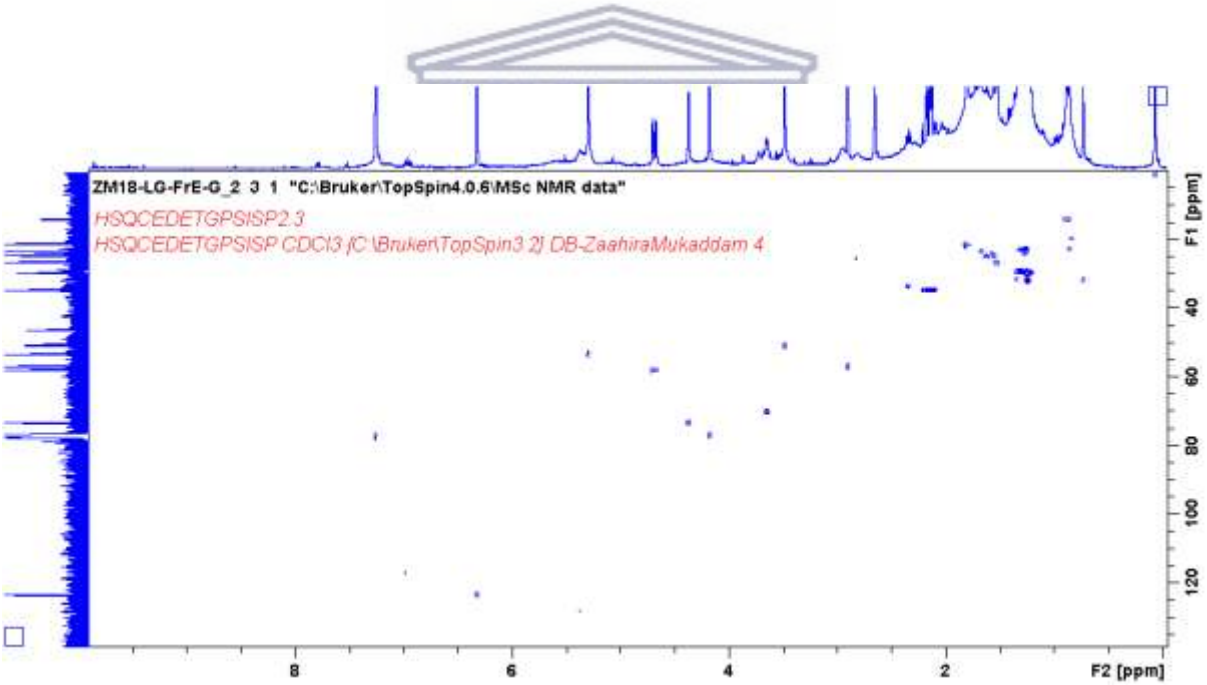

Figure S4.25: HSQC spectra of compound **4.29** ($CDCl_3$, 400 MHz)

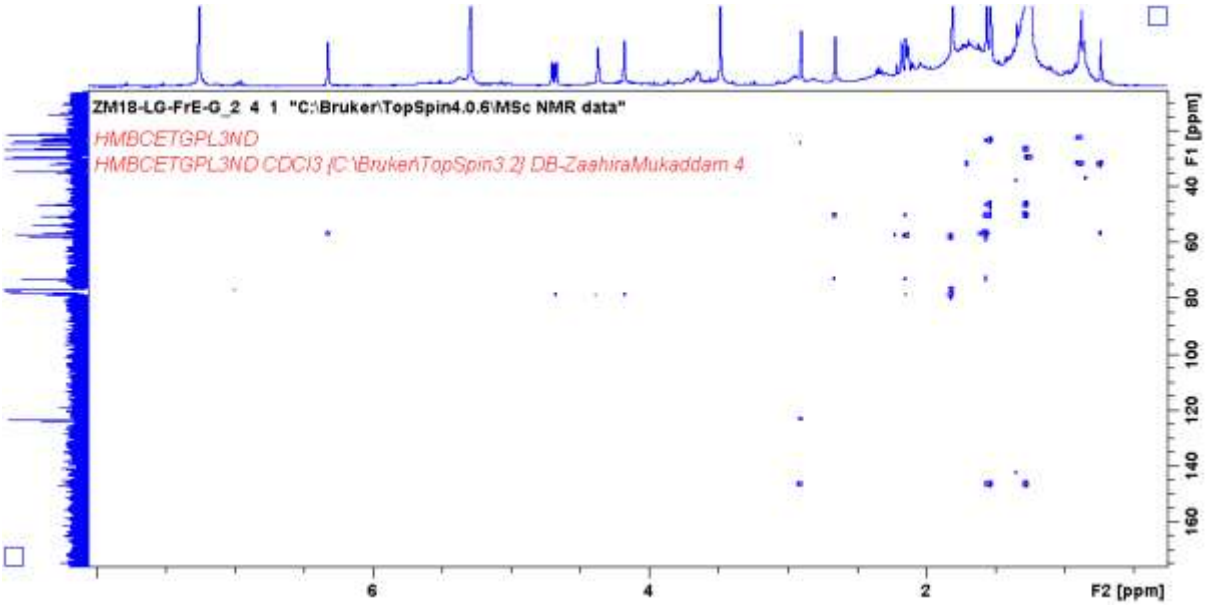

Figure S4.26: HMBC spectra of compound **4.29** ($CDCl_3$, 400 MHz)

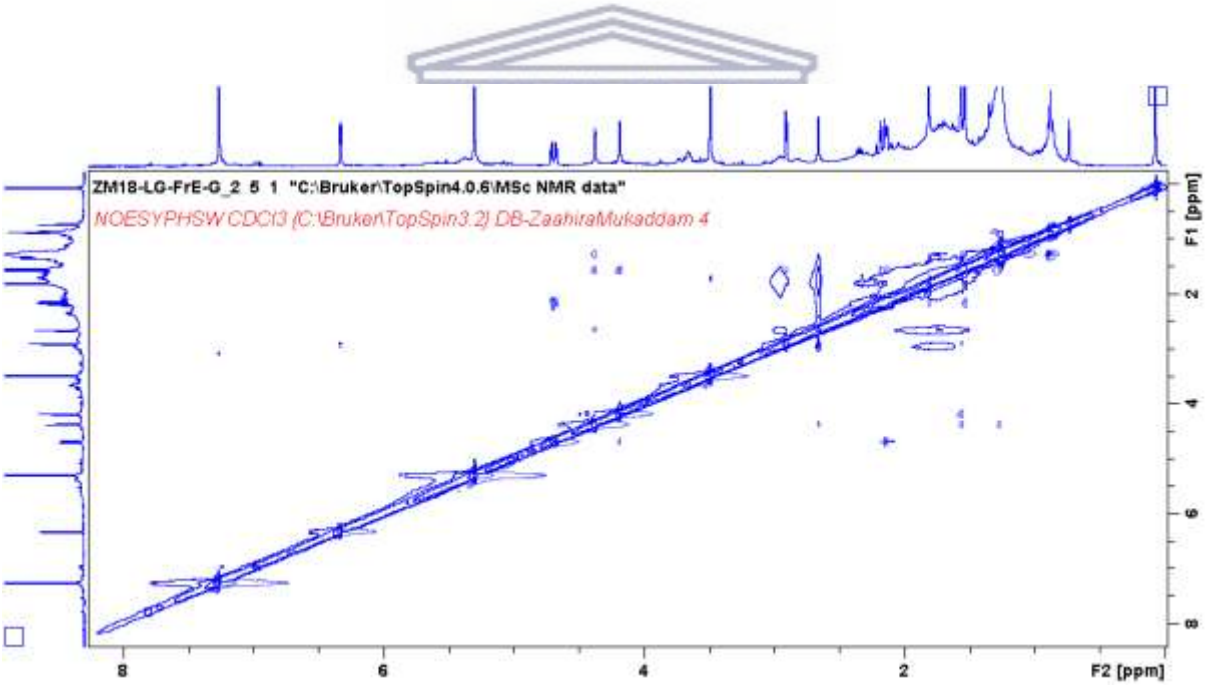

Figure S4.27: NOESY spectra of compound **4.29** ($CDCl_3$, 400 MHz)

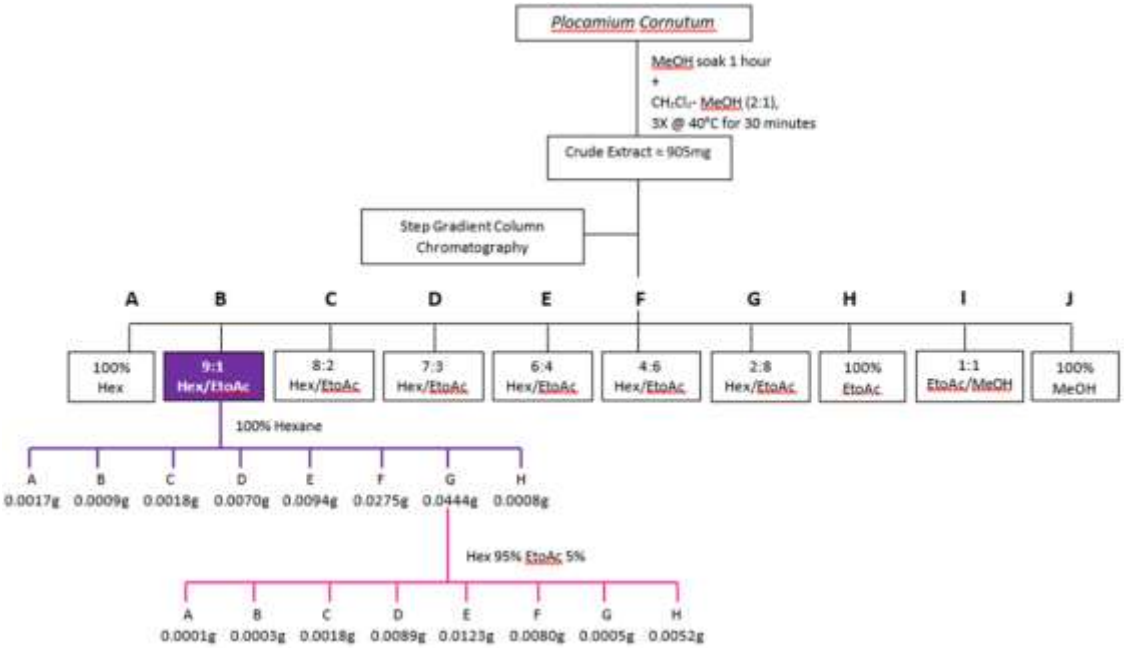

Figure S4.28: The total extraction and fractionation of *Plocamium cornutum*

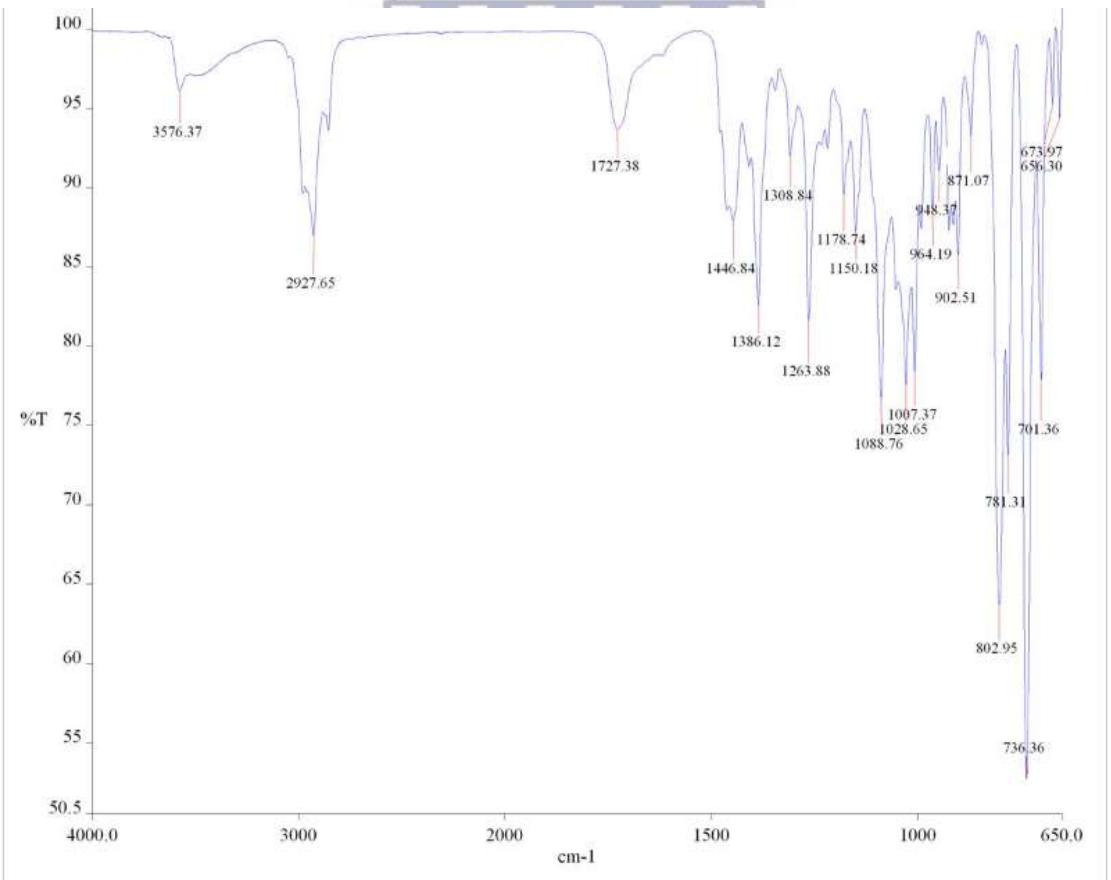

Figure S4.29: FTIR data for compound **4.30**

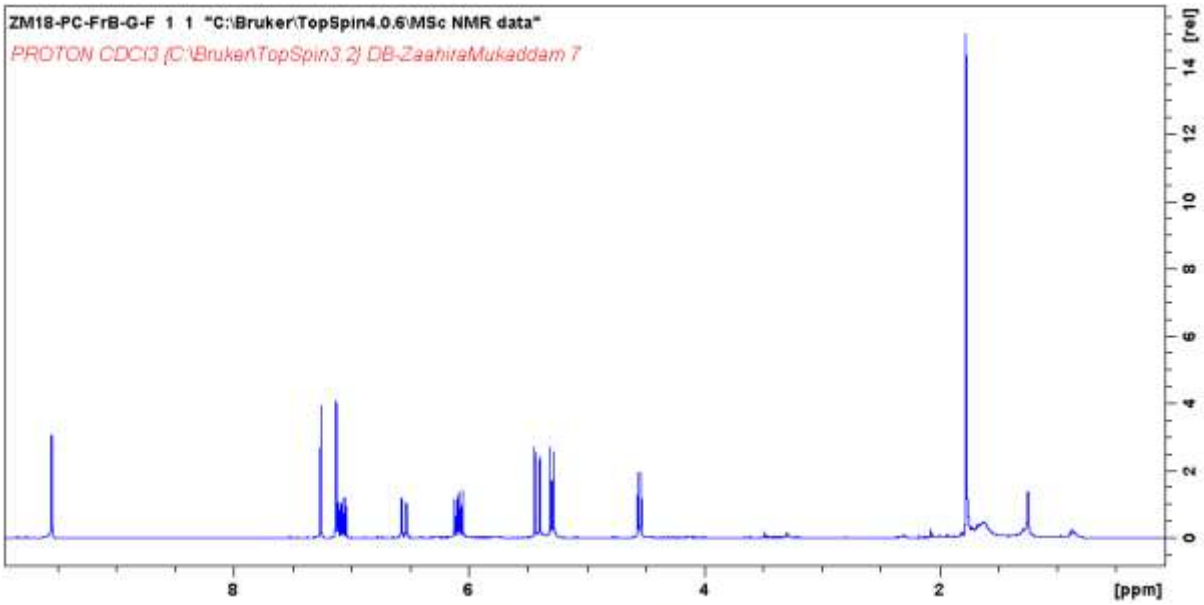

Figure S4.30: ^{1}H NMR spectra of compound **4.30** ($CDCl_3$, 400 MHz)

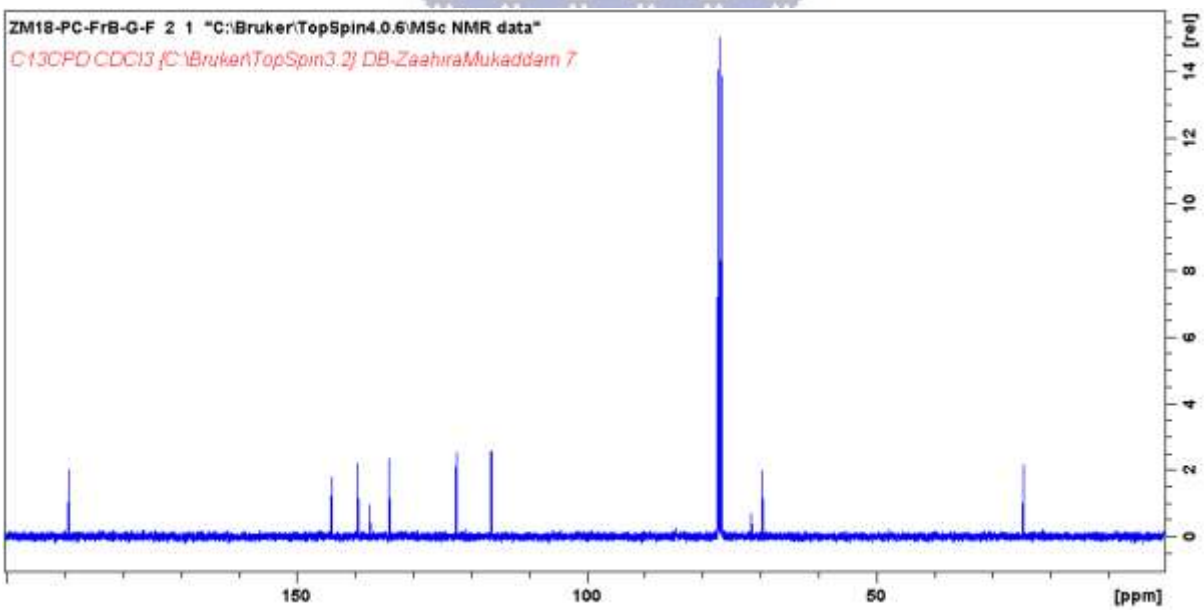

Figure S4.31: ^{13}C NMR spectra of compound **4.30** ($CDCl_3$, 400 MHz)

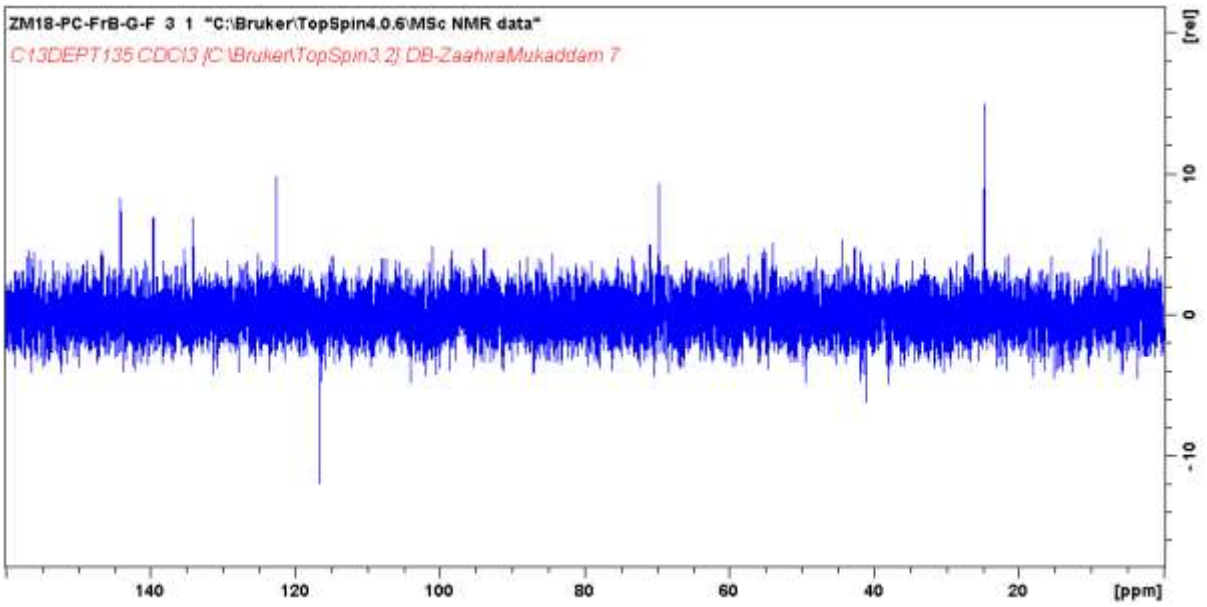

Figure S4.32: DEPT-135 spectra of compound **4.30** ($CDCl_3$, 400 MHz)

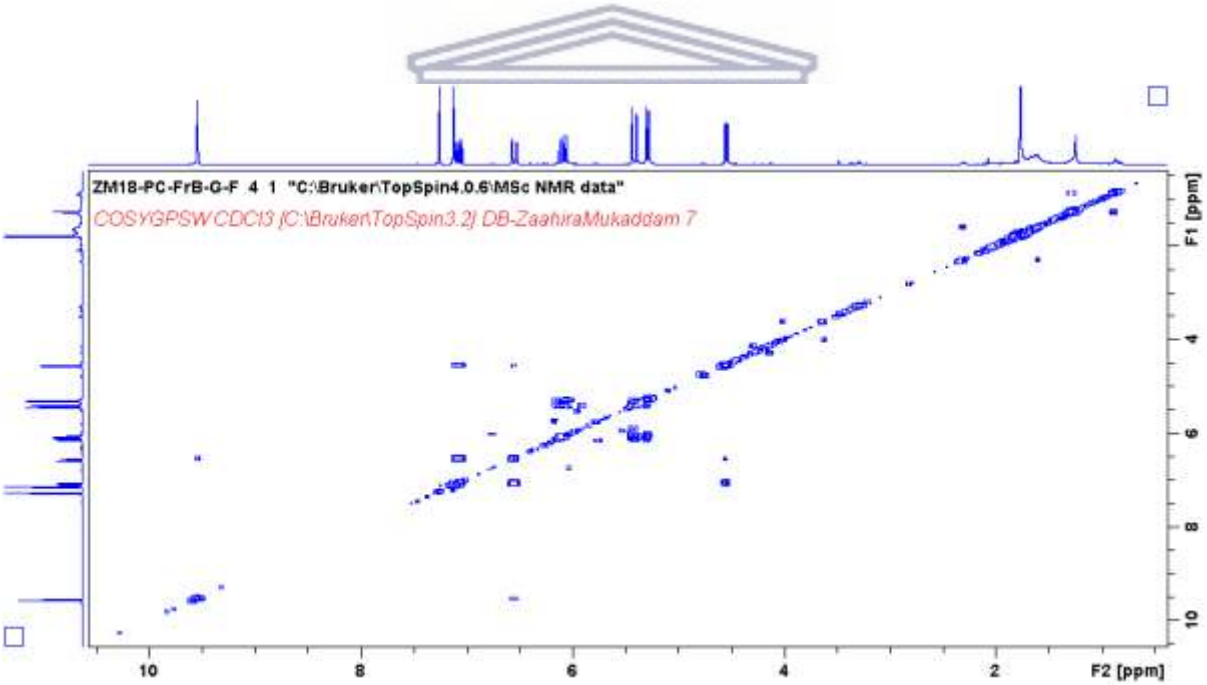

Figure S4.33: COSY spectra of compound **4.30** ($CDCl_3$, 400 MHz)

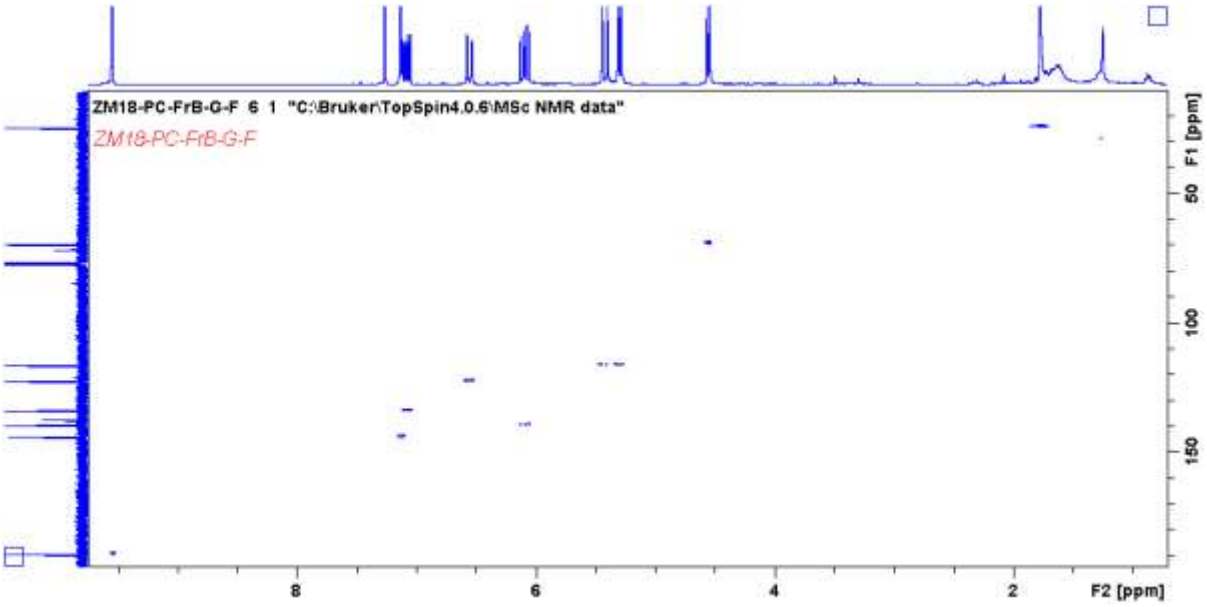

Figure S4.34: HSQC spectra of compound **4.30** ($CDCl_3$, 400 MHz)

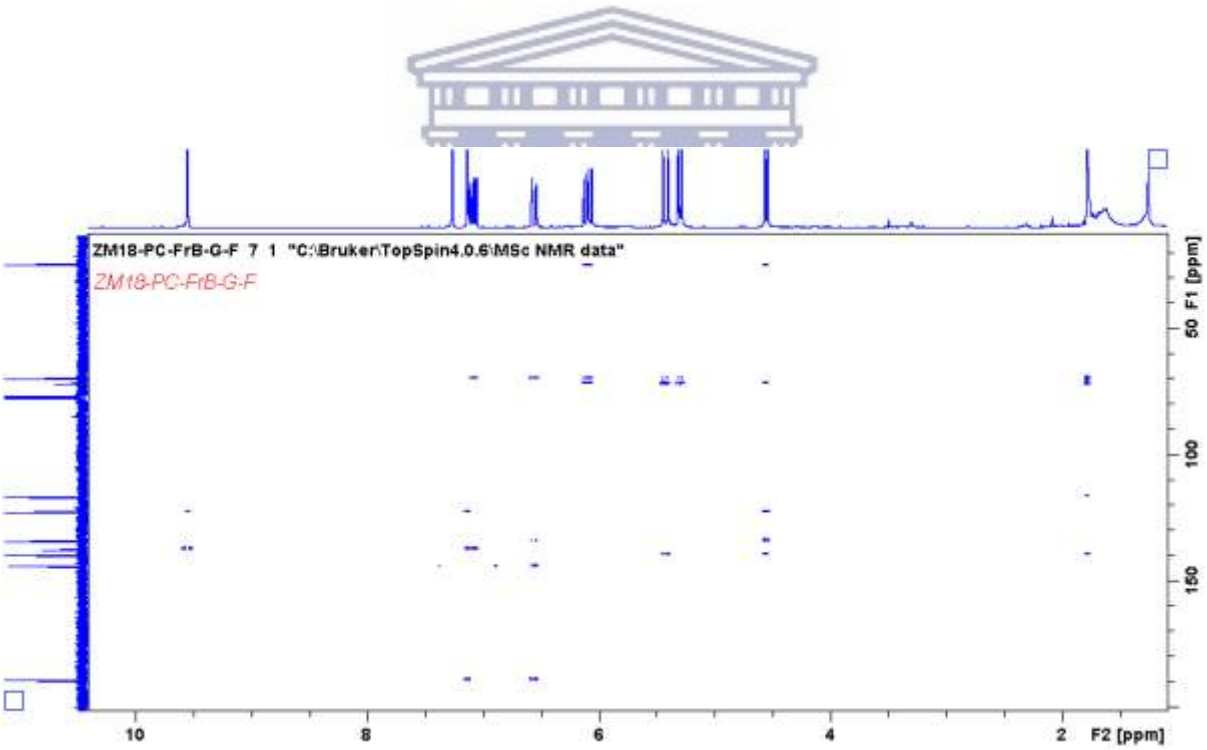

Figure S4.35: HMBC spectra of compound **4.30** ($CDCl_3$, 400 MHz)

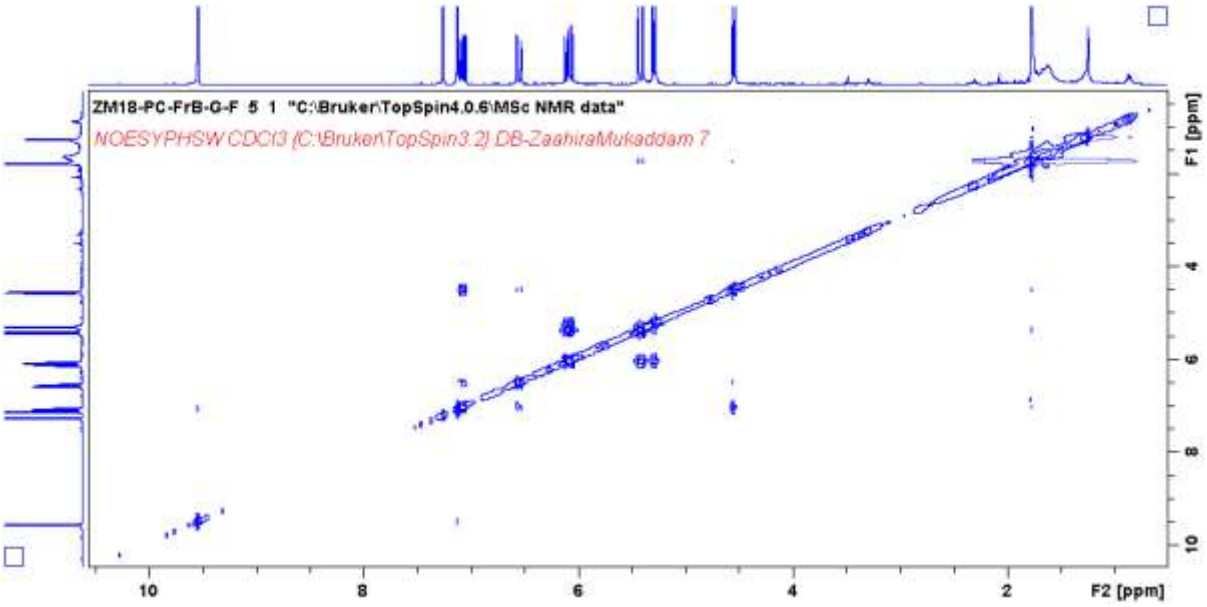

Figure S4.36: NOESY spectra of compound **4.30** ($CDCl_3$, 400 MHz)

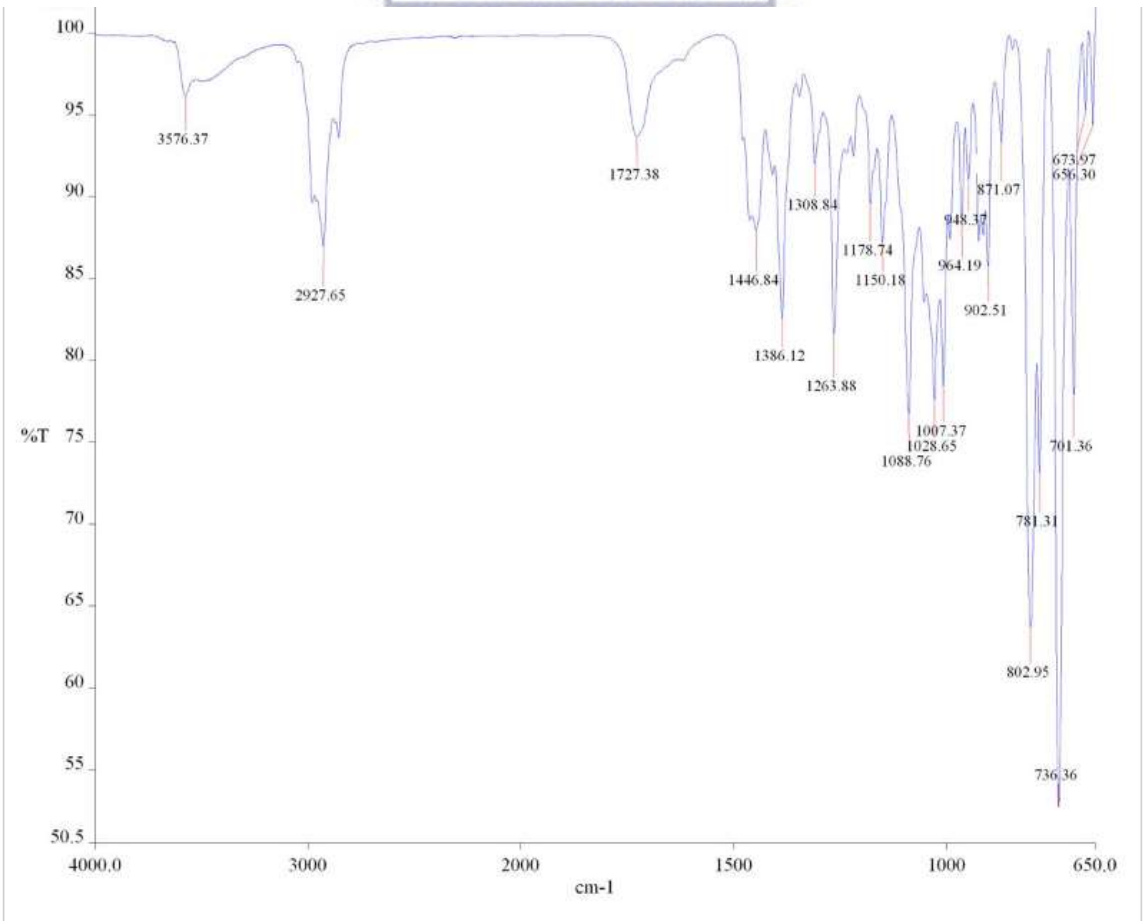

Figure S4.37: FTIR data for compound **4.31**

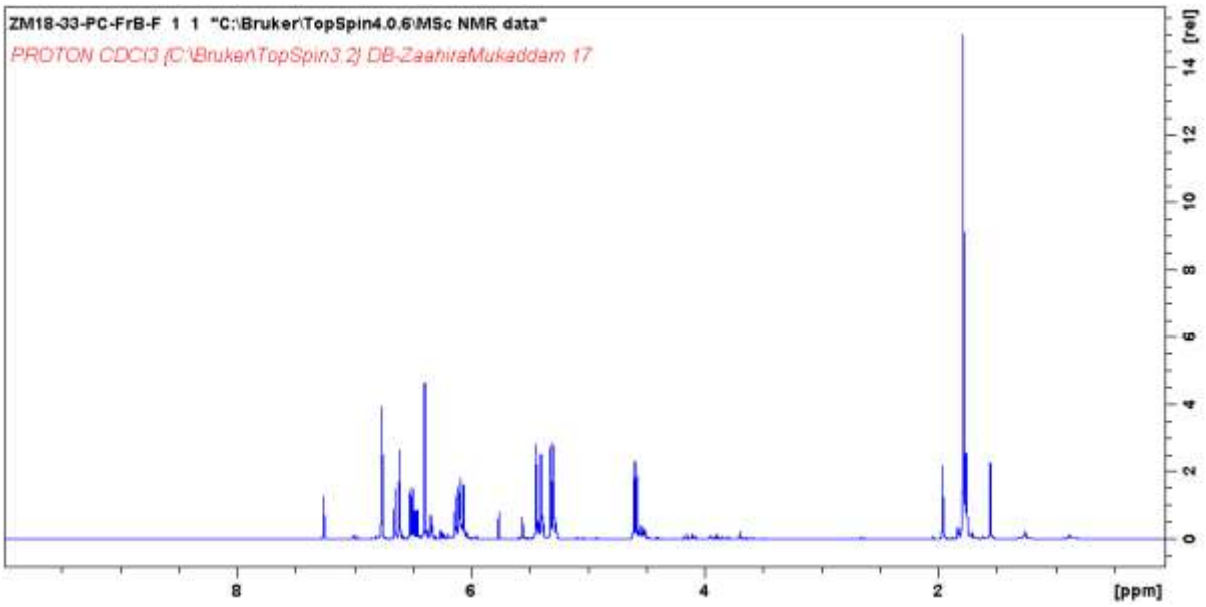

Figure S4.38: ^{1}H NMR spectra of compound **4.31** ($CDCl_3$, 400 MHz)

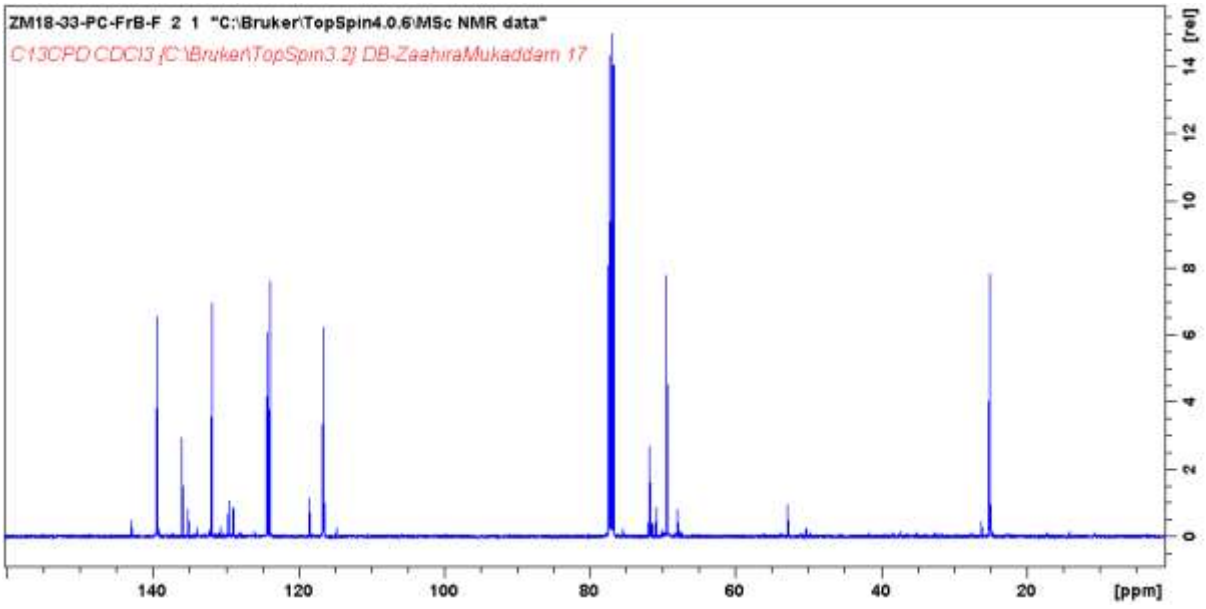

Figure S4.39: ^{13}C NMR spectra of compound **4.31** ($CDCl_3$, 400 MHz)

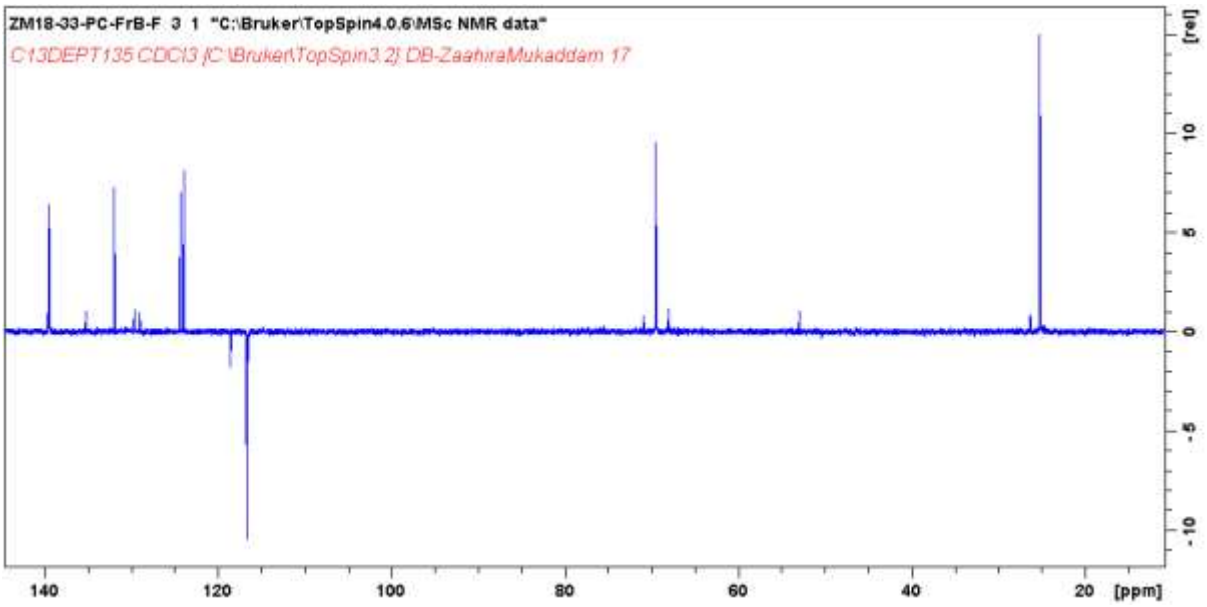

Figure S4.40: DEPT-135 spectra of compound **4.31** ($CDCl_3$, 400 MHz)

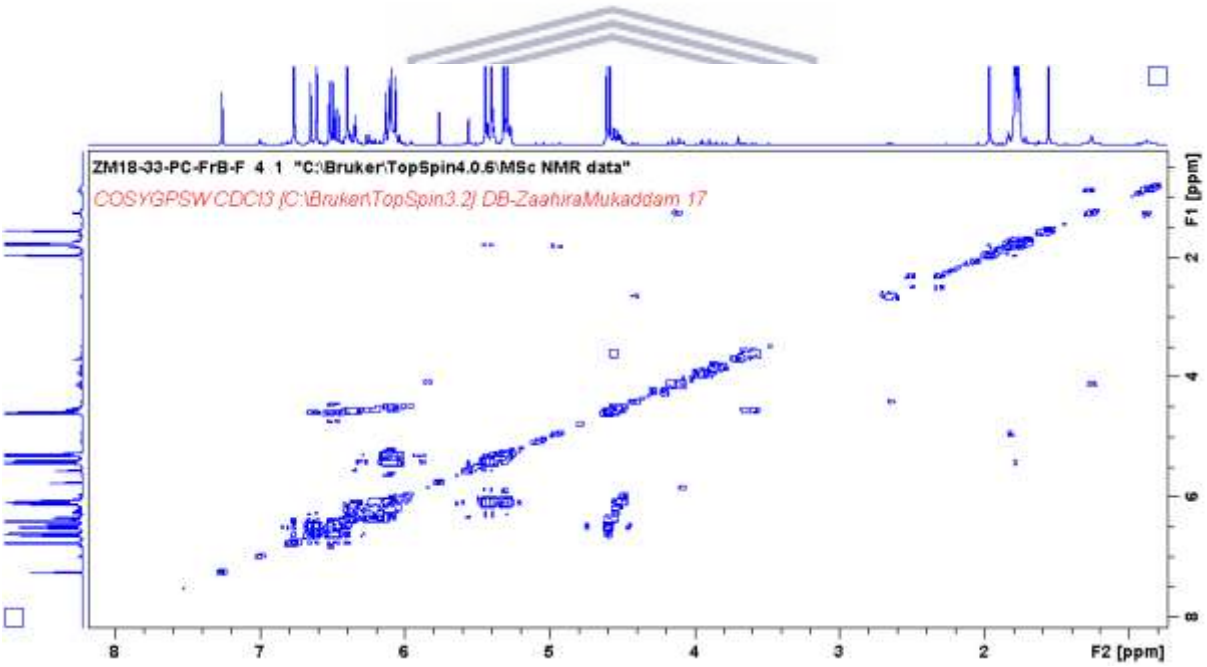

Figure S4.41: COSY spectra of compound **4.31** ($CDCl_3$, 400 MHz)

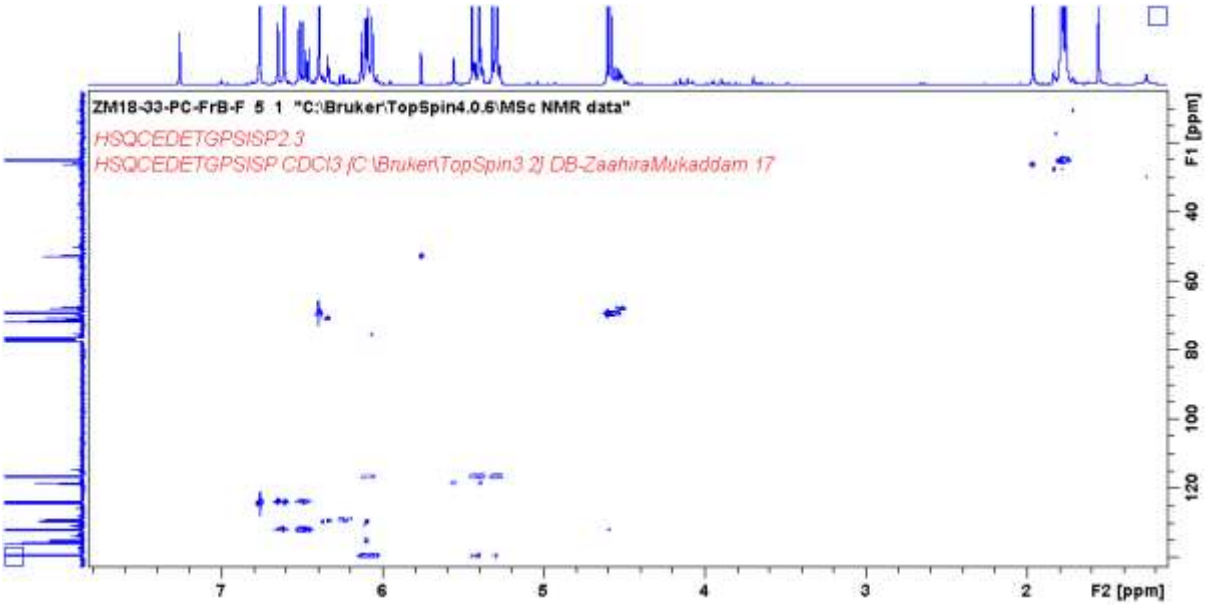

Figure S4.42: HSQC spectra of compound **4.31** ($CDCl_3$, 400 MHz)

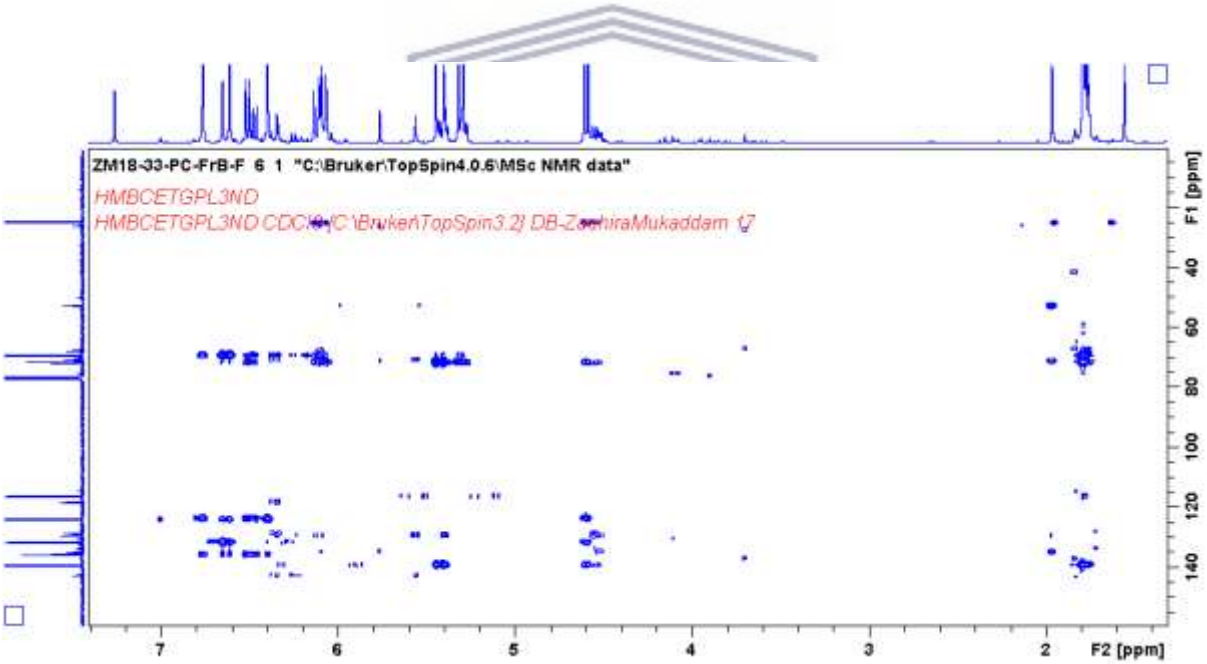

Figure S4.43: HMBC spectra of compound **4.31** ($CDCl_3$, 400 MHz)

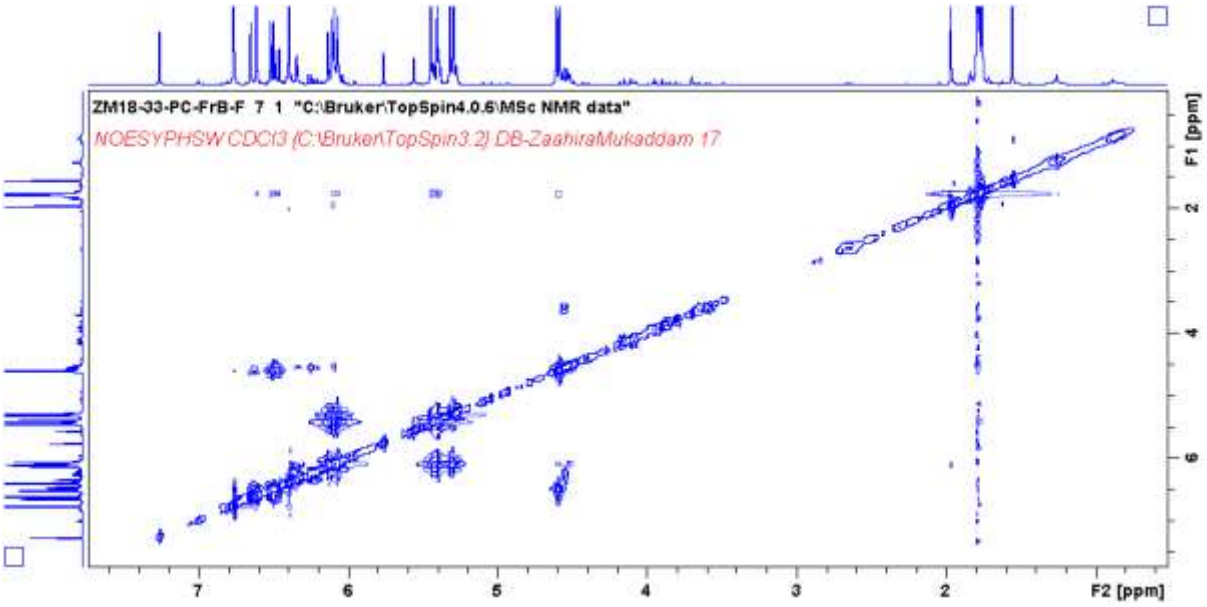

Figure S4.44: NOESY spectra of compound **4.31** ($CDCl_3$, 400 MHz)

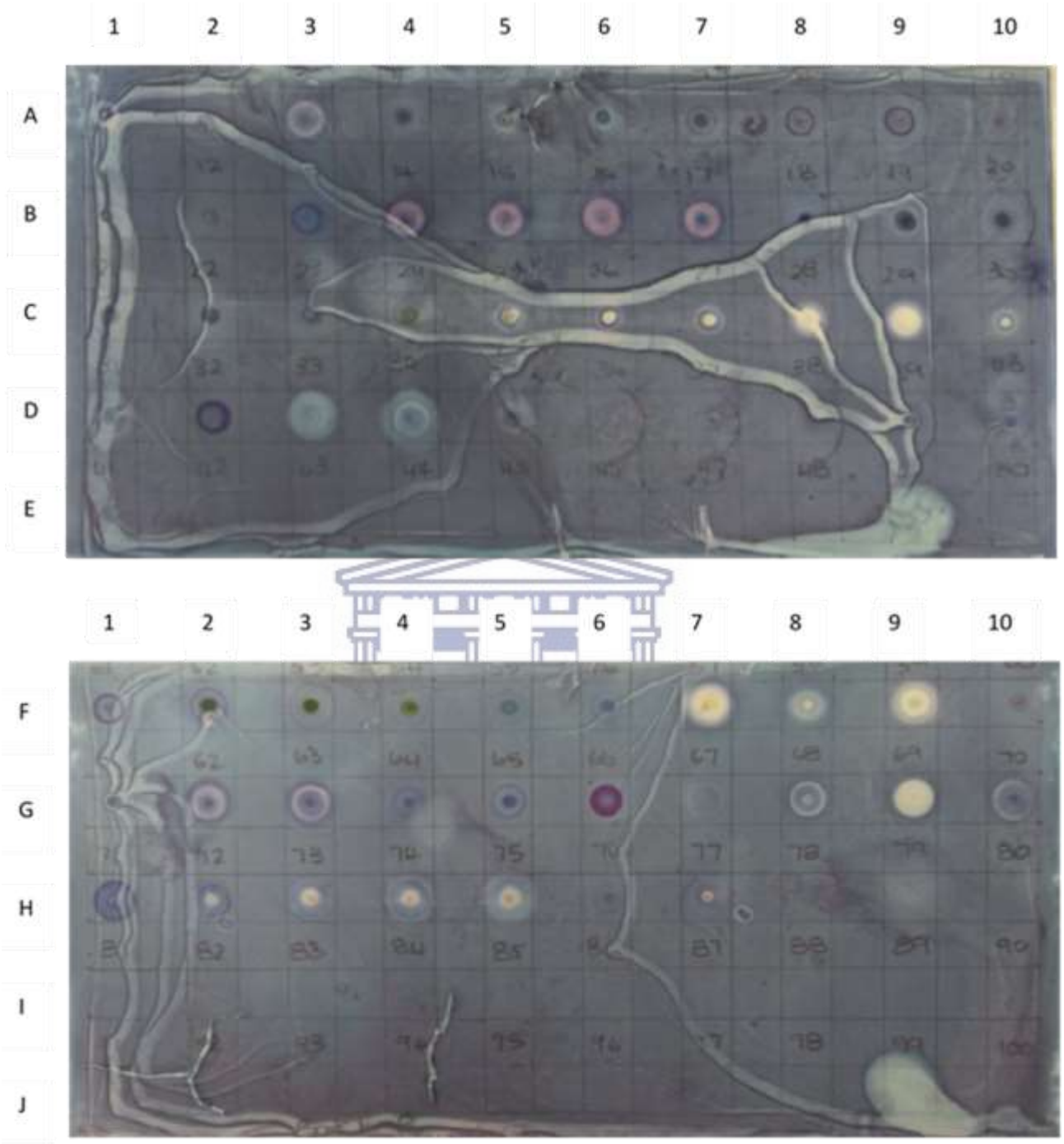

Figure S5.1: Photograph of the tested bioautography plates and the zones of activity observed for the various fractions against *M. aurum.*

	MCF-7	MCF-12
Untrt	100	100
LG Crude	77	103
LG-Fr-A	74	119
LG-Fr-B	58	61
LG-Fr-C	86	80
LG-Fr-D	100	106
LG-Fr-E	76	115
LG-Fr-F	102	119
LG-Fr-G	90	103
LG-Fr-H	103	117
LG-Fr-I	99	118
LG-Fr-J	86	45
LG-Fr-K	79	92
LG-DCMHP20	85	111
LG-Fr-E-G	87	62
DMSO	36	37
Untreated	**100**	100

Figure S5.2: Data for bar graph showing the effect of *L. glomerata* compounds on human breast cell lines.

Untreated	**100**	100
PC Crude	101	66
PC-Fr-A	84	144
PC-Fr-B	88	37
PC-Fr-C	83	52
PC-Fr-D	91	111
PC-Fr-E	78	34
PC-Fr-F	98	89
PC-Fr-G	89	45
PC-Fr-H	89	86
PC-Fr-I	81	86
PC-Fr-J	89	120
PC-Fr-B-F	85	20
PC-Fr-B-G-F	92	55
DMSO	36	37

Figure S5.3: Data for bar graph showing the effect of *P. cornutum* compounds on human breast cell lines.